Microstructure and macroscopic behaviour of polymer amended oil sands mature fine tailings

by

Tariq Mahmood Bajwa

A thesis submitted to the Faculty of Graduate and Postdoctoral Affairs in partial fulfillment of the requirements for the degree of

Doctor of Philosophy

in Geotechnical Engineering

Carleton University

Ottawa, Ontario

Examining Committee

Dr. Earnest Yanful, Civil and Environmental Engineering, Western University

Dr. Fred Afagh, Mechanical and Aerospace Engineering

Dr. Mohammad Rayhani, Civil and Environmental Engineering

Dr. Sai Vanapalli, Civil Engineering, University of Ottawa (Not in person)

Dr. Paul H. Simms, Supervisor, Civil and Environmental Engineering

Abstract

After several years following deposition, oil sands fine tailings settle to a solids content of 30 ~ 40% and are subsequently termed mature fine tailings (MFT). Once they have reached this state, MFT do not appreciably dewater, even after several decades. The particle size and dispersed structure of the fines (and possibly residual bitumen), negatively impacts the consolidation behavior of MFT.

Several technologies currently being trialed to accelerate dewatering of MFT, such as in-line flocculation, centrifuge, and tank thickening, flocculate the tailings using a polymer. The addition of polymer results in substantial dewatering in the short term (24 hours) after in-line flocculation, and increases dewatering in tank thickening and centrifugation. This is well understood in industry. However, the polymer may also change longer term dewatering behaviour by potentially changing the consolidation characteristics and water–retention characteristics of the tailings.

To assess the effect of polymer on all aspects of dewatering behaviour, column experiments simulating deposition of in-line flocculated tailings were undertaken for different times, different thicknesses, and under different environmental conditions. This allowed for the study to separate initial dewatering from self-weight consolidation, subsequent desiccation, and further consolidation of desiccated tailings when they are buried by fresh deposition. The behaviour was

analyzed by tracking fabric changes using mercury intrusion porosimetry and scanning electron microscopy.

Differences in dewatering behaviour following initial self-weight consolidation due to differences in polymer dose appeared to be minimal. Consolidation behaviour of previously desiccated tailings converged to the same properties by 80 kPa vertical effective stress. Optimizing for dose should therefore be done in terms of self-weight consolidation. It was observed that optimizing for yield stress may yield a higher optimal dose than for dewatering.

Key words: consolidation, desiccation, dewatering, hydraulic, microstrcuture, shear strength, suction, tailings, yield stress

Acknowledgements

I would like to take this special opportunity to thank my supervisor, Dr. Paul H. Simms, for his valuable guidance, technical and financial support, patience, and availability for each step of this study and providing me with the chance to work on this project. I would like to give my special thanks to Stanley Conley, Jason Arnott and Pierre Trudel (Civil Engineering Department), Dr. Marie Tudoret (Environmental Department) and other technical staff for their timely help while conducting the experimental work for this research. I also extend my thanks to Payal Chadha, Kristen Holtz, and Kay Casselman for their administrative support.

I offer my thanks to Dr. Jianqun Wang (Carleton University) for his comments, suggestions and help on the scanning electron microscopy (SEM) tests, and Tim Stephens (University of Western Ontario) facilitating mercury intrusion porosimetry (MIP) tests. My sincere gratitude to Dr. John Ripmeester, Dr. Moudrakovski Igor (National Research Council of Canada); Dr. Glenn A Facey, Glenn Poirier (University of Ottawa); Dr. Fred Gaidies and Keith Bourque (Carleton University) for their precious time to schedule technical sessions on various aspects of microstructure in the initial stage of my research program

I had the opportunity to meet and learn from many professors for last three years during my stay here at Carleton University. I offer my special thanks to Drs. Abd El Halim, George V. Hadjisophocleous, John Gales, Jules-Ange Infante, Karina

Lange, Majid Sartaj, Mohammad Rayhani, Paul Van Geel, Siva Sivathayalan and Shawn Kenny for their time and help.

I would like to express my sincere gratitude to Canada Oil Sands Innovation Alliance (COSIA), and the Carleton University for providing financial support throughout this research program. My thanks are extended to all my colleagues and friends Amandeep Singh, Jamal Sheikh, Oday Alshamary, Shoham Poudyal, Tessa Innocent and some others here at Carleton University, Ottawa, and abroad.

I love you so much, my sweeties, Shahmir I.U. Bajwa, Shayan S.U. Bajwa and Shawaiz I. U. Bajwa.

This thesis is dedicated to my father, who suffered a brain hemorrhage during my stay at Carleton University.

Table of Contents

List of Tables

List of Figures

List of Appendices

List of Abbreviations and Acronyms

Abbreviations

- AEV — Air entry value
- AOSD — Athabasca oil sands deposit
- bbl — Barrels
- Bm^3 — Billions cubic metre
- BSED — Backscattered electron detectors
- C_a — Calcium
- cd — Calendar day
- CEC — Cation exchange capacity
- cm / sec — Centimetre per second
- COF — Cyclone overflow
- CPSD — Cumulative pore size distribution

- CRS — Constant rate of strain
- Cs — Solids content
- CT — Composite tailings
- CT — Computed tomography
- CT — Consolidated tailings
- Cu — Copper
- d — Day
- EC — Electrical conductivity
- EDL — Electrical double layer
- ERCB — Energy Resources Conservation Board
- ESEM — Environment scanning electron microscopy
- FFT — Fluid fine tailings
- GSD — Grain size distribution
- Gs — Specific gravity
- GSED — Gaseous secondary electron detectors
- ILTT — In-line thickened tailings
- K — Potassium
- kg/m^3 — Kilograms per cubic metre
- kV — Kilovolts
- LI — Liquidity index
- Li — Lithium
- LIR — Load incremental ratio
- LL — Liquid limit
- meq — Milliequivalent
- MFT — Mature fine tailings
- Mg — Magnesium
- MIP — Mercury intrusion porosimetry
- mL/g — Milliliters per gram
- Mm^3 — Million cubic metres
- MPa — Mega Pascal
- MRL — Method reporting limit

- nm — Nano metre
- NMR — Nuclear magnetic resonance
- PI — Plasticity index
- PL — Plastic limit
- ppm — Parts per millions
- PSD — Pore size distribution
- RAPP — Regional aquatic Monitoring Program
- RH — Relative humidity
- rpm — Revolution per minute
- SCS — Soil classification system
- SEM — Scanning electron microscopy
- SFR — Sand to fine ratio
- SIS — Seepage induced settlement
- SL — Shrinkage limit
- SWCC — Soil water characteristics curve
- TSF — Tailings storage facility
- TT — Thickened tailings

Acronyms

- % — Percentage
- τ_y — Shear stress
- @ — At the rate of
- μ_a-μ_w — Matric suction
- µg/g — micron gram per gram
- µm — Micron metre
- µS/cm — Micro seimens per centimetre
- c_v — Coefficient of consolidation
- m_v — Coefficient of compressibility
- n — Porosity
- N_a — Sodium

- ^{o}C Degree centigrade
- S Degree of saturation
- u_a Pore air pressure
- u_w Pore water pressure
- V_s Volume of soil solids
- V_v Volume of voids
- π Osmotic suction
- ρ Density
- σ Stress
- Ψ Total suction

Chapter 1. Introduction

1.1 Background

The Athabasca oil sands deposit (AOSD), Alberta Canada is one of the world's largest unconventional reserves of crude bitumen or heavy crude oil, comprising sub-deposits associated with the Athabasca River, Peace River and Cold Lake (Masliya et al. 2004). The deposit is situated 75 kilometers north of Fort McMurray, Alberta, Canada, and is generally comprised of quartz, silt, clay, water, bitumen and some minerals like titanium, zirconium, tourmaline and pyrite. The deposit covers about 142,200 km^2, an area twice as large as the province of New Brunswick, Canada (Alberta Energy 2013). According to estimates, the deposit contains about 1.7 to 2.5 trillion barrels, of which 300 billion barrels of heavy crude oil are recoverable.

Oil sand deposits generally consists of 75 to 80 percent inorganic material, 13 to 16 percent bitumen and 3 to 5 percent water (Government of Alberta, Canada 2009; National Energy Board 2006; Caughill et al. 1993; Morgenstern et al. 1995). Commercial extraction of bitumen started in 1967. The oil sands operators follow two approaches for the extraction of bitumen, namely surface mining and in-situ extraction operations. After surface mining, bitumen is liberated from the ore using the Clark hot water process through the addition of hot water and caustic soda (Masliya et al. 2004). In the in-situ approach, the extraction of bitumen takes place at site and the operation involves cold flow, cyclic steam

simulation, steam assisted gravity drainage, solvent extraction, toe to heel air injection and combustion overhead gravity drainage. A huge volume of left over materials or waste material (oil sands tailings) is produced as a result of bitumen extraction form surface mining. The proportion of tailings to bitumen production from the reserve is quite high, as two barrels of tailings are generated for one barrel of crude oil (Mikula 2012 and Morgenstern and Scott 1995). The fine tailings contain water, residual bitumen, sands, silts, and clays. The water chemistry of the tailings is affected by the extraction process. For example, the concentration of sodium (Na) in the process water is high due to the addition of caustic soda.

After production, the oil sands tailings are transported hydraulically to the tailings storage facilities (TSF) bounded by engineered dams. At this time, the tailings have only a solids content (Cs) of 7 ~ 8 percent by mass. The sand particles settle out to the bottom or form beaches, trapping a fraction of the fines (silts and clays). Most of the fine particles remain in suspension, which slowly settles to form a suspension with Cs= 30 ~ 40 within a decade (~185% GWC). Once they have reached this state, the fine tailings, now termed MFT (mature fine tailings) do not appreciably dewater, even after several decades. The lack of dewatering of MFT is due to its poor consolidation characteristics (very low hydraulic conductivity) and thixotropic buildup of particle network structure that impedes consolidation (Jeeravipoolvarn 2005). Clay particles in MFT are in a relatively dispersed state, probably due to the chemistry of the extraction process (Beier

and Sego 2008). Despite thixotropic buildup, MFT does not develop any substantial strength (< 1 kPa), which prevents reclamation of the TSFs.

Due to high rates of production and low natural dewatering, the volume of tailings was reached to 741 Mm^3 in tailing storage facilities (TSF) until 2008 (Houlihan et al. 2010), which covered an area more than 175 km^2, i.e., 50% more than the city of Vancouver (NationMaster 2008) and the volume of water in Sylvan lake, Alberta, Canada. The volume of tailings is sufficient enough to fill Rogers Centre, Toronto, Canada, 47 times in a year. It is estimated that the volume of fine tailings may grow up to 1.3 B m^3 by 2060, if the tailings are produced at the current rate (Hale and Houlihan 2011).

The containment of this large volume of tailings for several decades in TSF poses a serious challenge to land reclamation and environment management responsibilities of the oil sands industry (Nix and Martin 2006; Rogers et al. 2001; Price 2011 and Environment Defence 2008). Gagne et al. (2012) suggested that the refining operations associated with oil sands tailings contaminated the Athabasca River. The oil sands tailings might cause chronic and chronicle diseases to aquatic and ecological receptors (Bothe et al. 2010). The Government of Canada is spending billions of dollars each year for cost effective management of fine tailings.

In the light of above mentioned issues, the Energy Resources Conversation Board (ERCB), Alberta, Canada introduced a legislation (Directive 074 - 2009),

which highlights the criteria for safe handling of this problematic and large volume of tailings. Directive 074 (2009) applies to all oil sands operations requiring reduction of fluid fine tailings (FFT) through its conversion into trafficable deposits. The legislation forced the industry to adopt technology achieving undrained shear strength of 5 kPa one year after deposition or 10 kPa after five years of tailings deposition in TSF for rapid trafficability, reclamation, which may minimize the adverse impacts to the environment. To achieve goals set out in the legislation, the oil sands operators may use a suite of technologies; however, they are bound to submit disposal plans that describe how they will achieve the criteria (Directive 074, 2009).

To achieve goals set out in Directive 074 (2009), the oil sand operators are following a number of technologies based on mixes of concepts to consolidate the tailings including freeze-thaw, composite tailings, addition of CO_2, thickening, centrifugation, or in-line flocculation, often with the addition of an amendment to promote flocculation of the dispersed clay particles (Zbik et al. 2009). Several of these technologies are currently being trialed at large scale by oil sand operators, using a polymer to assist flocculation in addition to relying on dewatering post-deposition by freeze-thaw, evaporation, and consolidation. After the introduction of polymer to the MFT and the subsequent initial dewatering process (e.g., thickening in a tank, or centrifuge), the MFT may be spread in thin lifts or thicker deposits. To place in context, in MFT 5 kPa is only reached when the solids content is above 65% solids, or lower than 55% water content.

Few findings in the public literature are available discussing the behaviour of polymer amended oil sands MFT. Mizani et al. (2013) reported that the low polymer dose showed more dewatering potential in thin lift (0.50 m). Mathews et al. (2011) reported that in-line mixing at the field scale increased the solids content from 30 - 35% to 45 - 55% within 24 hours after tailings deposition in thin lifts (0.60 m). Wells et al. (2011) stated that very thin lifts (0.2 - 0.3 m) gave 80% solids content within 10 days. Jeeravipoolvarn (2010) showed that the solids content changed from 3.7 to 32.6 % after 07 day on in-line polymer mixing of COF tailings. These works showed the effectiveness of polymer to assist in increasing the solids content of MFT, however, these studies were only focused highlighting the short term behaviour of polymer amended MFT examining only a few parameters of practical interest.

At least four mechanisms contribute to dewatering post-deposition: very short term water release (less than 24 hours) due to settling post-flocculation, which is called “initial dewatering” in this study, dewatering due to consolidation in the short term (in a few weeks), strength gain by desiccation once substantial water is no longer accumulating at surface, and long term consolidation at depth in a deposit. The scope of the study involves understanding the contribution of each mechanism to dewatering, and how these mechanisms interact. This is accomplished by tracking both macroscopic and microstructure characteristics of a polymer amended mature fine tailings as it dewaters through different mechanisms. The study examines the various parameters of practical interest, namely liquidity index (LI), sand to fine ratio (SFR), volume change, yield stress,

undrained shear strength, hydraulic conductivity, pore water chemistry, and soil water potential and furthermore, microstructure measurements using scanning electron microscopy (SEM) and mercury intrusion porosimetry (MIP) to track pore size distribution, pore shape, textural and geometric configuration. It is hoped that this fundamental study will provide information useful to assist optimization of current and future technologies employing polymer as an amendment in the oil sands industry.

All tests are performed on mature fine tailings mixed with a polymer and then subsequently deposited in columns. This most closely simulates the in-line flocculation technology. The mixing protocol for preparing the tailings in fact is taken from the protocols of one of the oil sand operators for producing “field equivalent” samples in the laboratory. This procedure is discussed in the methods chapter.

1.2 Originality of the research work

The originality of the work lies in the following:

1. In-depth study of dewatering behavior of polymer amended MFT for different post-deposition dewatering processes: initial dewatering, desiccation, and consolidation. No such study has been published in the public domain.
2. Analysis of microstructure of polymer amended MFT using MIP and SEM: while some limited study of microstructure of polymer amended cyclone overflow tailings by qualitative analysis of SEM images, neither quantitative analysis of

SEM images nor MIP has been applied to interpret behavior of MFT, polymer amended or otherwise.

1.3 Objectives

The research studies post-deposition dewatering of polymer amended MFT - to this end, the behavior of polymer amended MFT is studied at different times post-deposition. These times were selected to attempt to differentiate between initial dewatering (sedimentation), subsequent self-weight consolidation that occurs even in a relatively thin lift, desiccation, and consolidation under burial by new lifts. Figure 1 – 1 shows how polymer amended MFT dewatering behavior is different from the purpose of this study.

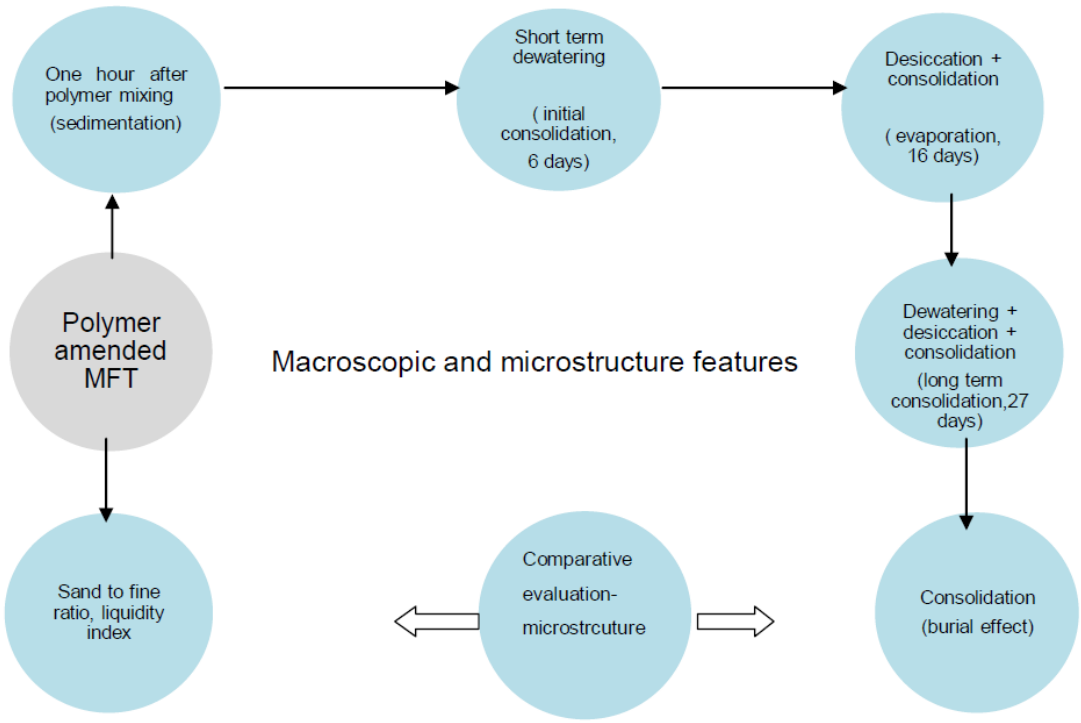

Figure 1-1: Scheme of specific objectives of the research program

1.4 Organization of thesis

Chapter 2: Literature review: The literature review provides a detailed description of Athabasca oil sands deposit (AOSD), oil sand tailings issues, tailings management perspectives, and fundamental engineering science on consolidation, desiccation, and microstructure of soils.

Chapter 3: The research study provides a detail description of the methods adopted to achieve the set objectives of the research program, as well as the procedure to prepare the polymer amended oil sands tailings

Chapters 4 through 9 document the individual studies developed to address Objectives 1 through 6

Chapter 10 analyses and synthesizes all microstructure data collected in the thesis

Chapter 11: Summarizes the research study, reports key finding, and presents recommendation for further research and tailings technology development

Versions of Chapters 4 and 7 were papers submitted to the Proceedings of GeoMontreal 2013 (Bajwa and Simms 2013) and ISSMGE 2013 (Bajwa and Simms 2013)

Chapter 2. Literature review

2.1 Athabasca oil sands deposit (AOSD)

The Athabasca oil sands deposit, Alberta, Canada (AOSD) is considered one of the world's largest unconventional reserves of crude bitumen and Athabasca River, Peace River and Cold Lake are parts of the deposit (Figure 2 – 1). The deposit is situated at latitude of 57° and longitude of -111°. It is 75 km north of Fort McMurray, Alberta, Canada (Hein et al. 2001) spreading over approximately 142,200 km^2, more than the area of New York State (USA) or twice the Province, New Brunswick, Canada.

It is estimated that the deposit contains about 1.7 to 2.5 trillion barrels of crude bitumen, out of which 300 billion barrels are recoverable. These reserves presume sufficient fulfilling the Canadians domestic oil need for next several centuries if extracted @ 2 million bbl. /cd. The volume of crude bitumen is absolutely comparable to the conventional reserves of Saudi Arabia (National Energy Board 2010; Government of Alberta, Canada, 2009; Morgenstern et al. 1995). Figure 2 - 2 highlights the world's proven oil reserves, production and their life.

It is presumed that the Albian Boreal Sea gave birth to Albian Sands about 100 million years ago as the Cretaceous generated from the Sea extended over the McMurray sands which deposited marine shale coverlet on the sandy floor (Hein

et al., 2001). The coverlet extracted the hydrocarbons of McMurray formation which consequently resulted in the formation of Albian sands

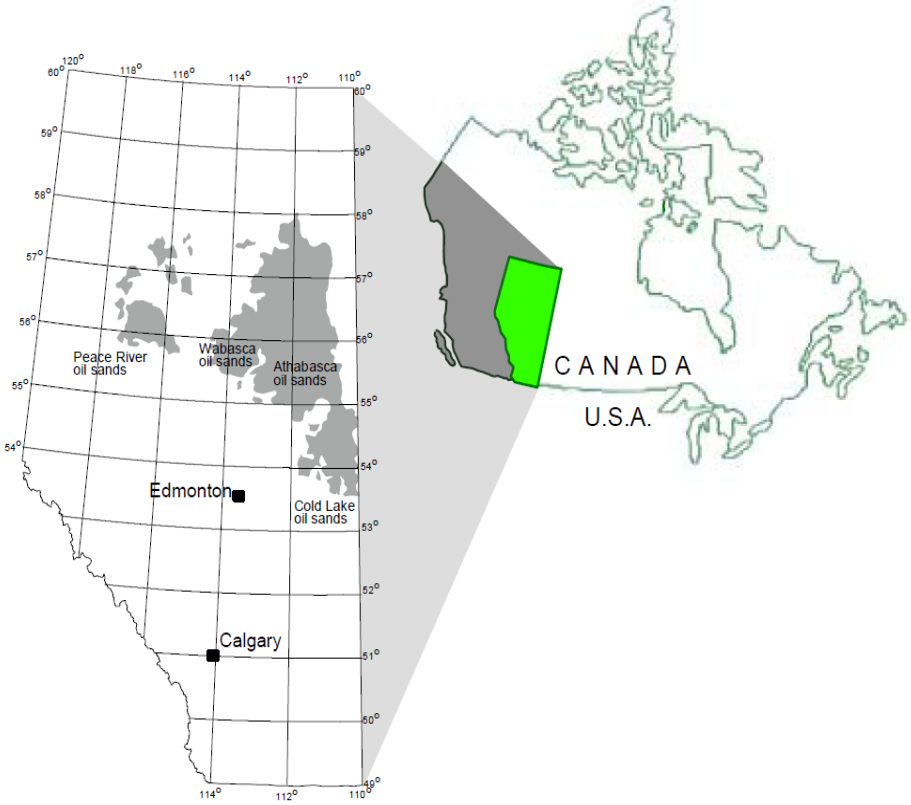

Figure 2-1: Location map of Athabasca oil sands deposit (Hein et al. 2001)

Figure 2 - 3 shows the stratigraphy of Athabasca oil sands deposit. The deposit generally comprises of quartz, silt, clay, water, bitumen and some minor amounts of minerals like titanium, zirconium, tourmaline and pyrite. The typical composition of deposit contains 75 to 80 percent inorganic material, 13 to 16 percent bitumen and 3 to 5 percent water (Morgenstern et al. 1995).

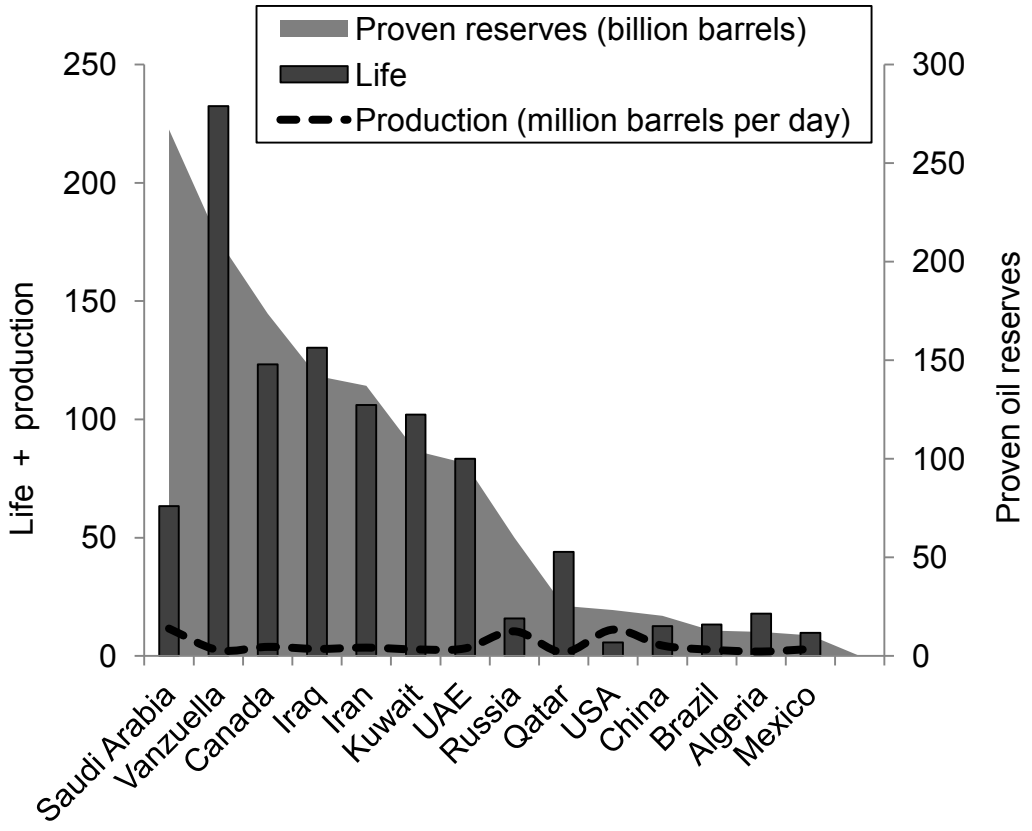

Figure 2-2: World's proven oil reserves (Bajwa 2013)

The major clay components of the McMurray formation include 40% - 70% kaolinite, 30% - 45% illite and 10% mixed layer illite/smectite (Beier and Sego 2008). The unique aspect of deposit is that an envelope or film of water about 10 nm thick surrounds the individual sand grains, which is further enclosed by bitumen film partially filled with voids (Zhu 2013). The underlying rock pore space upholds the bitumen in a similar fashion to that of conventional oil reserves. Caughill et al. (1993) stated that the pores space of Albian sands contained bitumen and associated gas, and the structural and geometric arrangement of

the Albian sands formation provided a lose bond between bitumen and sand grains which facilitated the bitumen extraction.

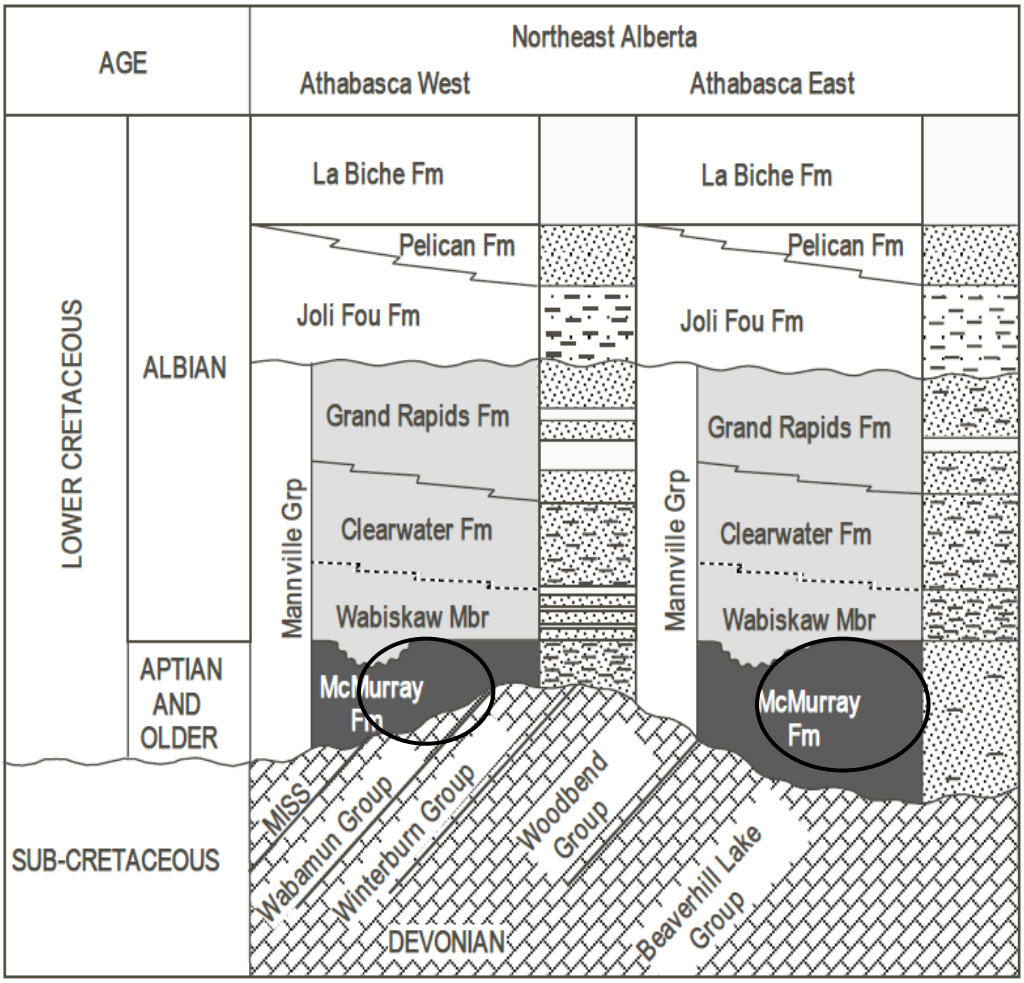

Figure 2-3: Stratigraphy of Fort McMurray area (Hein et al. 2001)

The oil sand operators follow two approaches to extract bitumen from the deposit such as ex-situ mining operation (surface mining) and in-situ extraction. The cost of ex-situ mining operation depends upon excavation, hydro transportation and energy extraction process where as the cost of in-situ mining

operations cost depend upon the followed approach, namely, cyclic steam stimulation (CSS) or steam assisted gravity drainage (SAGD).

The Athabasca oil sands deposit reserves are most commonly recoverable through surface mining operation (Government of Canada 2009). In this operation, one barrel of oil needs almost two tonnes of deposit to be processed, generating the proportion of waste materials to oil quite high. Subsequent to excavation, the oil sands are hydro-transported to the extraction plant *and* subsequent liberation of bitumen takes place using the Clark hot water process through the addition of hot water and caustic soda to the ore (Xu and Hamza 2003). Figure 2 - 4 shows the generic flow diagram of bitumen liberation using Clark hot water extraction process.

2.2 Production of oil sands mature fine tailings

The bitumen extraction from the oil sands mining operations results in the formation of two products such as an unwanted by-product - oil sands tailings and economically feasible product - crude oil. The crude oil contains a complex mixture of hydrocarbons- chains of carbon and hydrogen atoms and the typical composition contains approximately 84 percent carbon, 14 percent hydrogen, 1 to 3 percent sulphur and minor amounts of nitrogen, oxygen, metals and salt. The whole oil sands tailings are a heterogeneous mixture of clay, sand, fine silts, water, residual bitumen, salts, metals and organic compounds. The oil sands industry defines fines as mineral particles smaller than 44 μm.

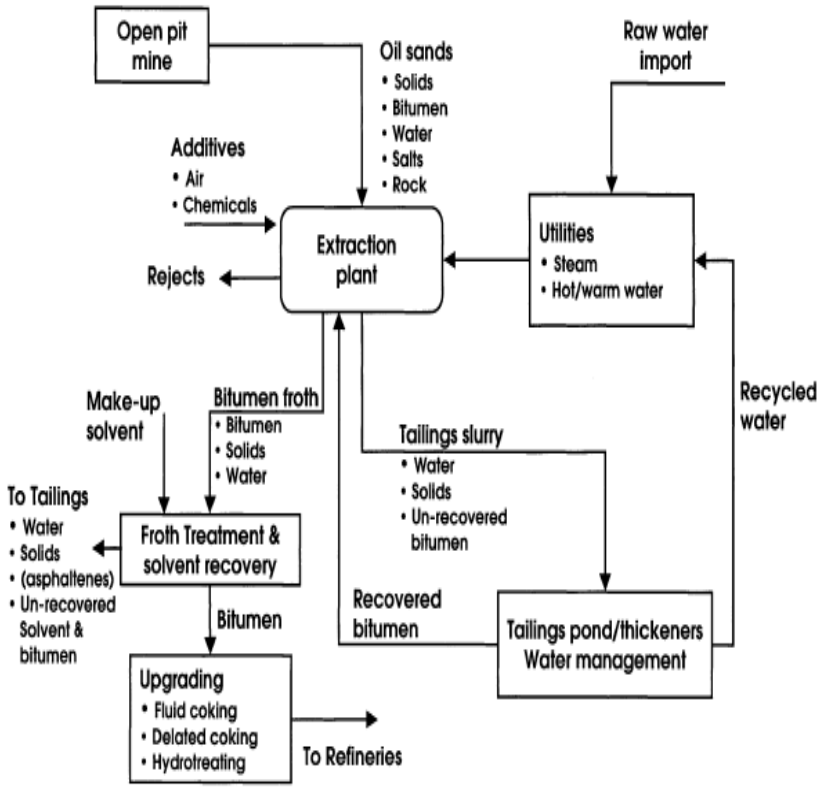

Figure 2-4: Scheme for oil sand processing using hot water extraction process (Masliya et al. 2004)

The whole tailings slurry consists of about 45% to 55% solids by mass (Jeeravipoolvarn 2010). Conventionally, the tailings are transported hydraulically to the tailings storage facilities (TSF). Upon deposition, the sand plus about one-half of the fines of whole tailings segregate dropping out to form dykes and beaches. The remaining water, bitumen, and fines flow into the tailings storage pond referred as thin fine tailings (TFT). These tailings at time of deposition contain only 7 ~ 8% solids content.

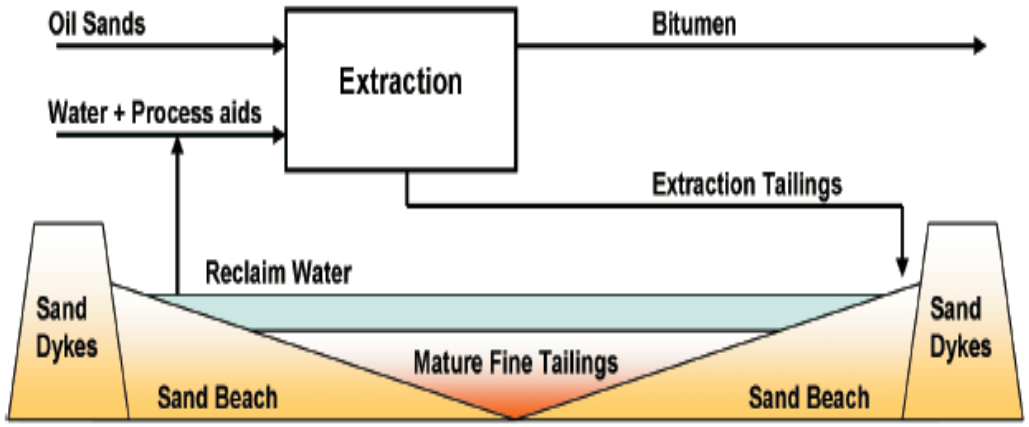

Figure 2-5: Conventional oil sands extraction and tailings disposal (Beier and Sego 2008)

After a few years of deposition, the coarse particles settle down forming a beach whereas the fine particles remain in suspension. After several years, the fine particle suspension reaches solids content of 30% - 40 %. These fine suspended particles remain in the same state for centuries, and are known as mature fine tailings (MFT). MFT remains in a fluid-like state for decades due to their very slow consolidation rate. MFT is problematic material due to its segregation nature, light weight behaviour, very low hydraulic conductivity and possibly due to development of pre-consolidation pressure through thixotropic development of a network particle structure (Scott et al. 2013, Jeeravipoolvarn 2005). Jeeravipoolvarn (2005) reported that MFT was only consolidated 3 meters by self-weight providing very little or no effective stresses when monitored in a standpipe of 10 m for more than 22 years and they showed an increase in percent solids from 30.6 to 40.6.

Despite the problem of MFT, almost 65% of the water used in the extraction process is recovered from tailings ponds and recycled in the extraction process. About 3 cubic metre of water per cubic metre of bitumen extracted is ensnared in mature fine tailings (BGC Engg. 2010 and Beier and Sego 2008).

In 2008, the tailing storage facilities (TSF) contained more than 830 million cubic metres of MFT, and the tailings ponds in Alberta covered about 77 km^2 (BGC Engg. 2010; Alberta Environment 1999). The volume of MFT may grow up to 1.2 billion cubic meters by 2030 and 1.3 billion cubic metres by 2060 in TSF, if bitumen is extracted at the same rate (Houlihan and Hale 2011). Figure 2 - 6 highlights the increasing trend of tailings in TSF from 1968 to 2060.

2.3 Oil sands mature fine tailings issues

The problems associated with the production of fine tailings include i-) land reclamation issue - MFT does not settle even after several decades of deposition due to its low weight aggregates and segregation behaviour, and ii-) environmental issue - the fine tailings may contain harmful contaminants, namely, naphthenic acids, polycyclic aromatic hydrocarbons, phenol compounds, ammonia, mercury and other trace metals (Rogers et al. 2002; Mackinnon et al. 2001; Nix and Martin 1992; Mackinnon and Boerger 1986).

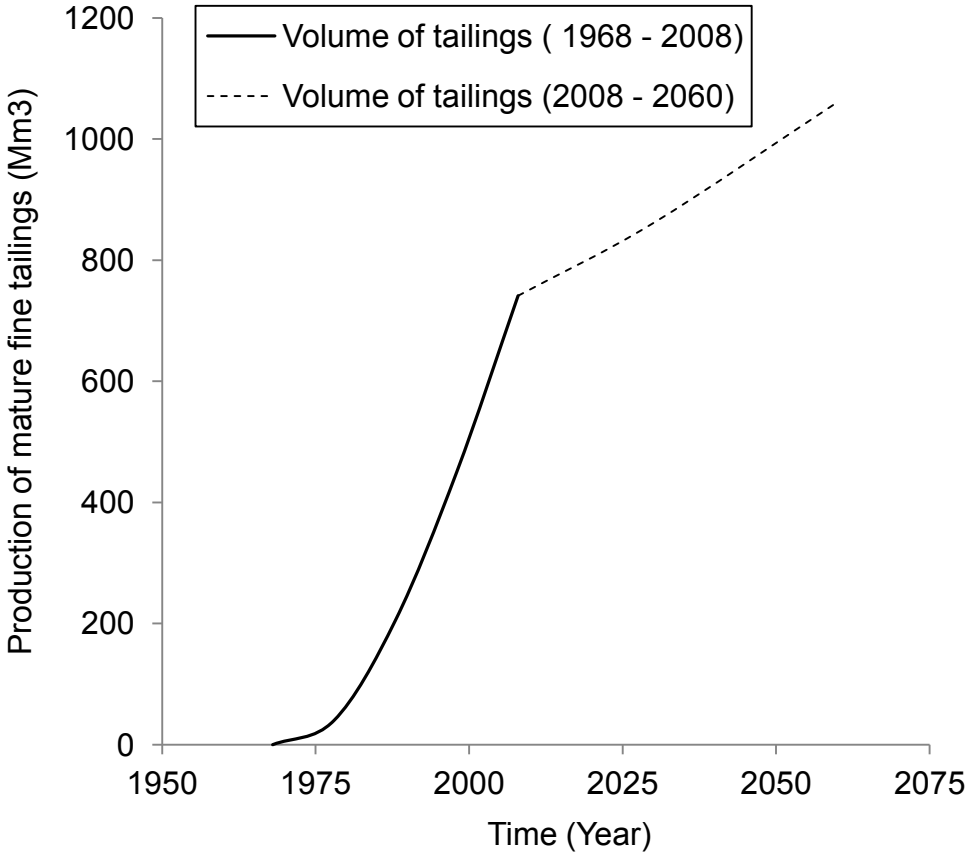

Figure 2-6: Expected trend of mature fine tailings generation (Houlihan et al. 2010)

The waters of oil sands tailing ponds may be acutely toxic to aquatic organisms and mammals. By some estimates, the TSFs leaked about 11 - 12.6 million of tailings each day which influenced the ground water quality (Price 2011 and Environment Defence 2008), however, the adverse impacts on ground water quality were not known to date and are still under investigation (Government of Canada 2009).

2.4 Management of oil sands mature fine tailings

The huge volume of oil sand tailings has emerged a critical issue for oil sands operators more than a decade. The Energy Resources Conversation Board (ERCB) Canada introduced a Directive 074 (2009) clarifying the criteria for safe handling of large volume of oil sands mature fine tailings. The Directive 074 compels the industry to adopt technology achieving undrained shear strength of 5 kPa after one year and 10 kPa after five years of tailings deposition. Though Directive 074 has been recently repealed (March 2015), newer policies still retain the 5 kPa criterion for what constitutes fluid fine tailings. In order to achieve guidelines as set out in Directive 074 (2009), the oil sands operators have accelerated development of alternative tailings disposal technologies. These include:

2.4.1 Composite or consolidated tailings (CT):

Composite or consolidated tailing (CT) is a tailings management process to expedite the settlement and consolidation behaviour of oil sands tailings. In this process, coarse sand and a chemical additive (coagulants) is mixed with fine tailings to transform their segregation nature to high density aggregates (Jeeravipoolvarn 2010).

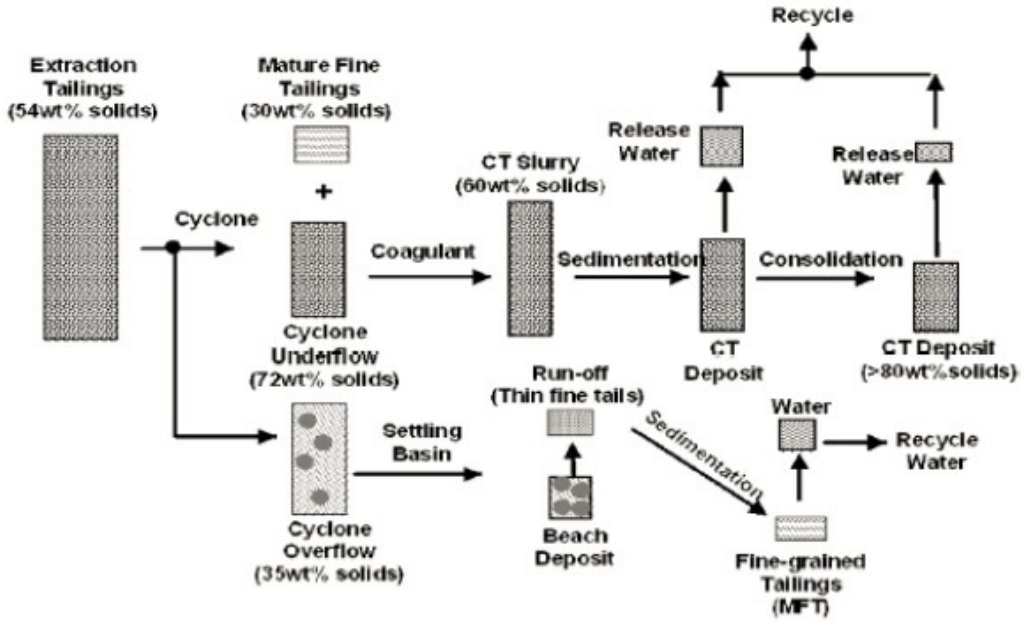

Figure 2-7: Schematic diagram of CT process (Jeeravipoolvarn 2010)

The addition of inorganic coagulants (such as calcium) results in the aggregation of fine suspended particles of tailings, which improves consolidation characteristics, while the addition of sands improves the strength at a given void ratio (Jeeravipoolvarn 2010). A schematic flow of CT process is shown in Figure 2 – 7. Suncor was the first operator to apply the CT process on commercial scale in 1995, followed by Syncrude conducting a field demonstration in the same year.

Hydrocyclones are used to isolate coarse and fine particles from the tailings stream prior to the CT process (Figure 2 – 7). The cyclone underflow (CUF) provides sands or coarse tailings and cyclone overflow (COF) is entrained with fine tailings. Cyclone underflow can be utilized for construction material and in the preparation of composite tailings (CT).

2.4.2 Centrifugation:

In this technique, the tailings are passed through vessels and a spinning action is utilized to induce dewatering through filters by centrifugal force. The use of a chemical additive improves the performance of the process. The process generated consolidated cake which minimized and eliminated the need of tailings containment in ponds (Xu and Dabrose 2011). Owolagba and Azam (2013) reported that the centrifugation process enhanced the solids content up to 60%, when tailings were tested at the pilot-scale. Syncrude is implementing centrifuge technology to dewater the fine tailings at the commercial scale.

2.4.3 Freeze-thaw:

In this technology, the CT or otherwise treated MFT are deposited in multiple thin layers allowing freezing and subsequent thawing of frozen mass takes place in the following summer. The freezing cycles consolidate the tailings forming peds that develops a fissured structure throughout the deposit. The tailings release water on thawing (Caldwell et al., 2014). Smaller lifts of tailings (5 – 15 cm) show the greatest degree of dewatering due to freeze-thaw (BGC Engg. 2010). MFT gets over-consolidated due to freeze thaw cycles taking place due to downward advancement of the freezing front in the deposit. The water movement within the vertical and horizontal ice lenses generates suction in the tailings developing a three dimensional interconnected ice network. During thaw, the ice develops a remnant fissure providing channels for the fluid to flow. The compacted

aggregated structure retains less water, which results in an increase in solids content. Proskin et al. (2010) stated that the freeze thaw and post thaw deposition of tailings resulted in an increase in the initial solids content from 30 to 55%.

2.4.4 In – line flocculation:

In in-line flocculation, MFT is combined with polymer in-line and discharged into a dedicated disposable area (DDA) to allow for drying and / or freeze-thaw. The polymer is mixed into the tailings in the pipe using turbulent flow. Figure 2 – 8 present in-line flocculation from the field batches of Shell, Canada. Mathews et al. (2011) reported that in-line mixing at the field scale increased the solids concentration form 30 - 35% to 45 - 55% within 24 hours after tailings deposition and 65% solids within two months in thin lifts (0.60 m). Wells et al. (2011) stated that very thin lifts (0.2 - 0.3 m) may give 80% solid concentration within 10 days. The studies showed that the polymer amended tailings deposited in thin lift provided a considerable gain in Cs over a very short period of time.

A thick lift may prove more beneficial than that of thin lift, while integrating the influence of natural processes like self weight consolidation and desiccation along with dewatering. The clay properties, tailings composition, flocculant selection and thickening procedure greatly influence the performance of both thin and thick lift tailings. To date, both Suncor and Shell, Canada are employing in-

line flocculation of MFT at the commercial scale. Suncor was the first operator to apply in-line flocculation at the commercial scale in 2004.

Figure 2-8: Example of in-line flocculation of MFT in the field (Mizani et al. 2013)

At least four mechanisms contribute to post-deposition dewatering strength gain of in-line flocculation i-) very short term water release (initial dewatering) takes place due to settling post deposition or sedimentation within hours, ii-) dewatering due to initial self weight consolidation and flocs formations in the short term (in a few weeks), iii-) strength gain by desiccation - the desiccation takes place at the surface of the tailings due to evaporation (natural process), iv-) consolidation - self weight consolidation (natural process) takes place throughout the depth of tailings when tailings are deposited in a single or when one layer of

tailings is buried over another layer, i.e., final stage of tailings. The following section reviews these different dewatering mechanisms.

2.5 Sedimentation induced by application of polymer

Particulate settling also known as a clarification region is defined as a condition when soil particles do not hinder each other (particles are far apart) and settle freely. This condition generally prevails in a mixture of very low solids content and the particles are far apart. During this stage, the heavier particles like sand settle quickly to the bottom of the basin whereas the fine particles such as clay and silt remain in suspensions with water and settle much slower rate. During this phase, the particle segregation or particle sorting takes place.

Sedimentation or hindered sedimentation commonly refers to the conditions of the soil particles when they settle together, en masse. The solids content of the soil solids increases due to the settling of the particles, and the mixture attain a zone in which the mixture transforms from suspension to a soil. The settling behaviour of soil mixture in this zone is not well defined and it can be either sedimentation or consolidation.

At the end of the hindered sedimentation, a condition prevails when grain to grain interactions are established and the effective stress is largely developed in the mixture. At this stage or in this type of settling, a typically clear interface exists between the top of the settling volume and supernatant fluid. The interface

generally moves down linearly with time during hindered sedimentation, resulting that the settling velocity is a unique function of solids dose. There is no development of effective stress in the zone of lower solids content during this stage. Motta et al. (2009) reported that the particle size, density and surface properties defined the tailings settling rate and the change in pH, salinity, and amount of flocculant influenced the above mentioned parameters.

Polymerization or flocculation is a technique that increases the dewatering and settling rate of fine suspended particles. It agglomerates the discrete, colloidal-sized particles providing chemical bondage to colloids (Rowe et al. 2004). Polymers or flocculants work on the principles of bridging developing bridges among individual particles of suspension.

Polymers are believed to promote flocculation by two mechanisms: bridging and charge neutralization. Bridging is a mechanism in which segments of a polymer chain adsorb on colloids and help particles to aggregate. Flocculants carry active groups with a charge to counterbalance the charge of particles (Suncor 2009). Charge neutralization takes place when a cationic flocculants or polymer is used, which reduces the net negative charge in tailings particles. Several processes occur within the suspension as a result of polymer addition that include transportation of polymer to the solid-liquid interface followed by adsorption of the polymer on the solid surface, rearrangement of adsorbed chains on the solid surface and collision among the particles (Rima 2014). Biggs et al. (2000)

reported that the polymer chemistry, polymer charge, particle surface area, polymer dose and the mixing regime influenced the bridging mechanism.

Li et al. (2014) reported that the flocculants bridged the fine particles providing large and rapid settling aggregates; furthermore the charge density and molecular weight influenced the performance of a polymer. Riley and Utting (2014) stated that the molecular distribution and specific functional group influenced the performance of polymer greatly. Figure 2 – 9 show the behaviour of colloids for an addition of flocculant.

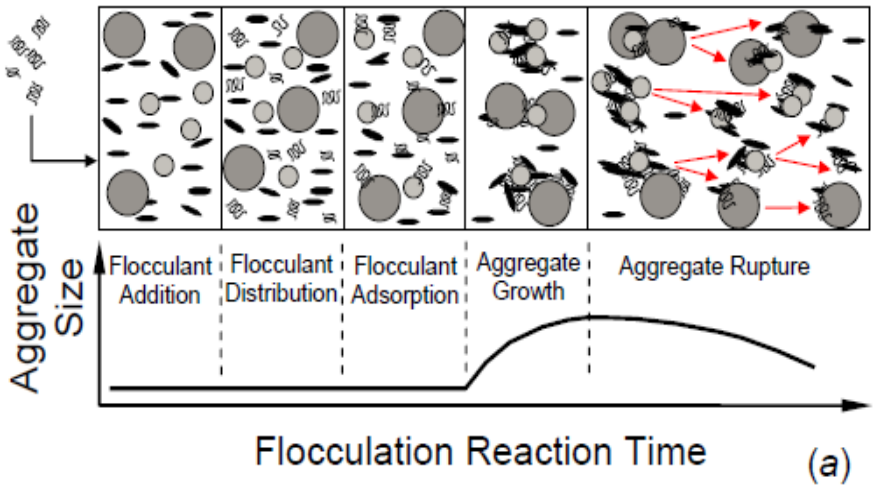

Figure 2-9: Behavior of colloids for an addition of flocculant (Jeeravipoolvarn 2010)

2.6 Evaporation and unsaturated flow

2.6.1 Evaporation

Evaporation is an important contributor to tailings dewatering in thin lift deposition and it may also improve the surface bearing capacity of thick deposits. Based on the water content availability in a medium, evaporation is categorized into three stages:, Stage I – the moisture availability may not limit the evaporation rate (maximum rate of evaporation) - this rate is often called potential evaporation (PE), and is a function of climatic parameters:, Stage II - the permeability at the soil surface decreases due to desaturation which results in an increase in the suction gradient exponentially to meet evaporative demand. The suction at the surface becomes sufficiently high (generally greater than 1 MPa) so as to reduce the relative humidity (RH) gradient between the soil pores and the atmosphere, which consequently results in the reduction of evaporation rate:, Stage III - the rate of evaporation eventually falls to a minimum level (Wilson et al. 1997).

Fisseha et al. (2010) studied evaporation in thickened hard rock tailings and emphasized the role of salt accumulation to suppress evaporation. Fujiyasu et al. (2000) described the roles of cracks in maintaining high evaporation rates in fine grained tailings. Innocent-Bernard (2013) showed that cracking maintained high evaporation rates in thickened oil sands tailings, despite the formation of a surface salt crust very early days after deposition.

Soleimani et al (2014) argued that cracks appeared essential pathways for dewatering in evaporation from field trials of in-line flocculated MFT. Rozina et al. (2015) showed that cracking increased evaporation rates in in-line flocculated MFT even temporarily above the potential rate.

2.6.2 Total, matric, and osmotic suction

Four components such as gravitational potential, matric potential, osmotic potential, and pressure potential define the total soil moisture potential (total suction) of a soil (Fredlund and Rahardjo 1993). Gravitational potential depends upon the gravitational field taking place due to position of water and the hydrostatic or pneumatic pressure induces pressure potential in the soil mass. Conversely to gravitational and pressure potential, the osmotic and matric suction greatly contribute to total soil suction (ψ).

As presented in Equation 2 - 1, total suction (ψ) is mainly a combination of two components, i.e., matric suction and osmotic suction (Fredlund and Rahardjo 1993)

$$\boldsymbol{\psi} = (\boldsymbol{u_a} - \boldsymbol{u_w}) + \boldsymbol{\pi} \qquad \textbf{Equation 2-1}$$

Ψ = total suction, $u_a - u_w$ = matric suction, and π = osmotic suction.

The change in soil suction generally occurs due to either one or both of these suction components. The concentration of dissolved ions defines the osmotic

suction in soils, so a change in salt concentration may affect the overall volume and shear strength of soil. The matric potential of a soil depends upon the water content and the soil-water characteristic curve (see next section). Negative pore-water pressures in soils are possible because of strong adsorptive short-range forces at the molecular level between water and mineral surfaces (reference), as well as the water-water cohesive forces that give rise to surface tension.

Osmotic suction can contribute significantly to total suction at the surface of oil sand tailings (Innocent–Bernard et al. 2014; Soleimani et al. 2014), which occurs due to accumulation of dissolved mass as it is transported to the surface by evaporation.

2.6.3 Soil water characteristic curve (SWCC) and shrinkage curve

The soil water characteristic curve (SWCC), also called the water retention curve (WRC) represents the moisture potential capability of a soil. A relationship between degree of saturation or water content and suction represents a typical water retention curve (WRC) of soil. The WRC provides a conceptual framework to understand the behavior of unsaturated soils (Barbour 1998). Figure 2 – 10 shows a typical soil water characteristic curve.

The air entry value or bubbling pressure, residual water content and degree of saturation are the key parameters of a typical water retention curve (WRC). At air entry value (AEV), the air starts entering the pores of the soil or drainage of the liquid from the soil pores begins. At the residual water content, the drainage of water from the soil pores becomes very small as the remaining water phase approaches discontinuity and the liquid permeability becomes extremely small. Further removal of water takes place under vapour migration.

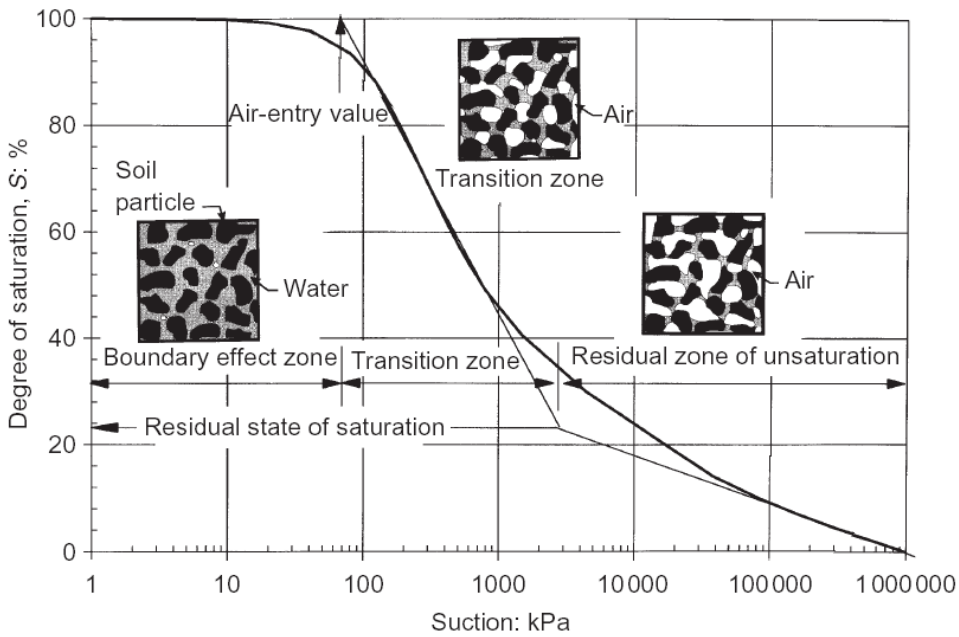

Figure 2-10: Typical soil water characteristics curve (Vanapalli et al. 1994)

Romero and Simms (2008) discussed that the capillarity and adsorption on particle surfaces at low suctions and clay inter layer at high suction influenced the water holding capability in clayey soils. The grain size distribution, plasticity and stress history were considered important factors influencing the behaviour of

water retention curve (Fredlund and Xing 1994). The matric suction varies with time depending upon the environmental changes and the most engineering problems related to unsaturated soils happen due to the environmental changes and the impact of osmotic suction is considered minimal in most practical applications. Figure 2 – 11 shows relationship between water content and void ratio (shrinkage curve) of a soil mass.

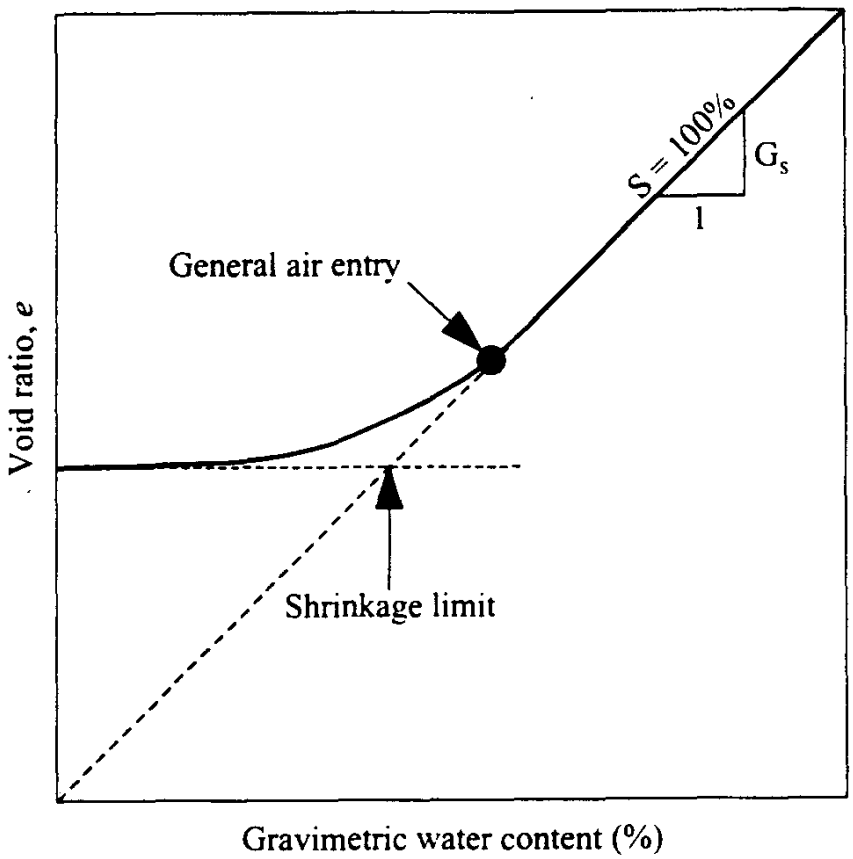

Figure 2-11: Volume mass relationship for the drying curve of an initially slurried soil specimen (Fredlund et al. 2002)

The shrinkage curve is another important property of unsaturated soils; which defines volume change as a soil dries out. While traditionally considered a unique relationship for a give soil, recent research has shown that the shrinkage curve may be affected by the initial water content and other condition for disturbed or artificial soils such as compacted clays and mine tailings. Heidarian (2012) showed that a larger initial void ratio resulted in higher air entry value (AEV) for MFT. Heidarian (2012) also found that adding polymer lowered the AEV as compared to the unamended MFT.

2.7 Consolidation in oil sands tailings

Consolidation phenomenon is a process by which soil undergoes substantial volume change due to change in effective stress. The soils gain effective stress during this process through a dissipation of excess pore pressure. Conversely to sedimentation, the effective stresses induced in the soil control the deformation of soil structure during consolidation. Jeeravipoolvarn (2010) argued on the basis of findings of Imai (1981); Sills (1998) and Bartholomeeusen (2003) that the boundary between sedimentation and consolidation was generally not predictable, as the void ratio at which the effective stress initiated is not uniquely defined, and varies with initial water content of the slurry. Figure 2 – 12 shows hydraulic void ratio relationships of various oil sands MFT.

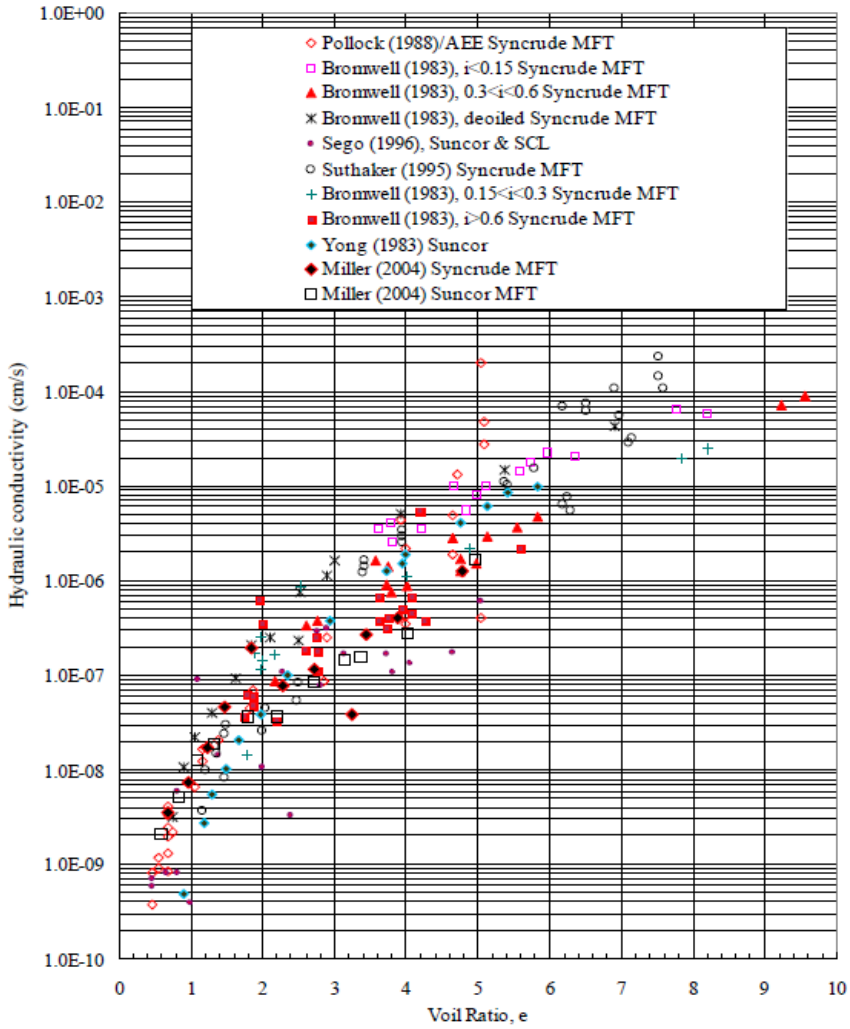

Figure 2-12: Hydraulic conductivity of oil sands MFT (Jeeravipoolvarn 2005)

Proskin et al. (2010) performed large strain consolidation test to examine the hydraulic conductivity, void ratio and microfabric of unamneded and polymer amended mature fine tailings of two Suncor lagoons. Figure 2 – 13 shows the test data of tested tailings.

The test results showed that both specimens provided separate compressibility curves despite that they were consolidated to same effective stress. The lower solids content exhibited higher compressibility, which resulted in less void ratio; despite that the initial void ratio was high.

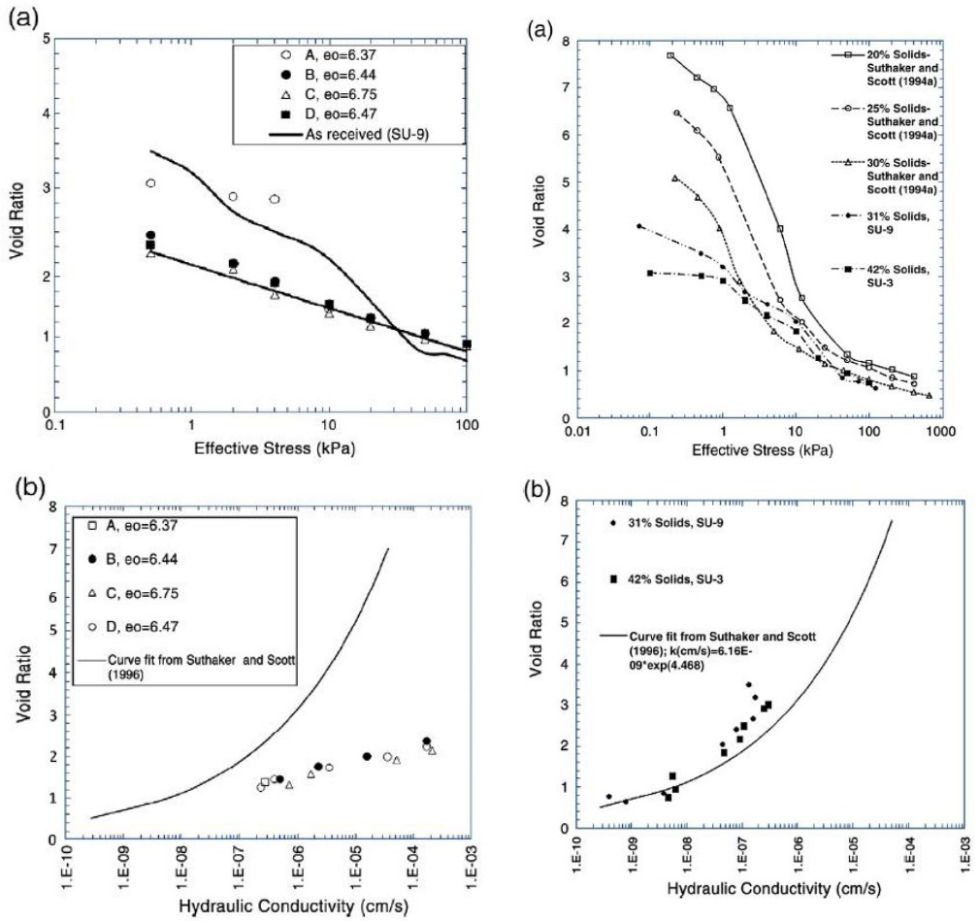

Figure 2-13: Consolidation test results, left: as received Suncor MFT, right: acid and quick lime amended freeze thaw MFT (Proskin et al. 2010).

Conversely, the higher solids content for lower initial void ratio provided lower compressibility. For an effective stress more than 10 kPa, both curves reached to a common line showing almost same void ratio. Similarly to void ratio, the hydraulic conductivity both unamneded and polymer amended freeze dried samples changed largely initially for each incremental stress level (Figure 2 – 13)

MFT and other oil sands fine tailings display considerable changes in compressibility and hydraulic conductivity with void ratio, and as such their deformation cannot be accurately predicted using classic Terzaghi small strain consolidation theory. The polymer amended MFT tailings exhibit similar behavior. Therefore, some form of large strain consolidation theory is used to analyze consolidation in these deposits.

For example, Jeeravipoolvarn (2010) developed a large strain consolidation model from the theory of Gibson, England and Hussey (1967) and successfully predicted both laboratory and field behavior of polymer amended cyclone over tailings. Jeeravipoolvarn (2009) analyzed the 10 m high columns of MFT allowed to settle over 30 years using a large strain consolidation model incorporating creep. Soleimani et al. (2014) incorporated large strain compressibility relationships into a coupled unsaturated flow – generalized consolidation software to predict dewatering of polymer amended MFT in the laboratory and in the field. Examples of compressibility and hydraulic conductivity relationships for polymer amended MFT (anionic polymer-Magnafloc 6260) generated by in-line

flocculation, and ATA (Anchor-Tether-Activator) amended tailings are shown in 2 -14 and 2- 15 respectively

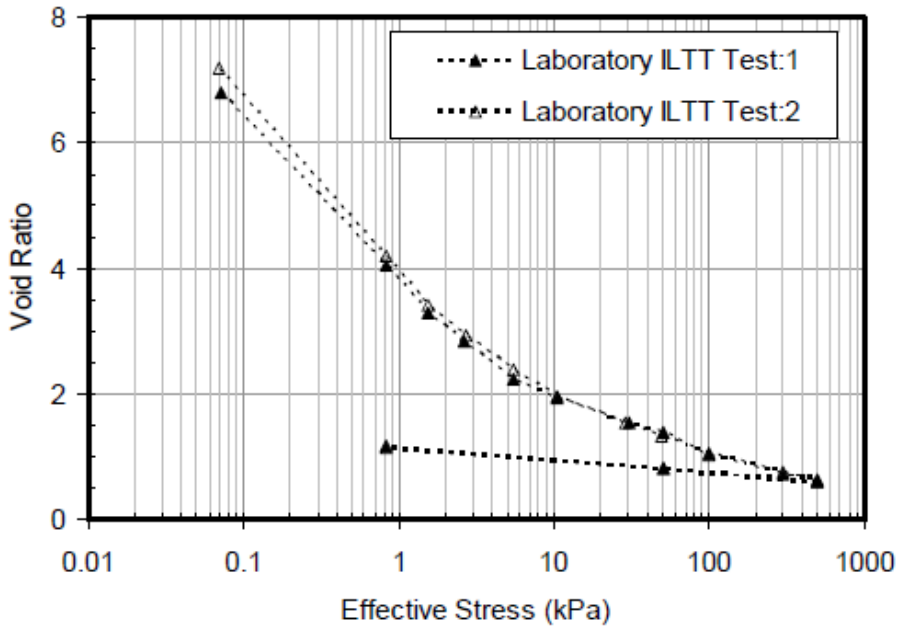

Figure 2-14: Compressibility of ILTT from large strain consolidation tests (Jeeravipoolvarn 2010)

2.8 Soil microstructure

The development on micromechanics theories in soil mechanics was started in 1970s and 1980s driven by the need to explain engineering behaviors such as basic characteristics of soils, the concepts of stress – strain relationships, consolidation, strength, hydraulic conductivity and soil suction. The microstructure defines the geometric, textural and structural configuration at various scales below the threshold of visibility by the naked eye (sub mm to nm). According to Mitchell and Soga (2005), fabric is defined as the particle and / or

pore space morphology in a soil whereas the structure refers to combined effects of fabric and inter particle forces. Soil is composed of a wide range of particles, but most fabric effects are associated with clays or clay size particles

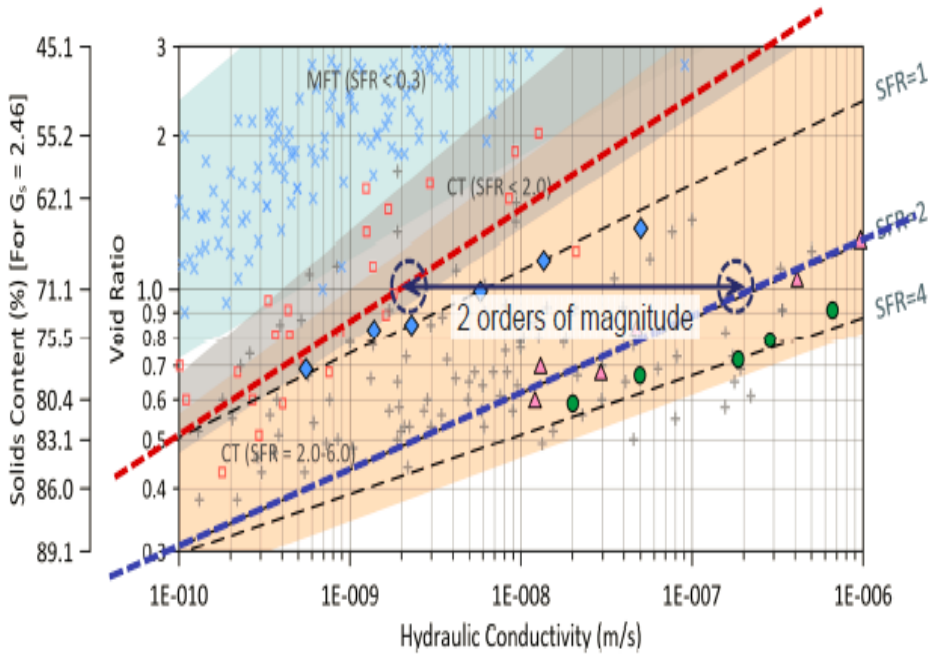

Figure 2-15: Compressibility of ATA tailings from consolidated undrained triaxial compression tests (Moore et al. 2014)

2.8.1 Clay structure

MFT generally consists of 80% kaolinite, 15% illite, 1.5% montmorrilonite, 1.5% chlorite and 2% mixed clay layers (FTFC, 1995). Kaolinite, Illite, and Montmorrilonite vary in their engineering behaviour primarily due to difference in inter-layer bonding: Kaolinite has very strong interlayer bonding and therefore has thicker particles and is less sensitive to changes in pore-water chemistry. Montmorrilonite has very weak interlayer bonding (only through molecular forces

due to the presence or interlayer cations), and consequently has thinner particles and is highly sensitive to changes in pore-water chemistry. Kaolinite typically shows little adsorption of water and its hydraulic conductivity is approximately > 10^{-09} m/sec in a pure sample. It has a cation exchange capacity (CEC) of 5 meq /100g. Individual particles are typically 100 x 100 x 50 nm size. The CEC of illite is 25 meq / 100 g and the typical particle thickness is 20 nm. The montmorrilonite generally contains particles of 100 x 100 x 10 nm size or less. It has larger potential for water adsorption and its CEC is 250 meq / 100 g. Chlorite is very stable and it is inactive mineral with CEC of 10 to 40 meq / 100 g.

2.8.2 Double layer theory

Oil sands MFT generally consists of fine clay particles. According to Kaminsky (2008), the clay particles produced highly negative electric charges in aqueous solution at neutral and high pH values. The charge variations at the interface and clay particles resulted in the formation of an electrical double layer (EDL) that affected the behaviour of soils.

A double layer comprises of stern and diffuse layers. The stern layer is composed of counter ions that are firmly attached to the colloid where as in the diffuse layer, the concentration of counter ion gradually decreases, and correspondingly the concentration of co-ions increases until a neutral charge is attained in the slurries. The combination of these two layers generates a double layer theory. The thickness of a double layer theory defines the flocculation

potential of particles. Mitchell and Soga (2005) stated that a thinner double layer provided higher flocculation of particles and the ionic valence and ions concentration influenced the double layer thickness.

2.8.3 Dispersion and Flocculation

Figure 2 – 16 shows the schematic of repulsive and attractive potential as a function of distance between particle surfaces.

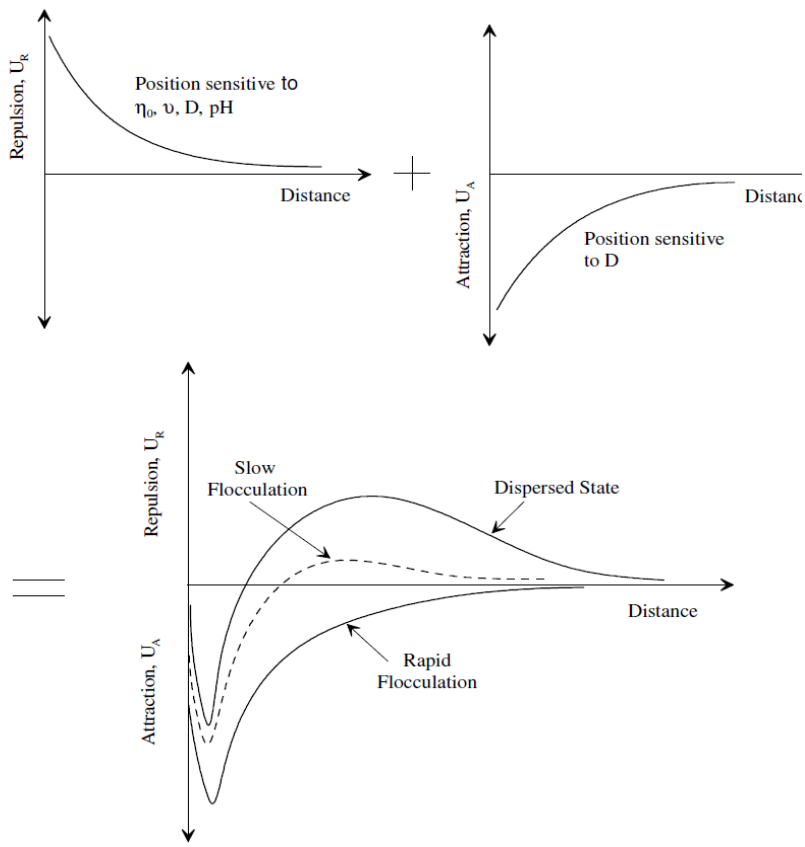

Figure 2-16: Schematic of repulsive and attractive potential as a function of distance between particle surfaces (Rima 2014)

Clay particles are negatively charged and the net negative charge is the primarily responsible to control clay dispersion. A reduction in the net negative charges overcomes the electrostatic repulsion allowing the particles come close to each other which results in flocculation.

The electrostatic repulsive forces (colloids of the same charge) and van der Walls attractive forces (colloids of the opposite charge) separate the charged colloids in a solution from each other, and the balance of these forces results in the dispersion and flocculation of the particles. The flocculation of the structure takes place when the attractive force dominates the repulsive force, so the net force behaves as an attraction and the particles are attracted to each other and a flocculated structure is formed. Conversely, the dispersion of the particles takes place if repulsive force exceeds the attractive force (Rima 2014; Jeeravipoolvarn 2005; Mitchell and Soga 2005)

2.8.4 Isomorphous substitution

Isomorphic substitution occurs on phyllosilicate clays. Cations are positively charged ions such as calcium (Ca^{2+}), magnesium (Mg^{2+}), and potassium (K^{+}) and aluminum (Al^{3+}) etc. The capacity of the soil upholding these cations is called the cation exchange capacity (CEC). The negatively charged clay in the soil hold these cations through electrostatic forces (negative soil particles attract the positive cations). The replacement of silica by aluminum in the clay minerals structure defines the isomorphous substitution, which develops negative surface

charge in clay particles. The soil as a whole does not have electric charge, the negative charge of the clay particles balances the positive charge of the cations in the soil. The negative charges associated with isomorphous substitution are considered permanent, that is, the charges do not change with pH changes, and it most commonly occurs in phyllosilicate minerals (Rima 2014; Mitchell and Soga 2005)

2.9 Imaging and quantification of soil microstructure

Microstructure techniques such as scanning electron microscopy (SEM), mercury intrusion porosimetry (MIP), micro computed tomography, optical microscope, and laser scanning microscope are being used successfully to examine the microstructure of geomaterials (Kochmanova and Tanaka 2010; Delage 2010; Romero and Simms 2008; Mitchell and Soga 2005; Nielson 2004).

X-ray computed tomography (CT) allows non-destructive imaging and it quantifies the internal features of a structure. According to Doan et al. (2012); Munkholem et al. (2012); Nielson (2004) and Pires et al. (2010), the μ computed tomography may visualize, isolate and quantify the resolved pore space of geomaterials. Motta et al. (2009) reported that NMR logging tools were used for quantitative observations of structure characteristics, e.g., permeability, porosity, and fluid saturation. Randall et al. (1997) discussed the probable use of spectroscopic and imaging modes of NMR to study the structural properties of soil. N_2 adsorption/desorption isotherms is also a quantitative technique to

characterize the variations in pore size distribution taking place due to chemo - hydraulic paths (Romero and Simms 2008).

Romero and Simms 2008) used scanning electron microscopy (SEM) technique to examine the changes taken place in unsaturated materials at aggregate and aggregate assembly scale. Delage et al. (2006); Simms and Yanful (2004); Griffith and Joshi (1989) used mercury intrusion porosimetry to characterize the pores size distribution of various soils. Scanning electron microscopy (SEM) and mercury intrusion porosimetry (MIP) techniques were used in this study for qualitative and quantitative measurements of oil sands mature fine tailings. Few samples were also tested with nuclear magnetic resonance to examine the microstructure but the soft and wet samples of tailings collapsed while inserting in NMR tube. NMR works on the principles that it detects protons in samples and the addition of water further enhances the chance of collapsing the tailings's structure. Weeman (1997) found that the application of NMR was quite limited in the field of soil science due to non homogeneous physical and chemical structure of soils. Both SEM and MIP techniques were chosen to quantify microstructure due to their relatively common usage and relative cost effectiveness.

2.9.1 Mercury intrusion porosimetry (MIP)

Mercury intrusion porosimetry (MIP) is an analytical approach defining the quantifiable aspects of porous geomaterials, e.g. pore size distribution, total pore volume or porosity, specific surface area and bulk density. Zhou et al. (2010)

stated that the pore size distributions provided the reliable data sets. Mercury intrusion porosimetry (MIP) was effectively used to differentiate the pore size distribution of porous materials and the approach worked efficiently for the pores size between 0.003 and 360 μm (ASTM 4404 -10; Romero and Simms 2008; Gieshe 2006).

Various studies in the literature were reported showing the successful use of MIP to characterize the pores size and volume of porous geomaterials. Lee et al. (2014) used MIP to examine the PSD of fly ash treated gold tailings. Simms and Yanful (2004, 2001) also applied MIP to investigate the volume change behaviour of Halton till and glacial till. Griffiths and Joshi (1989) employed MIP to characterize PSD of four different soils. Some other studies (Delage 2010; Delage et al. 2006) were also reported in the literature those employed MIP to study the microstructure of various soils. MIP data may provide strong correlations to permeability, consolidation characteristics, and water-retention behaviour (Romero and Simms 2008; Simms and Yanful 2005, 2004).

Though MIP is being used on extensive scale in various fields relating to geomaterials but the review still shows minimal use of this technology in oil sands industry. In this study, MIP was extensively used to examine the pore size distribution of oil sands mature fine tailings. MIP was also necessarily performed on dehydrated samples.

A pore-size distribution is obtained by intruding mercury into a dehydrated soil specimen under increasing pressures. The pressure applied to the mercury can be correlated to the smallest possible pore size at that pressure. The applied pressure is inversely proportional to the size of pores intruded. For a cylindrical pore model, Washburn equation provides relationship between pore size and applied pressure (ASTM D 4404 – 10).

$$d = \frac{-4\gamma cos\theta}{P_{abs}} \qquad \textbf{Equation 2-2}$$

In Equation 2 - 4, ɣ = surface tension of the mercury and its value is generally taken as 0.484 N/m at 25 ^{0}C, Θ = contact angle between mercury and pore wall and its value varies from 139° to 147°, d = entrance or pore throat diameter P_{abs} = P_G – P_L, P_L = absolute pressure causing intrusion, P_G = pressure of gas

2.9.2 Limitations of MIP

The main limitations of MIP include: i-) MIP does not measure pores surrounded by interconnected solids, ii-) constricted porosity is not detectable, iii-) unable to enter the smallest pores (non intruded porosity), iv-) limitations with the practical applications of minimum pressure – porosity is not detectable (ASTM D4404 - 10).

Zhou et al. (2010) stated that if the structure of the specimen is not uniformly distributed, mercury will not intrude into the large pores through smaller throat,

despite the pressure is sufficient to force the mercury to intrude into the smaller throat. In this case, the volume of large throat is considered as the volume of smaller throat and the phenomenon is known as accessibility effect. The ink bottle effect and accessibility effect may influence the credibility of test data in soils.

MIP demands pre-conditioning of the specimen and the ideal preconditioning of sample includes the drying procedure such as freeze drying to remove all the foreign liquids from the pores of the samples (ASTM D4404 -10; Romero and Simms 2008), without inducing suction and associated volume change in the process. Freeze thawing, oven drying, air drying and critical point drying are the techniques used to dry the sample (Romero and Simms 2008)

2.9.3 Scanning electron microscopy (SEM) tests

Scanning electron microscopy (SEM) is a microstructure technique used to study the structural arrangement of partially saturated geomaterials. Various findings in the literature are available which report successful use of this technique in various fields of applications. Monroy et al. (2009) used SEM in combination with MIP to examine the qualitative and quantitative measurements of compacted London clay. Zbik et al. (2008) examined the qualitative measurements of flocculated tailings for dewatering potential using scanning electron micrographs. Negre et al. (2004) differentiated the qualitative and quantitative measurements of soil colloids using SEM.

Findings such as Asmussen (2014); Desbois et al. (2012); Du et al. (2010); Zbik et al. (2009); Mitchell and Soga (2005 and Makula and Manuz (2000) were also reported in the literatures those employed SEM techniques to evaluate the microstructure of various porous medium. Some other studies Yilmaz et al. (2011); Delage (2010); Delage et al. (2006); Jeeravipoolvarn (2005); Simms and Yanful (2005, 2004) and Griffith and Joshi (1989) reported to use SEM for qualitative and quantities measurements of some other materials such as oil sands tailings, glacial till, compacted silt, and cement paste backfill etc. for change in macroscopic behaviour.

In SEM, a beam of electrons is directed towards a sample under vacuum. The electron gun releases a beam of electron, which hits the sample; secondary electrons are generated from the samples. Backscattered electron detectors (BSE) and gaseous secondary electron detectors (GSED) detect these electrons and generate an image. Danilatos (1993) explained that BSED often gives better quality images in comparison to GSED. Photoelectrons can be considered an example of secondary electrons and diffuse reflections of waves, particles and signals are the examples of backscattered electron. As in secondary electron detector, the emitted secondary electron strikes with the water molecules due to the existence of water vapour inside the microscope chamber that generates positive ions. This phenomenon causes overcharging of the sample that affects the quality of the secondary electron images.

A vacuum inside the chamber assures an effective operation of the electron gun; however, it may cause overcharging of the sample influencing the quality of an image. SEM device is facilitated to adjust the vacuum for wide range. It has the potential to establish the difference in pressure with progressive reduction in pressure and it works under controlled environmental conditions eliminating the need of conductive coatings to the samples. Under low vacuum, SEM can examine the microstructure of geomaterials preserving their fully hydrated and chemically unconfined (original) state., though low vacuum sacrifices resolution. SEM is most often performed using dehydrated samples in order to coat the surface with conductive material (such as gold) and so as to establish a vacuum that minimizes scattering of the electron beam aimed at the sample.

However, dehydrating samples in an uncontrolled manner will induce matric suction on the material and alter the microstructure, and also possibly inducing changes due to interlayer collapse of certain clays. Therefore, sample preparation techniques were developed that attempted to rapidly dehydrate the samples, such as critical point drying (Romero and Simms 2008), and freeze-drying followed by sublimation (Ahmed et al. 1974). The second technique was employed in this thesis. Delage et al. (1996) showed that important difference between these two procedures at both microscopic and macroscopic levels such as superficial fissuration with direct immersion, and a change was also observed in the volume and the PSD curves. ESEM or low vacuum SEM, by contrast, does not require sample dehydration. The sample is placed in a small chamber that is not under vacuum, so as to minimize the distance the electron beam has

to travel where air is present. Scattering does result, but various practical innovations have been applied to ESEM devices to minimize scattering. Nevertheless, resolution is limited for ESEM compared to SEM. Some results on clay sand mixture using ESEM include Viola et al. (2005) as discussed in Romero and Simms (2008) and ours are shown in Figure 2 – 17. The advantages in being able to see the effect of progressive dehydration on soil samples is clear, despite the relatively low resolution in these samples.

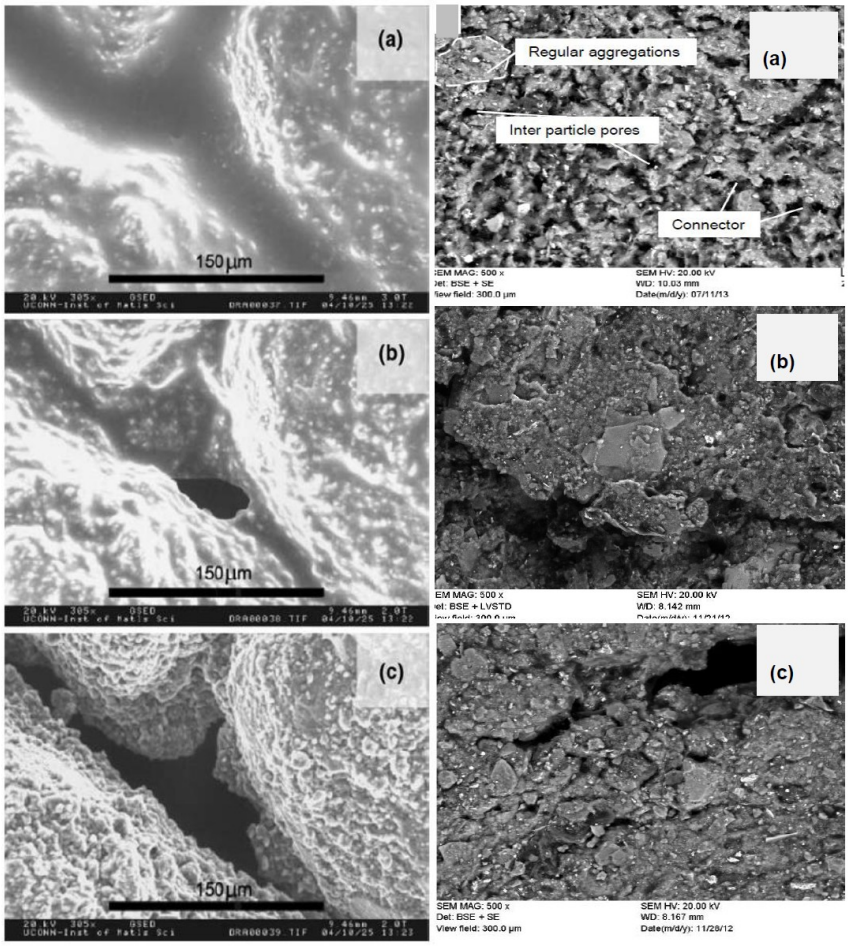

Figure 2-17: ESEM images (Left – clay sand mixture, Right – polymer amended oil sands tailings

2.9.4 SEM / CT investigation on oil sands tailings

Jeeravipoolvarn (2005) reported SEM test results performed by Tang et al. (1997) examining the effects of bicarbonate, NaOH, organic matter, sodium naphthenate, gypsum, and processing temperature on the fabric of MFT.

Kaminsky (2008) compared SEM data sets of oil sands tailings solids content with three other types of solids content and discussed that various solids content phases were unable to provide any major difference in area fraction while analyzed for phase fraction; however, mottled particles were far more common in other solids rather than tailings solids content.

Fard (2011) conducted ESEM tests to study the unamended oil sands ores and concluded that the water layer of oil sands ores contained very fine clay particles which were also attached to the sand grains and inside the bitumen phase. The results contradicted the results of old model of Camp (1976), which considered that the clays were only in a water film of the oil sands ores. Jeeravipoolvarn (2005) examined the fabric of oil sands MFT performing SEM tests with samples collected from 10 m stand pipe, and concluded that the MFT showed card-house floc structure, and the structure appeared more compressed at the bottom

Jeeravipoolvarn (2010) reported a comparative evaluation of micro structure of CT (23% solids content) and ILTT (24% solids content), and stated that the SEM micrographs of both tailings showed several large booklets of clay platelets with

the majority of the isolated clay plates. Based on the mode of particle association, the CT provided mild edge-to-face flocculated and dispersed whereas edge-to-face and edge-to-edge flocculated and aggregated patterns dominated the ILTT.

The CT tailings provided larger pores space with an average spacing of 5.5 μm, however in-line thickened tailings, the pore space was smaller and it was about 3.5 μm. Furthermore, Jeeravipoolvarn (2010) discussed the SEM images of both CT and ILTT for solids content of around 70% (void ratio of about 1) when consolidated to a stress level of 500 kPa. The consolidated SEM micrographs of both tailings looked quite similar showing random and packed clay structures, and there were no signs of parallel cardhouse structure in higher solids content of CT as noted in the CT of lower solids content.

The microstructure clearly defines the structural units of a porous medium, however, the arrangement of these units in a macroscopic scale is not so well understood for oil sands mature fine tailings and the data is quite limited in this scenarios. The volume of oil sands tailings changes due to change in polymer dose, dewatering, desiccation and consolidation which influences the overall characteristics of tailings. The volume change behaviour affects the geo- physical and performance properties, i.e., hydraulic properties, macroporosity, rheological properties and mechanical properties and the performance properties/macroscopic properties are dependent upon the microstructure arrangement of oil sands fine tailings.

2.10 Conclusions

The typical composition of AOSD consists of 75 ~ 79% inorganic constituents, 13 ~ 16% bitumen and 3 ~ 5% water

The oil sands operators follow surface mining and insitu mining operations for the extraction of bitumen from oil sands deposit.

The production of bitumen from tar sand resulted in the formation of oil sands tailings and until 2008, the TMF contained about 830 Mm^3 volumes of fine tailings. The oil industry followed various approaches such as centrifuge, composite tailing (CT), freeze drying and inline thickening etc. for the management of oil sands mature fine tailings. Many of these technologies employed a polymer at some stage; however, the research in the oil sands tailings is still in the trial stage.

The desiccation, consolidation and dewatering post deposition behaviour were considered essentially important to accelerate the settlement behaviour of in- line thickened oil sands fine tailings, however, the polymer selection, environmental conditions and tailings layout may greatly influence the performance of these mechanisms. Examination of the microstructure of clay sand mixture was reported as an example.

Chapter 3. Methods used and materials preparation

3.1 General

The specific objectives of this chapter are:

- to discuss methods followed to evaluate the macroscopic features
- to discuss methods followed to characterize tailings fabric
- to discuss materials and procedure used in the preparation of polymer amended fine tailings

3.2 Macroscopic features of oil sands fine tailings

3.2.1 Specific gravity

Specific gravity of soil is defined as the ratio of mass of particles to the mass of an equivalent volume of water. Sand has higher specific gravity where as organic matter shows lower specific gravity. The specific gravity of most of geomaterials varies from 1 to 5 (Onuaguluchi and Eren 2013; Kuyucak et al. 2010; Jeeravipoolvarn 2010 and McCarthy 2004), though for soils commonly encountered in geotechnical practice (inorganic materials of natural genesis) the range is usually restricted between 2.6 and 2.7. For oil sands tailings, determination of specific gravity is somewhat controversial due to the effect of attached residual bitumen on the solids phase (COSIA 2014). The Athabasca

bitumen shows a specific gravity of about 1.03 (Alberta Innovates 2012; Jeeravipoolvarn 2005).

Specific gravity of both polymer amended MFT and unamended MFT was estimated following the guidelines as discussed in standard ASTM D 854 – 10. The standard reported two methods for deairing a sample, i-) vacuum method and ii-) boiling method, while determining the specific gravity of soils. Jeeravipoolvarn (2005) reported that the boiling method demanded special attention due to the floating of bitumen within the existing specific gravity jar, so the vacuum method was employed to examine the specific gravity of both unamended and polymer amended oil sands fine tailings.

Two issues were noted while performing specific gravity tests of fine tailing. MFT provided considerable quantity of entrapped air, which required sufficient time to remove the entrapped air. Also, bitumen floated on top of the distilled water disguising the Pycnometer mark.

3.2.2 Grain size distribution

The studies such as Fall et al. (2010) and Jeeravipoolvarn (2010) employed sieve analysis and hydrometric analysis to characterize the grain size distribution of treated oil sands tailings. Koyukuk et al. (2010) employed Fritisch laser particle analyzer in combination with sieve analysis for the gradation of uranium tailings. Marques et al. (2010) and Fourie and Gawu (2010) reported grain size

distribution of slurry type materials but the adopted methods were not reported in the studies.

In oil sands industry, SFR is defined as the ratio of particles over to under 44 microns. The coarse fraction (coarse silt and sand - nominally > 44 μ m) of oil sands tailings settled down and the finer fraction (predominately < 44 μm silt and clays - mainly illite and kaolinite) flown as a suspension to a quiescent settling area (BGC Engg. 2010).

As with specific gravity, the determination of distribution of fines in MFT is controversial, or at least known to be sensitive to the method (laser versus hydrometer, type of dispersant). This topic is the subject of investigation of working group commissioned by COSIA (2014).

The grain size distribution of both unamended MFT and polymer amended MFT was determined to classify the sand to fine ratio (SFR), and the procedure as discussed in standard ASTM D 422 – 63 (2007) was followed. The tests were performed with and without dispersion agent, i.e., sodium hexametaphosphate**.** It was common practice to use air dried sample for grain size distribution tests, so MFT was placed in open and wide pan for drying. After drying, the unamended MFT showed a hard and sticky nature, not easily breakable with hands. The tailings were then preserved at a certain water content to eliminate the need of crushing that might disturb the original SFR. The size of sample was estimated on a dry mass basis of the preserved wet samples.

3.2.3 Index properties

The liquid limit (LL) and plastic limit (PL) of both unamended and polymer amended MFT was determined to classify the consistency of oil sands tailings. It is the most common practice to use the standard Casagrande device to determine the liquid limit of a soil. However, few studies such as Koumoto and Houlsby (2001) and Keedwell (1984) preferred to use fall cone method for the determination of liquid limit of slurry type materials.

Based on this argument, the fall cone method was preferred to examine the liquid limit of oil sands fine tailings. In this test, a soil paste (about 80 grams) was placed in a small container and the cone was held with the point in contact with the paste surface. The cone was then released for 5 ± 1 seconds and the penetration of the cone in the slurry paste was measured. The liquid limit of tailings was the water content corresponding to a penetration of 20 mm. Koumoto and Houlsby (2001) discussed the theory and practice of fall cone test in detail.

The plastic limit of tailings was examined to identify the demarcation boundary between the liquid and semi - solid states, and the procedure as outlined in standard ASTM D 4318 – 10 was used to perform PL tests. The LL and PL were then used to define the liquidity index (LI) and plasticity index (PI). The shrinkage (SL) of tailings was evaluated monitoring volume change behaviour of tailings during various drying tests.

3.2.4 Organic and inorganic contents

The organic and inorganic contents of unamended and polymer amended MFT were determined following the procedure as outlined in standard ASTM D 2974 – 07 (a). The standard discussed the two steps procedure to determine the water content rather different to the routine water content determination.

First, the sample was dried at room temperature and then the particular sample was placed in oven at a temperature of 105 ^{0}C to determine the water content. After estimating the water content, the sample was ignited in a muffle furnace at a temperature of 440 ^{0}C to characterize the organic and inorganic content. At 440 ^{o}C, the organic content of the sample was ignited and the left over materials (residue) was the ash i.e., the inorganic content of the sample. The inorganic contents of the sample were estimated as a percentage of the total mass of the oven dried sample after ignition. The organic contents of the sample were determined subtracting the percent inorganic content from one hundred.

3.2.5 Pore water chemistry

Pore water obtained by either bleed water or centrifuging of solids samples was collected and sent to commercial laboratories for pore water chemistry one hour after polymer mixing.

3.2.6 Hydraulic conductivity

Falling head test method was followed to determine the hydraulic conductivity of oil sands MFT during earlier stage of deposition, essentially as an index test, as the permeability varied considerably with void ratio. The initial hydraulic gradient was set constant to assure similar conditions for all tailings. Equation 3-1 shows the mathematical expression of Darcy's law for falling head test.

$$\boldsymbol{k} = \frac{\boldsymbol{a L_f}}{\boldsymbol{A_t}} \mathbf{ln} \left(\frac{\mathbf{H_1}}{\mathbf{H_2}}\right) \qquad \textbf{Equation 3-1}$$

A = area of specimen, a = x-sectional area of falling head reservoir, L_f = length of specimen, H_1 and H_2 are the heads after time t_1 and time t_2.

3.2.7 Suction

A Decagon WP 4 Dewpoint Potentiameter was used to examine the total suction of oil sands tailings. The Potentiameter estimates the total suction of geomaterials equilibrating the relative humidity of the sample and the device chamber. Total suction measurements use chilled mirror hygrometer (Wenglor WP4 Potentiameter). Such hygrometers measure the vapour pressure in porous media by decreasing the temperature in a confined space with the sample, until water condenses on a mirror.

Thus the saturated vapour pressure at this controlled temperature is known, which equal to the vapour pressure at the ambient temperature of the sample. The relative humidity is equated to total suction, based on the well-known Kelvin-Laplace equation. The range of this device is theoretically from 0 up to 500 MPa of total suction, but precision is limited to ±0.1 MPa. Samples were generated in different developed experimental scheme to perform total suction tests.

The osmotic suction of tailings was determined from electrical conductivity measurements. To carry out EC tests, the procedure as discussed in Dunmola and Simms (2010) was followed. The study reported using 1: 5 tailings slurry (tailings: deionised water) to estimate the electrical conductivity of tailings. The mixture of tailings and deionized water was thoroughly mixed using an electrical shaker and after then the solution was centrifuged at 3000 rpm for 2.5 minutes.

A traceable conductivity meter (VWR International, Friendswood, TX) was used to perform EC tests. The device automatically availed the temperature changes during the experimentation. The saturation extraction procedure was then employed to transform the electrical conductivity of pore water to osmotic suction which corresponded to natural water content of tailings. Peroni and Tarantino (2005) reported an empirical equation to estimate the osmotic suction form electrical conductivity (Equation 3 – 2).

$$\boldsymbol{\pi = 0.0191EC^{1.074}} \qquad \textbf{Equation 3-2}$$

π = Osmotic suction (kPa), EC = electrical conductivity (μS/cm)

Abedi - Koupai and Mehdizadeh (2007) reported another relationship (Equation 3 - 3) for the determination of osmotic suction from the electrical conductivity.

$$\boldsymbol{\psi_{os}} = -36EC_e \qquad \textbf{Equation 3-3}$$

ψ_{os} = osmotic suction (j / kg) and EC_e (dS / m)

3.2.8 Yield stress

Various findings like Boger (2013, 2006); Mizani and Simms (2010); Pashias et al. (1996) and Nguyen and Boger (1992) were reported in the literature, those employed cylindrical slump to determine the yield stress of slurry type suspended materials. A paste like material was placed in a cylindrical container - opened from both ends. The column was then lifted gently and the deformed specimen height corresponding to original cylinder was reported as measured slump (Pashias et al. 1996).

In this study, the cylindrical slump tests of oil sands fine tailings were performed with various polymer doses and aspect ratio. Pashias et al. (1996) reported Equation 3 - 4 to determine the yield stress of slurry type materials from cylindrical slump tests.

$$\tau'_y = \frac{1}{2} - \frac{1}{2}\sqrt{S'} \qquad \textbf{Equation 3-4}$$

τ'_y = yield stress dimensionalized for ρgH, S' = measured slump dimensionalized for H, H = depth of cylinder, ρ = density of suspension, g = acceleration due to gravity.

The procedure as discussed in Pashias et al. (1996) was followed to conduct the slump tests for both unamended and polymer amended oil sands fine tailings.

3.2.9 Undrained shear strength

A vane shear device was employed to determine the undrained shear strength of thickened oil sands fine tailings. A shear vane was consisted of four thin steel plates of equal sizes welded orthogonally to a steel rod. The vane was pushed into the materials at the specified depth and the torque was applied at the top of the torque rod. The vane was rotated until the tailings failed in shear. In all tests, the vane blade was inserted into the soil to a depth at least twice the length of the vane blade which ensured shearing on the vertical edges of the vane blade, and also minimized disturbance of the adjoining soil surface. The guidelines as discussed in standard ASTM D 2573 - 08 was followed to perform the vane shear tests of polymer amended oil sands tailings.

3.2.10 Consolidation tests

For soft fine grained materials such as MFT, specialized tests are commonly used to estimate the large strain consolidation properties. Self-weight column devices are developed to impersonate sedimentation and very low stress consolidation of high water content materials, however because of use of only gravity driven stresses, the experiment durations may be extremely long. The constant rate of strain (CRS) devices examines the stress state of the specimen throughout the consolidation process at low stress levels, but, again, very low strain rates results in lengthy experiment durations.

In seepage induced settlement tests (SIS), the water flows through the sample downward continuously, a difference in pressure is generated across the sample and resultantly, the consolidation of the soil sample takes place. The SIS tests provide compressibility and hydraulic conductivity relationship in a single step test maintaining a single hydraulic gradient.

Imai (1979) established a seepage-induced consolidation testing device to simulate the downward seepage consolidation stress superimposed on stress due to specimen self weight. Been and Sills (1981) developed a 2 m high self weight consolidation column of Combwich Estuarine mud of initial density between 1.02 and 1.15 to get experimental data to validate their own theoretical study on sedimentation and consolidation of soft soils.

Berilgen et al. (2006) performed seepage induced settlement (SIS) tests to investigate the relationships between index properties and consolidation of three different kinds of slurry type clayey soils. These tests were conducted to simulate the consolidation behaviour of higher water content soils for very low effective-stress range.

Meric (2010) reported the findings of Berry and Poskitt (1972), and discussed that the authors used Rowe cell to test amorphous granular and fibrous peat (initial void ratio = 7) to generate data for modeling peat consolidation. Tsutsumia and Tanakab (2012 examined the strain rate of a clayey soil for temperature variations performing special constant rate of strain (CRS) loading tests. Jeeravipoolvarn et al. (2009) simulated large scale consolidation behaviour of oil sands tailings. Three 10 m large stand pipes were used in the study for theoretical verification of experimental data sets. The study concluded that the unamneded MFT was only consolidated more than 30% over a period of 25 years, and they were enabled to provide very little or no effective stress due to self weight consolidation. Comparatively, the mix of sand and fine tailings provided quite high effective stress due to larger consolidation.

Nevertheless, conventional one dimensional consolidation tests (oedometer tests) were performed to examine the consolidation behaviour of polymer amended oil sands fine tailings. Conventional interpretation of these tests may still yield accurate estimates of hydraulic conductivity if the amount of volume change is sufficiently low, alternately, the deformation measured in these tests

can be modeled by large strain consolidation software, and therefore the large strain consolidation relationships can be back calculated from the data.

First, the soft polymer amended MFT (initial water content > 153%) was desiccated in columns to various degrees, which alternately enhanced the initial solids content and lowered the initial void ratio of polymer amended tailings.

The consolidation tests were carried out following the procedures as described in standard ASTM D 2435/D2435M – 11. For consolidation tests, the consolidation pressure was applied in conventional manner with load incremental ratio (LIR) of 1 which was obtained by doubling the total axial load on the tailings rising from 2.5 kPa to 80 kPa i.e., 1, 2.5, 5, 10, 20, 40, and 80 meaning that $\Delta\sigma/\sigma$ was kept at 1; $\Delta\sigma$ is the step load increment and σ is the effective stress on the specimen before the application of the incremental step load.

Each sample was consolidated for a particular loading up to 24 hours, until it reached to maximum consolidation capacity. The load of 80 kPa was selected on the argument that the calculations by experts showed that a deposit yield of 1.1 - 2 dry tonnes per seq. m per annum was desirable to attain the goals as set out in Directive 074 (2009) on economic grounds (Caldwell et al. 2014).

Keedwell (1984) suggested two methods to remove the loads after consolidation test. In first method, the load was removed at once, while in second method, the loads were removed in stages. The latter method was more practical while

examining the swelling behaviour of a material. In our study, the loads were removed all at once as the work examined the macroscopic and microstructure behaviour of thickened MFT for successive increase in stress level rather than the swelling behaviour of polymer amended tailings.

At the end of each test, the wet and dry weight of the sample was determined to determine the variations in water content and percent solids by mass for each stress level. Some samples for stress levels of 20, 40 and 80 kPa were collected from the consolidometer to perform the microstructure tests. The microstructure tests were also carried out on unconsolidated (0 kPa) samples desiccated to various initial solids content. The total suction and electrical conductivity tests were performed with consolidated and unconsolidated tailings.

The standard one dimensional consolidation method is based on Terzaghi's consolidation theory computing the coefficient of consolidation, c_v. Both logarithm-of time-method (Equation 3 – 5) and square-root-of-time method (Equation 3 – 6) were used to estimate the coefficient of consolidation of fine tailings following the procedure as discussed in Das (2008).

$$c_v = \frac{0.197H^2}{t_{50}} \qquad \textbf{Equation 3-5}$$

$$c_v = \frac{0.848H^2}{t_{90}} \qquad \textbf{Equation 3-6}$$

c_v = coefficient of consolidation, H = length of drainage path, t_{50} = time for 50% consolidation, t_{90} = time for 90% consolidation

After then, coefficient of consolidation, c_v was used to determine the hydraulic conductivity of tailings using another empirical relationship (Equation 3 – 7)

$$c_v = \frac{k}{m_v \gamma_w} = \frac{k}{\left[\frac{\Delta e}{\Delta \sigma}(1+e_{av})\right]\gamma_w} \qquad \textbf{Equation 3-7}$$

m_v = coefficient of compressibility, Δe = change in void ratio, e_{av} = average void ratio, $\Delta\sigma$ = change in stress level, k = hydraulic conductivity

Besides oedometer tests, thick and thin lifts (20 cm, 30 cm, 82 cm) were also developed to simulate the consolidation behaviour of tailings. Furthermore, the hydraulic conductivity of amended tailings was also determined at high water content incorporating the effect of SIS, and the falling head tests were performed in this respect as discussed earlier in Section 3.2.6

3.3 Microstructure of oil sands mature fine tailings

3.3.1 Mercury intrusion porosimetry tests

For MIP tests, the samples of polymer amended tailings were cut into a piece of 7 ~ 8 cubic millimetres. The samples were freeze in liquid nitrogen and n-pentane. A cylindrical container was filled with n-pentane (C_5-H_{12}) - a non polymerized liquid. The n- pentane container was cooled in liquid nitrogen (-210

^{o}C to - 196 ^{o}C) initially for 30 seconds. After then, the sample holder including samples was dipped in n - pentene while keeping it submerged in liquid nitrogen all the time. The sample holder and samples kept moving up and down ensuring that the sample did not freeze and stick in n- pentane container and liquid nitrogen. The freezing process continued for 45 to 60 seconds until the samples turned white.

A sample holder was especially designed and manufactured to freeze four samples at once. After freezing, the samples were dried in a developed set up of vacuum pump, desiccator, desiccant, ice packs and liquid nitrogen for 7 ~8 hours. The desiccant was placed in an oven at 110 ^{o}C for 16 hours prior to use.

The method was modified to criteria of freeze drying as discussed in Simms (2003) for compacted clay. It appeared rather difficult to collect samples of too wet tailings, so small molds of 1 cm^3 were used to collect the samples of tailing at higher water contents. The freeze drying method preserved the microstructure features of the sample, only small change in volume. The argument was stated on the evidence of Romero and Simms (2008) that the process eliminated the surface tension forces taking place as a result of air water interface utilizing temperature and pressure conditions, and it was assumed that the shrinkage of soil structure did not occur on drying which could change its structure. Figure 3 - 1 shows a scheme of developed set up to freeze dried the samples of oil sands fine tailings.

After freeze dried, the samples were tested using mercury porosimeter (AutoPore IV 9500) at University of Western Ontario and Tescan Vaga II – XMU at Carleton University, Canada for microstructure analysis.

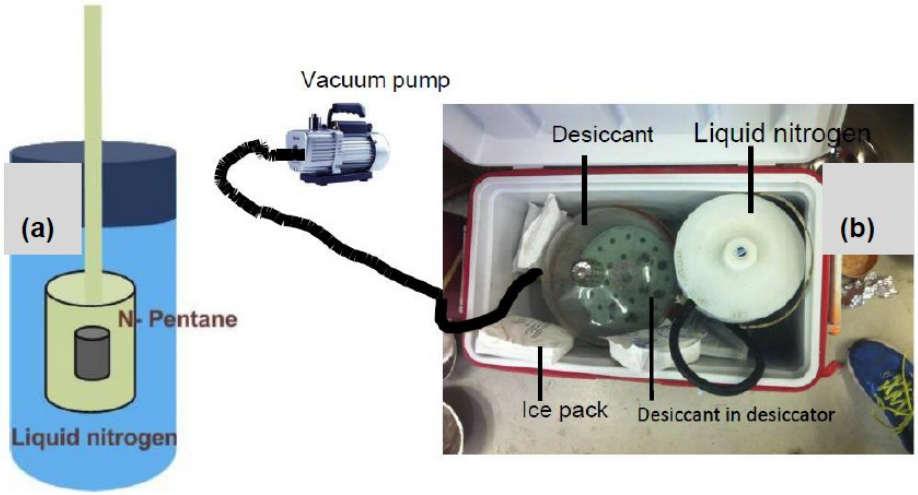

Figure 3-1: Scheme of developed freeze drying set up, (a)- freezing of sample, (b) - drying of sample); (Modified from Simms 2003)

3.3.2 Scanning electron microscopy (SEM)

SEM can magnify a sample from 20 to 30,000 x with spatial resolution of 50 to 100 nm. The device can image an area of approximately 1 cm to 5 microns in width. It has potential to perform analysis of selected point locations for a particular sample. SEM generally applies two vacuum conditions while analyzing a sample: i-) low vacuum scanning electron microscope (LVSEM); ii -) high vacuum scanning electron microscope (HVSEM).

Figure 3 – 2 shows schematic cross section of an ESEM. A Tescan Vega-II XMU SEM device at Carleton University was used for image analysis of polymer amended tailings. The tests were carried out at various scale and magnifications to visualize and quantify pores of all ranges. Some samples were collected directly from the experimental chambers to perform the ESEM tests. A rapid freezing stage of -50 ^{o}C was applied to hydrated samples in the vacuum chamber and the samples were tested at a vacuum of 10^{-3} Pa. SEM tests were also performed on dehydrated (freeze dried) samples as discussed in Section 3.3.1. In addition to this, SEM tests were carried out with freeze dried samples coated with gold palladium.

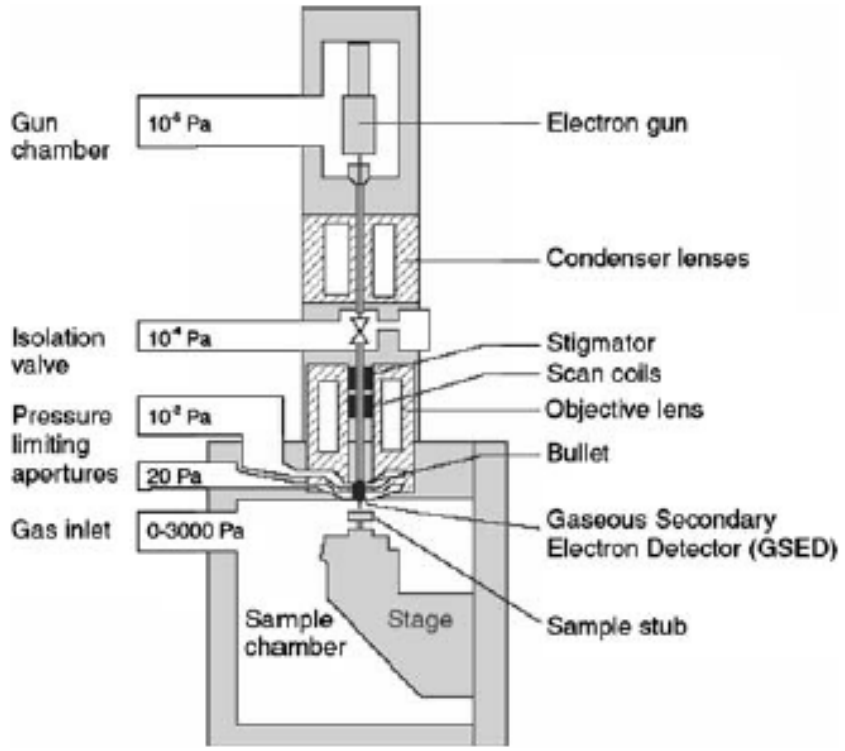

Figure 3-2: Schematic of cross section of an ESEM (Romero and Simms 2008)

ImageJ software was used to conduct the gray pixel analysis of SEM micrographs for quantitative measurement of oil sands fine tailings fabric (Ferreira and Rasband 2012). The software works on the principle that it classifies an image categorizing the grayscale value: gray scale is a single number based on the brightness of a pixel. First of all, SEM micrographs of oil sands tailings were optimized for adjusting the threshold (0 – 255), typically zero was taken as black, and 255 as white and the values in between composed of different gray shades.

The image analysis could be performed with a specified selected area or considering the entire image, and in this study; the analysis was performed with images of 300 μm view field. The particle analyzer was then utilized to extract the features of already threshold image to define the circularity range (0 – 1) of pores within the fabric. For a perfect circle, the software defined circularity value of 1, while zero value defined an increasingly elongated shape. ImageJ software automatically adjusted these values considering the shape of pores within the fabric.

The most appropriate way was to analyze the particles tracing their size and circularity by outer edge or flood filling, but the flood filling approach was followed in this study while identifying the pores of tailings fabric. Finally, the particle analyzer reported the summarized particle count, total particle area, average particle size and area of the simulated pores.

There was an option to define area in square pixels or in calibrated square units such as mm^2 and μm^2 etc. The number of pixels was then counted based on number of pixels per micron of the image. The estimated area of each individual pore was then changed to pores diameter. The cumulative diameter of pores of equal size was estimated classifying the frequency of pores of equal magnitude; labeling them into a series of bins ranging from 100000 to 1. Finally, the classified bins and pores diameter were used to quantify the microporosity of SEM micrograph.

3.4 Materials preparation

The unamended MFT and reclaim water were got from the tailings storage facilities (TSF) of Shell, Canada. A 0.4% solution of polymer was prepared with reclaim water following the procedure as discussed in Shell Canada Protocol, 2012 to produce field representative samples (Shell 2012). Figure 3 – 3 presents a few pictorial views of laboratory preparation of polymer amended oil sands MFT.

Reclaim water is treated water reclaimed from conventional tailings impoundments with low solids and certain impurities. Table 3 – 1 shows a chemical analysis of pore water of oil sands MFT. A 0.4% solution was prepared using four blade impeller of 8.5 cm radius fixing a speed of 225 rpm. The 0.4% solution was left over 24 hours in air tight container for homogeneity. After then

0.4% flocculated solution was mixed with 1800 g of unamended MFT using four blade impeller fixing a speed of 260 rpm for 22 seconds.

Figure 3-3: Laboratory preparation of polymer amended oil sands MFT

The prepared MFT was then transferred to developed experimental scheme in order to perform the microstructure and macroscopic tests (Figure 3 – 3). Figure 3 – 4 shows the SEM micrograph of 0.4% solution prepared using polymer SNF A3338 and reclaim water.

Table 3-1: Pore water chemistry of oil sands MFT (Guo 2012)

Cations	Concentration (mg/L)	Cations	(mg/L)	Cations	Concentration (mg/L)
Na	599.55	Ba	0.1	Rb	0.06
Ca	9.68	Cu	0.11	Sr	0.36
Mg	9.03	Fe	0.02	V	0.01
K	19.73	Ni	0.01	Zn	0.01
Al	0.04	Pb	0.01	-	-
Anions	**Concentration (mg/L)**	**Anions**	**Concentration (mg/L)**	**Anions**	**Concentration (mg/L)**
Chloride	278.5	Nitrate	2.6	Sulphate	29.1
Hydroxide	328.5	-	-	-	-
pH =8.88				EC = 3.59 mS/cm	

Polymer amended tailings prepared in the laboratory using this procedure was compared to field samples collected during full-scale deposition of in-line flocculated tailings. In the field, the polymer was injected into tailings in-line using turbulence flow some metres before the end of the pipe, and the polymer amended tailings were deposited 8’ 11’’ from mixing point (Figure 3 - 5). The samples generated in the laboratory and in the field were at least roughly equivalent (Figure 3 - 6). Figure 3 – 7 shows stress growth yield stress of laboratory prepared and field generated samples of polymer amended MFT, 1/2 hour after preparation.

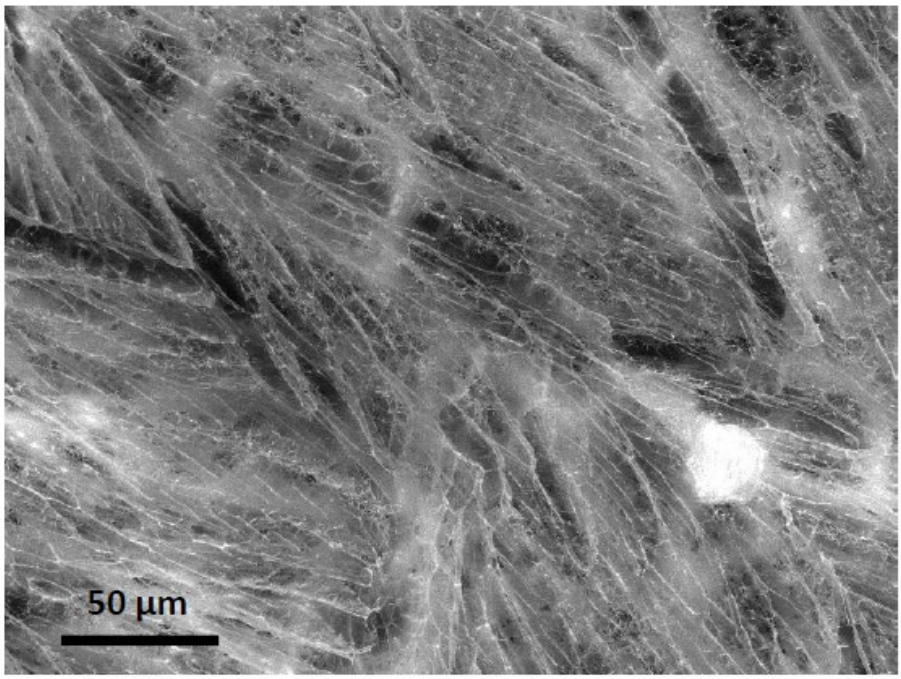

Figure 3-4: SEM micrograph of 0.4% solution prepared with polymer and reclaim water (Mizani et al. 2013)

Figure 3-5: Example of in-line flocculation of MFT in the field (Mizani et al. 2013)

Figure 3-6: Laboratory appearance of polymer amended MFT

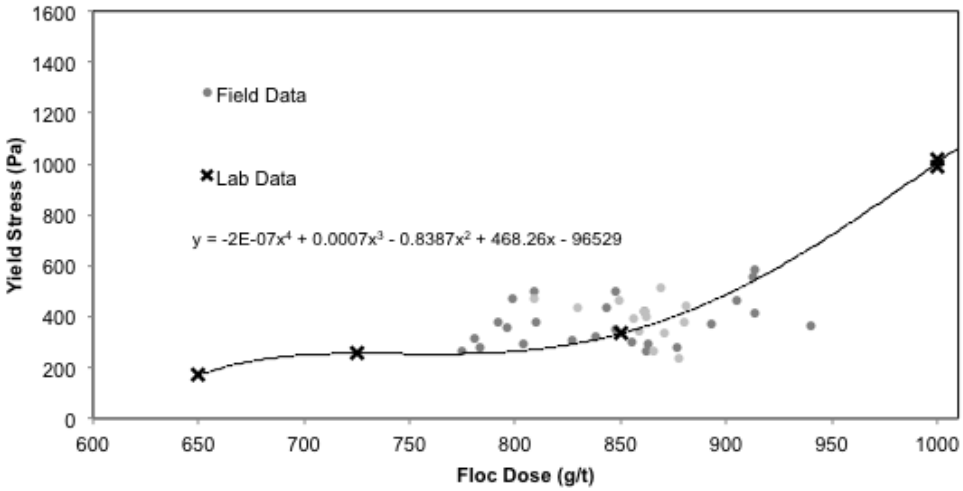

Figure 3-7: Stress growth yield stress of laboratory prepared and field generated samples of polymer amended MFT, 1/2 hour after preparation (Mizani et al. 2013)

3.5 Conclusions:

Various experimental schemes were developed in the laboratory with an aim to achieve the objectives as defined in Chapter 01. A series of slump tests, vane shear tests, suction tests, hydraulic conductivity tests, and consolidation tests etc., were performed to study the macroscopic behaviour of tailings. Figure 3 – 8 reports the methods used in the study.

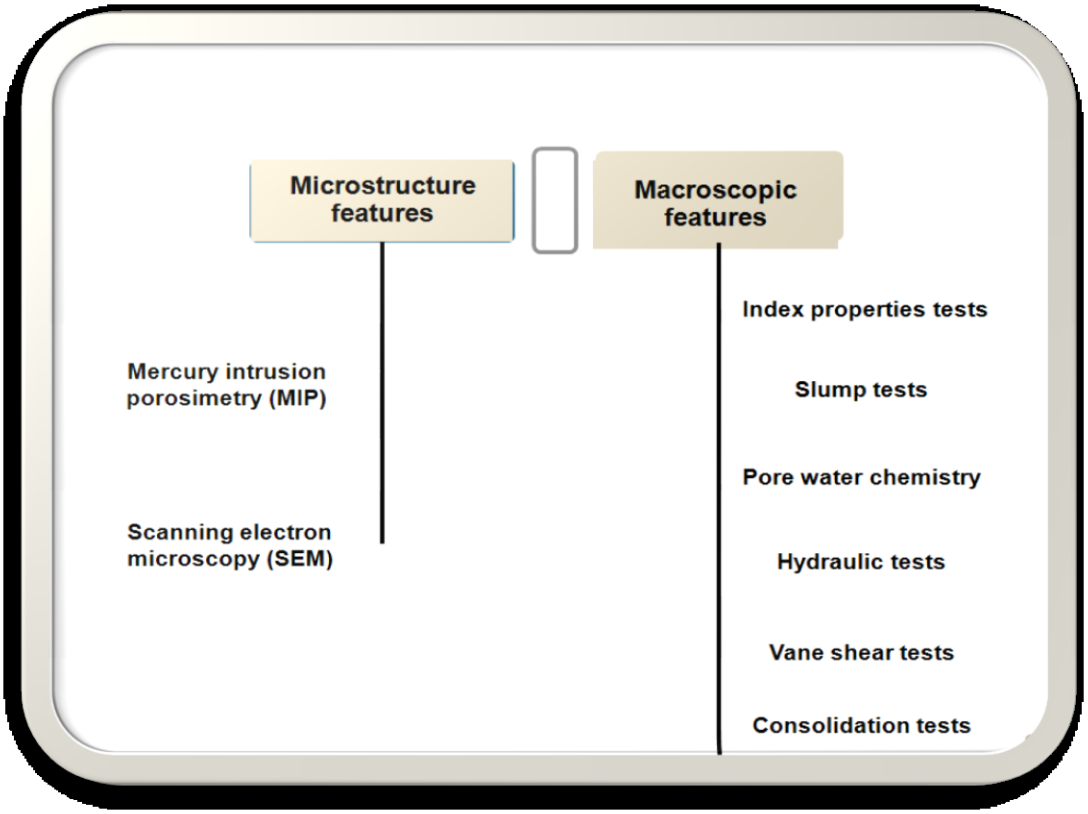

Figure 3-8: Summarized microstructure and macroscopic tests

To examine the fabric of tailings, mercury intrusion porosimetry (MIP), environmental scanning electron microscopy (ESEM) and scanning electron

microscopy (SEM) techniques were employed. Gray pixel analysis (ImageJ) was performed to quantify fabric of tailings from ESEM and SEM micrographs.

Chapter 4. Influence of polymer dose on Atterberg limits and particle size distribution of polymer amended oil sands mature fine tailings [1]

Abstract

Sand to fine ratio (SFR), specific gravity (G_S) and Atterberg limits are used to quantify the effects on geotechnical behaviour of polymer amended fine tailings. In this study, the specific gravity, sand to fine ratio (SFR) and Atterberg limits of oil sands fine tailings were determined for wide range of polymer doses. The test results showed that the addition of polymer modified the segregation nature to agglomeration of mature fine tailings, which alternately enhanced apparent sand to fine ratio (SFR) and also LL values.

4.1 Introduction

The oil sands MFT has no significant strength, and deposits several decades old have not appreciably dewatered. Figure 4 -1 presents the schematic of the production of oil sands MFT. The MFT is posing serious threat to our environment and land use values due to its high volume and segregation behaviour. The mineral surface properties of MFT did not show any dewatering potential due to greater water holding capacity and slow consolidation rate (Beier and Sego 2008).

[1] A version of this chapter was published in proceedings of GeoMontreal 2013 (Bajwa and Simms 2013)

As such, many technologies were tested to accelerate dewatering which attempted to modify the electrochemical interactions of the fines by altering the pore water chemistry (e.g. adding lime or gypsum), or introducing a charger polymer to bridge dispersed particles.

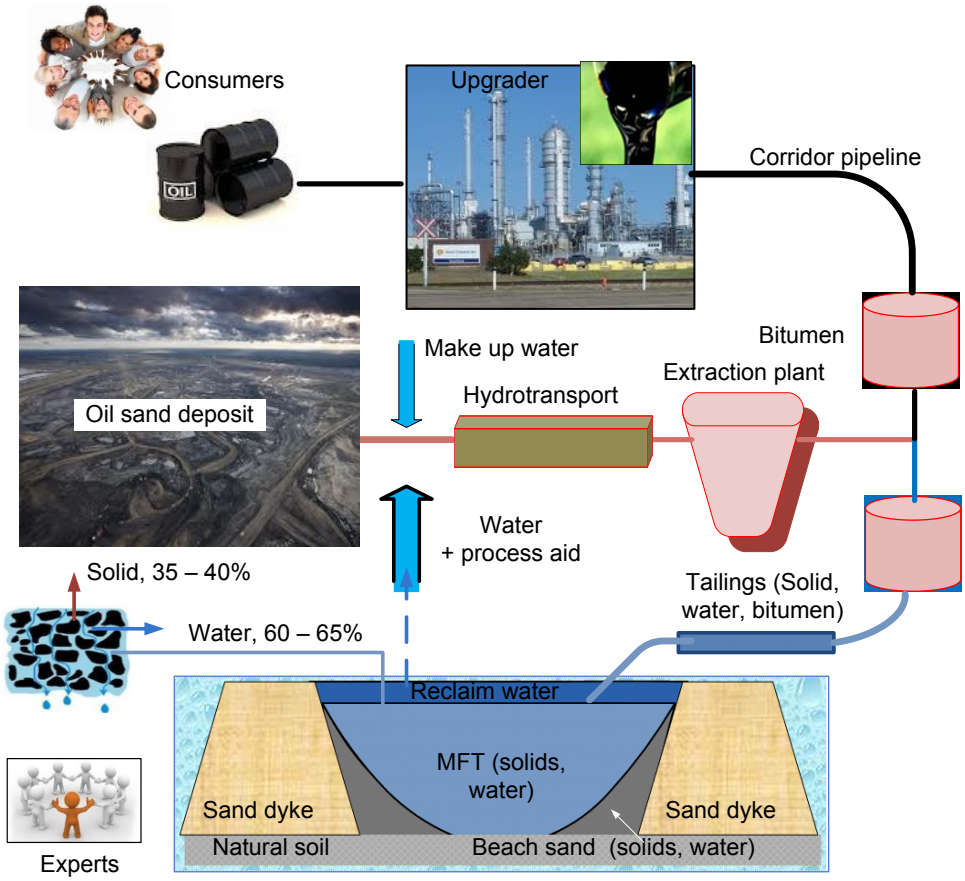

Figure 4-1: Scheme of oil sands mature fine tailings production (Modified from Beier and Sego 2008)

In order to promote reclamation of water from the tailings and to drive reclamation of MFT deposits, the Alberta Regulators have adopted the guidelines as set out in Directive 074 (ERCB 2009), which mandates that fine tailings need

to achieve a schedule of shear strength criteria to ensure that the tailings are on the path to trafficability and reclamation. Oil sand operators are pursuing a range of technologies to achieve these criteria, including conventional thickening, centrifuging, increasing fines capture in coarse tailings beaches, improving the existing CT (composite tailings) technology, and in-line mixing of fine tailings with a polymer.

SFR is an oil sands industry definition, and is defined as the ratio of particles over to under 44 microns (BGC Engg. 2010). The efficiency of any treatment to increase flocculation of individual particles may be partly evaluated by the increase in SFR of the treated tailings relative to the untreated tailings.

The Atterberg limits and SFR may greatly influence the post deposition behaviour of oil sands tailings controlling some important properties such as tailings water potential, strength and hydraulic conductivity etc. Few studies were found in literature, those discussed the impact of polymer in terms of LL and SFR in oil sands fine tailings for a limited range of polymer doses.

Jeeravipoolvarn (2010) examined the grain size distribution of ILTT and COF tailings focusing on various shearing rates, and few tailings were considered for Atterberg limits. Owolagba (2013) discussed the gain size distribution of centrifuged oil sands MFT and as received tailings showing major attention on soil water potential. In this study, the SFR and Atterberg limits of oil sands fine tailings were examined for wide range of polymer doses (0 – 4000 ppm) with an

aim to provide an understanding towards the implications of polymer dose beyond a certain threshold.

4.2 Materials preparation and methods used:

The polymer amended fine tailings were prepared following the guidelines as described in Chapter 3. After mixing, the prepared tailings were transferred to cylindrical columns of 20 cm dia. and 30 cm depth and left for air drying. A wide range of polymer doses ranging from 500 to 4000 ppm was used in this study. The prepared tailings were then used to perform the specific gravity; grain size distribution and Atterberg limit tests. For these tests, triplicate samples were generated in columns, and an average value of these parameters was reported in this study.

4.3 Results and discussions

4.3.1 Preliminary characteristics of oil sands mature fine tailings

The unamneded MFT provided a water content of 140% with 42 % solids content. The wet density was 1200 kg / m^3. Porosity was high (76 %) but all the pores were almost filled with water (S = 0.99) giving an entrapped air content of only 0.8 %. The average water content of the polymer amended MFT varied between 149 and 212 % for polymer doses ranging from 500 to 4000 just after the polymer mixing. The increase in water content occurred due to the addition of

reclaim water while mixing the polymer. The polymer amended MFT showed an average bulk density of 1220 kg / m^3 ~ 1300 kg / m^3.

4.3.2 Specific gravity of oil sands fine tailings

Figure 4 - 2 shows the test results of specific gravity for polymer amended MFT with standard deviation error bars.

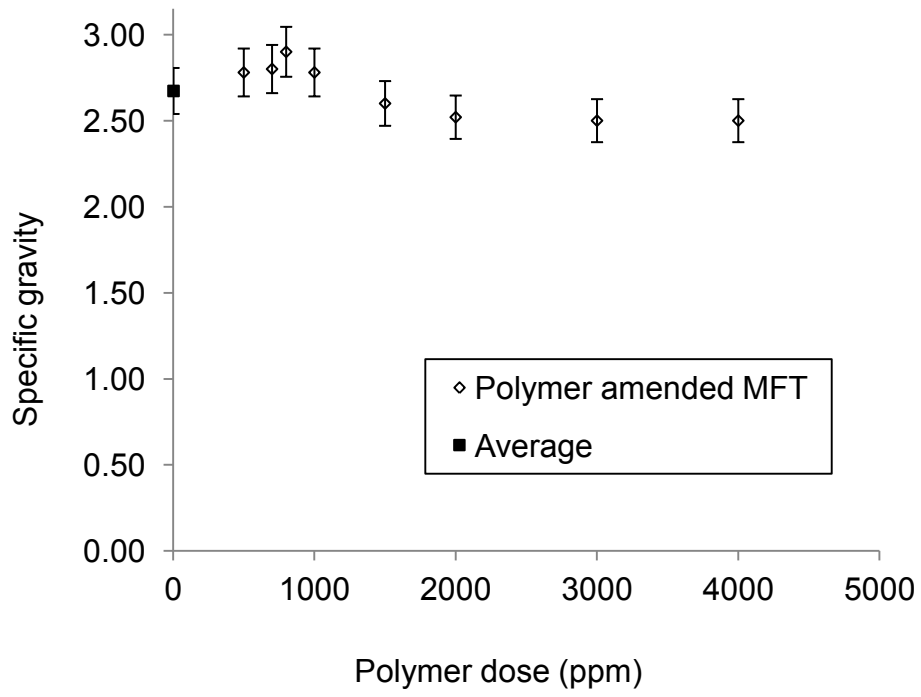

Figure 4-2: Specific gravity of polymer amended tailings for error bars with percentage (5%)

To test our method, we compared the obtained value of unamended MFT (2.22) to other reported values. Jeeravipoolvarn (2005) reported a value of 2.28. For polymer amended MFT, the increase in specific gravity was quite high in

comparison to unamended MFT. The polymer amended MFT showed specific gravity of 2.90 for polymer dose of 800 ppm (Figure 4 - 2).

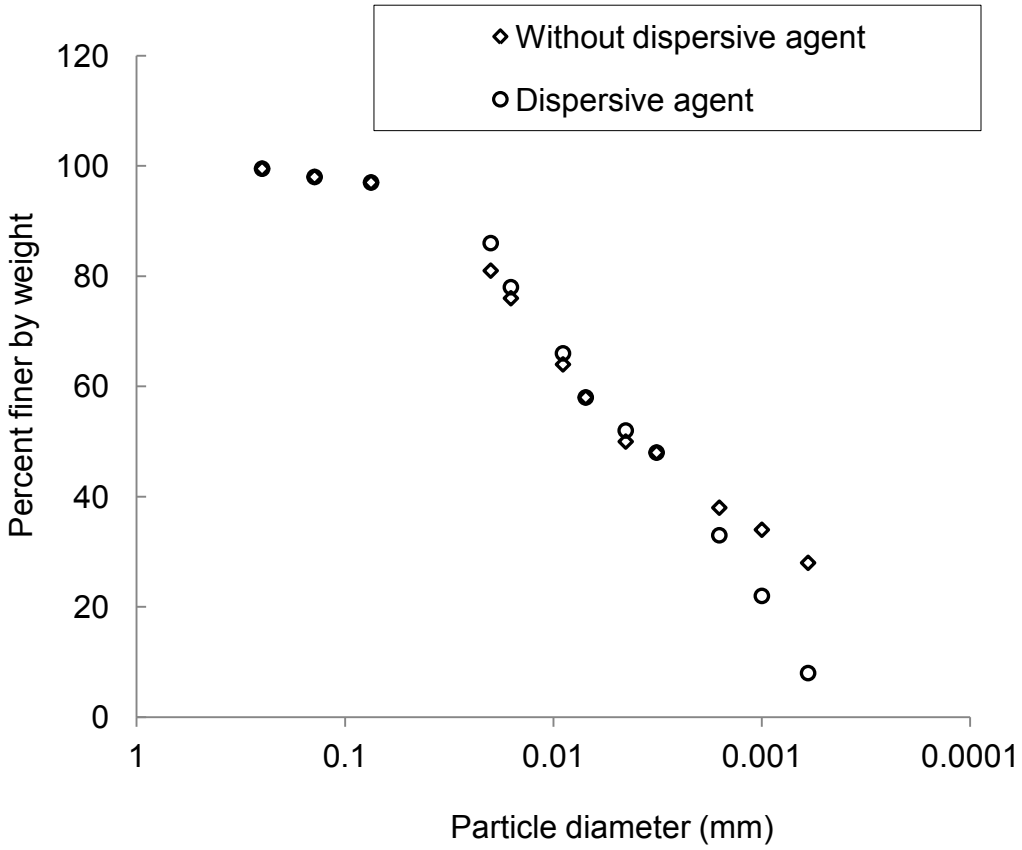

Figure 4-3: Particle size distribution (PSD) of oil sands mature fine tailings (MFT)

Jeeravipoolvarn (2010) reported the specific gravity of anionic flocculant (CIBA Magnafloc 6260) amended cyclone overflow (COF) tailings and in-line thickened tailings (ILTT) and it varied from 2.45 to 2.54. Innocent-Bernard (2013) discussed the specific gravity of thickened oil sands tailings and it varied between 2.50 and 2.70. The somewhat higher value of this study was attributed to the different

flocculation process and flocculant. This difference in measured specific gravity occurred due to different degrees of dissociation of residual bitumen from the clays (Jeeravipoolvarn 2010).

The polymer amended tailings were desiccated in the column, so there was chances of isolation of bitumen from the clay contents while their deposition in columns, which raised the specific gravity. The addition of polymer changed the mineralogical properties of tailings which might also enhance the specific gravity. This higher specific gravity of polymer amended tailings may affect the self-weight consolidation behaviour of polymer amended tailings in succeeding chapters.

4.3.3 Grain size distribution test results:

Figure 4 - 3 shows the grain size distribution curve of unamended MFT with and without the dispersing agent. The curves of unamended MFT overlapped to each other except for finer particles less than 0.003 mm size. It means that the addition of dispersion agent did not show any influence on the grain size distribution of unamended tailings.

A comparison of polymer amended MFT and unamended MFT showed that the addition of polymer altered the percentage of sand, silt and clay content quite largely (Figure 4 - 4). The percent silt was increased from 58% to 82% for a particular polymer dose of 800 ppm showing considerable increase in particle

sizes. The SFR of unamended MFT was estimated to be 0.10, which was quite low in comparison to polymer amended MFT (Figure 4 – 5). The nature of unamended MFT curve in Figure 4 - 4 verified this statement showing quite low percent of silt.

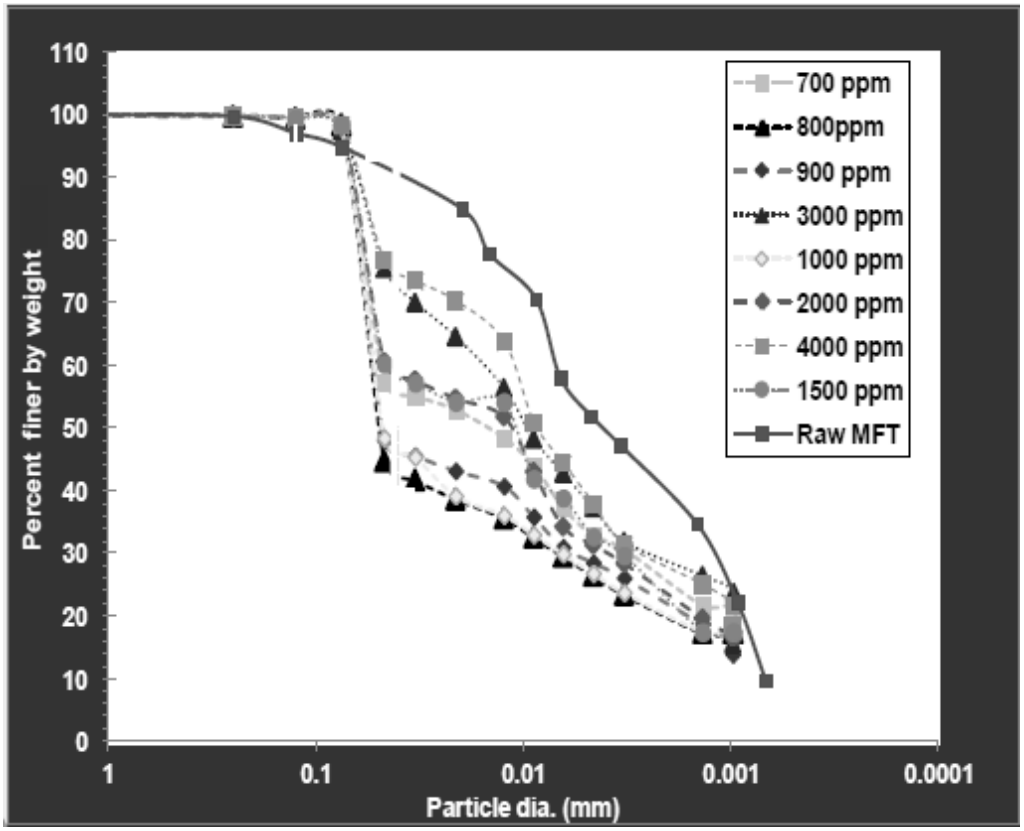

Figure 4-4: Particle size distribution of polymer amended fine tailings for various polymer doses

According to soil classification systems, the unamended MFT showed 40% clay, 58% silt and only 2% sands content and the particles diameter varied from 0.3 mm to 0.0006 mm (Figure 4 - 3). Figure 4 - 4 shows the particle size distribution

of polymer amended MFT for various polymer doses ranging from 0 to 4000 ppm.

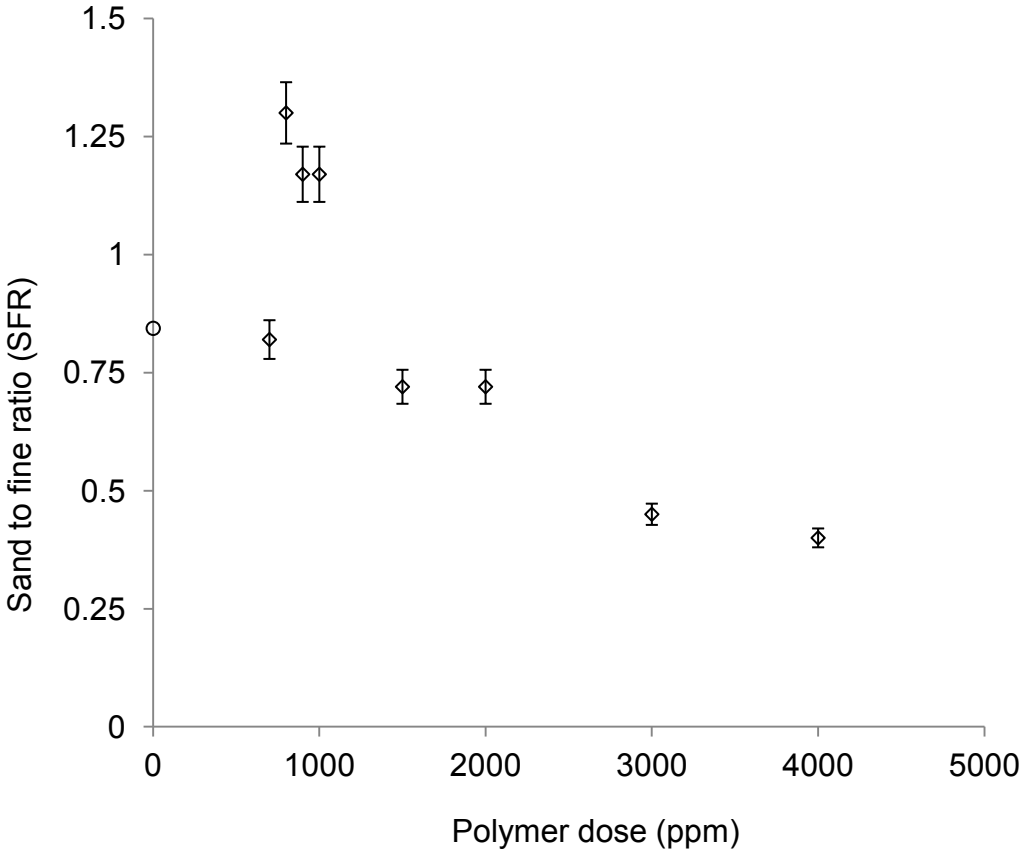

Figure 4-5: Sand to fine ratio (SFR) of polymer amended tailings for error bars with percentage (5%)

For a particular range of polymer dose (700 -1000 ppm), the SFR looked more stabilized, however, SFR for 700 ppm was less in comparison to 800 ppm but still quite high in comparison to unamended MFT. Similar to the specific gravity test results, the polymer dose of 800 ppm showed peak SFR (1.30), and generally SFR varied between 0.40 and 1.30 for doses ranging from 700 to 4000 ppm

(Figure 4 - 5). Innocent-Bernard (2013) discussed SFR of thickened oil sands tailings over time and it varied between 0.67 and 1.17, and these values appeared close to the current study. However, the reported study utilized dry samples whereas the dry mass was estimated on the basis of wet samples in this study. The wet samples were used to eliminate the crushing of tailings particles that might disturb the SFR, as the tailings provided too sticky and stiff structure on drying.

The test results showed a clear optimal dosage in terms of altering the apparent grain size distribution. This suggested industry to consider SFR while optimizing polymer dosage in addition to other mechanisms such as capillary suction time. The addition of flocculant physically bridged the finer particles to form larger particles, which resulted in an increase in SFR.

4.3.4 Index properties test results:

Unamended MFT showed a liquid limit (LL) of 45 and plastic limit (PL) of 19 with liquidity index (LI) of 4.65 (Figure 4 - 6). Jeeravipoolvarn (2005) reported the LL and PL of mature fine tailings of 46 and 21 respectively. The LL of polymer amended MFT varied from 70 to 82% and it attained a peak value of LL (82%) for a polymer dose of 800 ppm giving LI of 2.49 (Figure 4 - 6). Innocent – Bernard (2013) reported the findings of Yao et al. (2010), and the liquid limit of these tailings varied between 40 and 70%.

The mode of particle arrangement due to inter particle arrangement controlled the liquid limit of kaolinite dominant soils (Di Maio et al. 2002). The clay particles of oil sands MFT showed negative charges and the net negative charge primarily controlled the clay dispersion. With an addition of polymer, the segment of polymer chain adsorbed on the tailings colloids. The thickness of diffuse double layer suppressed due to changes in the dielectric constant, electrolyte solution, and cationic valence. Mitchell and Soga (2005) stated that the ionic valence and ions concentration influenced the double layer thickness and a thinner double layer provided higher flocculation of particles.

These changes in pore medium chemistry due to double layer theory and isomorphous substitution affected the interparticle attractive and repulsive forces. The electrostatic repulsive forces (colloids of the same charge) and van der Walls attractive forces (colloids of the opposite charge) separated the charged colloids in a solution from each other, and the balance of these forces resulted in the dispersion and flocculation of the particles. A reduction in the net negative charge overcame the electrostatic repulsion allowing the particles to come closer to each other.

Resultantly, the repulsive forces reduced and net attractive forces increased due to an increase in net shearing resistance at the particles level and these conditions favored flocculation which resulted in an increase in liquid limit and SFR of polymer amended tailings. For a polymer dose of 700 ~ 1000 ppm, the van der Wall attractive forces most apparently dominated the electrostatic

repulsion forces, and the polymer doses of this range showed more agglomeration giving high SFR and LL.

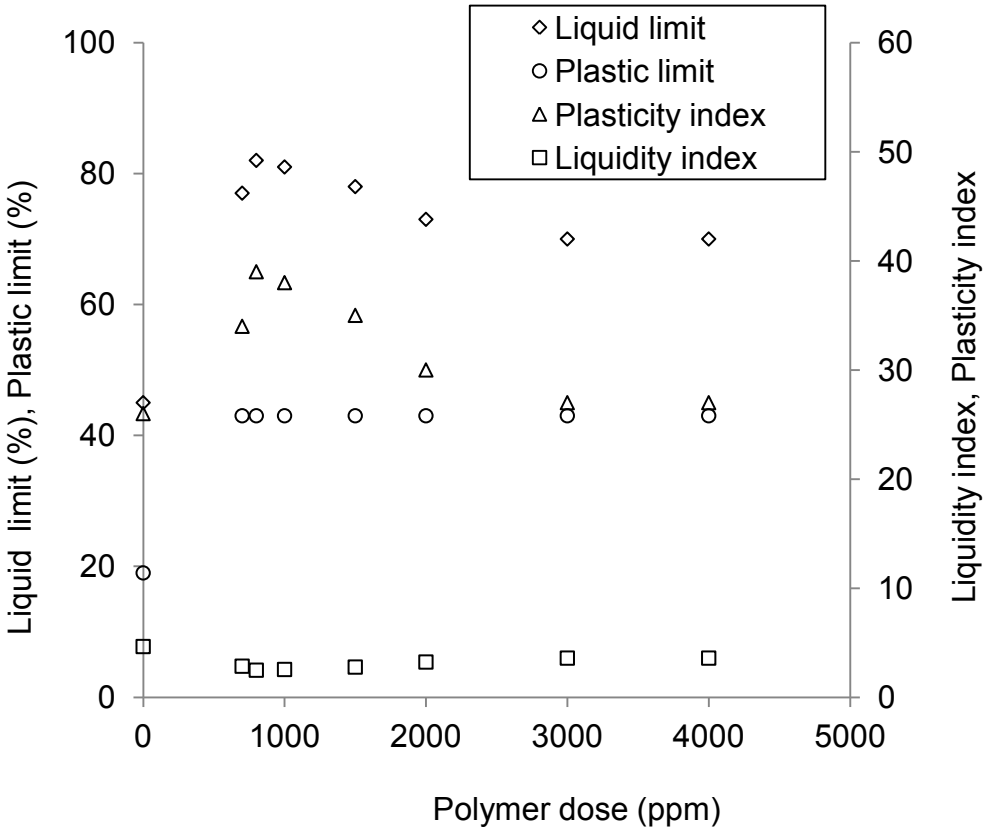

Figure 4-6: Index properties of fine tailings for various doses

Interestingly, the plastic limit of the polymer amended FT was the same, though different from the original MFT. This reflected the evolution of microstructure shown in the succeeding chapters using both scanning electron microscopy (SEM) and mercury intrusion porosimetry (MIP), that polymer amended MFT for a wide range of doses collapsed to the same microstructure beyond a certain degree of desiccation.

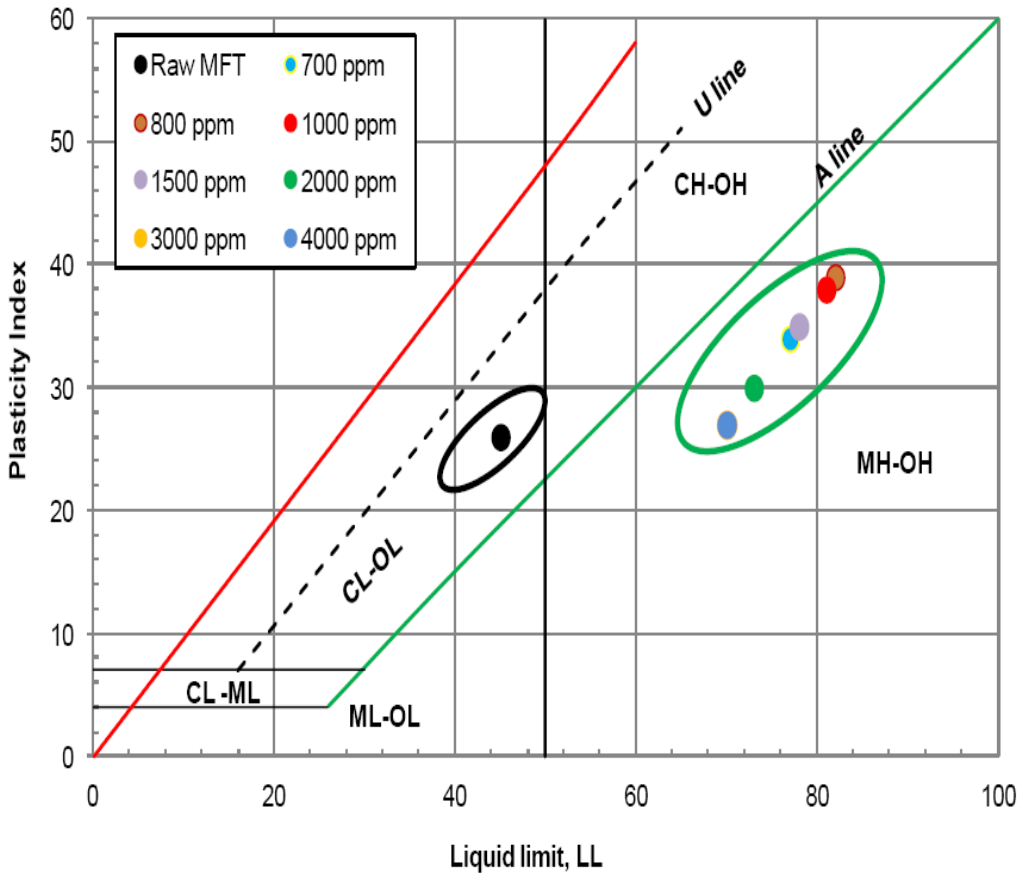

Figure 4-7: Plasticity chart of polymer amended fine tailings

The tailings at higher water content showed differences in inter – aggregate porosity, however the differences were much less apparent at the lower water content for various polymer doses. This validated the argument that tailings for various polymer doses behaved in similar fashion beyond a certain degree of desiccation. The unique plastic limit of tailings for various polymer doses also authenticated this fact. The addition of polymer changed the grain size distribution of MFT shaping all the samples to fall in inorganic MH - OH region of plasticity chart categorizing it as elastic silt, and comparatively, unamended MFT fell in CL - OL region (Figure 4 - 7).

4.4 Conclusions:

The addition of polymer modified the behavior of mature fine tailings, raising apparent sand to fine ratio (SFR) and lowering the liquidity index (LI) values. For SFR, specific gravity, and LI, a peak value was reached at 800 or 1000 ppm. The plastic limit was the same for all polymer doses (700 to 4000 ppm), but was substantially less than the value for unamended MFT.

There was a clear optimum for polymer (800 ppm) in terms of LL, Gs, and SFR. This would be compared to other optimums in terms of short and long term dewatering in subsequent chapters.

Chapter 5. Evolution of macroscopic and microstructure features of polymer amended oil sands mature fine tailings one hour after polymer mixing

Abstract:

The oil sands industry has developed various approaches to dewater fine tailings, most of which employ a mixes of concept in order to increase fine tailings's strength to meet the ERCB Directive 074 (2009) guidelines. One common step in many tailings management strategies is the addition of a polymer to facilitate flocculation of dispersed clay particles and therefore to improve dewatering. Dewatering takes place through several mechanisms, including sedimentation of new flocs, subsequent self-weight consolidation of polymer amended tailings days to weeks after deposition, desiccation due to surface processes (evaporation and freeze-thaw), and further self-weight consolidation in the long term and / or by burial under fresh tailings or other surcharge, and thixotropic strength growth.

Optimizing polymer dose for one mechanism does not necessarily optimize deposition for all dewatering steps. Therefore, in this thesis, we attempted to study the influence of polymer on different stages of dewatering. In this study, the influence of polymer on macroscopic (yield stress, hydraulic conductivity, suction, pore water chemistry) and microstructure (flocs formation) features of oil sands fine tailings were examined one hour after polymer mixing, so as to differentiate

between flocs formation and immediate settling and subsequent self-weight consolidation.

The test results showed that the tailings fabric changed with a change in polymer dose. The dose of 700 ppm provided the highest yield stress associated with its higher drain off potential as a comparison to other doses. Furthermore, SEM images showed larger and more interconnected flocs at higher doses, showing that such structures impeded dewatering and associated strength development due to dewatering after 1 hour.

5.1 Introduction

Various studies were found in the literature, those discussed the benefits of adding a chemical additive to accelerate the drain off potential of oil sands fine tailings. Ren et al. (2014) discussed the effects of mixing energy on the drain off potential of flocculated oil sands mature fine tailings. Wang et al. (2014) stated that the treated tailings released more water, which consequently increased their yield stress. Aida and Mamadou (2013) used a super absorbent polymer (SAP) to examine the impact of water release on the undrained shear strength of tailings. Mizani et al. (2013) reported that flocs formation in polymer amended tailings resulted in considerable release of water after 24 hours of polymer mixing. Chalaturnyk et al. (2002) treated oil sands tailings with cationic polyacrylamide (PAM) in order to expedite their drain off potential. Hamza et al. (1996) used anionic polycrylamide in order to increase the dewatering rate of

lime treated oil sands tailings. Figure 5 – 1 highlights the mechanism of the release of water taking place due to flocculation during earlier stage of polymer amended tailings.

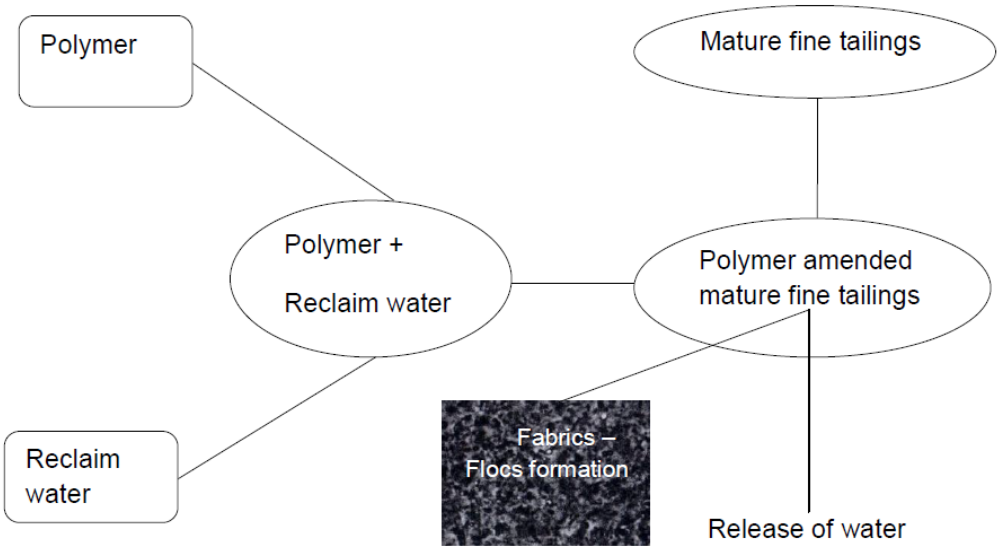

Figure 5-1: Schematic diagram illustrating the mechanism of water release of polymer amended oil sands mature fine tailings

The previous research was mainly focused on the drain off and consolidation potential of treated tailings after several hours of deposition, and the studies were only limited to a few parameters of practical interest. So, in this study, the dewatering and related properties were examined after 1 hour to attempt to separate flocculation from self weight sedimentation. A series of slump tests, hydraulic conductivity tests, suction tests, pore water chemistry tests and microstructure tests (ESEM) were conducted for various polymer doses.

5.2 Materials preparation and methods used:

The polymer amended MFT was prepared following the guidelines as described in Chapter 03. The geotechnical and microstructure tests were carried out one hour after depositing the polymer amended tailings in columns. A series of slump tests was performed to examine the yield stress of tailings for various polymer doses. A polymer dose of 500 to 4000 ppm was used in this study.

For slump tests, the tailings were transferred to cylindrical columns of 10 cm dia. and 10 cm depth. Each column was supplemented with drainage system at the bottom to monitor the drain off potential for respective dose. The schematic of slump tests of polymer amended fine tailings is shown in Figure 5 – 2.

The base plate of each column was removed before conducting the slump tests. Two fans were used to simulate the field conditions in the laboratory, though it was not so important to examine the evaporation potential of tailings one hour after polymer mixing as the small evaporation rate at this time might not able to alter the yield stress.

For unamended MFT, prior to test, MFT for each sample was mixed uniformly with a mixing device and brush, after then the sample was transferred to the mold with a small spatula. The sample was transferred carefully minimizing the chances of any gap that might influence the overall solids to water content fractions for a particular sample. A small wooden hammer especially

manufactured for this purpose was used to compact the samples in the mold for any space. The mold was filled in three equal layers. The mold was lifted gently to avoid any turn or stress on the mold and the slump height was determined immediately with the measuring tape.

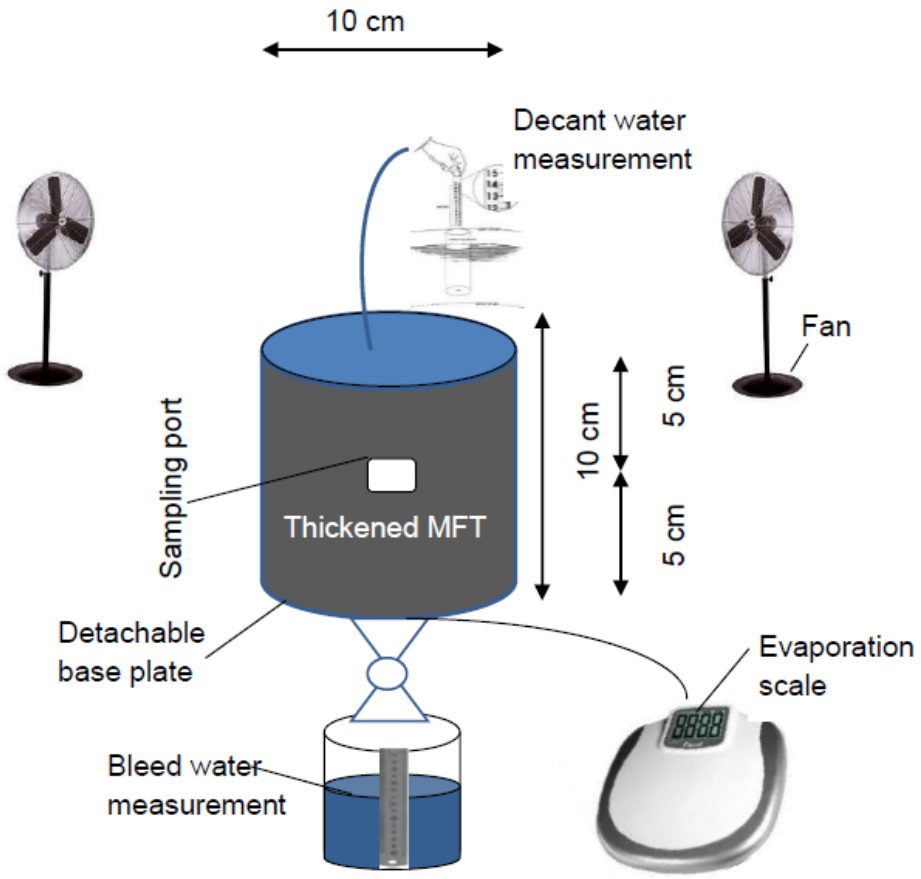

Figure 5-2: Schematic of ILTT one hour after polymer mixing

The same process was repeated for all the tests with each increase in water content. For particular water content, duplicate samples were generated to define

the average slump. For polymer amended MFT, triplicate samples were generated for each dose and an average slump was reported in this study.

For hydraulic conductivity, the falling head test method was followed and the tailings were prepared in the cylindrical columns of 30 cm depth and 15 cm diameter. The polymer amended MFT was transferred to the permeater one hour after polymer mixing and the test was continued for 24 hours for each polymer dose. Tailings water potential was monitored performing total suction and electrical conductivity tests. For total suction tests, a WP4 Dewpoint PotentiaMeter was used and the electrical conductivity was calculated using a traceable conductivity meter. The osmotic suction was estimated transforming the electrical conductivity to osmotic suction using USDA equation (Peroni and Tarantino 2005). The saturation extraction procedure was followed to transfer the electrical conductivity to osmotic suction.

The pore water chemistry of tailings was examined for polymer doses of 700, 1000 and 1500 ppm one hour after polymer mixing. For pore water chemistry, the samples of various doses were sent to Exova, Ottawa, Canada. The procedure as outlined in standard ASTM D 2974 – 07 (a) was followed to determine the organic and inorganic contents of tailings. For suction, the same samples were used for which we did the slump tests and for pore water chemistry, the samples were generated one hour after polymer mixing, and sealed in a polyethylene bags, which corresponded to water contents as discussed in Section 5.3.3., one hour after polymer mixing, as those were sent to Exova, Ottawa for chemical

analysis. However, the analysis of metals was reported on a dry sample basis and N-NH_3 was analyzed as collected.

For these tests, the ESEM technique was selected to examine the microstructure, as opposed to MIP and SEM on freeze-dried samples. This was done to avoid any effects associated with flash freezing of samples of very high water content (Newson et al. 2014). The cylindrical columns of 10 cm depth and 10 cm diameter were developed for various polymer doses to examine the fabric of tailings one hour after polymer mixing. The samples for perspective dose were extracted from a depth of 5 cm from the top. A small mold of 1 cm^3 was placed at a depth of 05 cm from the top, while depositing the tailings in the columns. There was chance of the mold to move down due to the soft tailings, so the mold was held with a thread and adhesive tape at the particular position.

After one hour, the tailings were dug to the specified depth and the molds including samples were taken out. The samples were collected from the columns one hour after tailings deposition and the analysis was performed one hour after collecting the samples. The actual time to perform microstructure tests on samples was approximately two hour. A Tescan Vega – II XMU device was used to perform the ESEM tests, and ImageJ analysis was used for quantitative measurements of tailings fabric.

5.3 Results and discussions

5.3.1 Organic and inorganic contents of oil sands mature fine tailings

The unamended MFT showed 6.5% organic and 93.5% inorganic contents and the polymer amended MFT gave almost similar organic (6%) and inorganic (94%) contents. The addition of polymer did not alter the fractions of organic and inorganic contents of MFT. The organic contents were found quite low in both treated and untreated tailings. Innocent – Bernard (2013) reported that the unamneded tailings provided average organic contents of 2 %, and the reported value was slightly lower than our results and this difference might occur because of variation in MFT composition.

5.3.2 Pore water chemistry of oil sands mature fine tailings

Table 5 – 1 shows the pore water chemistry test results of both unamneded and polymer amended oil sands tailings. Most metal constituents of both unamended and polymer amended tailings appeared comparable; however the difference in the concentration of a few metals was quite large and as an example, unamended MFT showed 5700 µg/g of Ca whereas the concentration of Ca in polymer amended tailings was about 3000 µg/g. Moreover, the tailings for various doses did not provide major variations in metal constituent except Na, and the polymer doses of, 700, 1000 and 1500 ppm gave 1000, 1100 and 1700 µg/g of Na respectively (Table 5 -1).

The higher concentration of Na in treated tailings generally represented the higher level of soluble salts. The concentration of Ca in polymer amended tailings was significantly decreased for all polymer doses when compared to unamended MFT. In addition to this, the concentrations of Cu, K, Li and Mg of polymer amended MFT were also less for all polymer doses in comparison to unamneded MFT.

Table 5-1: Pore water chemistry of unamneded and polymer amended fine tailings

Group	Units	Analyte	MRL	Unamended MFT	Polymer amended MFT (PPM)		
					700	1000	1500
Agri. Soil	ppm	HNO3	1	-	<1	<1	<1
-	ppm	HNO3	1	-	<1	-	-
-	ppm	-	25	-	-	<25	<25
General chemistry	-	-	1	7.47	7.56	7.65	7.58
Metals	µg/g	Ca	100	5700	3000	2800	2800
-	µg/g	Cu	1	17	12	12	14
-	µg/g	K	100	1000	900	900	900
-	µg/g	Li	1	10	6	6	7
-	µg/g	Mg	100	1800	1100	1100	1200
-	µg/g	Na	100	1200	1000	1100	1700
Nutrients	µg/g	N-NH3	100	<100	<100	<100	<100
	µg/g	N-NH4	100	<100	<100	<100	<100
Others	µg/g	N-NH3	100	<100	<100	<100	<100
	Method reporting limit		parts per millions		micron gram per gram		

The addition of polymer did not provide any major change in the concentration of nutrients and both treated and untreated tailings approximately showed comparable concentration of nutrients (Table 5 -1). The pH of both unamended

and polymer amended MFT was more than 7 showing their trend towards alkalinity and comparatively, the pH of polymer amended MFT was high for all polymer doses in comparison to unamended MFT (Table 5 -1). Moore et al. (2014) reported that both unamended and silica treated MFT provided pH of 7.74 and 7.89 respectively, and both treated and untreated tailings showed almost same concentrations of Na and Ca. The addition of polymer provided major changes in the concentration of metals of polymer amended oil sands tailings for all doses as compared to unamended MFT.

5.3.3 Gravimetric water content and percent solids by mass of oil sands mature fine tailings

The initial water content of unamended MFT was 140% showing 42 percent solids by mass. The addition of 0.4% solution as discussed in Chapter 03 for various polymer doses resulted in an immediate increase in water content or decrease in percent solids by mass for all polymer doses just after polymer mixing (Figure 5 - 4).

The tailings started draining off water after the polymer mixing which resulted in an increase in percent solids by mass (Figure 5 – 4). The sand to fine ratio (SFR) of polymer amended MFT changed greatly with the addition of polymer and a lower polymer dose showed high SFR than that of high polymer dose (Chapter 4).

Though the polymer amended MFT released water for all polymer doses during first hour of polymer mixing, but all the added water in the polymer solution did not drain off. The polymer amended MFT still gave quite high water content one hour after polymer mixing as a comparison to initial water content of unamended MFT (140%). However, 500 and 700 ppm gave less water contents than that of original water content (Figure 5 - 3).

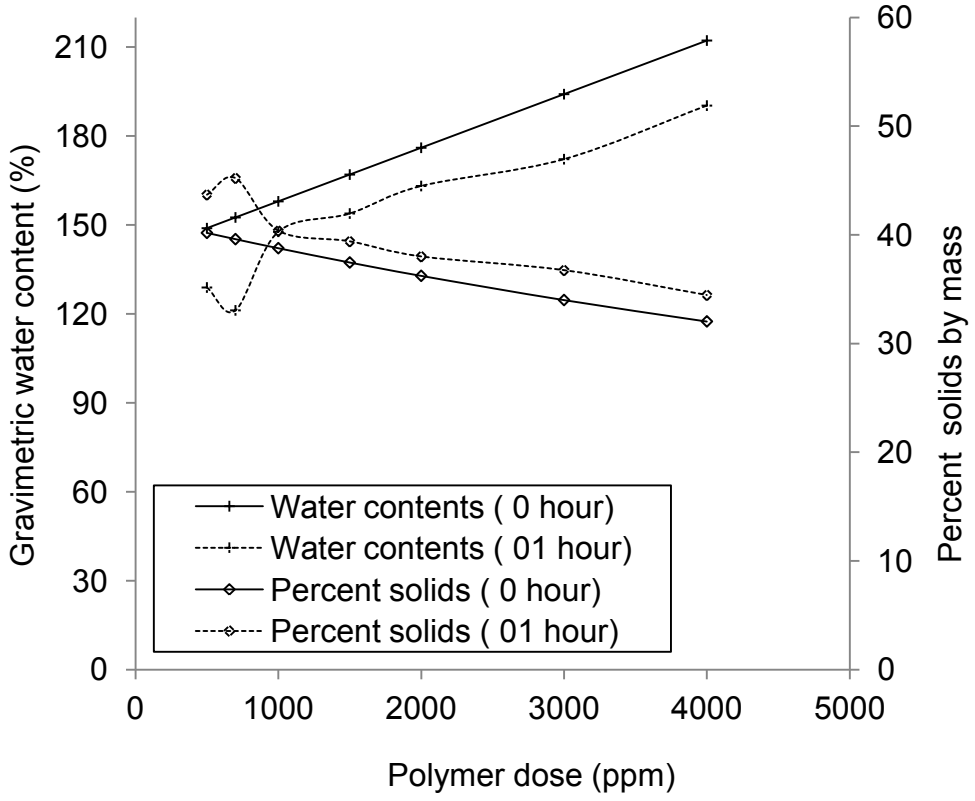

Figure 5-3: Gravimetric water content and percent solids of polymer amended oil sands mature fine tailings

The polymer doses of 700, 1000 and 1500 ppm released 115, 20, and 17 mL water respectively after one hour of polymer mixing. For a polymer dose higher

than 2000 ppm, the tailings did not show any release of water one hour after polymer mixing. However, tailings for all doses showed approximately same evaporation potential (~15 mL) one hour after polymer mixing.

5.3.4 Water potential of polymer amended oil sands mature fine tailings

The total suction of polymer amended MFT varied from 300 kPa to 210 kPa for various polymer doses one hour after polymer mixing.

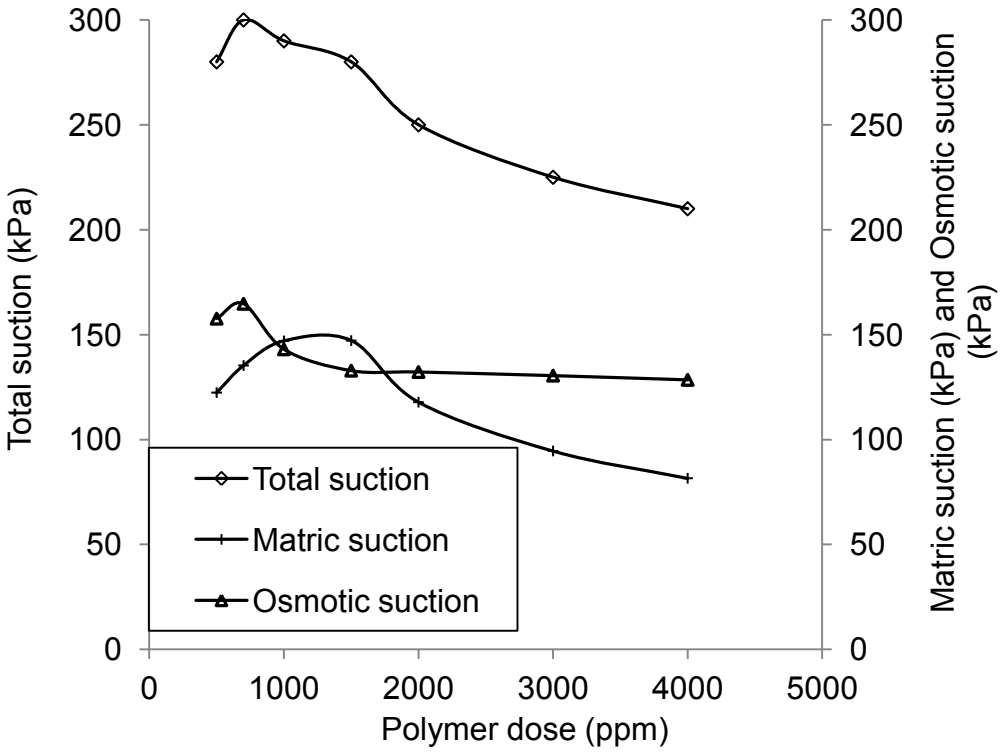

Figure 5-4: Soil water potential of polymer amended fine tailings

The tailings gave slightly higher suction for lower polymer dose in comparison to higher polymer dose; however the difference was not too large. The tailings showed higher osmotic suction in comparison to matric suction, however, minor variations were noted in osmotic suction for various doses (Figure 5 – 4)

The osmotic suction depends upon the concentration of dissolved salts in a material (Fredlund and Rahardjo 1993). The osmotic suction of tailings might be biased to some extent as the saturation extract procedure was used to transform the electrical conductivity of pore water to osmotic suction corresponding to natural water content of tailings. Fredlund and Rahardjo (1993) reported that the saturation extract procedure was unable to provide exact measurement of osmotic suction.

The polymer amended tailings were almost fully saturated due to higher water content, so they showed minimum matric suction. The matric suction of polymer amended MFT one hour after polymer mixing was also biased a little as the WP 4 Dewpoint Potentiameter measured total suction with an accuracy of ± 0.1 (Figure 5 - 4). Murray and Sivakumar (2010) stated that the sum of osmotic suction and matric suction might not be true replicate of total suction measured individually for a particular material.

In comparison to polymer amended MFT, the unamended MFT provided a total suction of 190 kPa corresponding to a water content of 140% which was comparable to polymer amended tailings.

5.3.5 Yield stress of oil sands mature fine tailings

The slump tests were performed to examine the yield stress, dimensionalized slump, solids content and gravimetric water content of unamended MFT (Figure 5 – 5).

Figure 5-5: Pictorial views of slump tests for unamended oil sands mature fine tailings

The unamended MFT behaved like flowing liquid for water content greater than 84%. The yield stress was only 2 Pa for 84% water content (Figure 5 – 6). Goodbille and Moffett (2014) reported that the unamended MFT was unable to provide strength for solids content less than 60%.

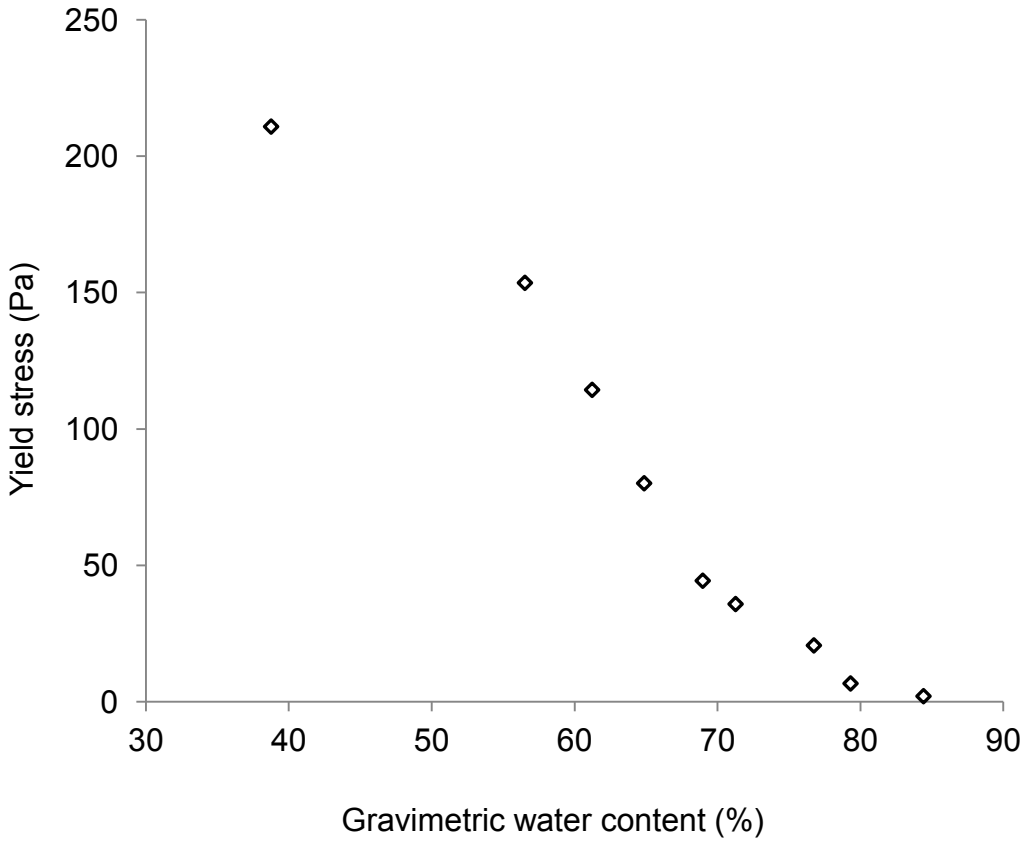

Figure 5-6: Yield stress and gravimetric water content relationships of unamended oil sands mature fine tailings

The tailings showed minimum slump (0.03%) for a water content of 39% giving maximum yield stress of 211 Pa corresponding to 34 percent water content (Figs 5 – 6 and 5 - 7). Practically, unamended MFT needs several decades enable getting the particular water content of 84% in tailings management facilities (Jeeravipoolvarn 2005).

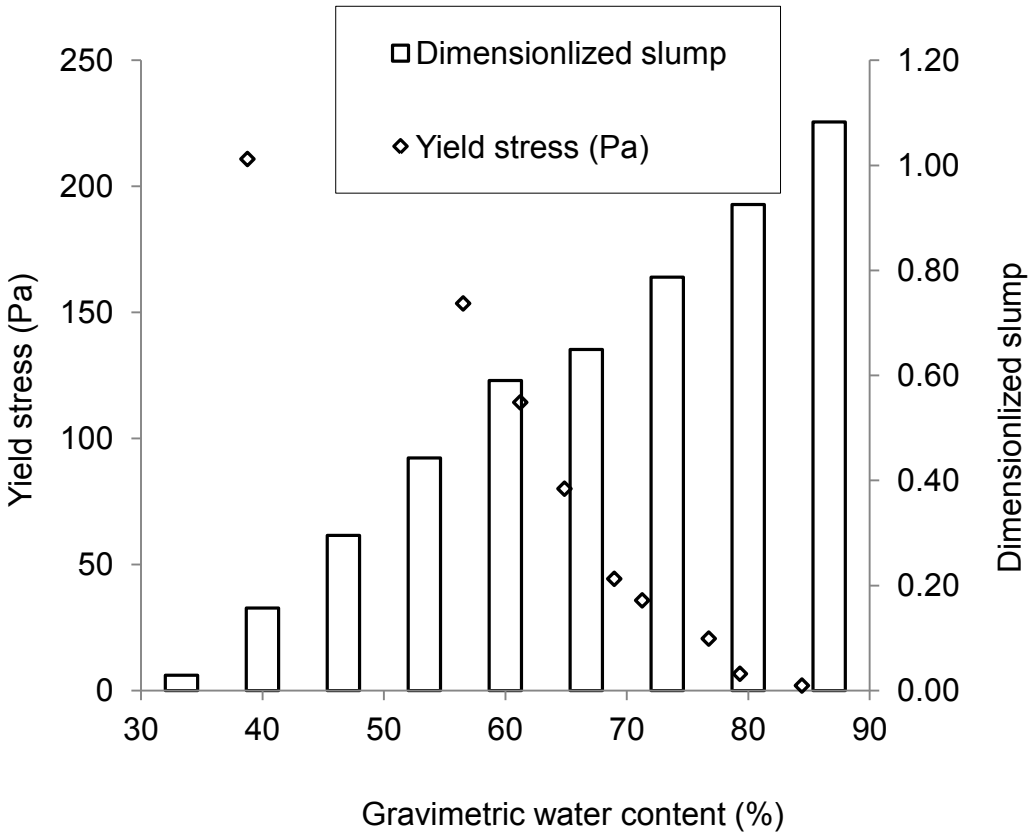

Figure 5-7: Interactions of yield stress , dimensionalized slumps and water content of unamended oil sands mature fine tailings

The yield stress, dimensionalized slump, percent solids by mass and gravimetric water content of polymer amended MFT were examined for various polymer doses (Figs 5 – 9 and 5 - 10). The polymer dose of 700 ppm gave maximum yield stress of 68 Pa and the water content was 121 one hour after polymer mixing. The yield stress was less for polymer doses more or less than 700 ppm. The stress varied between 68 and 2 Pa for polymer doses ranging from 500 – 4000 ppm. The polymer dose of 4000 ppm showed minimum yield stress of 2 Pa for 190% gravimetric water content (Figure 5 - 9).

Figure 5-8: Pictorial view of slump tests of polymer amended MFT for various polymer doses

However, the difference in yield stress of treated tailings was not too large for polymer doses ranging from 500 – 1000 ppm. The polymer amended MFT provided higher slumps beyond a polymer dose of 1500 ppm and the tailings were also appeared so thin for 4000 ppm one hour after polymer mixing. The polymer dose of 700 ppm provided smooth and stabilized slump in comparison to all other doses (Figure 5 - 8).

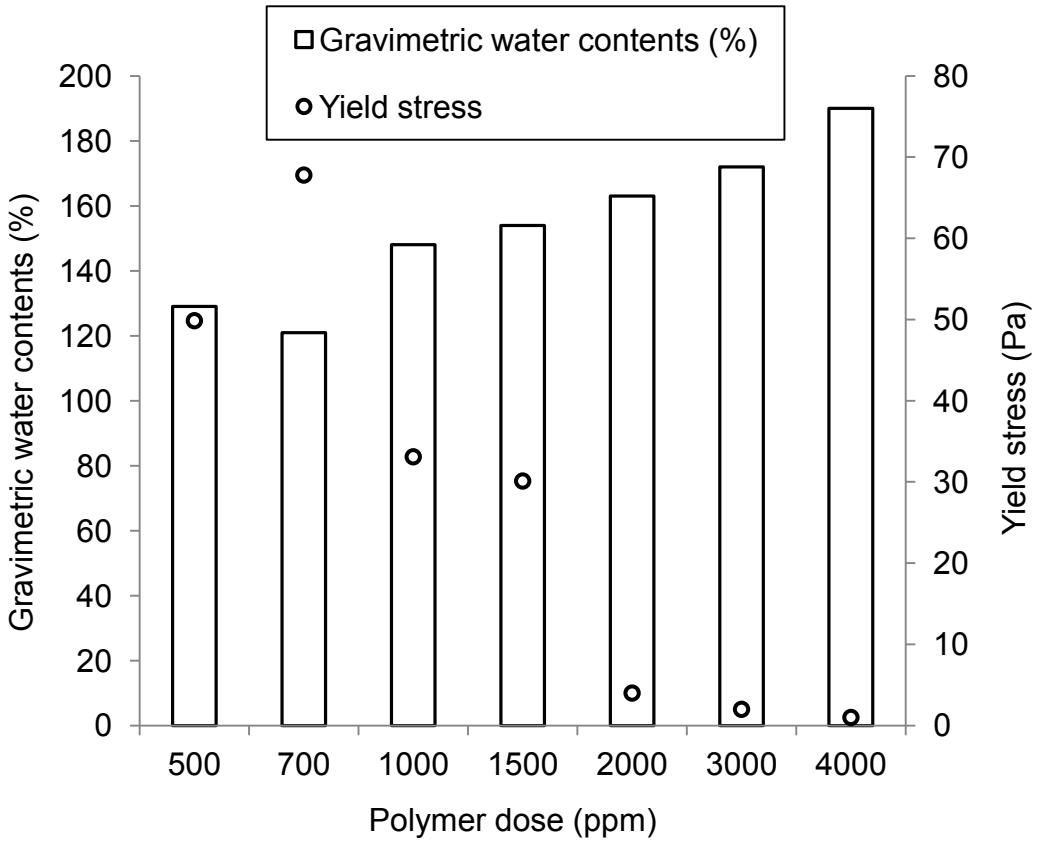

Figure 5-9: Interactions of yield stress, gravimetric water content and polymer dose of polymer amended fine tailings

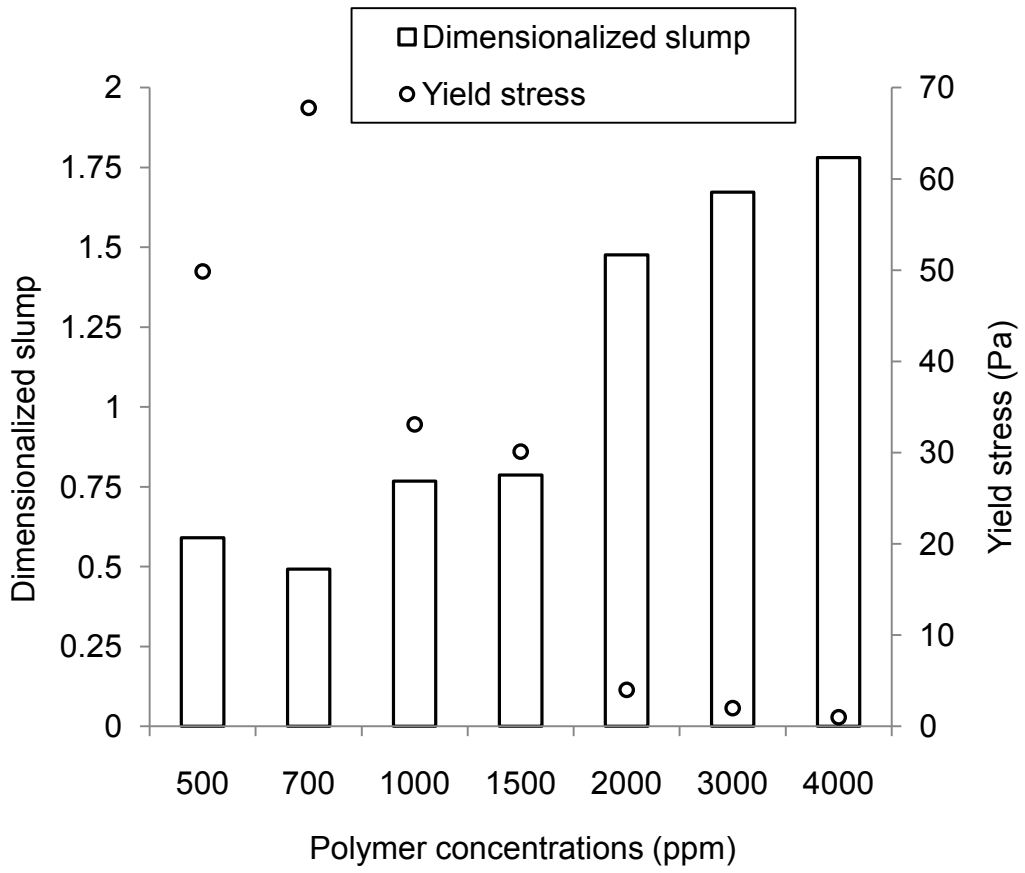

Figure 5-10: Interactions of yield stress, dimensionalized slump and polymer dose of polymer amended oil sands mature fine tailings

For slump tests, the polymer amended MFT provided peak yield stress (68 Pa) for 700 ppm corresponding to dimensionalized slump of 0.49 and 121% water content or we can say that 700 ppm is the reference value/best dose. Goodbill and Moffett (2014) examined the strength of silica treated oil sands fine tailings and discussed that the tailings showed shear strength of 100 Pa one hour after additive treatment. This difference in yield stress was attributed to use of different flocculant and thickening procedures.

Jeeravipoolvarn (2010) observed that the behaviour of treated tailings was directly related to the effect of flocculants in ILTT process. Generally the changes in fabric and water content of treated tailings contributed to these variations in slumps as the tailings for various doses showed entirely different flocs formation as discussed in Section 5.3.7.

The high polymer treated tailings dewatered less in comparison to low polymer treated tailings. The larger water release and higher density explains the higher slumps for the lower polymer dose materials, rather than any structure effect imparted by the polymer (Figure 5 -10).

Figs 5 – 11 and 5 - 12 show relationships between yield stress and void ratio of polymer amended and unamneded oil sands fine tailings respectively. As in Figure 5 – 11, the tailings for 700 ppm showed maximum yield stress relating to void ratio of 3.38, however for unamneded MFT, the void ratio and yield stress relationship varied linearly (Figure 5 – 12).

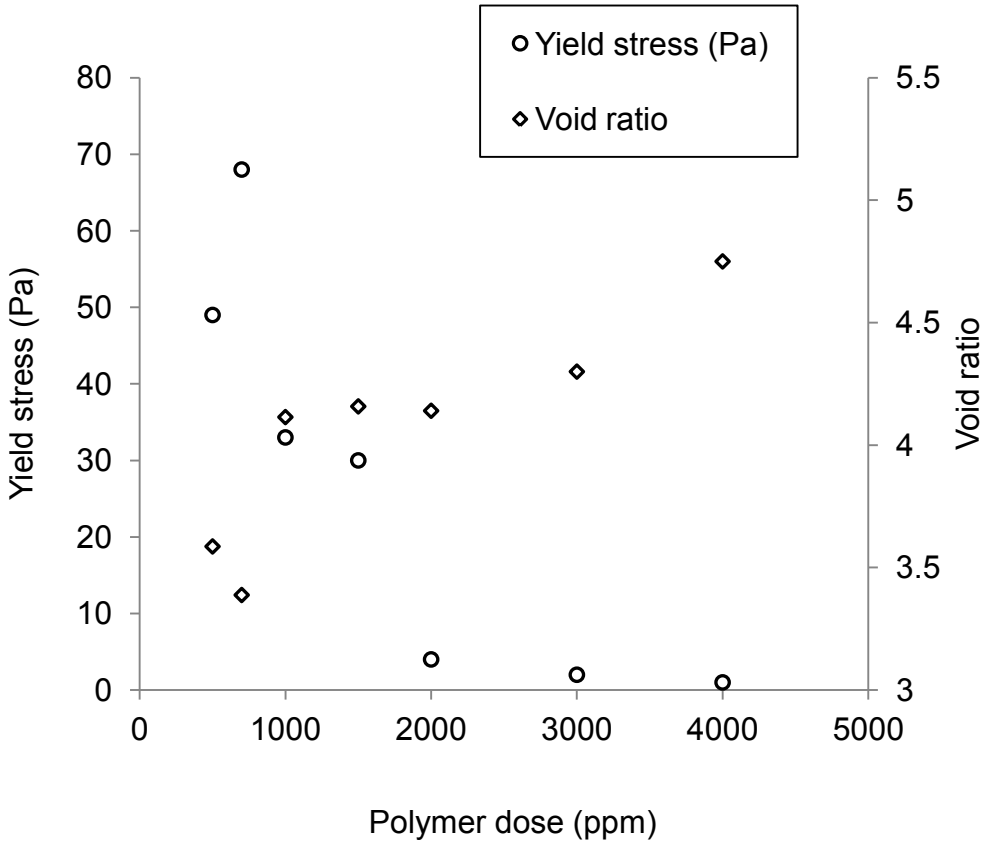

Figure 5-11: Yield stress and void ratio relationships of polymer amended oil sands tailings

The void ratio of polymer amended MFT varied between 3.38 and 4.75 for polymer doses ranging from 500 to 4000 ppm (Figure 5 - 11), and correspondingly, the amended tailings provided almost 100% degree of saturation for all doses. It was quite natural as the water contents were quite high in the treated tailings one hour after polymer mixing (Figure 5 - 9). The polymer dose of 700 ppm showed minimum void ratio (3.38) in comparison to all other polymer doses (Figure 5 -11).

The void ratio increased with an increase in polymer dose except for a slight decrease for 700 ppm; however, the change in initial void ratio as a function of dose was small.

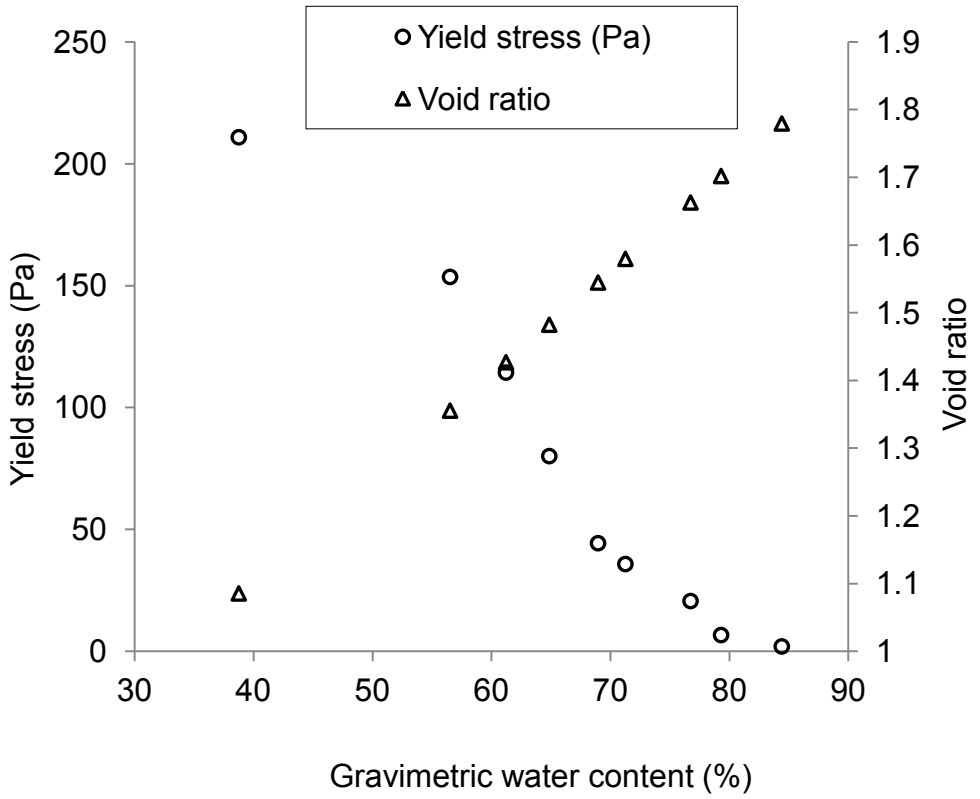

Figure 5-12: Yield stress and void ratio relationships of unamneded oil sands MFT

5.3.6 Hydraulic conductivity of oil sands mature fine tailings

The hydraulic conductivity of polymer amended MFT varied from 3.5 x 10^{-06} cm / sec to 7.8 x 10^{-06} cm / sec. for 1 hour after polymer mixing for various polymer doses (Figure 5 - 13).

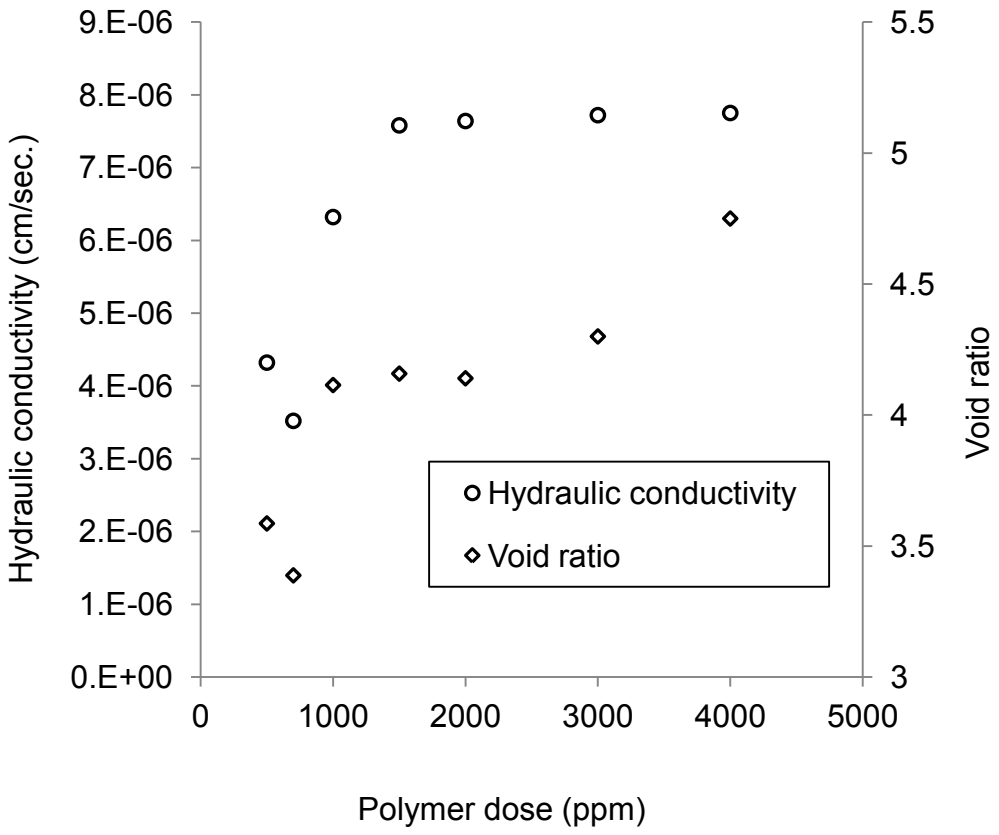

Figure 5-13: Interactions of void ratio, hydraulic conductivity and polymer dose of polymer amended oil sands mature fine tailings

Overall, the hydraulic conductivity of tailings increased for an increase in polymer dose and the polymer dose of 4000 ppm showed higher hydraulic conductivity of 7.58 x 10^{-06} cm / sec. and correspondingly, the polymer dose of 700 ppm provided minimum hydraulic conductivity of 3.52 x 10^{-06} cm / sec., (Figure 5 -13). The higher dewatering potential of 700 ppm resulted in its lower void ratio, which correspondingly reduced the k value. Mitchell and Soga (2005) stated that the variations in fabric, void ratio and water content influenced the hydraulic conductivity of a material from 2 to 3 orders of magnitude.

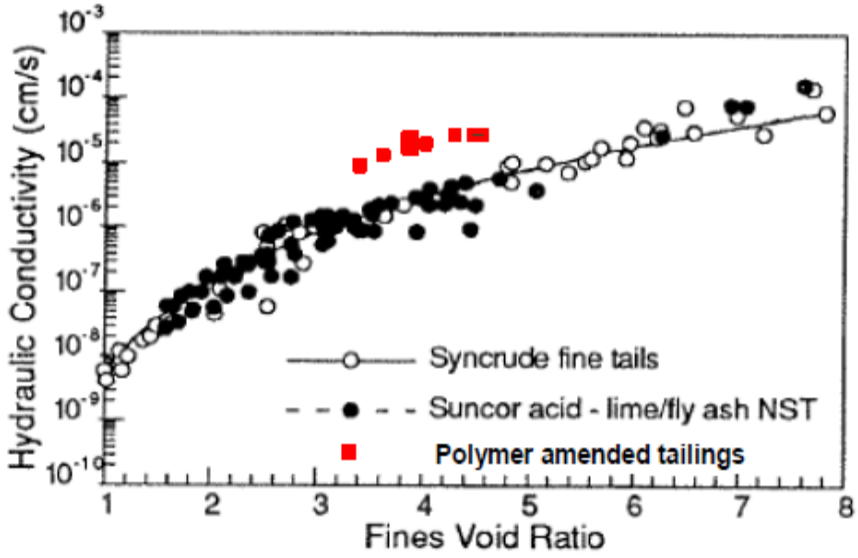

Figure 5-14: Comparison of Hydraulic conductivity of polymer amended tailings and Suncor acid – lime / fly ash NST

The test results showed that though the change in polymer dose changed the hydraulic conductivity of tailings, but the difference in k was not too influential; showing variation in the same order of 10^{-06} for all polymer doses one hour after polymer mixing.

The reported void ratios might be somewhat higher than the true values, as the tailings consolidated further in permeater due to the length of the test (24 hours). The k tests of tailings for each sample continued up to 24 hours, and the polymer dose of 700 ppm showed maximum settlement of 3 cm in the permeater. However, the settlement of various tailings varied from 1.56 to 3 cm during the tests. Suthakar and Scott (1996) reported the hydraulic conductivity of Suncor acid – lime / fly ash tailings and Syncrude fine tailings, and as a comparison, the

polymer amended oil sands fine tailings showed quite higher k values for a particular void ratio (Figure 5 – 14).

5.3.7 Microstructure of polymer amended oil sands mature fine tailings

The scanning electron micrograph of polymer amended oil sands mature fine tailings showed that the addition of polymer changed the fabric of the tailings and the features of the fabric appeared different for various polymer doses one hour after polymer mixing (Figs 5 -15 to 5 - 18). The size and pattern of inter assemblage pores looked different for various polymer doses. For high polymer doses such as 4000 ppm, the fabric appeared scattered and over flocculated (a network structure is seen but no aggregation is seen) and any apparent aggregation was not observed in its fabric (Figure 5 – 18). Comparatively, for 500 ppm, the flocs were smaller in size (Figure 5 – 15).

Mitchell and Soga (2005) classified aggregations or flocs as regular and irregular depending upon the circularity of aggregations. The tailings for polymer doses of 500, 700, 1000 and 1500 ppm showed different flocs formation than that of 4000 ppm, and SEM micrographs of these tailings showed that the size of aggregation increased for an increase in polymer dose from 500 to 1500 ppm. Comparatively, 1500 ppm showed more irregularity in aggregation to that of other doses, however, inter-assemblage and interparticle pores were quite visible in all tailings (Figs 5 -15 to 5 - 17).

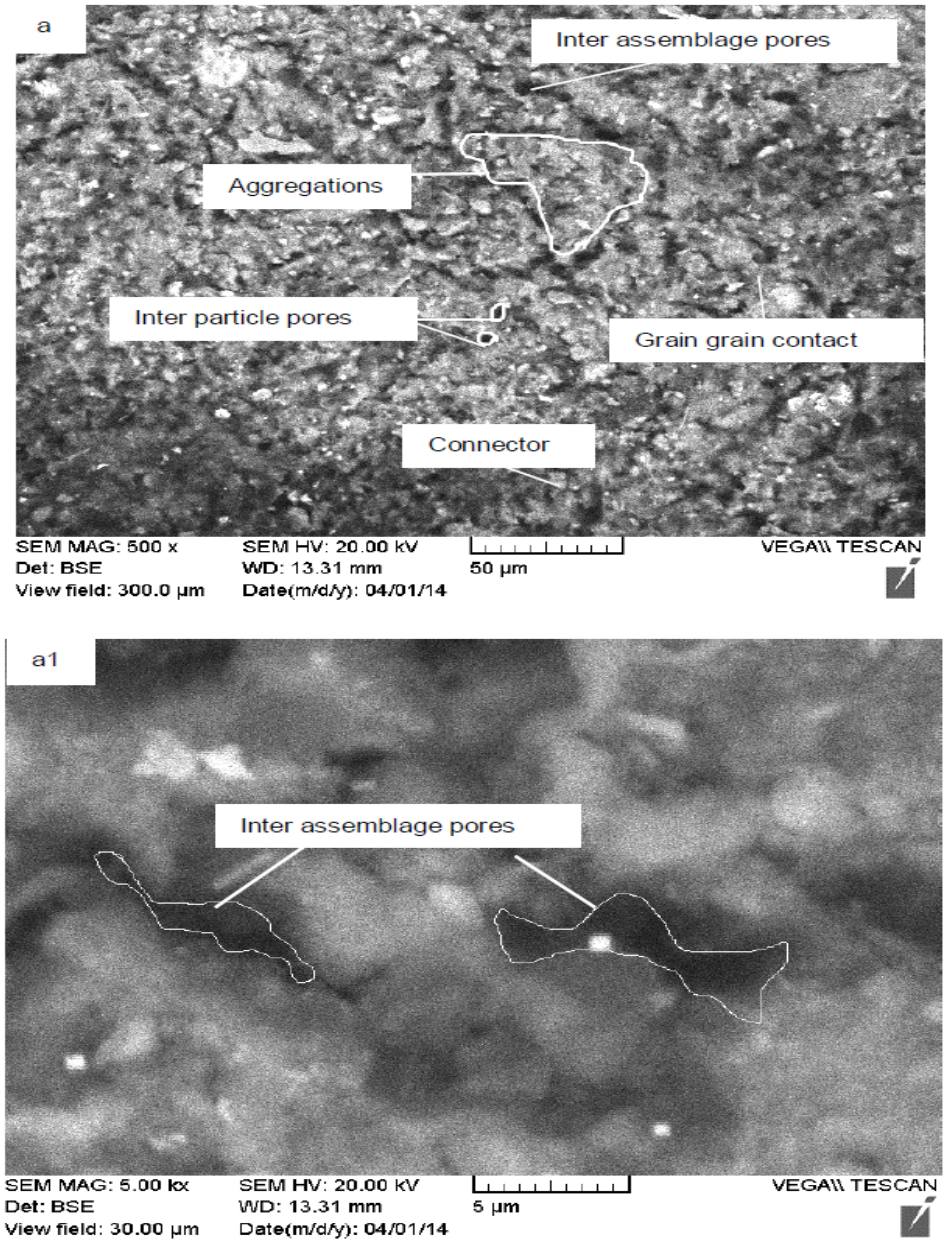

Figure 5-15: Backscattered environmental scanning electron micrographs of fine tailings for a polymer dose of 500 ppm; a –magnification - 500 x, scale - 50 µm, view field - 300 µm; a1 -magnification - 5 kx, scale - 5 µm, view field - 30 µm

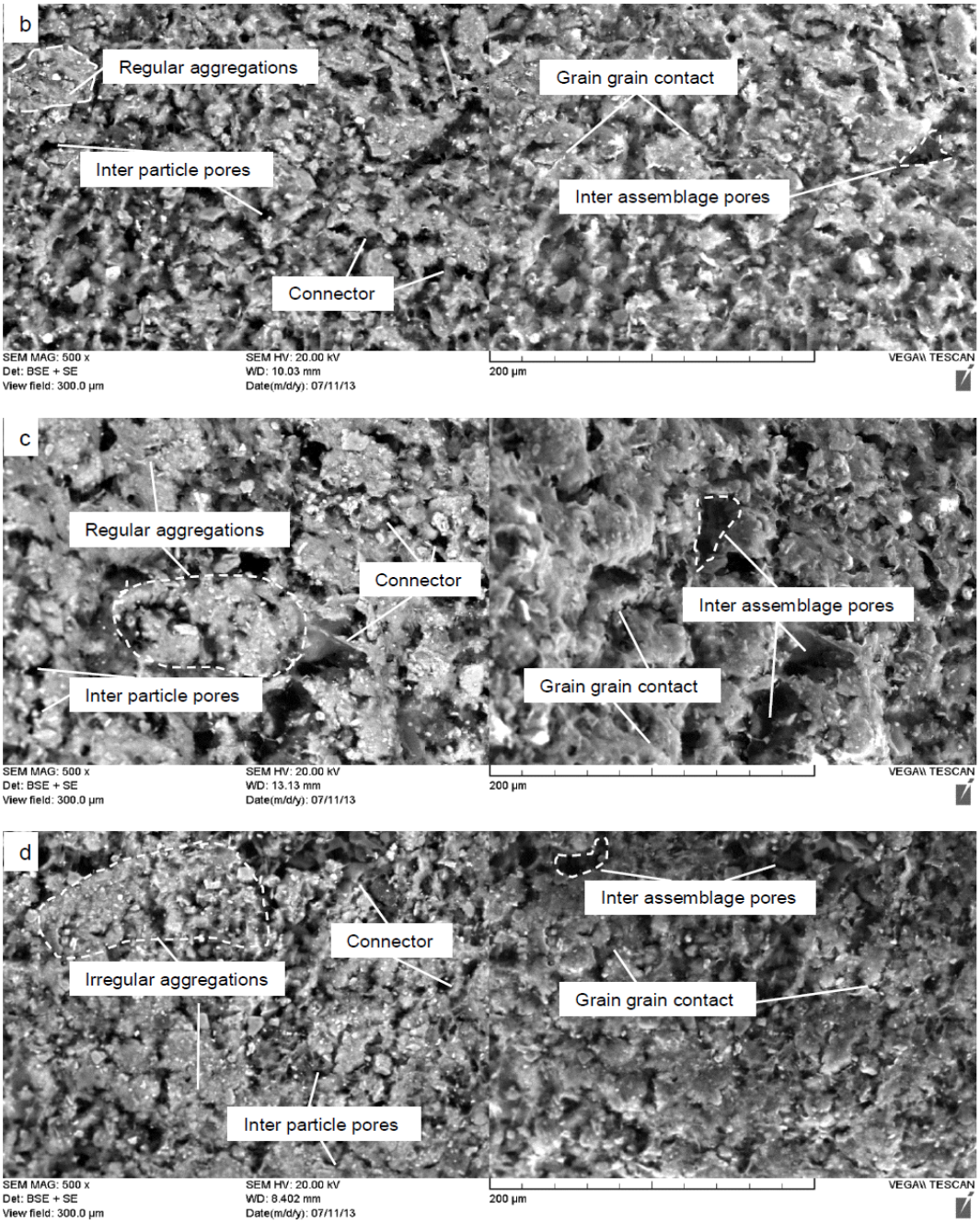

Figure 5-16: Environmental scanning electron micrographs of fine tailings; left - backscattered electron, right – secondary electron, (b – 700 ppm, c – 1000 ppm, d – 1500 ppm); magnification - 500 x, scale - 200 µm, view field – 300 µm

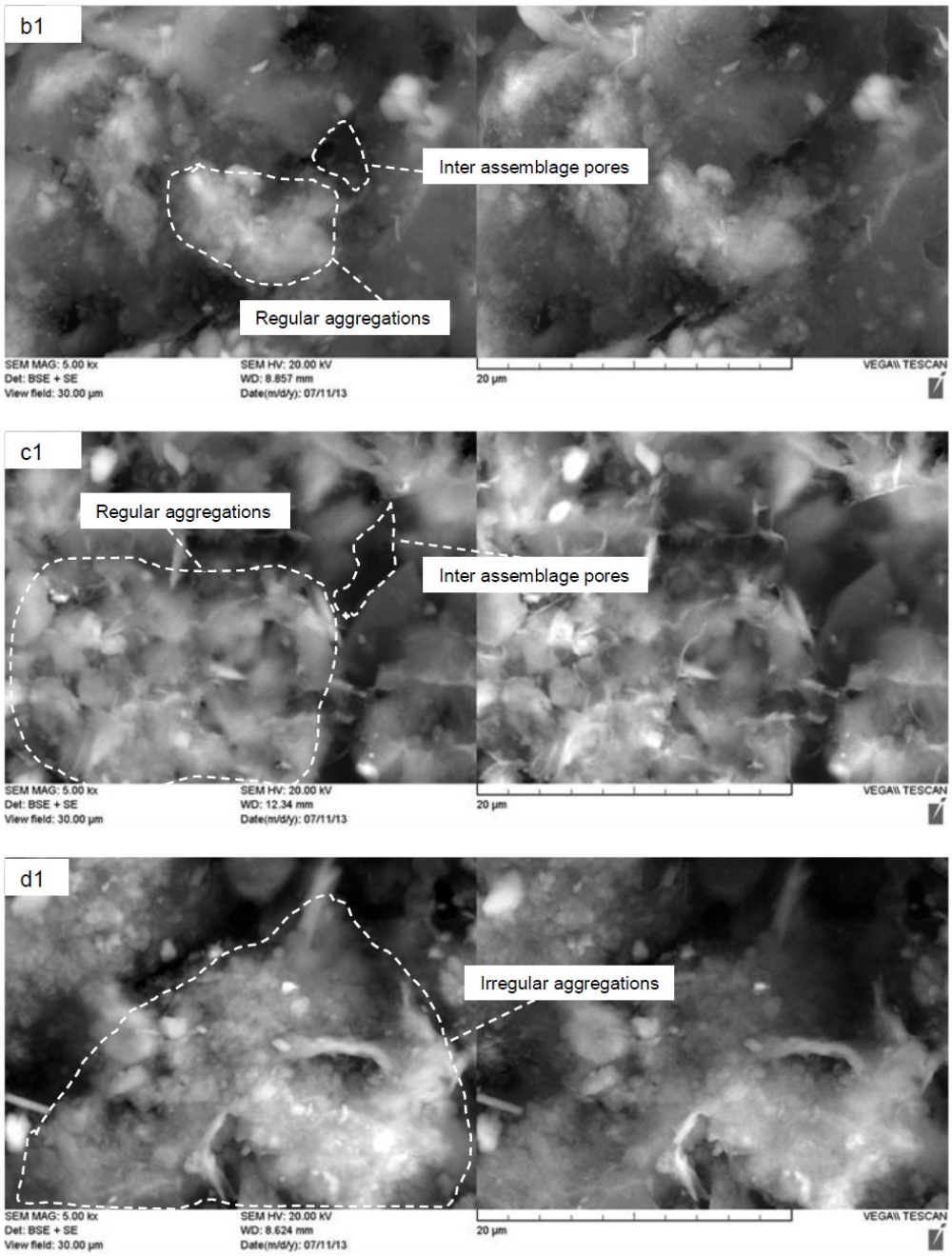

Figure 5-17: Environmental scanning electron micrographs of fine tailings; left – backscattered electron, right – secondary electron, (b1 – 700 ppm, c1 – 1000 ppm, d1 – 1500 ppm); magnification - 5 kx, scale - 20 µm, view field – 30 µm

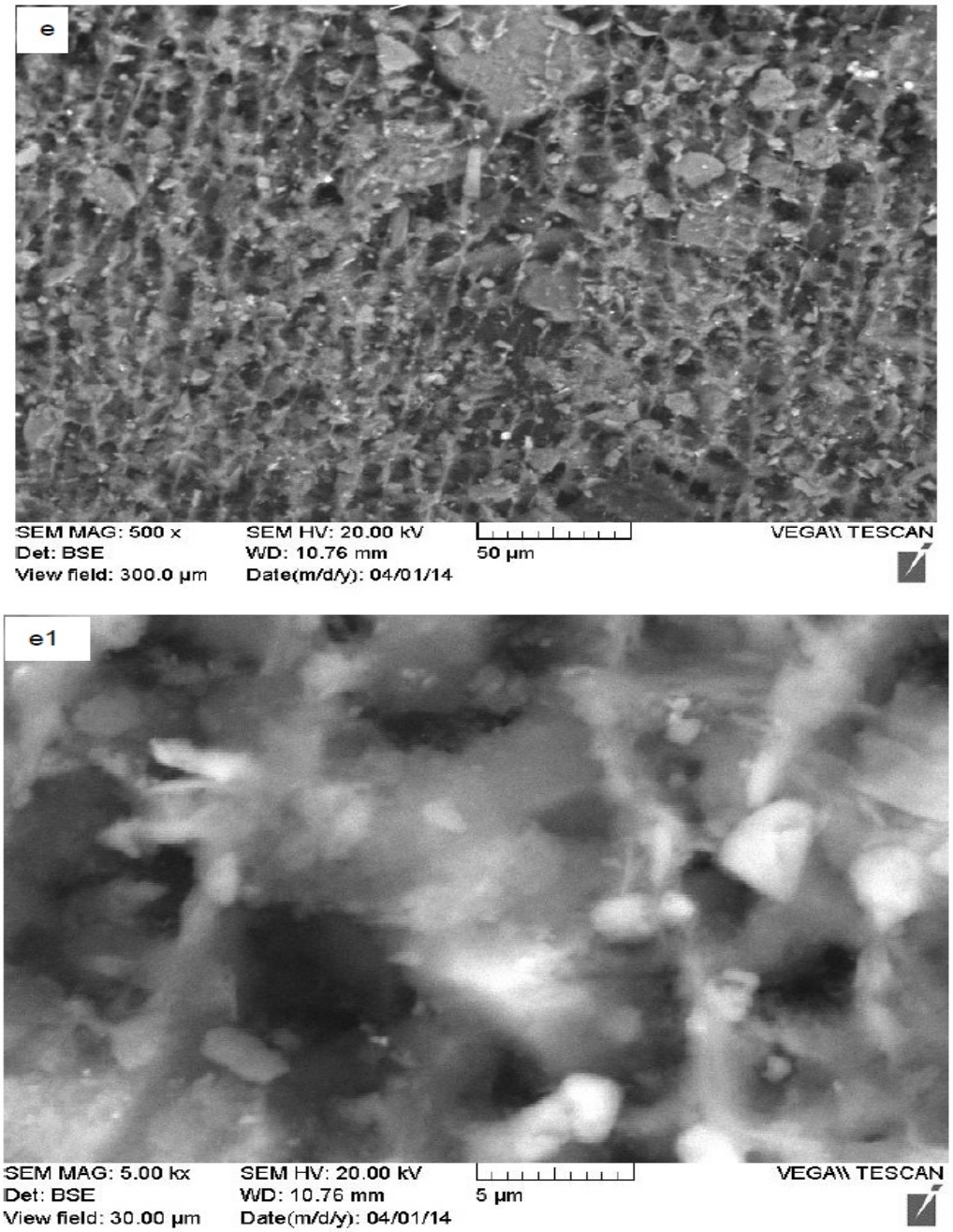

Figure 5-18: Backscattered environmental scanning electron micrographs of fine tailings for a polymer dose of 4000 ppm; a –magnification - 500 x, scale - 50 µm, view field - 300 µm; a1 -magnification - 5 kx, scale - 5 µm, view field - 30 µm

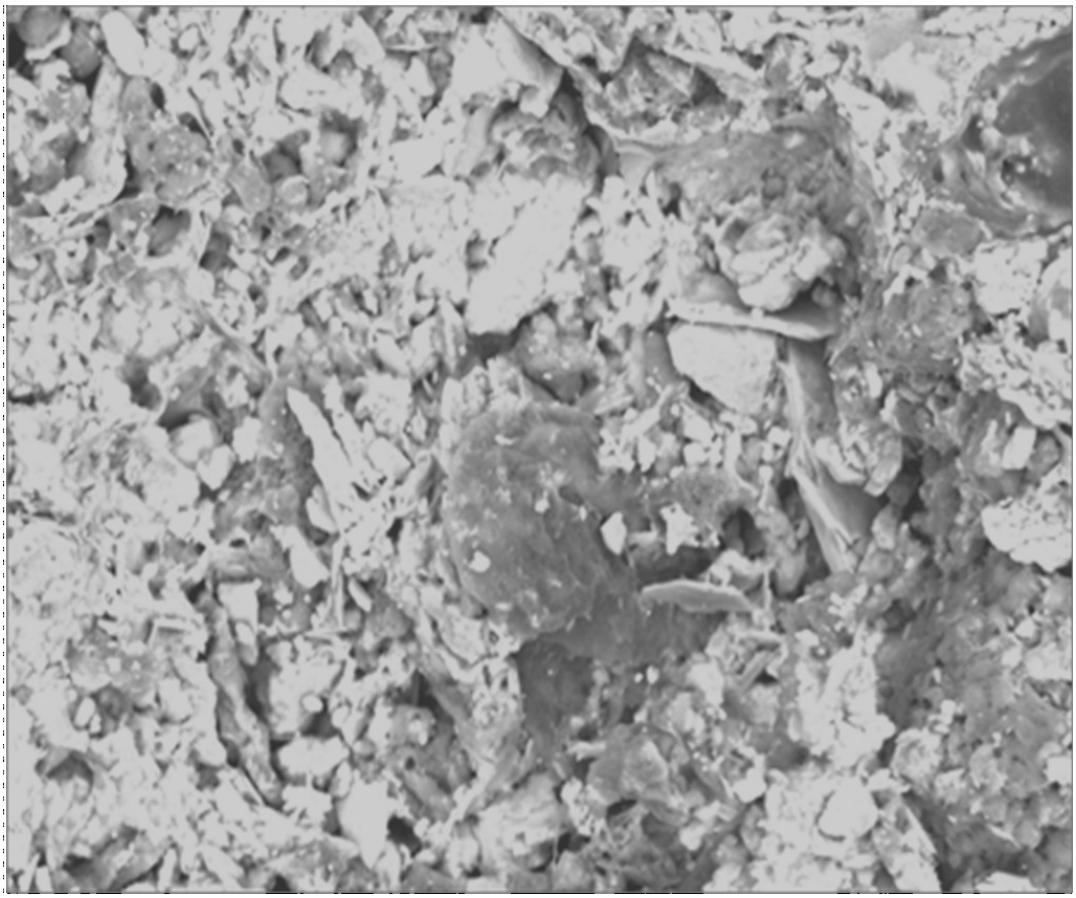

Figure 5-19 : Backscattered environmental scanning electron micrograph of unamended oil sands mature fine tailings; magnification - 5 kx, scale - 5 µm, view field - 30 µm

All tailings for various doses provided more likely edge to face and edge to edge flocculated and aggregated fabric. Moreover, the polymer amended tailings showed entirely different fabric (Figs 5 -15 to 5 - 18) when compared to unamended tailings (Figure 5 - 19).

The flocculated tailings for each polymer dose behaved in different fashion due to different flocs configuration, structural as well textural arrangement and it was the change in fabric as a result of polymer addition which enabled tailings to give

different dewatering potential, and consequently a gain in strength within hours irrespective of quite high water content. Table 5 – 2 shows the summary of test results of polymer amended tailings one hour after polymer mixing.

Table 5-2: Summary of test results of polymer amended oil sands fine tailings

Features	Parameters	Units	Polymer dose (ppm)						
			500	700	1000	1500	2000	3000	4000
			One hour after tailings deposition						
Macroscopic	Gravimetric water contents	%	129	121	148	154	163	172	190
	Solids content	%	44	45	40	39	38	37	34
	Cu. evaporation	mm	0.5	0.8	0.5	0.5	0.5	0.5	0.5
	Cu. dewatering	mm	2.09	2.77	0.15	0.06	0.03	0.03	0.03
	Void ratio, e	-	3.58	3.38	4.11	4.15	4.14	4.30	4.75
	Total suction	kPa	280	300	290	280	250	225	210
	Dimensionalized slump*	-	0.59	0.49	0.76	0.78	1.47	1.67	1.78
	Yield stress	Pa	49	68	33	30	4	2	2
	Hydraulic conductivity	cm /sec	4.32E-06	3.52E-06	6.38E-06	7.58E-06	7.64E-06	7.72E-06	7.75E-06
Microstructure	ESEM	µm	Small and scattered aggregation	Regular aggregation	Regular aggregation	Irregular aggregation	-	-	Over flocculated
*** aspect ratio – 1**									

5.4 Interaction of macroscopic and microstructure features of polymer amended oil sands mature fine tailings

The tailings showed an increase in void ratio for an increase in polymer dose. The lower polymer doses drained off more water due to the formation of regular and smaller aggregation, which consequently provided lower void ratio. The formation of larger and irregular aggregation suppressed sedimentation, consequently reducing dewatering and maintain higher void ratio, which resulted in an increase in hydraulic conductivity.

Mitchell and Soga (2005) stated that the interassemblage pore and transassemblage pore controlled the hydraulic conductivity whereas regular aggregation and interassemblage pores controlled the yield stress. The formation of larger irregular aggregation and high void ratio for high polymer doses impeded settling, which resulted in their lower yield stress. The percent solids by mass were higher (low void ratio) for 700 ppm in comparison to other doses due to the formation of smaller regularized aggregation and consequent higher density 1 hour after polymer mixing. However, at a given density, the polymer amended tailings showed higher yield stresses as compared to unamended MFT. Therefore, fabric as well as density affected the yield stress.

The ImageJ analysis of SEM micrographs as in Figure 5 – 20 validated the above discussion showing that the microporosity of tailings increased for an increase in polymer dose. The polymer dose of 4000 ppm showed quite high

microporosity, and it might be due to over flocculation. The tailings for 700 ppm polymer dose showed lower microporosity in comparison to higher doses. However, the microporosity test results might be exaggerated somewhat because at this stage, the influence of flocs was quite visible in the tailings, and most probably in higher dose; which provided higher microporosity as expected at this stage of tailings deposition.

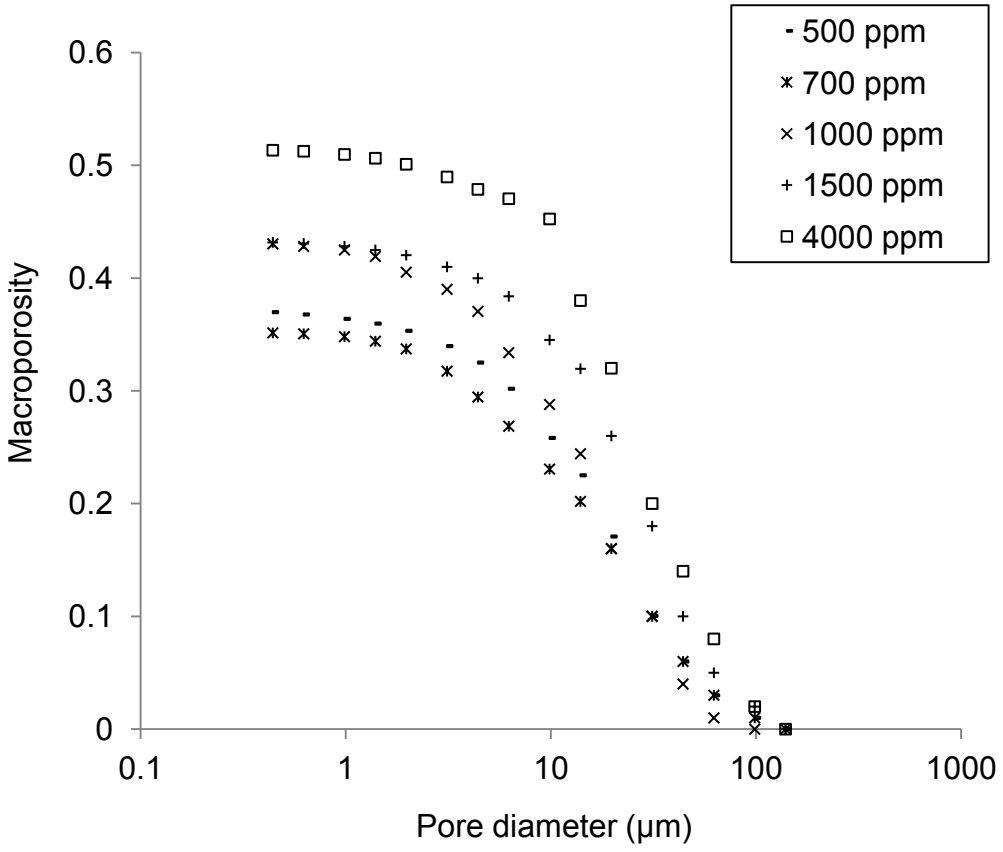

Figure 5-20: Gray pixel analysis of polymer amended tailings one hour after polymer mixing

The gray pixel analysis was performed with ESEM micrographs of 0.5 kx magnifications, 1536 x 648 resolutions and 300 μm view field. Figures (5 – 16, 5 – 17 and 5 – 19) present ESEM images used in analysis. The micrographs of tailings were optimized adjusting for threshold to clearly distinguish the particles, background and adjacent grains boundaries.

At this stage, i.e., one hour after polymer mixing, the formation of flocs definitely influenced the drain off potential of polymer amended tailings for various doses which resultantly changed the hydraulic conductivity, void ratio and yield stress. However, further release of water or change in desiccation level may modify the fabric of polymer amended tailings greatly, and this will be discussed in succeeding chapters.

5.5 **Conclusions**

The addition of polymer changed the features of tailings fabric and the tailings released water due to the agglomeration of colloids and flocs formation. The tailings for various doses provided different drain off potential due to different fabric, and an increase in dose was correlated with larger and more irregular flocs. Though the water content of polymer amended tailings for all polymer doses was quite high one hour after polymer mixing but the changed features of the fabric enabled to raise their yield stress greatly.

The tailings for various polymer doses were unable to provide major variations in the total suction but the osmotic suction dominated the total suction during earlier stage of deposition. Furthermore, the addition of polymer lowered the metal ingredients and raised the alkalinity of the tailings but it did not change the inorganic and organic content of tailings. The change in pore water chemistry like lowering the pH value may further increase the agglomeration behavior of treated tailings. The replacement of Na with Ca may increase the fertility of the tailings. The strength of tailings can be raised increasing the organic content making fiber to act as reinforcement.

Both the amount of dewatering and the yield stress were highest for a polymer dose of 700 ppm. This was apparently due to optimal floc formation. The higher doses resulted in larger and more irregular floc formation. The formation of larger flocs actually impeded sedimentation.

The optimal dose of 700 ppm was not the same as identified in the previous chapter in terms of Atterberg limits and grain size. The polymer dose of 800 ppm showed higher SFR in comparison to 700 ppm. Succeeding chapters will investigate longer term dewatering due to self-weight consolidation and desiccation of polymer amended tailings.

Chapter 6. Evolution of yield stress and microstructure of polymer amended oil sands mature fine tailings for short term dewatering

Abstract:

The mechanisms such as flocculation, short term self-weight consolidation, desiccation and long term consolidation contribute to strength gain of polymer amended oil sands fine tailings. Optimization of polymer dose is usually done for a relatively short time. It is possible that optimization for short term dewatering may not result in optimization for long term dewatering. In this study, the yield stress and microstructure behavior of oil sands fine tailings were monitored for short term consolidation (up to 6 days). Polymer doses of 500, 700, 1000 and 1500 ppm were used in the study.

The test results showed that the tailings released water which consequently increased their yield stress during earlier stage of deposition. The polymer dose of 700 ppm showed marginally more dewatering than that of other doses one hour after polymer mixing. This was similar to earlier chapters, where the 700 ppm dose indicated a higher degree of dewatering at 1 hour after sample preparation with respect to all other doses. Higher doses (1000 and 1500 ppm) showed substantially less dewatering and 500 ppm showed comparable dewatering to 700 ppm. ImageJ software was used to perform the gray pixel analysis of scanning electron micrographs. This was compared to MIP data.

Finally, the fabric data was used to explain the variability in dewatering for different polymer doses.

6.1 Materials preparation and methods used

The polymer amended MFT was prepared following the protocol as discussed in Chapter 3. After mixing, the prepared MFT was transferred to cylindrical columns to perform the microstructure and macroscopic tests. A drain off system was provided at the bottom of each column to record the potential release of water from tailings.

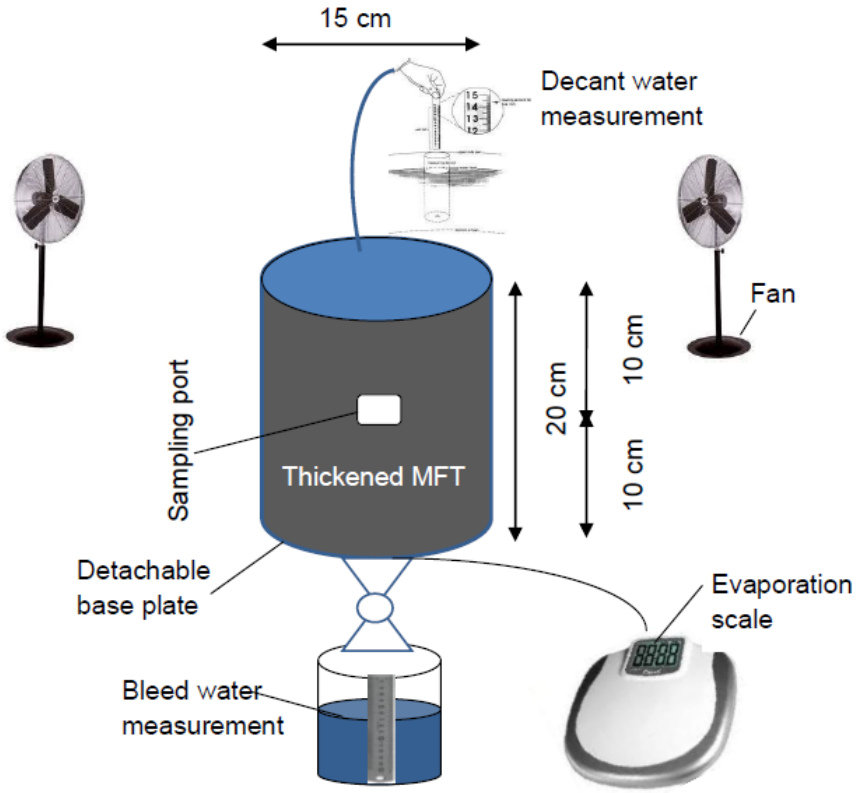

Figure 6-1: Schematic of thin lift experiment

The bottom of each column was removed while performing the slump tests. Every 24 hours, any water accumulated at the surface (decant water) of the tailings was collected by using a small beaker (250 ml) and a syringe. A graduated cylinder was used to determine the quantity of water. Two fans were used to control the potential evaporation rate of tailings in the laboratory. Figure 6 – 1 shows a schematic of the experimental setup.

Figure 6 – 2 shows the experimental set up to examine the yield stress of polymer amended tailings during short term dewatering. The cylindrical columns of 15 cm dia., and 20 cm depth (aspect ratio ~1.33) were used for this purpose. The tests were conducted every 24 hours, starting from one hour after polymer mixing and continuing up to 6 days. Triplicate samples were generated for each specimen to perform the slump tests and an average slump was reported in this study.

For hydraulic conductivity measurements, the tailings were prepared in cylindrical columns of 15 cm diameter and 30 cm depth. The polymer amended MFT was transferred to the permeater after 01 and 144 hours of polymer mixing and the test was continued for 24 hours for each polymer dose. Soil water potential was measured after each slump test using a WP4 Dewpoint PotentiaMeter..

The drainage (release of water from bottom) and surface flux (evaporation + decant water) from each column were monitored to estimate the total water lost. The overall gravimetric water content and void ratio were obtained by weight and by measuring vertical settlement. Destruction of column replicates facilitated measurement of depth profiles of water content, total and osmotic suction. Scanning electron microscopy (SEM) and mercury intrusion porosimetry (MIP) techniques were used to examine the microstructure of tailings

Figure 6-2: Laboratory experimental set up to examine the yield stress of polymer amended tailings for short term dewatering

For microstrcuture and suction tests, the samples were collected at the depth of 10 cm from the top. A small mold of 1 cm^3 was used to collect the samples from the columns. For MIP and SEM tests, the freeze dried samples were used. The freeze dried samples were coated with gold palladium and then Tescan Vega-II XMU was used to perform SEM tests.

An AutoPore IV 9500 porosimeter was used to perform MIP tests. ImageJ software was used to perform the gray pixel analysis of SEM images.

6.2 Results and discussions

6.2.1 Dewatering potential:

Total dewatering is sum of drainage collected from the bottom columns, and total surface flux (evaporation and bleed water) reporting to the surface of the tailings. The polymer dose of 500 ppm showed higher drainage releasing 15 mm of water and in comparison to this, the polymer doses of 700, 1000 and 1500 ppm released 13, 5 and 4 mm of water 144 hours after polymer mixing. Drainage potential for the polymer doses of 500 and 700 ppm was quite high in the beginning and the tailings for polymer dose of 700 ppm reached their 40% drain off potential just after one hour, and the doses of 500 and 700 ppm attained almost 62 and 72% drain off potential respectively 24 hours after tailings deposition. For first 24 hours, the dewatering rate for all doses varied linearly, and the doses of 1000 and 1500 attained their maximum drainage after 72 hours;

comparatively, the polymer doses of 500 and 700 ppm still showed a small release of water after 144 hours of tailings deposition (Figure 6 – 3). Mizani et al. (2013) observed similar findings and reported that the lower polymer doses showed more dewatering potential in comparison to higher doses.

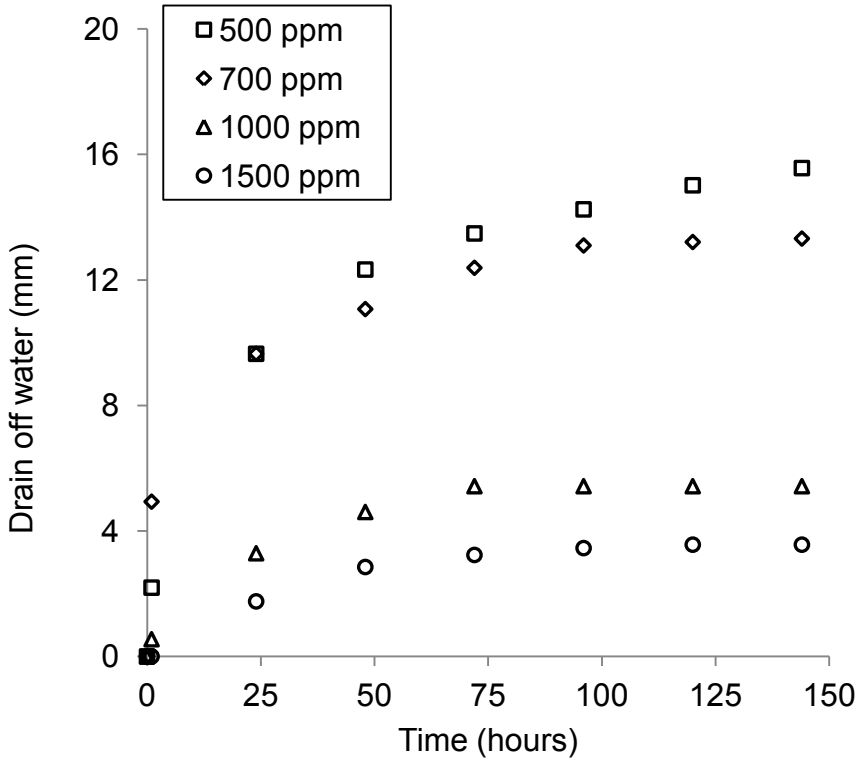

Figure 6-3: Cumulative bottom drainage for short term dewatering

Figure 6 – 4 shows the cumulative surface flux (evaporated and collected water) of tailings. The rate of consolidation water reporting the surface exceeded the evaporation rate for the first two days. Subsequently, surface flux more and less equaled the potential evaporation rate for the remainder of the experiment for all polymer doses.

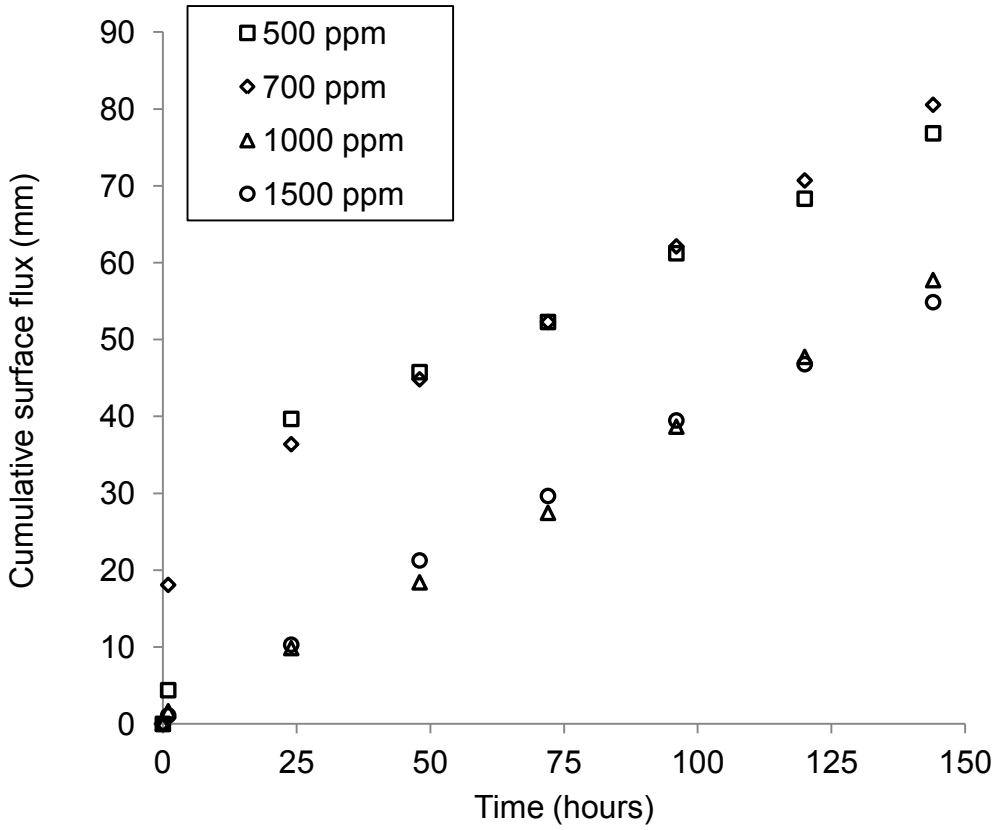

Figure 6-4: Cumulative surface flux of polymer amended tailings

The amount of consolidation water reporting to the surface was substantially higher for 500 and 700 ppm samples. Comparatively, the polymer dose of 700 ppm provided higher surface flux in comparison to other doses, which enabled it to provide maximum release of water (drainage + surface flux) 144 hours after tailings deposition.

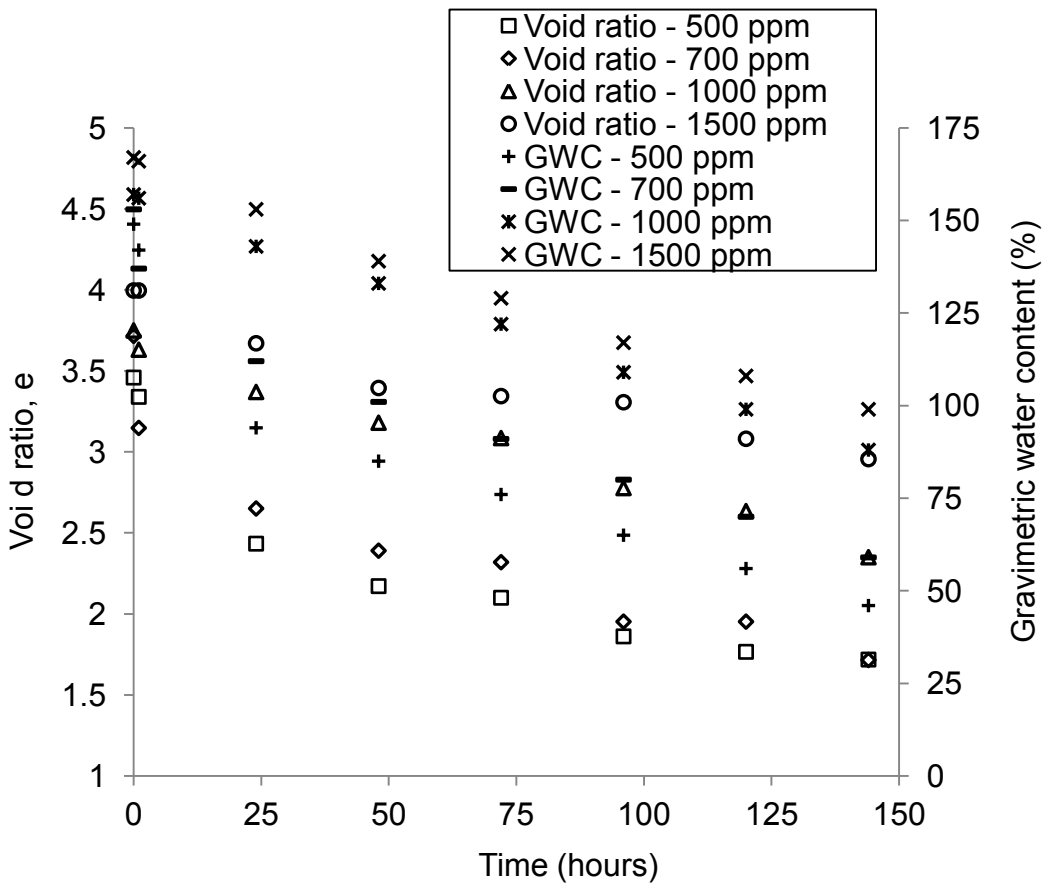

Figure 6-5: Void ratio, gravimetric water content relationships over time of polymer amended tailings

Water content and void ratios showed similar trends, as the degree of consolidation was enhanced in the 500 and 700 ppm dose samples compared to 1000 and 1500 ppm. It was seen by comparing the water contents with the void ratio data, that the tailings started to desaturate at the top of the tailings, but saturated conditions remained in at least part of the tailings as all samples continued to drain from the bottom to the end of the test.

Water content was lowest at the end of the 500 ppm test (46%) and increased to 96% for the 1500 ppm material (Figure 6 – 5). Similarly, the shrinkage curves of

tailing showed that the polymer doses of 500 and 700 ppm provided more consolidation in comparison to 1000 and 1500 ppm, and 700 ppm was still showed further trend of consolidation, however, volume change leveled off in the 500 ppm sample, perhaps as it was approaching its shrinkage limit (Figure 6 – 6).

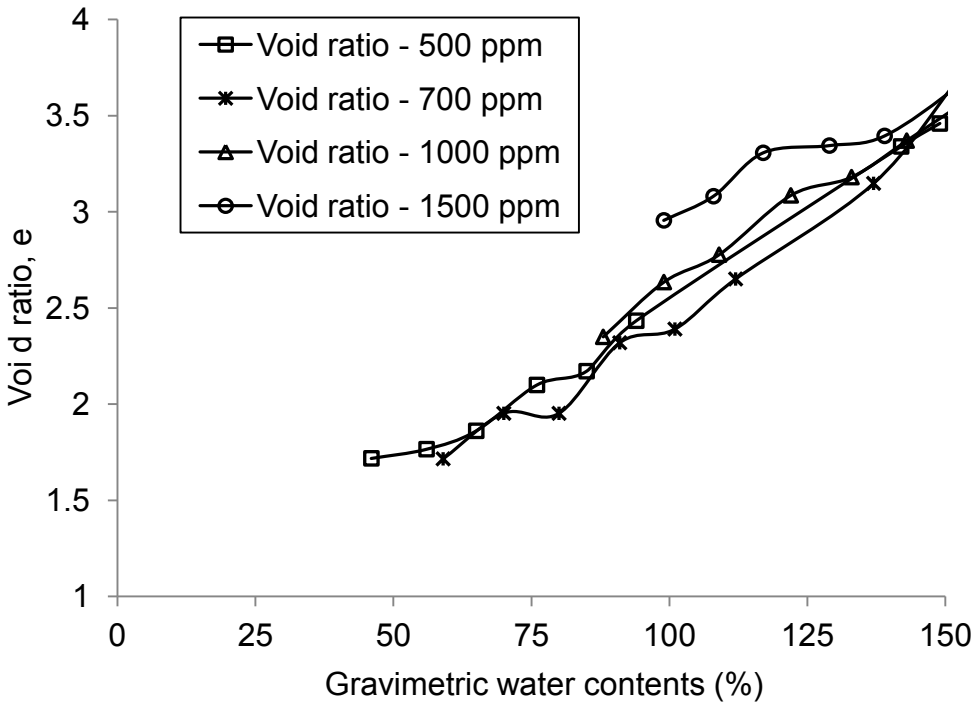

Figure 6-6: Shrinkage curves of polymer amended tailings

6.2.2 Slump tests:

Figure 6 - 7 shows the dimensionalized slumps of polymer amended tailings for polymer doses of 500, 700, 1000 and 1500 ppm during short term dewatering. The dimensionalized slumps of tailings for various doses showed almost similar

nature and the curves converged to each other over time. All tailings showed notable differences in slumps in the first 48 hours for each dose; however, thereafter, they did not show any significant difference in slump.

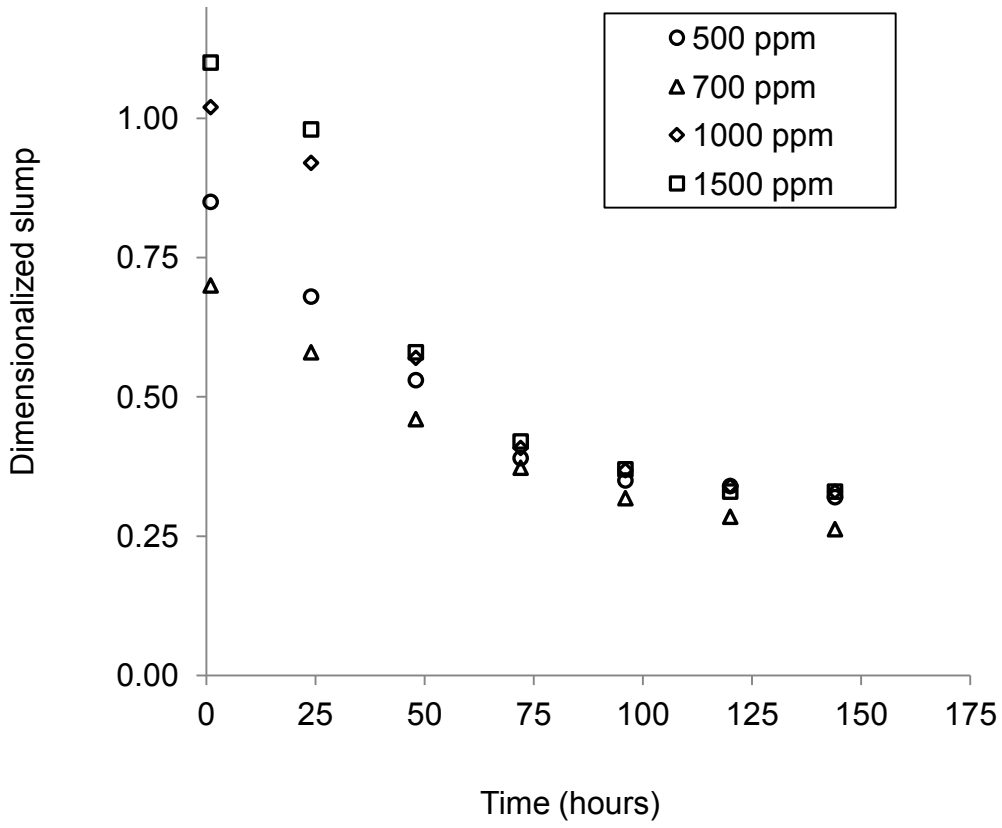

Figure 6-7: Dimensionalized slumps of polymer amended tailings

Practically, the tailings released significant quantity of water up to 48 ~ 72 hours, which enabled them to provide stabilized slumps. The polymer doses of 500, 700, 1000 and 1500 ppm provided slumps of 0.85, 0.70, 1.02 and 1.1 one hour after polymer mixing (Figure 6 – 7).

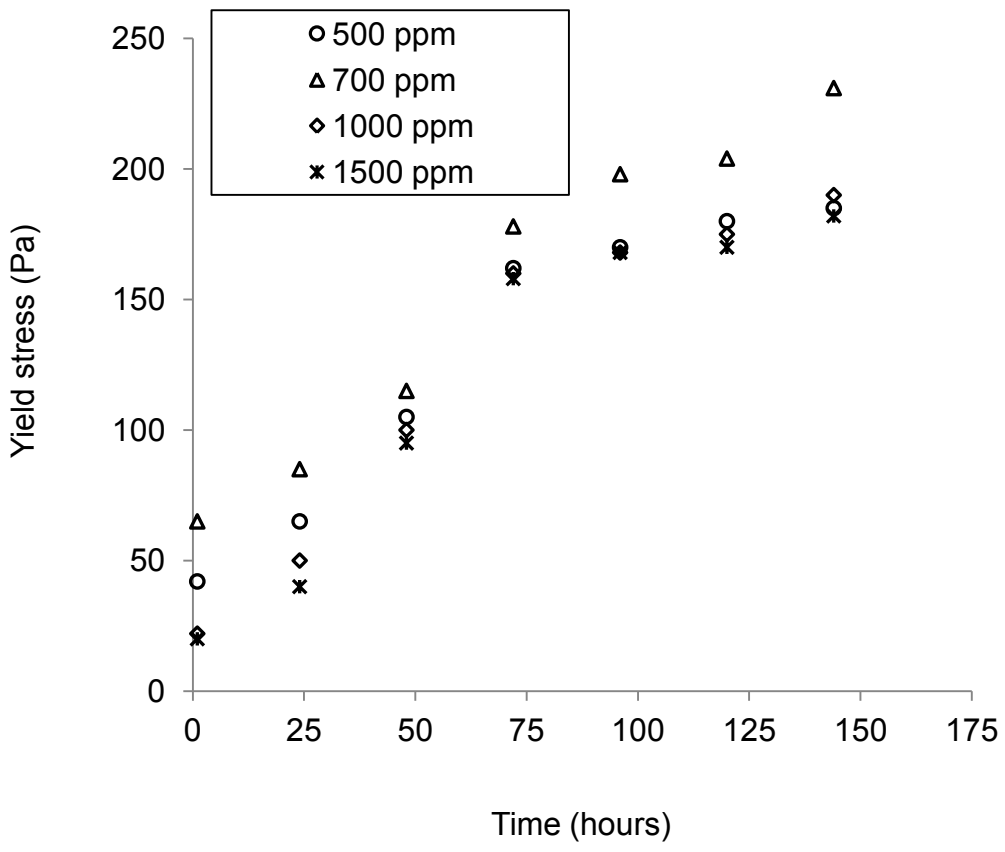

Figure 6-8: Yield stress of polymer amended tailings

There was one important observation to note that the dose of 700 ppm drained off 5 mm of water which was substantially higher when compared to 2, 0.5 and 0 mm of 500, 1000 and 1500 ppm doses one hour after tailings deposition (Figure 6 – 3). The higher amount of dewatering of 700 ppm enabled these tailings to provide lower slump (Figure 6 – 7), and consequently higher yield stress (Figure 6 – 8).

Based on the variations in slump values, the polymer doses of 500, 700, 1000 and 1500 ppm showed yield stress of 42, 65, 22 and 20 Pa respectively one hour

after tailings deposition, and they showed yield stress of 185, 231,190 and 182 Pa respectively 144 hours after tailings deposition (Figure 6 – 8). Generally, the slumps of various tailings did not differ too much irrespective of the variations in their drain off potential especially after 72 hours of tailings deposition. Overall, the polymer dose of 700 ppm showed higher yield stress in comparison to other doses. Mizani et al. (2013) reported that the yield stress of polymer amended mature fine tailings varied between 10 and 250 Pa for various polymer doses and using a similar anionic high molecular weight polymer, when tailings were tested using slump tests and other techniques.

The slump tests for aspect ratio of 1.33 provided comparative but lower yield stress, when compared to slump tests for an aspect ratio of 1 as discussed in Chapter 5. Pashias et al. (1996) observed similar observations while conducting slump tests with flocculated suspensions for various aspect ratios. The study stated that smaller aspect ratio provided lower slumps, whereas, too large aspect ratio resulted in the collapse of the slump.

Figure 6 – 9 shows variations in the physical appearance of slumps for various aspect ratios of 500 ppm one hour after polymer mixing and Figure 6 – 10 shows the variations in the slumps of 500 ppm after 01, 48, 72 and 144 hours after tailings deposition.

Figure 6-9: Appearance of slumps for 500 ppm one hour after polymer mixing (left: aspect ratio – 1, right: aspect ratio – 1.33

Similarly in Figure 6 – 11, the polymer dose of 700 ppm gave lower void ratio for short term dewatering, which can be attributed to its higher degree of dewatering, which consequently enabled these tailings to provide higher strength. However, for a particular void ratio, 1500 ppm provided higher yield stress and this higher yield stress of 1500 ppm for larger void ratio associated with larger flocs. This means that two components, i.e., floc formation and dewatering, each contributed to strength gain of polymer amended tailings.

Generally, the test results showed that the major difference in the behaviour of tailings was noted for this narrow range of polymer doses (500 - 1500 ppm) between 01 and 144 hours after polymer mixing, and the polymer dose of 700 ppm performed well in comparison to other doses; when compared taken into account their drain off potential, yield stress, slump appearance and especially,

the release of water during initial stage of tailings deposition, i.e., one hour after polymer mixing.

Figure 6-10: Physical appearance of slumps over time for 500 ppm (aspect ratio – 1.33)

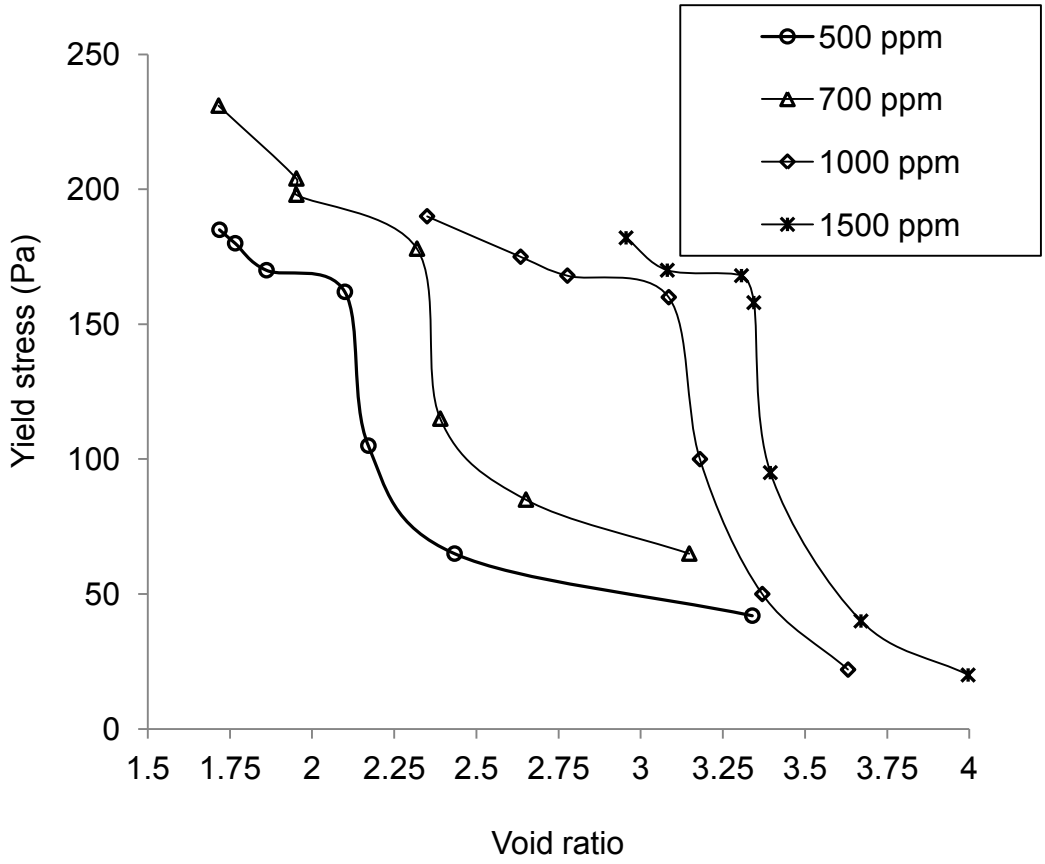

Figure 6-11: Yield stress and void ratio relationship of polymer amended tailings

Mizani et al. (2013) reported similar findings showing that 700 ppm gave higher dewatering potential than that of other doses. In terms of slump appearance, as shown in Figure 6 -12, the 500 ppm and 700 ppm samples provided more stiff, stabilized and compacted slump in comparison to 1000 and 1500 ppm polymer doses. The slump of 1000 and 1500 ppm still looked soft, collapsible and spreadable 144 hours after tailings deposition due to their low degree of dewatering.

Figure 6-12: Appearance of slumps after 144 hours of tailings deposition for various polymer doses (aspect ratio – 1.33)

6.2.3 Hydraulic conductivity and suction tests:

Total suction was measured in samples with polymer doses of 500, 700, 1000 and 1500 ppm to be 280, 300, 290 and 280 kPa one hour after polymer mixing, and 600, 650, 420 and 410 kPa respectively 144 hours after polymer mixing. The soil water potential of polymer amended MFT did not vary too much for various polymer doses after 01 hour, however, the polymer doses of 500 and 700 ppm showed relatively high suction in comparison to 1000 and 1500 ppm 144 hours

after polymer mixing. This is probably due to concentration of ions and the associated increase in osmotic suction in the more highly dewatered samples (500 and 700 ppm).

The polymer doses of 700, 1000 and 1500 ppm polymer doses showed hydraulic conductivity of 4.3 x 10^{-06}, 3.5 x 10^{-06}, 6.4 x 10^{-06}, and 7.6 x 10^{-06} cm/sec., one hour after polymer mixing. The final void ratio of polymer amended MFT for all doses was less than the reported value as the tailings were consolidated further in the permeater during the test.

6.2.4 Scanning electron microscopy (SEM) tests and ImageJ analysis:

Figs 6 – 13 to 6 – 16 show the scanning electron micrographs of polymer amended oil sands tailings 01 and 144 hours after polymer mixing. The images were captured with a magnification of 5 kx and at a scale of 5 μm.. The SEM micrographs showed that the addition of polymer changed the tailings's fabric and the structure of the tailings was different for all doses 01 and 144 hours after polymer mixing.

The polymer doses of 500 and 700 ppm provided more round and regular flocs in comparison to 1000 and 1500 ppm one hour after polymer mixing. Moreover, 500 and 700 ppm showed more packed and compacted structure showing notable changes in fabric after 144 hours of polymer mixing (Figs 6 – 13 and 6 – 14).

Comparatively, the SEM micrographs for 1000 and 1500 ppm doses showed more porous nature after 144 hours in comparison to one hour of polymer mixing.

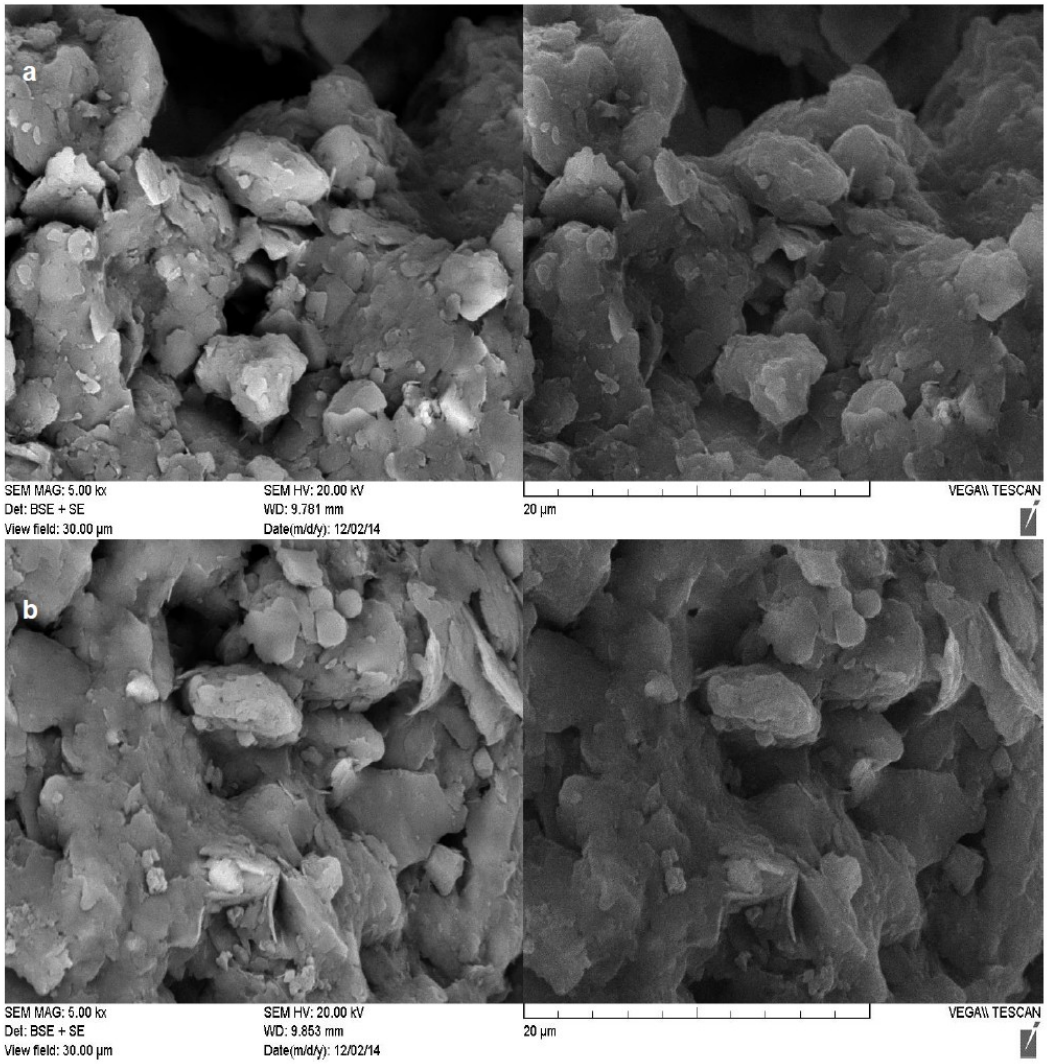

Figure 6-13: Scanning electron micrographs of polymer amended oil sands tailings for polymer dose of 500 ppm (a – one hour after polymer mixing; b – 144 hours after polymer mixing)

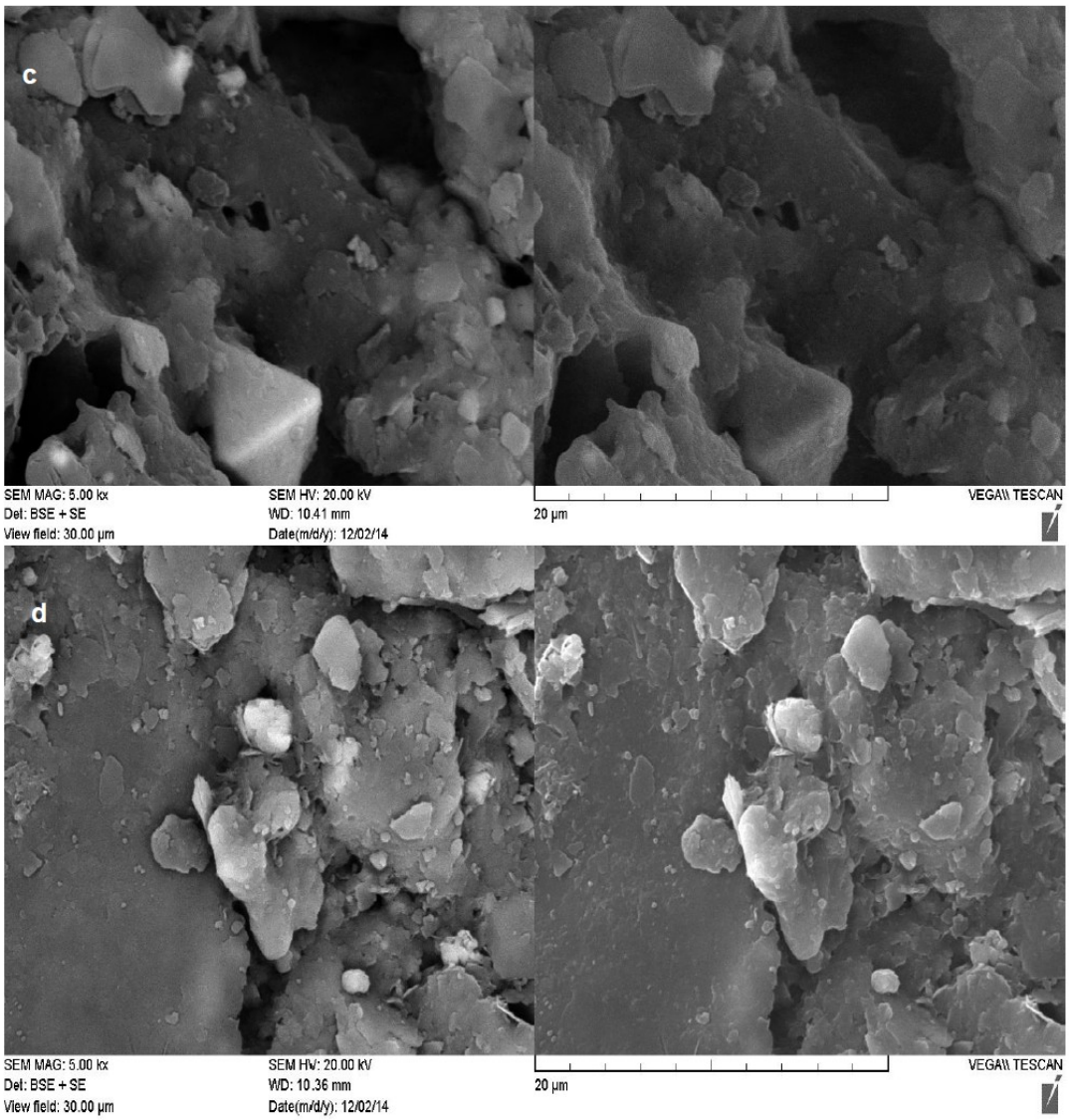

Figure 6-14: Scanning electron micrographs of polymer amended oil sands tailings for polymer dose of 700 ppm (c – one hour after polymer mixing; d – 144 hours after polymer mixing)

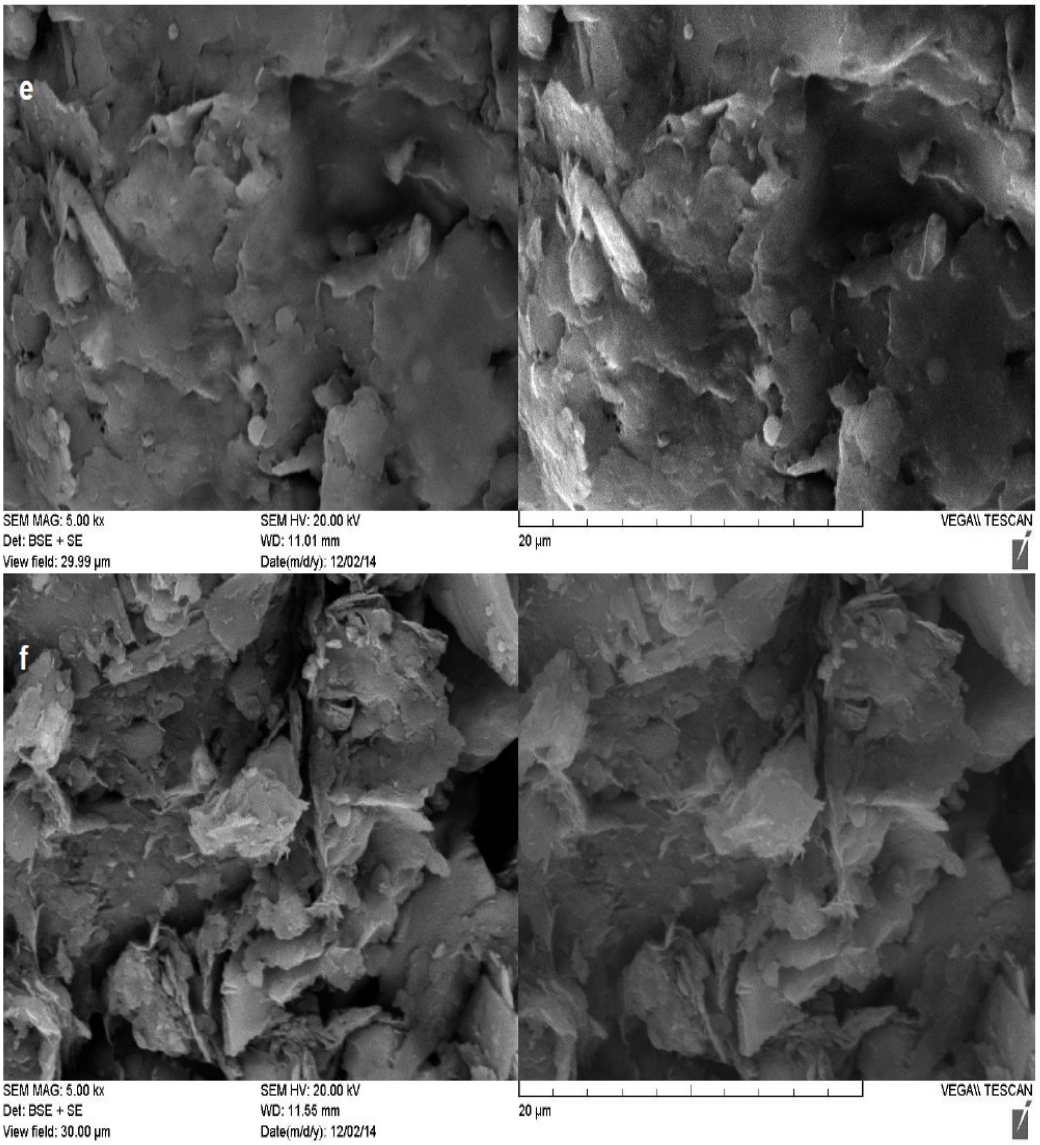

Figure 6-15: Scanning electron micrographs of polymer amended oil sands tailings for polymer dose of 1000 ppm (e – one hour after polymer mixing; f – 144 hours after polymer mixing)

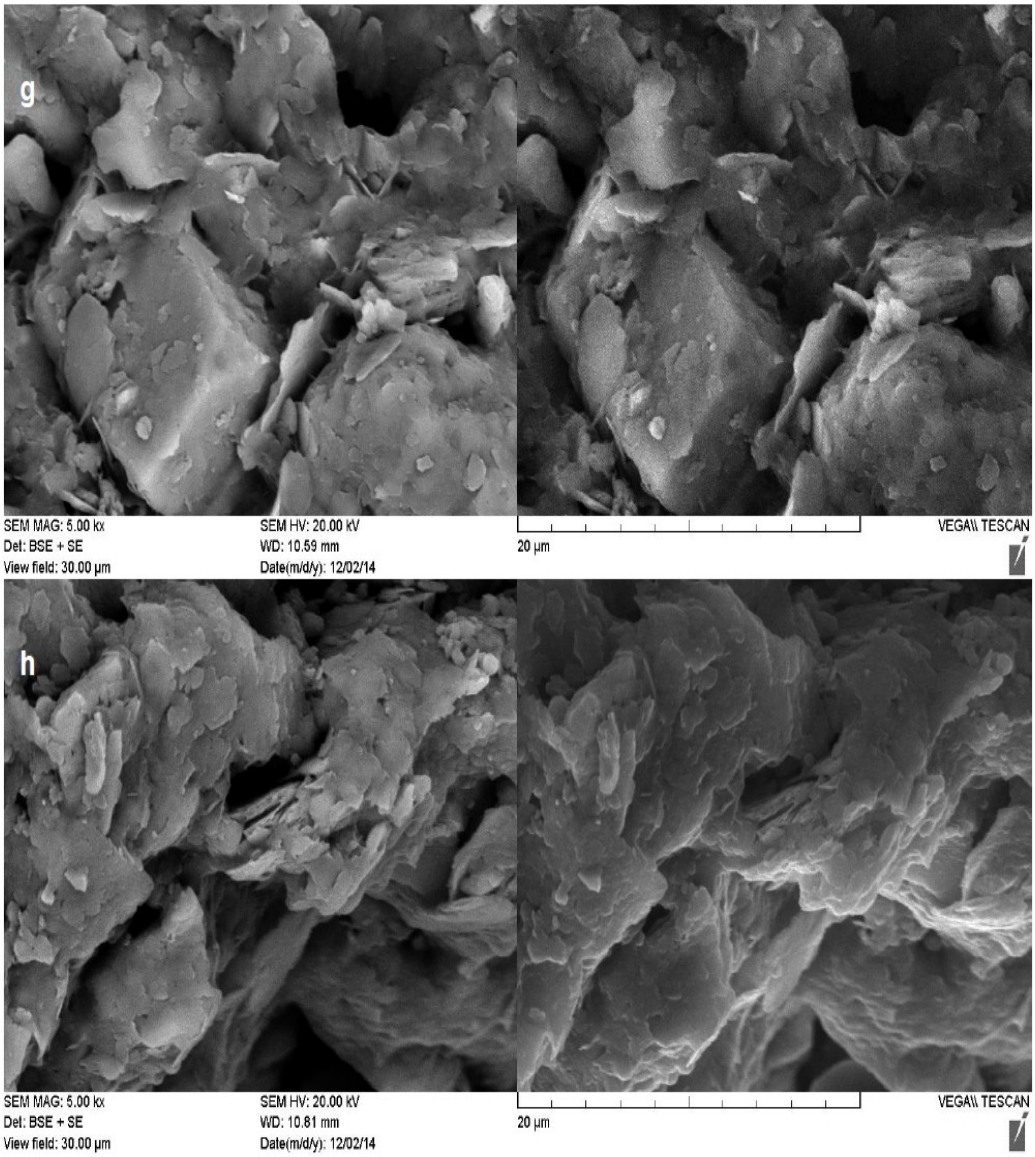

Figure 6-16: Scanning electron micrographs of polymer amended oil sands tailings for polymer dose of 1500 ppm (g – one hour after polymer mixing; h – 144 hours after polymer mixing)

Figs 6 - 17 and 6 - 18 show gray pixel analysis of polymer amended tailings 01 hour and 144 hours of tailings deposition. The imageJ analyses was performed with BSE images of 0.5 kx magnification, 1536 x 648 resolution and 300 μm view field. The SEM micrographs used in image analysis are presented in Appendix 1. The specific magnification was selected to maximize the scope of analysis considering the particle size distribution of tailings. The BSE micrographs of tailings were optimized adjusting their threshold to clearly distinguish the particles, background and adjacent grains boundaries.

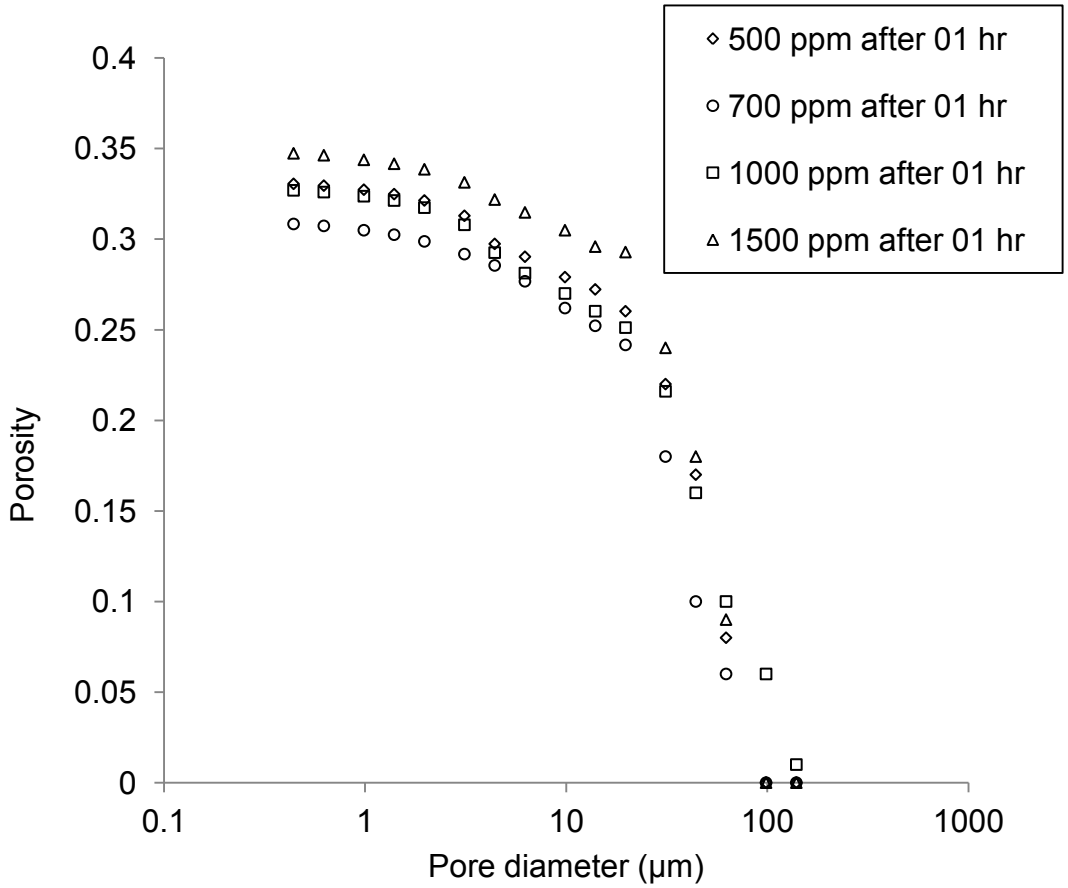

Figure 6-17: Gray pixel analysis of SEM micrographs 01 hour after polymer mixing

The gray pixel analysis showed that the lower polymer dose showed less microporosity in comparison to higher doses, and 700 ppm showed minimum microporosity after both 01 and 144 hours of polymer mixing. Resultantly, the tailings provided microporosity of 0.33, 0.31, 0.33, 0.35 for polymer doses of 500, 700, 1000 and 1500 ppm respectively (Figure 6 – 17), and they showed microporosity of 0.25, 0.27, 0.31, and 0.32 respectively 144 hours after polymer mixing (Figure 6 – 18).

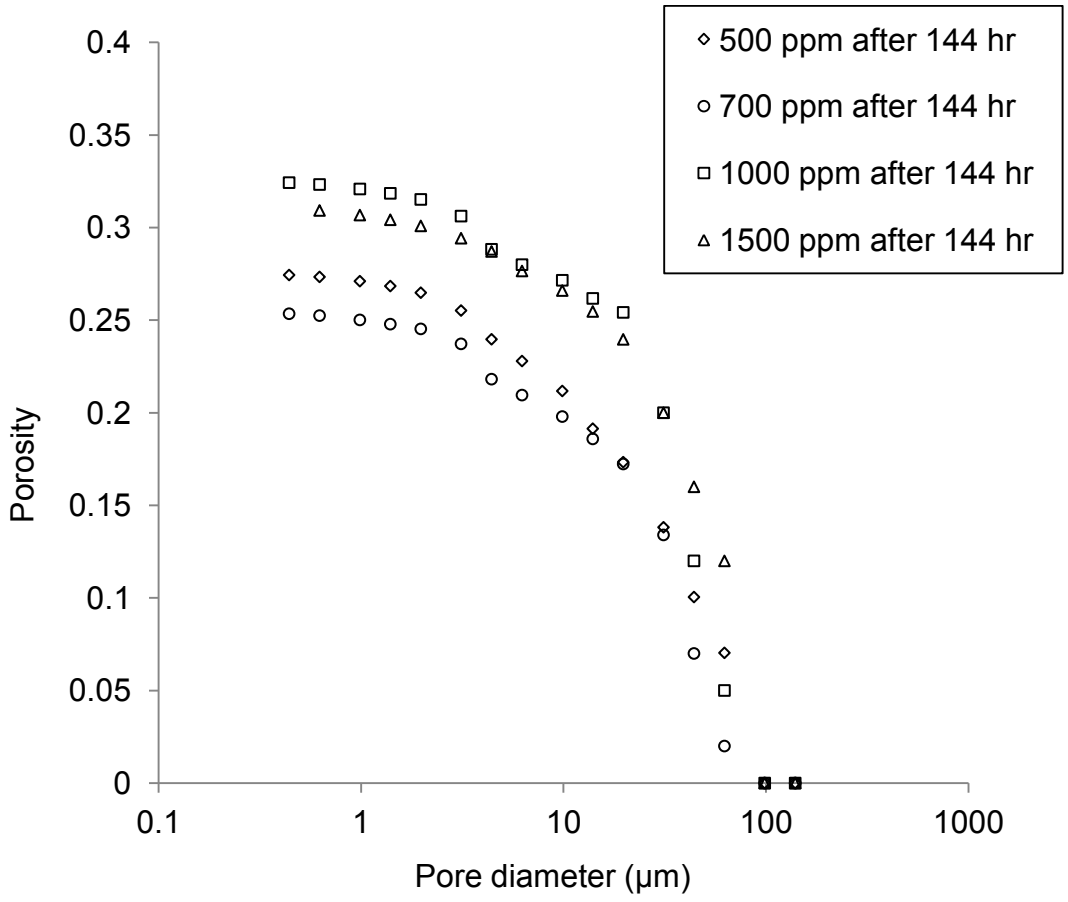

Figure 6-18: Gray pixel analysis of SEM micrographs 144 hours after polymer mixing

Comparatively, the lower polymer doses showed more decrease in microporosity in comparison to higher doses between 01 and 144 hours of tailings deposition. As we already discussed that the SEM micrographs of 500 and 700 ppm appeared more compacted than that of 1000 and 1500 ppm especially after 144 hours of tailings deposition, which alternately enabled tailings to provide lower microporosity. Comparatively, the tailings provided more trends towards smaller diameter for successive release of water, and the microporosity curves shifted towards smaller pores diameter especially for 500 and 700 ppm, which resulted in larger number of smaller pores after 144 hours in comparison to 01 hour. However, for 1000 and 1500 ppm, the curves did not show any important difference in microporosity 01 and 144 hours after tailings deposition.

The test results showed that SEM approach was effectively used to classify the microstructure of polymer amended oil sands tailings like that of other materials such as fine grained rock salts, flocculated kaolinite suspensions, smectite suspensions, clay sand mixture and compacted FEBEX bentonite etc. as discussed by Desbois et al. (2012); Du et al. (2010); Romero and Simms (2008); Morris and Zbik (2009); Zbik et al. (2008); and Makula and Manuz (2000). However, ImageJ analysis still needs more investigation to optimize and simulate the gray value of oil sands tailings as they contain residual bitumen and polymer. Furthermore, ImageJ analysis provided pores of larger diameter in comparison to MIP data set as presented in succeeding section.

6.2.5 Mercury intrusion porosimetry (MIP) tests:

Figure 6 – 19 shows cumulative pores size distribution (CPSD) of polymer amended oil sands fine tailings. As in Figure 6 – 19, the cumulative intrusion pore volume of tailings decreased with a release of water and as expected, the tailings showed lower cumulative intrusions 144 hours than that of 01 hour after tailings deposition.

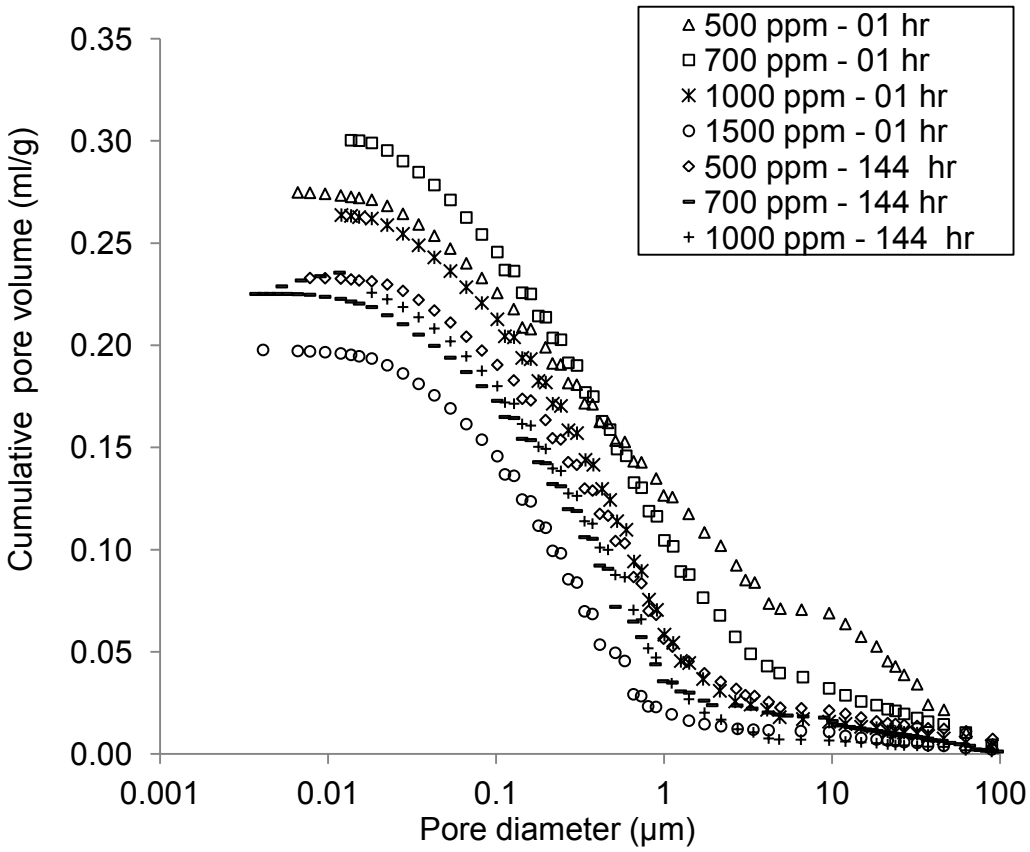

Figure 6-19: Cumulative pore volume distribution of polymer amended tailings

Comparatively, the polymer doses of 500 and 700 ppm showed higher cumulative intrusion in comparison to 1000 and 1500 ppm after 01 hour of polymer mixing, and these tailings gave lower intrusion 144 hours after polymer mixing. Similar to SEM micrographs, the cumulative intrusions curves of 1000 ppm showed minor difference in pores volume 01 and 144 hours after polymer mixing.

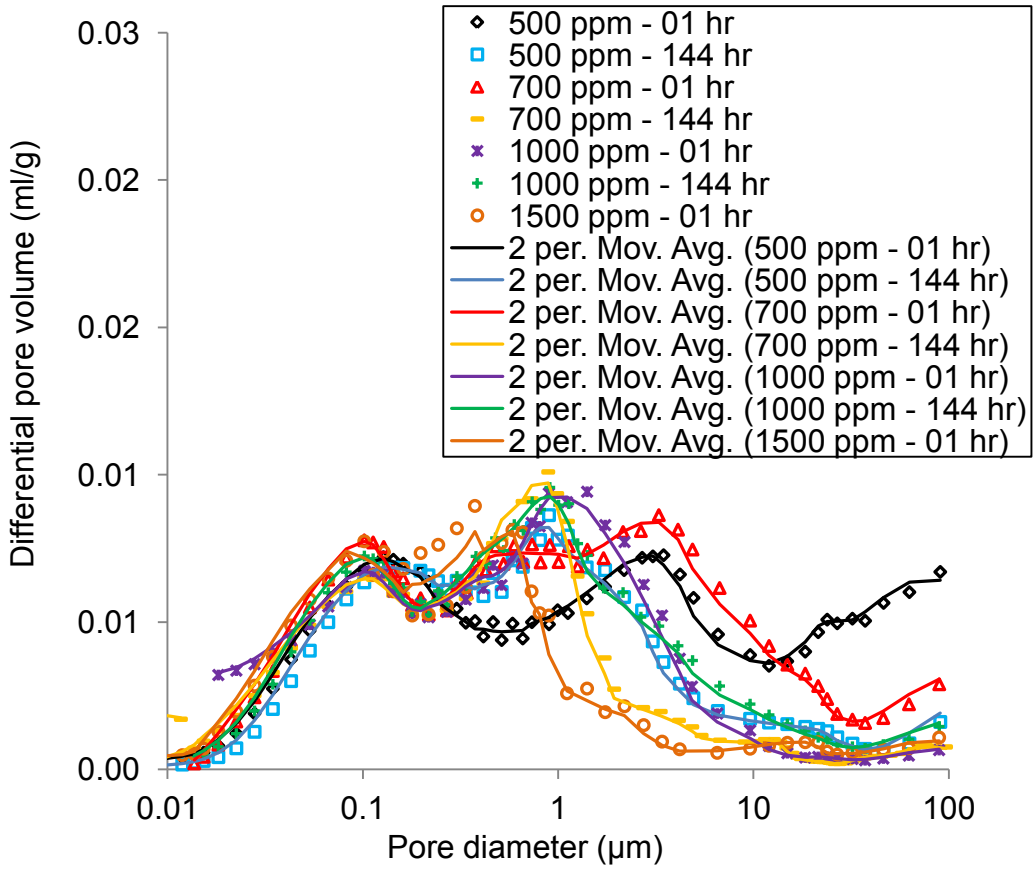

Figure 6-20: Differential pore volume distribution of polymer amended tailings

As in Figs 6 – 20, the tailings were spread between 0.003 and 100 μm pores diameter, and the peak of pores mode lowered for release of water 144 hours after polymer mixing. However, the sample split into pieces while performing MIP tests for 1500 ppm 144 hours after polymer mixing, so the data was not presented herein.

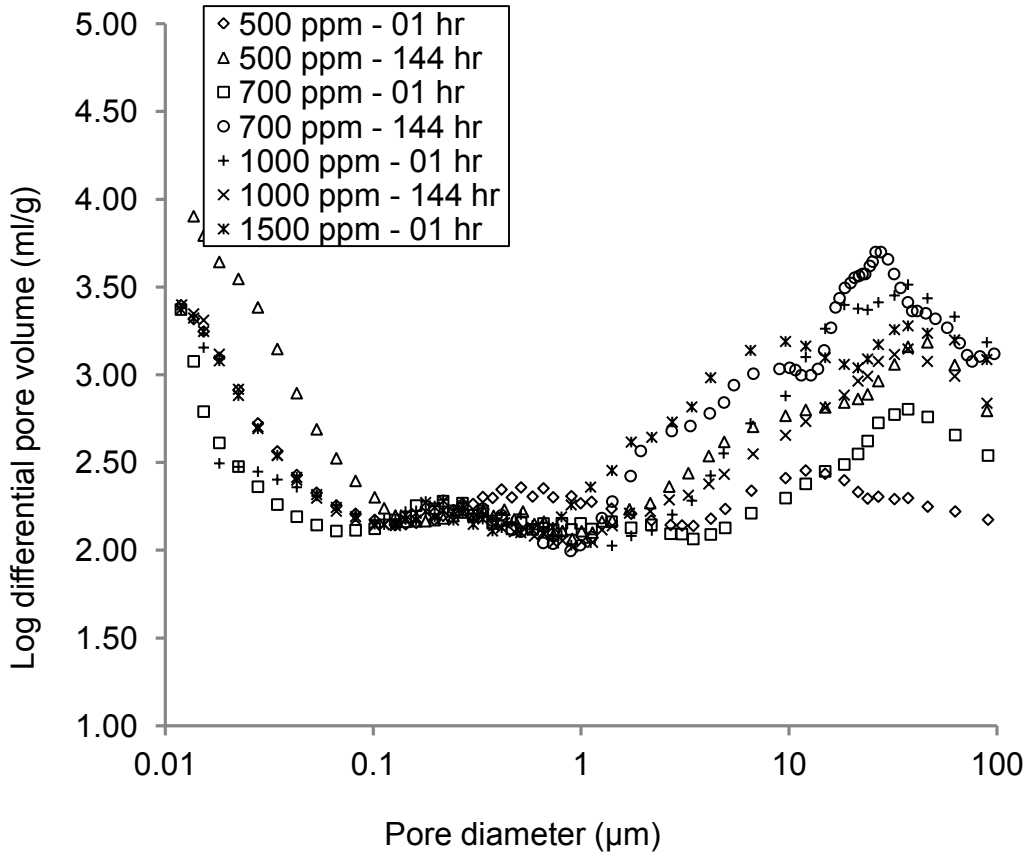

Figure 6-21: Log differential pore volume distribution of polymer amended tailings

The differential curves of tailings gave different pores size distribution for an increase in polymer dose and comparatively, the peak pore modes converged for

a release of water after 144 hours of tailings deposition. Furthermore, the differential curve (data points) of 700 ppm compressed for 144 hours in comparison to 01 hour after polymer mixing. However, all the tailings provided bimodal pore size distribution 01 and 144 hours of polymer mixing (Figure 6 – 20).

Similarly, as in Figure 6 – 21, the log differential pore volume distribution showed higher peak towards the larger pores diameter after 144 hours of polymer mixing showing notable decrease in microporosity; however, major differences were observed in all tailings for pores diameter ranging between 1 and 10 μm.There was clear indication that inter – aggregate pores centered at pores diameter of 0.1 and 1 μm (Figs 6 – 20 and 6 - 21).

MIP test results showed that the tailings behaved in similar fashion (Figure 6 – 19) to that of volume change as shown in Figure 6 - 5, 144 hours after polymer mixing. The tailings gave less void ratio for various doses with respect to specific time, but the difference in void ratio was more for various doses 01 and 144 hours after tailings deposition (Figure 6 - 5).

There was one important observation to note here that MIP and SEM results presented here might be biased to some extent as the tailings were tested at very high water content (129~ 165%), which were likely to give more percent change in volume, and alternately, showed somewhat lower microporosity of tailings to the original value, despite that few special arrangements were

undertaken to collect and preserve the microstrcuture samples. However, taken into account these high water content data sets, both MIP and SEM were efficiently used to simulate the structural, geometric and textural configuration of oil sands fine tailings, even at very high water content. Generally, the test results showed that the tailing treated with polymer was more propitious to drain off the water which solidified the structure of polymer amended tailings enhancing their yield stress. Table 6 -1 shows a comparative summary of test results for short term dewatering

Table 6-1: Comparative summary of macroscopic test results 01 and 144 hours after tailings deposition

Features	Parameters	Units	Polymer dose (ppm)							
			500		700		1000		1500	
			1 hour**	144 hours**	1 hour	144 hours	1 hour	144 hours	1 hour	144 hours
Macroscopic	Gravimetric water content	%	143	46	137	59	157	88	167	99
	Drain off water	mm	2	15	5	13	0.55	5	0	4
	Surface flux	mm	4	77	18	81	2	58	1	55
	Void ratio, e	-	-	1.71	-	1.71	-	2.34	-	2.95
	Total suction	kPa	280	600	300	650	290	420	280	410
	Dimensionalized slump*	-	0.85	0.32	0.7	0.26	1.02	0.33	1.1	0.33
	Yield stress	Pa	42	185	65	231	22	190	20	182
	Hydraulic conductivity	cm /sec	4.32E-06	2.01E-07	3.52E-06	1.37E-07	6.38E-06	3.52E-07	7.58E-06	7.58E-07

* aspect ratio - 1.33

** time after polymer mixing

6.3 Interaction of macroscopic and microstructure features of polymer amended tailings

The tailings released water as an addition of polymer providing a change in volume which resulted in a decrease in water content for all doses. Comparatively, 700 ppm showed lower void ratio especially 144 hours after tailings deposition due to its high dewatering potential and it consequently provided more suction, lower hydraulic conductivity and higher yield stress. The MIP and ImageJ analysis showed that the tailings shifted towards pores of smaller diameter with a release of water showing important volume changes after 144 hours in comparison to one hour of tailings deposition.

Furthermore, the scanning electron micrographs showed that the tailings fabric appeared more compacted 144 hours in comparison to 01 hour after polymer mixing particularly for 500 and 700 ppm. The microporosity test results of 1000 and 1500 ppm did not differ too much after 01 and 144 hours supporting their lower drain off potential and smaller changes in volume. The higher drain off potential of 500 and 700 ppm was attributed to smooth, uniform aggregation and the channelized structure in the beginning; conversely, SEM micrographs for 1000 and 1500 ppm did not show porous or channelized structure in the beginning.

Similarly, the macrostructure behaviour of tailings showed that 500 and 700 ppm behaved in different fashion that that of 1000 and 1500 ppm and the

microstructure analysis validated this test data. Generally, the test results showed that the scanning electron micrographs, MIP test data in combination with ImageJ analysis supported the macrostructure behaviour of tailings for short term dewatering, despite the microstructure results were biased to some extent as the tailings were tested at higher water contents that more likely resulted in higher percent change in volume during preconditioning of the samples.

6.4 Conclusions:

The lower polymer doses of 500 and 700 ppm showed higher dewatering potential in comparison to higher polymer dose. The hydraulic conductivity varied in the same order 01 hour and 144 hours after tailings deposition, however the hydraulic conductivity for a particular dose decreased with time due to initial self weight consolidation. The tailings showed more suction after 144 hours than that of 01 hour and the difference was more for 500 and 700 ppm. Comparatively, the polymer dose of 700 ppm showed higher yield stress in comparison to other doses, however, for a particular void ratio, the polymer dose of 1500 ppm showed higher strength and it happened due to its larger flocs. It means that both dewatering and fabric contributed to strength gain of tailings.

In addition to this, the microstructure of the tailings changed for a change in the polymer dose, and the release of water as well. The treated tailings for each polymer dose behaved in different fashion due to various flocs configuration, structural and textural arrangement and it was the change in fabric as a result of

polymer addition which modified the macroscopic features of oil sands tailings for successive release of water during short term dewatering. Taken into account the macroscopic features (especially considering bottom drainage and surface flux 01 hour after polymer mixing) of tailings, the 700 ppm was optimal dose up to this point.

Chapter 7. Influence of desiccation on microstructure and vane strength of polymer amended oil sands mature fine tailings[2]

Abstract

In this study, the evolution of strength and microstructure of polymer amended MFT during desiccation was examined for desiccation. Polymer amended tailings for doses of 500, 1000, and 1500 ppm were desiccated and consolidated in a simple laboratory simulation of thin-lift drying. Unlike the previous chapter, the fabric was tracked using ESEM on fresh samples and MIP on freeze-dried samples. The tests were allowed to continue longer than the column experiments in earlier chapters to allow for greater desiccation. Strength was evaluated using vane tests rather than slump tests.

The test results showed that the differences in microstructure disappeared due to polymer dose as desiccation progressed, and the peak pore mode shifted towards smaller pores diameter. However, the polymer amended MFT showed higher cumulative pore size distribution (CPSD) than that of unamended tailings even after desiccation beyond the shrinkage limit. Some differences in strength – void ratio relationships were observed between samples with different polymer

[2] A version of this Chapter was published in the Proceedings of ISSMGE Paris Conference (Bajwa and Simms 2013), and some information was included in the Proceedings of GeoMontreal Conference (Bajwa and Simms 2013)

doses. The water retention curves and shrinkage curves showed some minor differences depending on polymer dose.

7.1 Materials preparation and methods used:

The polymer amended MFT was prepared following the guidelines as discussed in Chapter 3. After mixing, the prepared polymer amended MFT was transferred to three columns of 30 cm diameter and 45 cm depth. Three polymer doses of 700, 1000, and 1500 were used in the study, and the tailings were deposited in a lift of 30 cm. Figure 7 - 1 shows a schematic of the experimental setup to examine the microstructure and macroscopic features of polymer amended tailings in thin lift. The addition of polymer resulted in the release of water and each day the water accumulated at the surface was removed using a small beaker and syringe. Each column rested on a scale, which allowed for direct measurement of evaporation.

A vane was used to estimate the undrained shear strength. The vane tests were performed at a depth of 15 cm from the top of the column (Figure 7 – 1). The vane was driven gently to the specified depth in a single thrust and the tailings were sheared until they failed. Peak and residual values were recorded. Generally, the residual undrained shear strength was measured after five to ten vane rotations in a vane shear test. Figure 7 - 2 shows laboratory experimental set up to examine macroscopic and microstrcuture behaviour of polymer amended oil sands tailings.

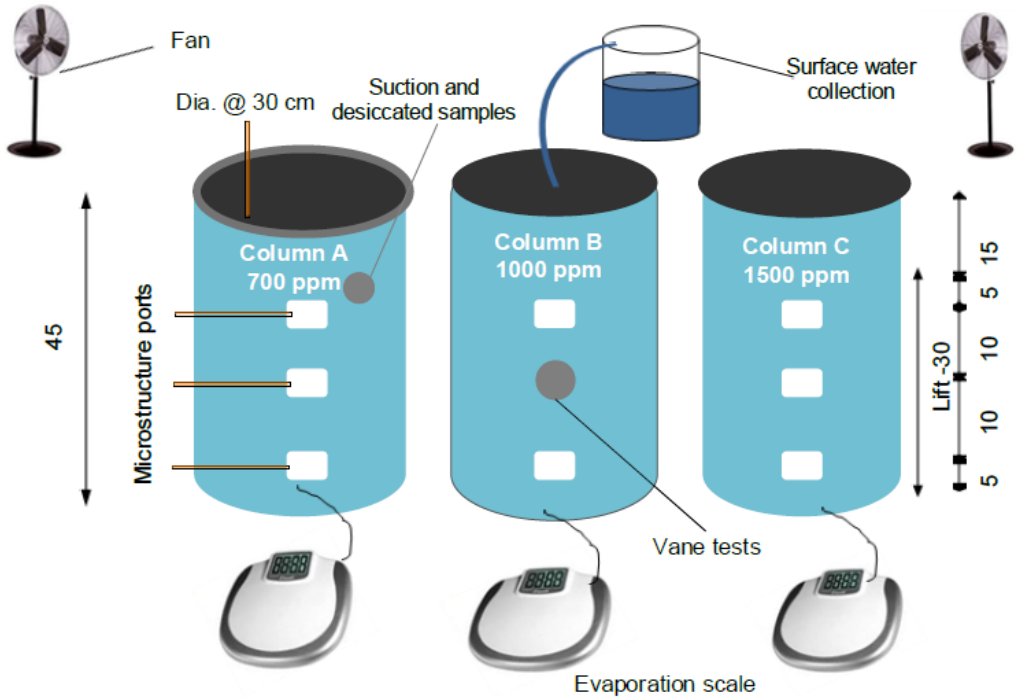

Figure 7-1: Schematic of set up of polymer amended mature fine tailings for desiccation

Tescan Vega-II XMU SEM device was used to conduct scanning electron microscopy (ESEM) tests. The backscattered electron (BSED) and gaseous secondary electron (GSED) were employed to capture the images and these approaches followed an iterative approach setting the scale of the images. In this study, the BSED micrographs were analyzed based on the qualitative comparison between BSED and GSED images.

The analysis was carried out applying a rapid freezing stage of -50 ^{o}C before application of vacuum (10^{-3} Pa). The charging of non-conductive specimens was adjusted varying voltage such that the incoming beam current was equal to sum

of out coming secondary and backscattered electrons currents. It usually occurred at accelerating voltages of 0.3 – 4 kV.

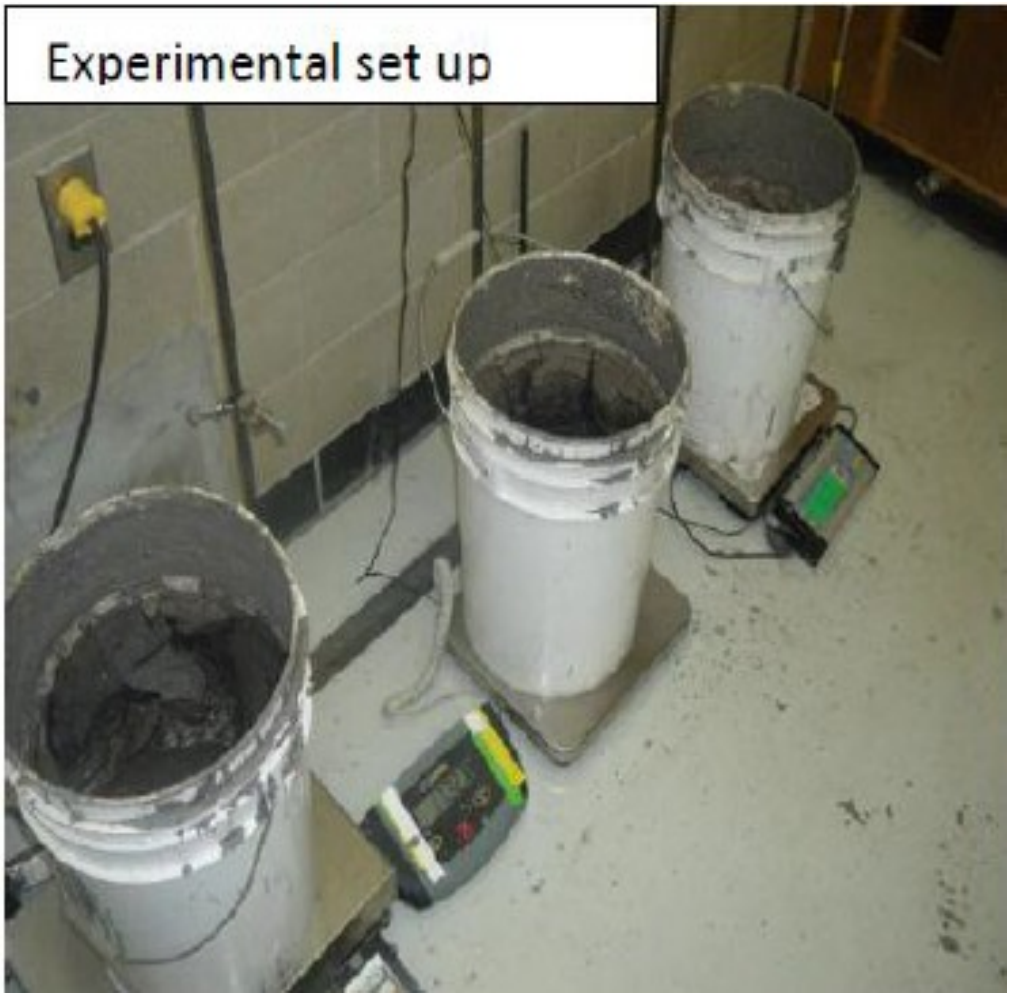

Figure 7-2: Laboratory experimental set up to examine desiccation behaviour of polymer amended oil sand mature fine tailings

For ESEM tests, some samples were obtained from 2 ~ 3 cm from the top of column for various degree of desiccation, and other samples were collected from 5, 15, and 25 cm depths from the top after 16 days of tailings deposition (Figure 7 – 1). The gray pixel analysis of SEM micrographs was performed for

quantitative measurements. The micrographs were captured at three random spots per sample.

Total suction measurements were carried out using chilled mirror hygrometer (Wenglor WP4 PotentiaMeter). Samples were extracted from the porous media and placed in a container for insertion in the WP4 device. The desiccated samples for total suction tests were collected from 2 ~ 3 cm from the top of the column each 24 hour after tailings deposition.

7.2 Test results and discussions

7.2.1 Total suction and volume change behaviour of polymer amended oil sands tailings

As shown in Figure 7 - 3, evaporation proceeded at the potential rate of ~ 6 mm /day, until about day 10.

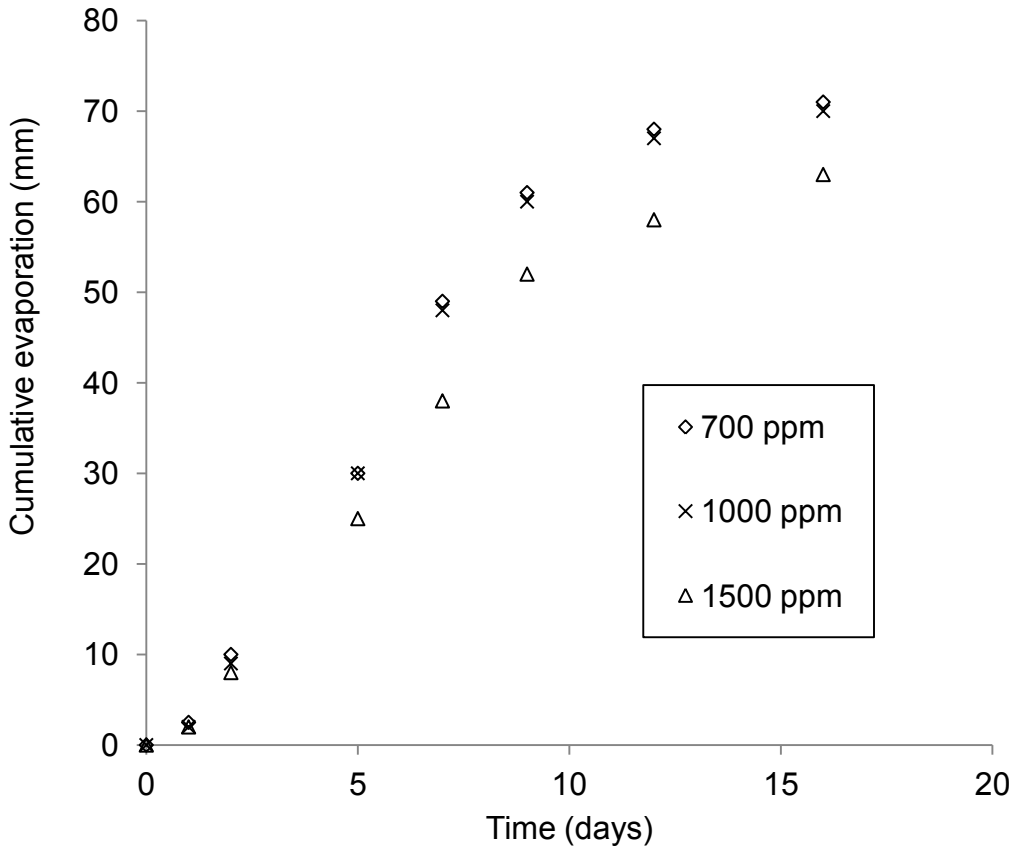

Figure 7-3: Cumulative evaporation of polymer amended MFT in thin lift

This corresponded to an average water content of 75%, and at 65% water content, polymer amended MFT provided peak undrained shear strength in excess of 5 kPa (Matthews et al. 2011). For this relatively short layer thickness (30 cm initial height), the drying was quite uniform with depth.

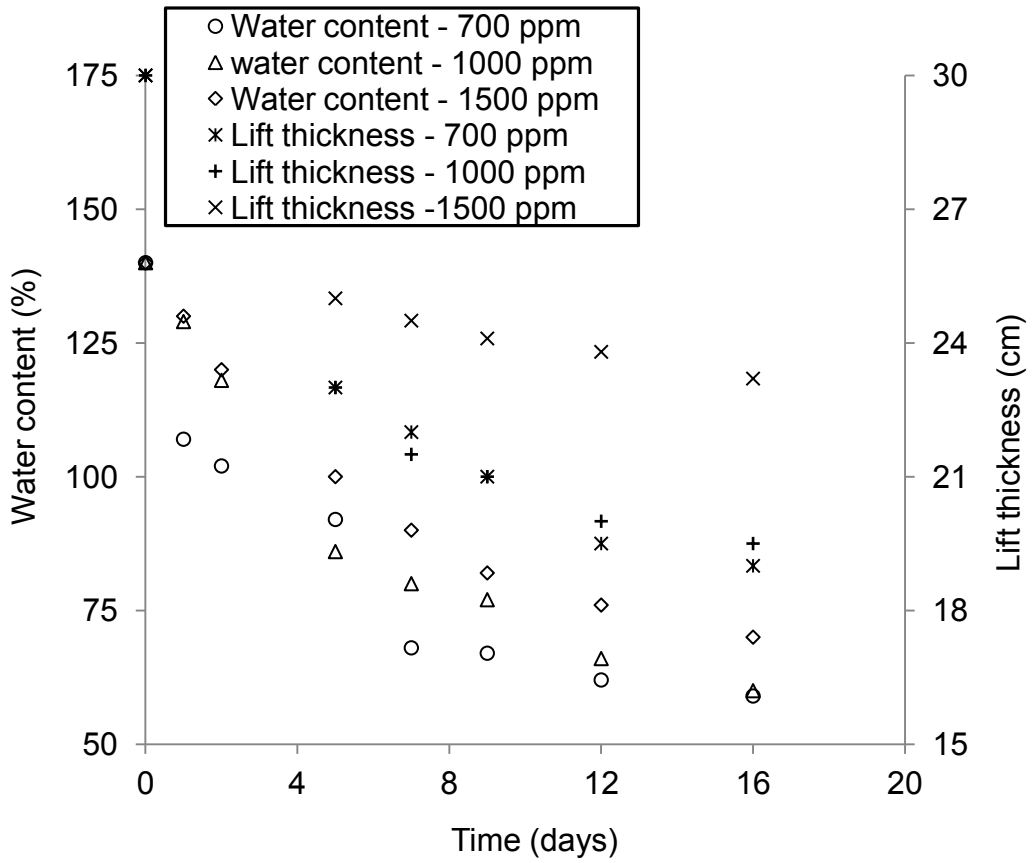

Figure 7-4: Water content, lift thickness relationship over time of polymer amended tailings

Total suction values near the (~2 cm) surface increased above 0.70 MPa at this point (10 days), correlating with the onset of stage II drying (actual evaporation declined largely compared to potential evaporation).

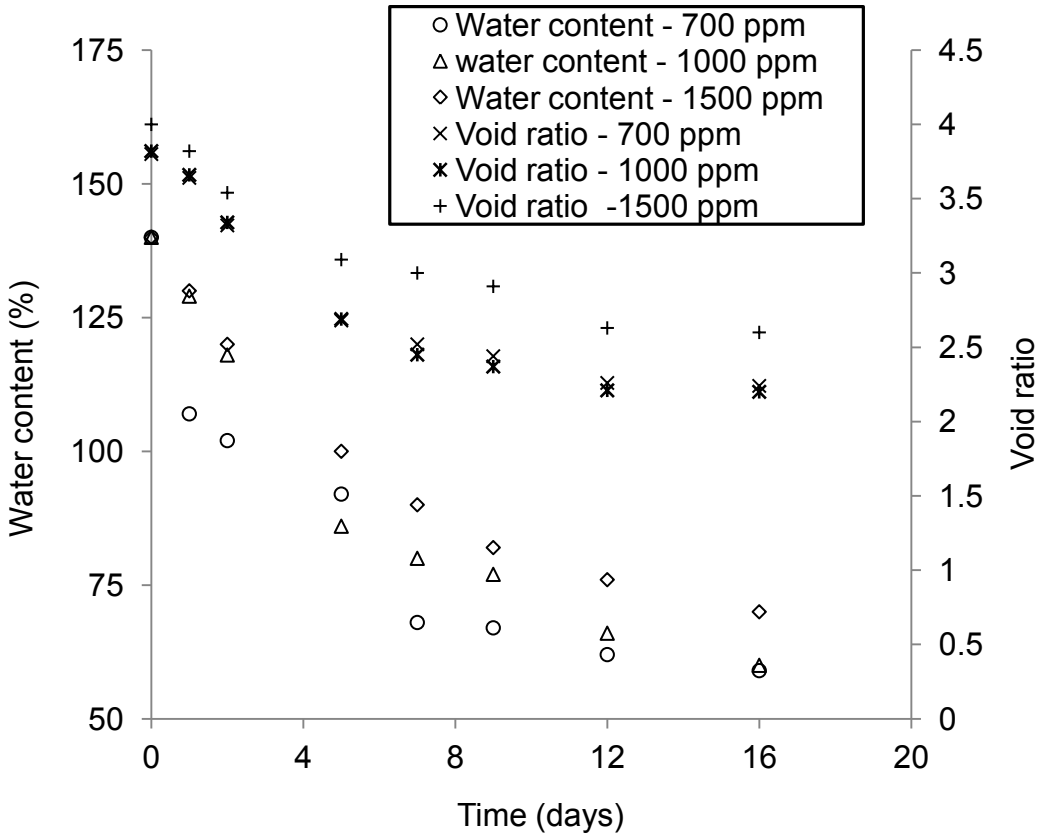

Figure 7-5: Water content, void ratio and time interaction of polymer amended tailings

As described in Wilson et al. (1997), evaporation declined as a function of total suction at the soil surface. In our tests, the decline became significant for total suction in excess of 3 MPa, which conformed to the point where the relative humidity was expected to decline as per Equation 2.2.

The volume change behaviour of tailings is shown in Figs 7 – 4 and 7 - 5 (showing relationships among water content, void ratio, time, and lift thickness) and Figure 7 - 6 (the shrinkage curves).

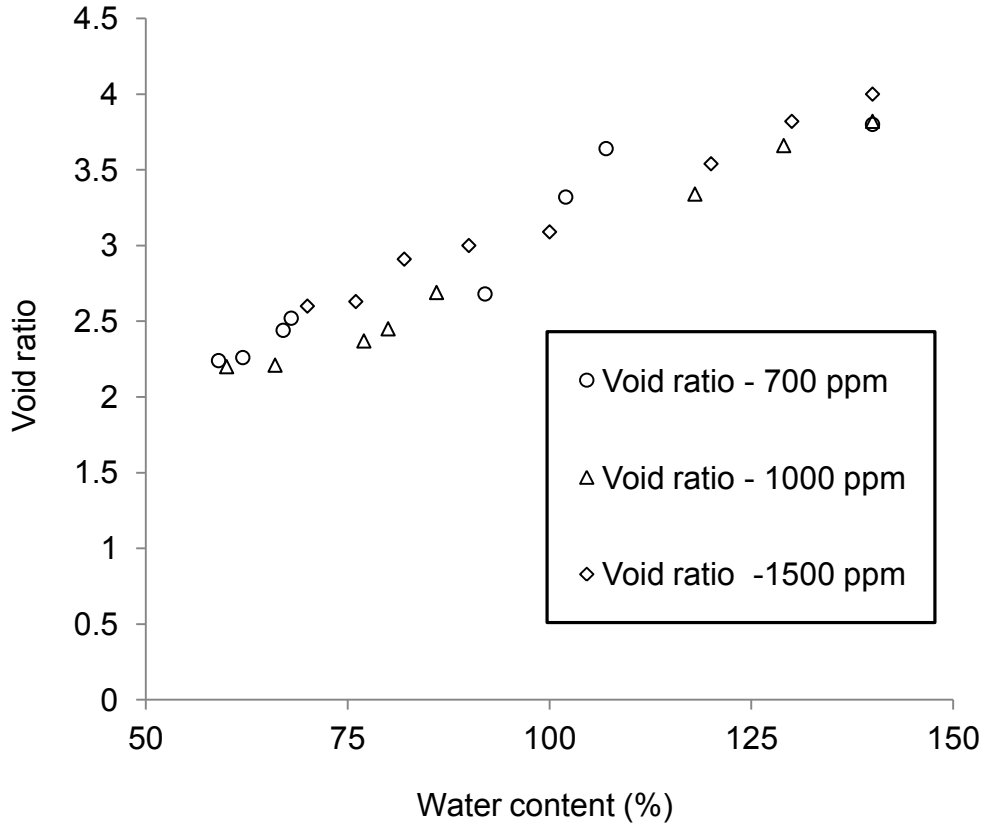

Figure 7-6: Shrinkage curves of polymer amended MFT

The shrinkage curves showed that the tailings for all doses provided two steps desaturation; first, the volume of tailings initially decreased due to desaturation, then stabilized showing less change in volume for a while, and after then the second step desaturation initiated which resulted in higher shrinkage of tailings enabling them to attain shrinkage limit. The inter-aggregate pores contributed to this initial desaturation whereas the soil matrix inside the aggregates resulted in second point desaturation. The tailings for 1500 ppm showed higher void ratio in comparison to 1000 and 700 ppm at the apparent shrinkage limit.

Plotting total suction versus water content data from the same samples, a rough water-retention curve (WRC) was obtained for the polymer amended tailings for various polymer doses (Figure 7 - 7). For AEV water content from Figs 7 - 6 and 7 - 7, a total suction of about 350 ~ 400 kPa was found.

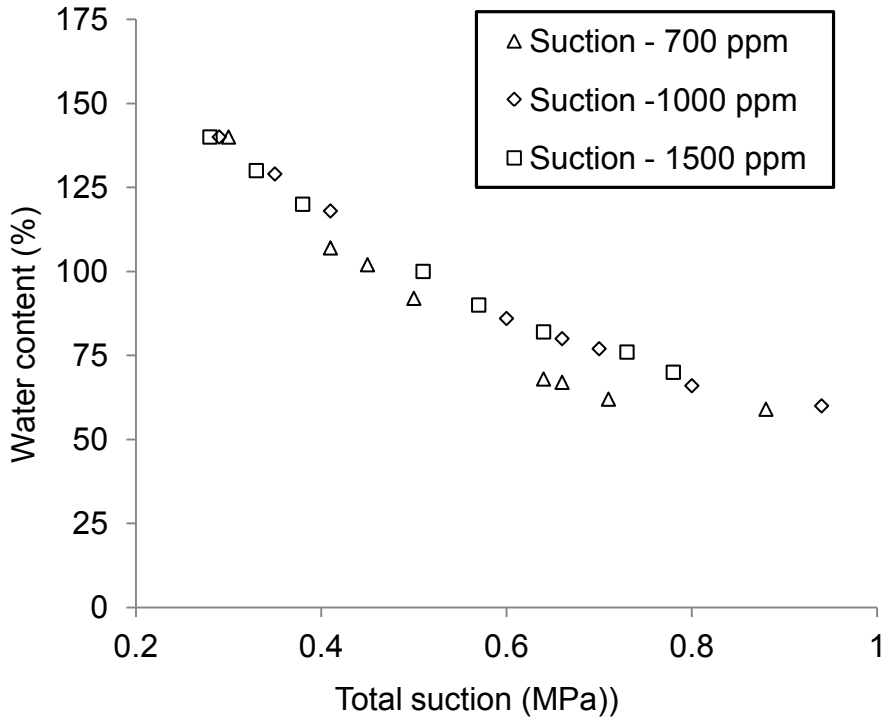

Figure 7-7: Water-retention curves of polymer amended MFT

7.2.2 Undrained shear strength of oil sands fine tailings

Figure 7 - 8 shows results from the vane tests. In the beginning for less desiccation or higher volume of water content (120 - 105%), the data points of all tailings appeared converging to each other showing almost same strength.

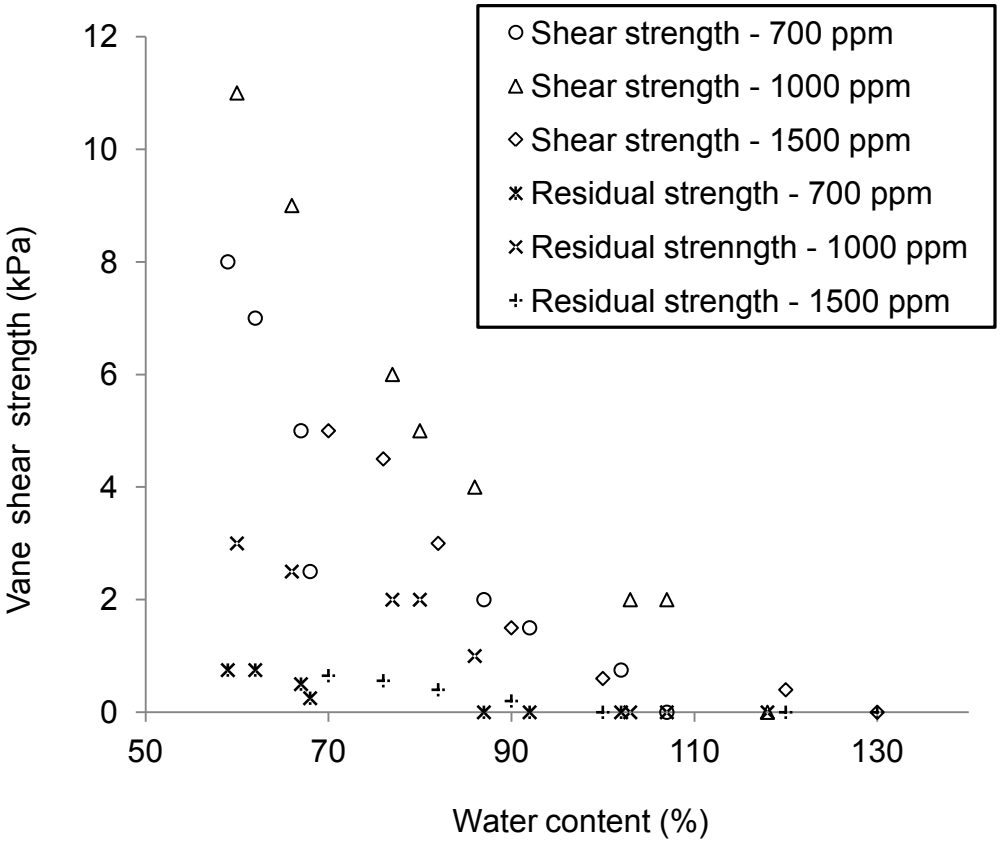

Figure 7-8: Undrained shear strength and water content relationships of polymer amended tailings

The curves appeared divergent to each other showing some differences in strength at lower water contents. For 1500 ppm polymer dose, the strength-water content curve fell below than 700 and 1000 ppm, however, for a particular void ratio; the polymer dose of 1500 ppm gave higher strength in comparison to other doses, and it happened due to larger flocs formation.

The residual shear strength of the polymer amended MFT showed the same trend as that of undrained shear strength for all polymer doses (Figure 7 - 9). In

both residual and peak strength, the 1000 ppm dose showed a consistently higher, but probably not practically large increase in strength over the other two doses. The undrained shear strength and void ratio relationships of polymer amended tailings are presented in Figure 7 – 9. The strength was almost same in the beginning for all doses but overall 700 and 1000 ppm showed more strength in comparison to1500 ppm for lower void ratio, and this happened due to the higher shrinkage limit of the 1500 ppm tailings.

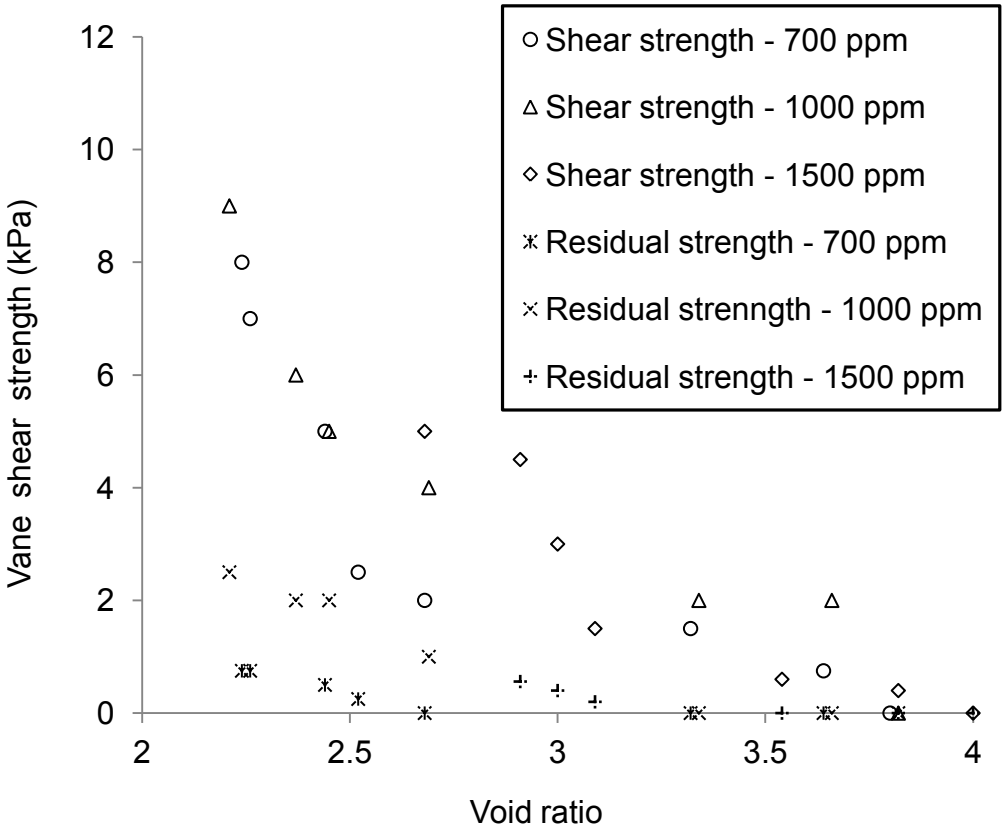

Figure 7-9: Undrained shear strength and void ratio relationships of polymer amended tailings

7.2.3 Scanning electron microscopy (SEM) test results:

Figs 7 - 10 and 7 - 11 show ESEM images of polymer amended tailings. The samples were collected at the depths of 5 cm, 15 cm, and 25 cm for various doses. As shown in Figure 7 - 3, the evaporation rate was almost the same and comparable in all columns but the water content was different with depth, and the profile somewhat changed with the polymer dose, though perhaps not significant (Figs 7 -10 and 7 – 11). It should be noted that the variation in water content with depth was not necessarily representative of field conditions, as crack patterns in the field were not adequately simulated by these small diameter tests.

Also similar from observed field behaviour and laboratory tests on thicker layers (~0.5 to 1 m), Mizani et al. (2013) and Matthews et al. (2011) showed lower water content at the bottom, likely reflecting self-weight consolidation. In these tests of 0.30 m, the 1000 ppm tailings gave lowest water content at the bottom (0.25 m).

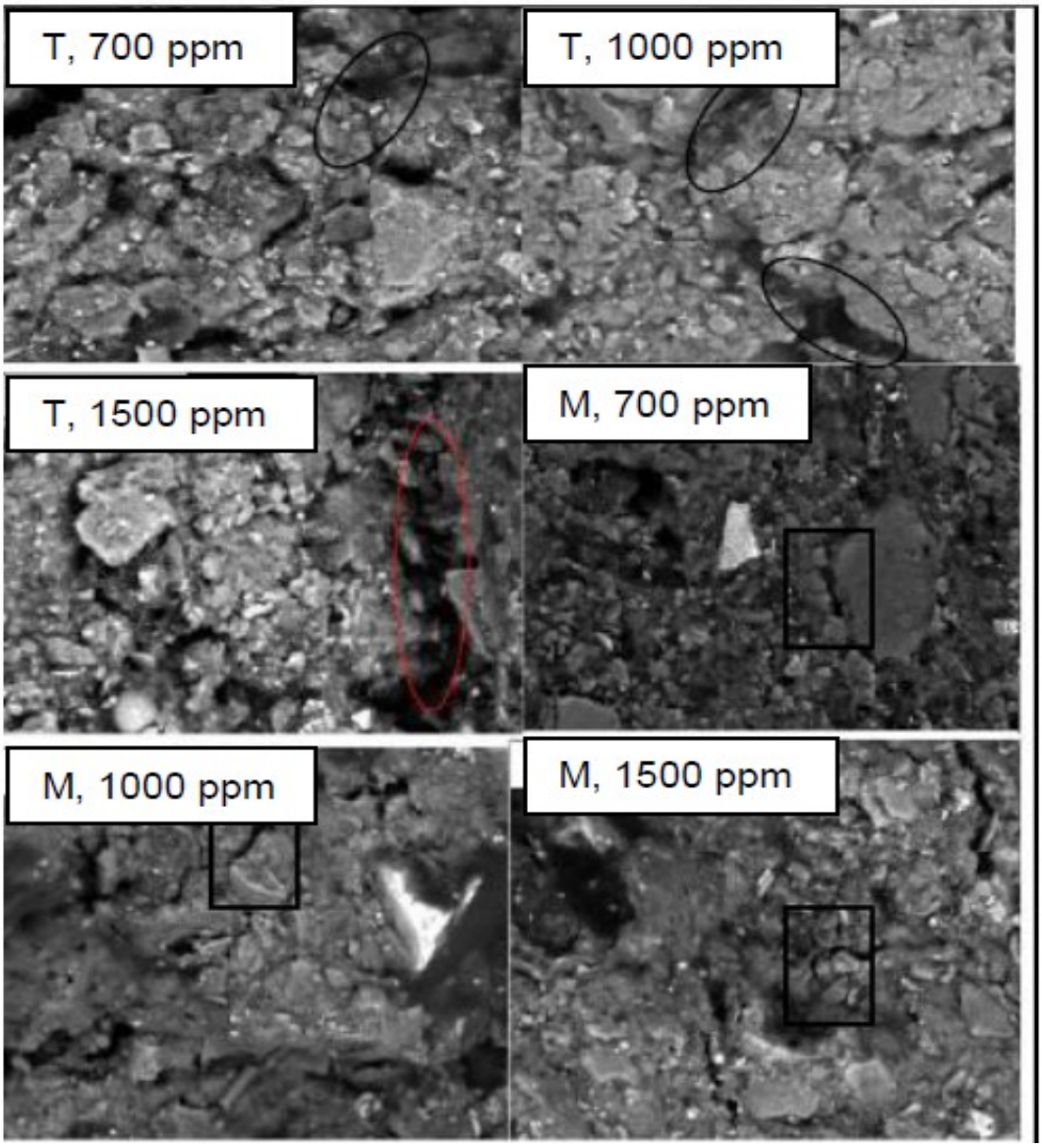

Figure 7-10: Environmental scanning electron microscopic (ESEM) micrographs of polymer amended mature fine tailings for depth profile; w = 36 % for top layer (700 ppm), w = 34 for top layer (1000 ppm), w = 35% for top layer (1500 ppm), w = 61% for middle layer (700 ppm), w = 48 % for middle layer (1000 ppm), w = 55 % for middle layer (1500 ppm); T, M, B represents middle and bottom layer profiles; Images are 100 by 100 microns

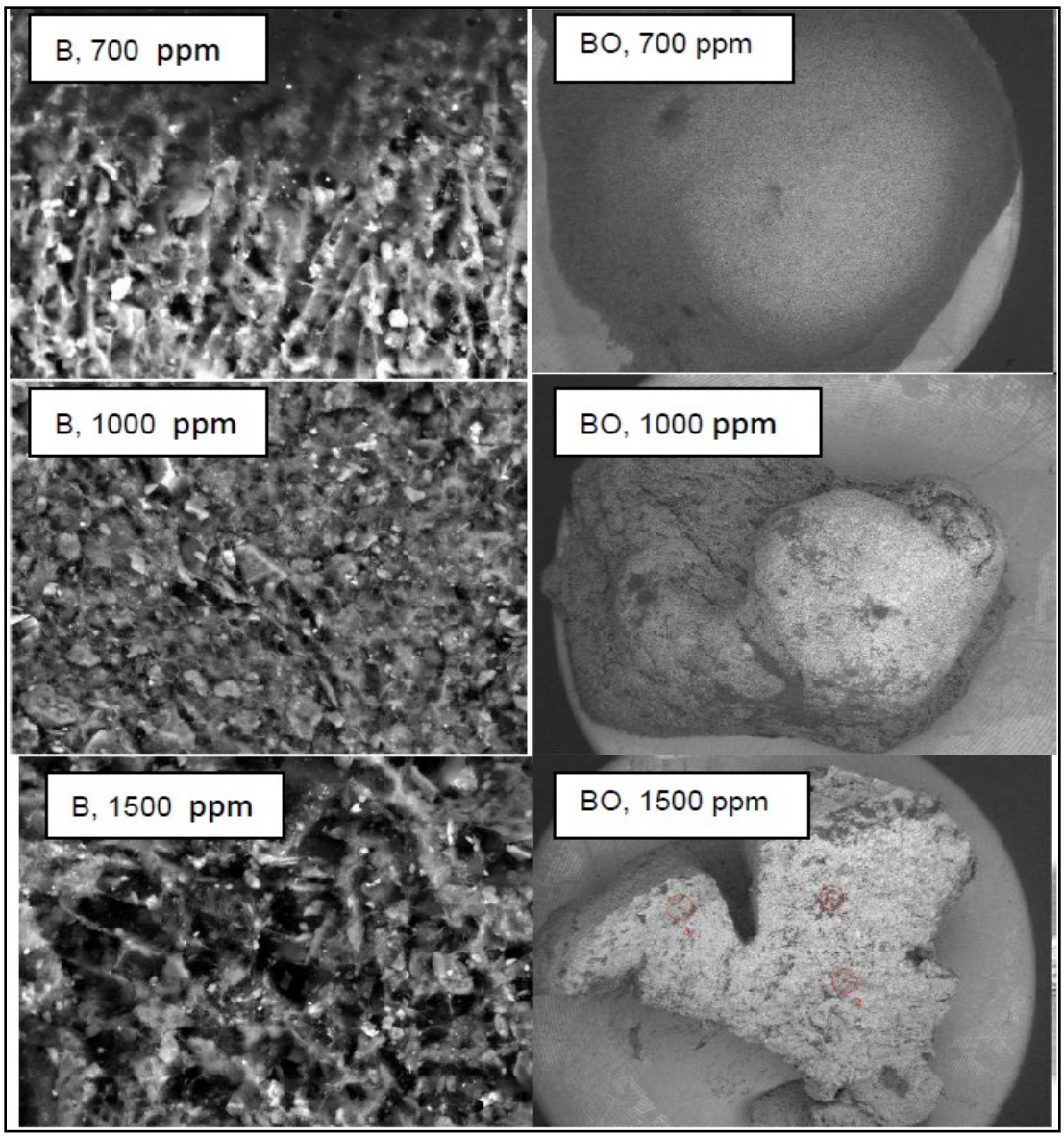

Figure 7-11: Environmental scanning electron microscopic (ESEM) micrographs of polymer amended mature fine tailings for depth profile; w = 98% for bottom layer (700 ppm), w = 89% for bottom layer (1000 ppm), w = 93% for bottom layer (1500 ppm); Images are 100 by 100 microns

Mizani et al. (2013) showed better longer term water release for less flocculated samples, which reflected the better consolidation characteristics of those materials. In general, with decreasing water content a micro crack network developed as desiccation progressed – micro cracks and pores opening up between contracting aggregates were highlighted in the images for the top and bottom of the columns. At the middle wetter layers, the fabric appeared more regular. The 1000 ppm and 1500 ppm tailings showed comparable fabric in terms of water content, but the 1500 ppm tailings showed much larger pores and clearer flocs.

Figure 7 -12 shows gray pixel analysis providing a more quantitative and unbiased analysis of ESEM images. The imageJ analysis was performed with BSE images captured at a magnification of 0.5 kx and at a scale of 200 μm. All SEM micrographs with a resolution of 1536 x 648 and a view field of 300 μm were selected to conduct the analysis. Appendix 2 shows ESEM micrographs used in image analysis. The optimization of backscattered SEM micrographs was carried out adjusting the threshold to clearly distinguish the particles, background and adjacent grain boundaries.

The microporosity of tailings differed but not so large at a particular depth for various polymer doses, and the data points of tailings appeared overlapping to each other. However, a major difference in microporosity was noted for a specific dose with respect to various depths. The data points of tailings varied between

0.4 and 100 μm for all depths and various doses as well (Figure 7 – 12). The microporosity of tailings lowered for an increase in degree of desiccation.

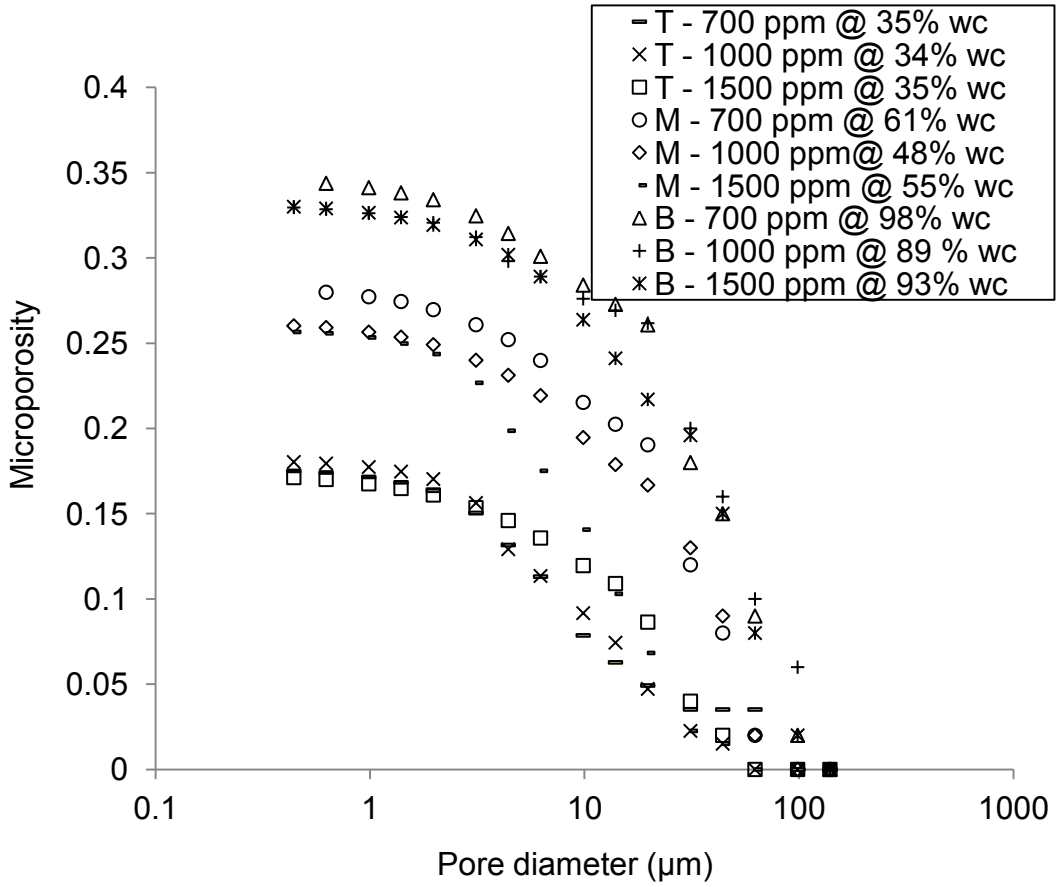

Figure 7-12: Microporosity of polymer amended tailings for various depth layers (T- top depth, M - middle depth, B - bottom depth)

As in Figure 7 – 10, the ESEM micrographs showed that the tailings fabric appeared different for a specific degree of desiccation; and for an increase in degree of desiccation, the tailings fabric appeared more compacted and packed, which alternately lowered the microporosity of tailings as presented in Figure 7 – 12.

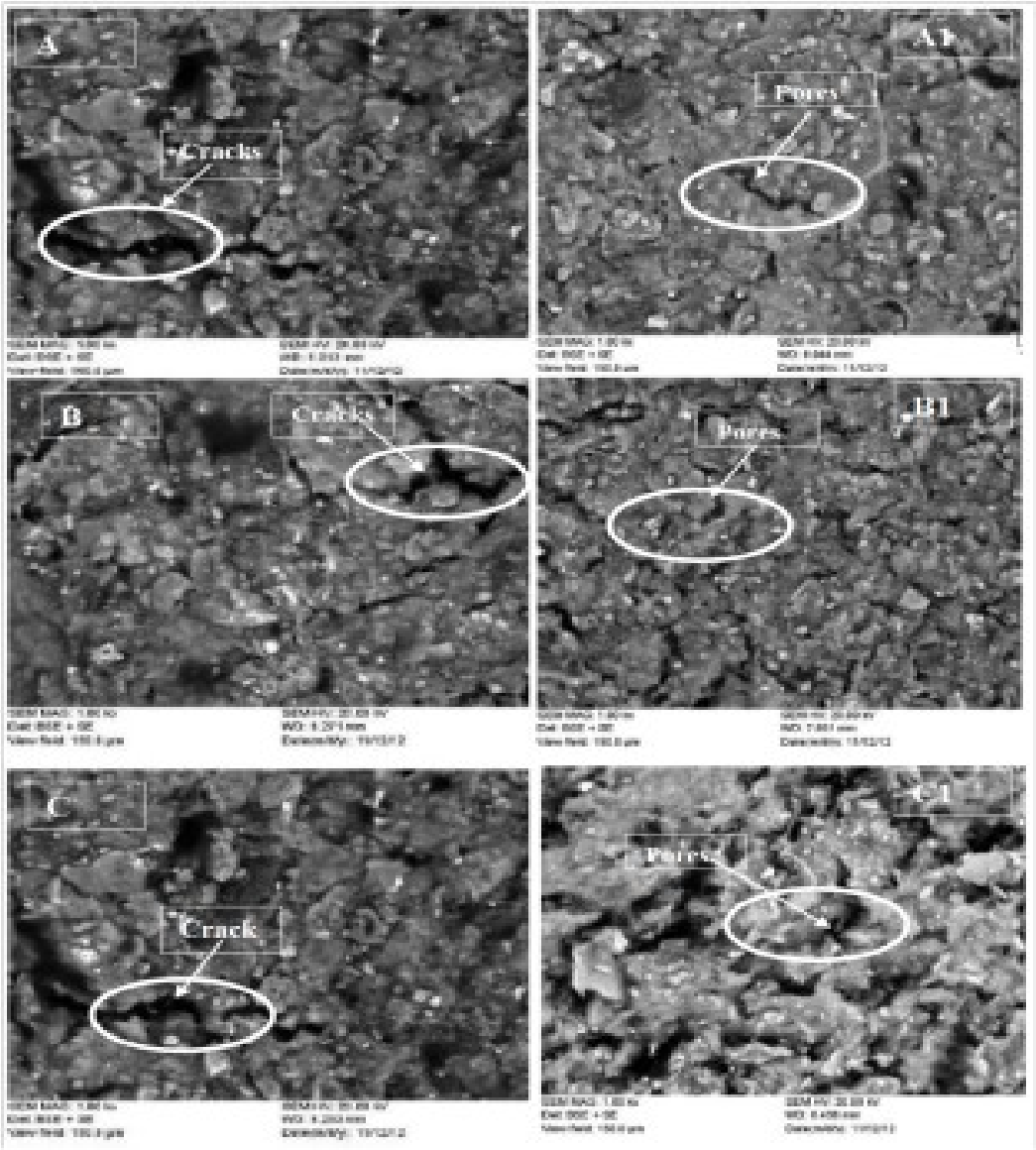

Figure 7-13: Environmental scanning electron microscopic (ESEM) micrographs of polymer amended MFT (left; w = 50% for 700, 1000, and 1500 ppm from top to bottom and right; w =103% for 700, 1000, and 1500 from top to bottom. Images are 100 by 100 microns.

The ImageJ analysis validated the fact that the tailings provided more packed structure showing lower porosity at the top in comparison to other layers and it happened due to the prevalence of desiccation, which resultantly intensified the size of pore cracks (Figure 7 – 10). According to Kodikara (2000), desiccation

resulted in the formation of cracks and the cracks were produced in the clayey soil as the tensile stress overcame the tensile strength of the medium as a result of an increase in suction.

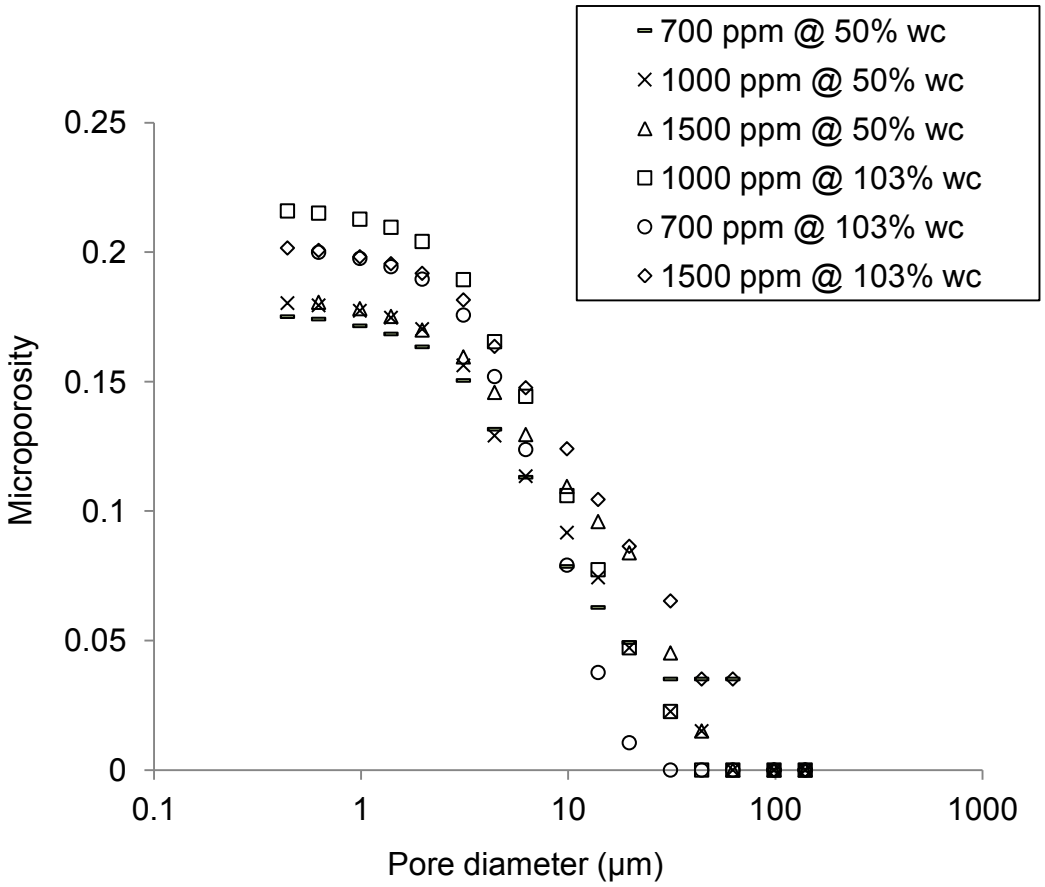

Figure 7-14: Microporosity of polymer amended tailings for various levels of desiccation

Two samples for each level of polymer dose are shown in Figure 7 - 13 for two different water contents of ~100 % and 50% (+/- 5%). Interestingly, while the samples at the higher water content appeared to show differences in inter-aggregate porosity, the differences at the lower water content were much less

apparent. In the 1500 ppm sample at the higher water content, the shapes of the pores looked more round giving the structure more flocculated than that of the other doses.

The appearance of tailings fabric at lower water content appeared quite different in comparison to higher water content. At the lower water content, the fabric showed a greater frequency of cracks. However, the difference between samples with different polymer dose was less remarkable than at the higher water content.

The gray pixel analysis of ESEM micrographs validated the qualitative judgement value. Appendix 3 presents ESEM micrographs used in image analysis as shown in Figure 7 – 14. These results, by themselves, suggested that desiccation substantially altered the microstructure, similar to other clayey soils (Romero and Simms 2008), and as desiccation progressed, the differences in microstructure between samples prepared with different polymer doses became less.

The gray pixel analysis as shown in Figure 7 -14 showed that the microporosity of tailings decreased with a decrease in water content for all doses. Again, the porosity curves of various doses overlapped to each other showing minimal difference in porosity for a particular degree of desiccation, however the difference was quite significant for the change in degree of desiccation for a specified dose. The microporosity of various doses for lower water content did not differ largely validating the argument that the change in volume was not so important for various doses beyond a certain degree of desiccation

7.2.4 Mercury intrusion porosimetry test results

Cumulative pore-size distributions (CPSD) from MIP are shown in Figs 7 – 15 to 7 – 17. Figure 7 - 15 shows the CPSD for the three treatments of polymer amended MFT and untreated MFT at the initial water content (140%).

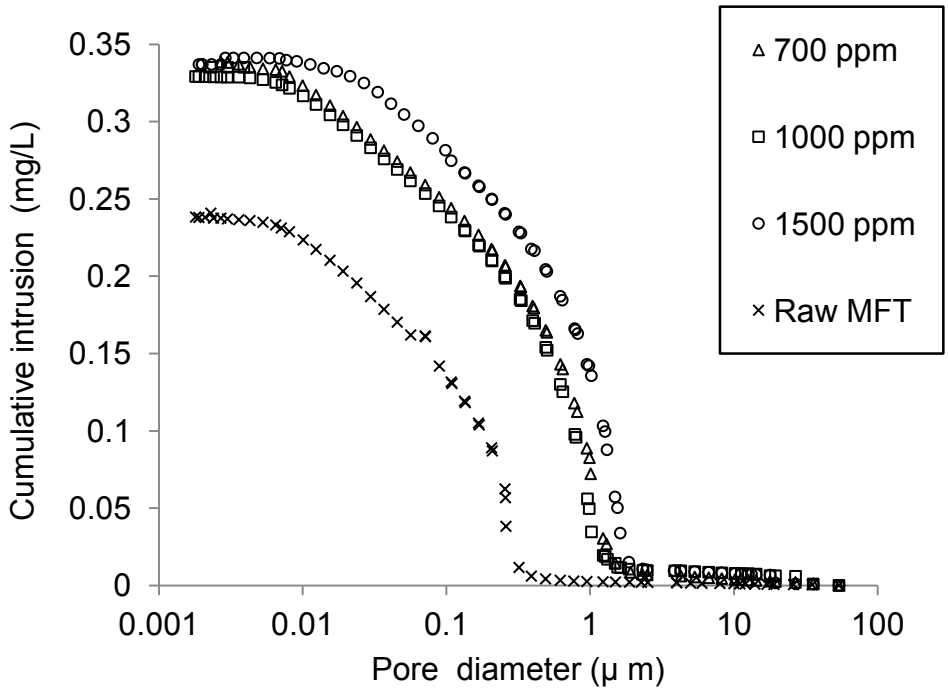

Figure 7-15: Mercury intrusion porosimetry test results, showing cumulative pore-size distributions (intrusion) for polymer amended MFT for a water content of 140% for 700, 1000, 1500 ppm and unamended MFT.

As expected, the treated MFT showed much more porosity in the high pore sizes than untreated MFT. The treated MFT CPSD was very close together, and the 1500 ppm sample gave somewhat larger pore sizes than the other two treatments. As shown in Figure 7 – 16, the changes in CPSD with desiccation

showed the same trend as the SEM images. There was very little difference in fabric was noted between the samples desiccated to 100%.

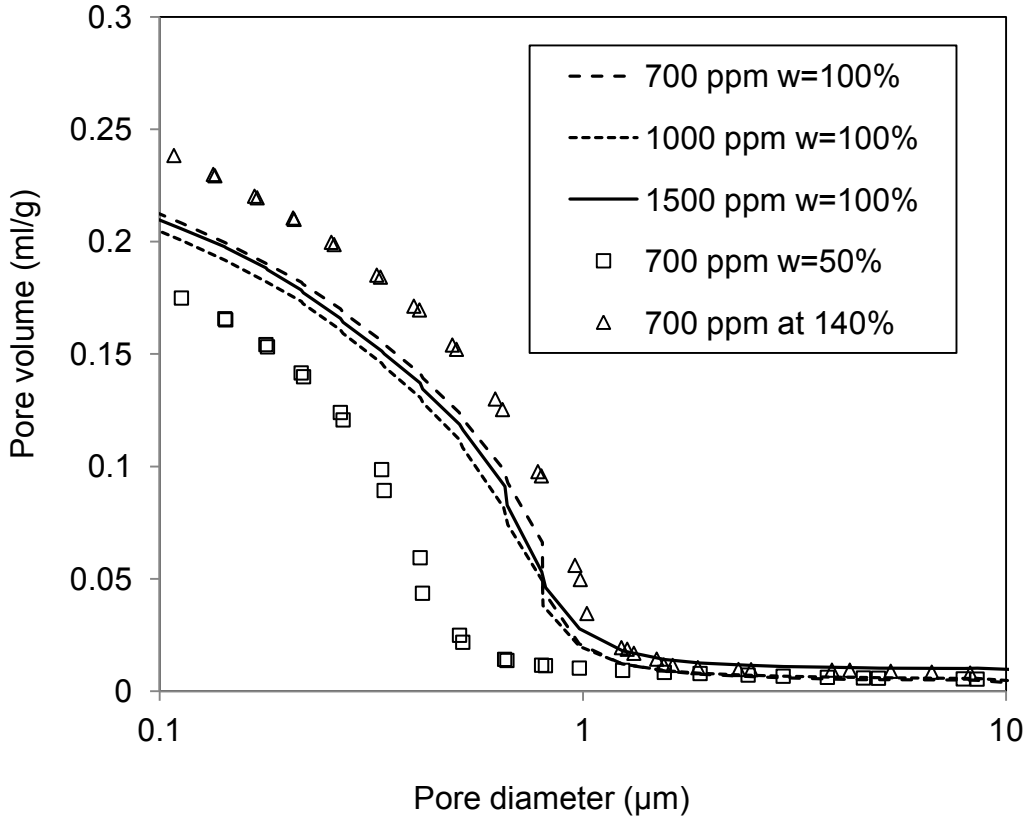

.

Figure 7-16: Cumulative pore-size distributions of polymer amended tailings at different degrees of desiccation

This agreed with the relatively small differences in the water retention curve at higher suctions – by the time the AEV was reached (Figure 7 - 7), and the difference in microstructure appeared relatively small. However, the MIP data did not apparently explain the slightly higher shrinkage limit of the 1500 ppm treatment, however 1500 ppm showed higher cumulative intrusion. After

desiccation to 50% water content, the polymer amended tailings still showed a greater porosity in the larger pores, compared to the unamended MFT at 140% as shown in Figure 7 -17.

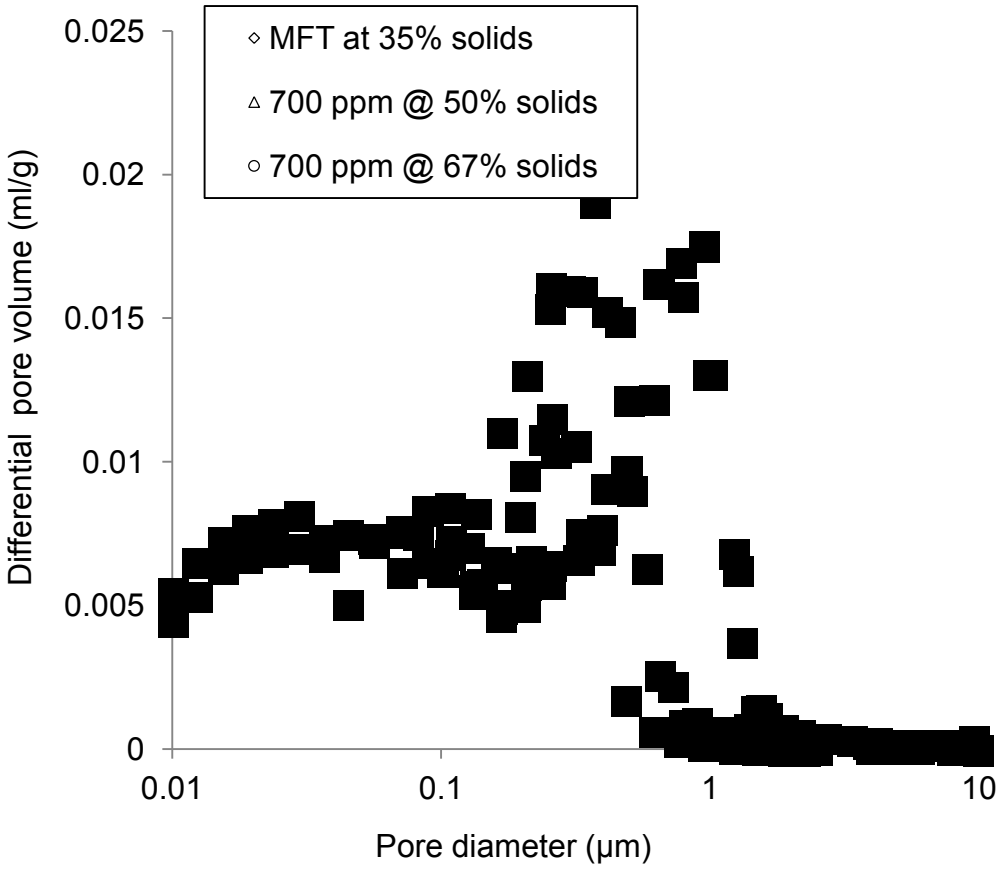

Figure 7-17: Differential pore-size distributions of polymer amended tailings for different degrees of desiccation

As in Figure 7 -17, the peak pore mode shifted towards smaller pores diameter, showing an increase in smaller pores diameter with an increase in percent solids and consequently the PSD of tailings centered at pores diameter of 0.9 and 0.4 µm for percent solids of 50 and 67% respectively. These results were in close

agreement to SEM micrographs and Image analysis. The SEM micrographs showed more compacted structure for 67% solids content and the microporosity of tailings also decreased for an increase in degree of desiccation.

7.3 Interaction of microstructure and macroscopic features of polymer amended tailings

For higher water content (103%), the pores appeared more open, wide and the structure was more flocculated, and conversely, the structure appeared more compact for lower water content (50%) which resulted in narrow, less open pores but initiation of cracks. Comparatively, the tailings showed lower microporosity at lower water content, and similar observations were noted in the scanning electron micrographs.

This decrease in microporosity as an increase in degree of desiccation resulted in an increase in strength beyond certain water content for all tailings. Both techniques showed that the pore-size distributions of the different treatments (polymer doses of 700, 1000, and 1500 ppm) converged with increasing desiccation. This correlated with the very similar water-retention curves of the different treatments, though not with the slightly higher shrinkage limit of the 1500 ppm sample. Based on this analysis, it appeared that the desiccation behaviour beyond the initial water release during settling appeared relatively insensitive to the range of polymer applied in this study.

7.4 Conclusions

As expected, the polymer amended MFT gave much more porosity with high pore sizes than unamended MFT. Furthermore, for a polymer dose of 700 ppm, the peak pore mode shifted towards smaller pores diameter for an increase in degree of desiccation. While some differences were detected in evaporation and shear strength - water content relationships for polymer doses of 700, 1000, and 1500 ppm, there appeared not to be practically significant changes. These results suggested there is no benefit to efficiency of dewatering through desiccation to increase the polymer dose beyond a certain threshold. However, up to this point, 700 ppm was the optimal polymer dose.

Chapter 8. Evolution of microstructure and undrained shear strength of polymer amended oil sands mature fine tailings in thick lifts (~ 80 cm)

In this study, the strength and microstructure of polymer amended oil sands fine tailings were examined in experiments simulating thick lift deposition (~ initial height of 80 cm). The test results showed that both consolidation and desiccation greatly influenced the strength of polymer amended tailings. Consolidation controlled the strength near the bottom and middle of the lift while desiccation dominated the strength under the crest. The osmotic suction contributed largely to total suction at higher water contents. The tailings shifted towards pores of smaller diameter with an increase in degree of desiccation and consolidation, and the peak pore mode compressed for an increase in degree of consolidation. Shear strength at a given void ratio was stronger in the thick lift than in the thin lift test described in the previous chapter. This is correlated to a more flocculated structure present in the thick lift experiments.

8.1 Introduction:

The regulatory changes have forced the oil sands industry to adopt new methods for an effective management of oil sands tailings. The attainment of the guidelines of ERCB Directive 074 (2009) would help to; i-) minimize and eventually eliminate long-term storage of fluid tailings in the reclamation landscape; ii-) minimize fresh water import maximizing process water recycling; iii-) reduce resource sterilization associated with tailings ponds; iv-) minimize and

eliminate the hazardous environmental impact. Oil sands operators are testing several alternatives to transform the fluid MFT into a trafficable deposit in order to achieve these objectives. The inventory of fluid MFT contained in the tailings ponds would continue to grow until the new technologies were implemented. Various technologies were being trialed for several years now, but remained expensive to implement on a commercial scale (Sobkowicz 2013). In-line flocculated tailings is a simple approach to enhance the settling behavior discharging tailings in-line (Figure 8 – 1).

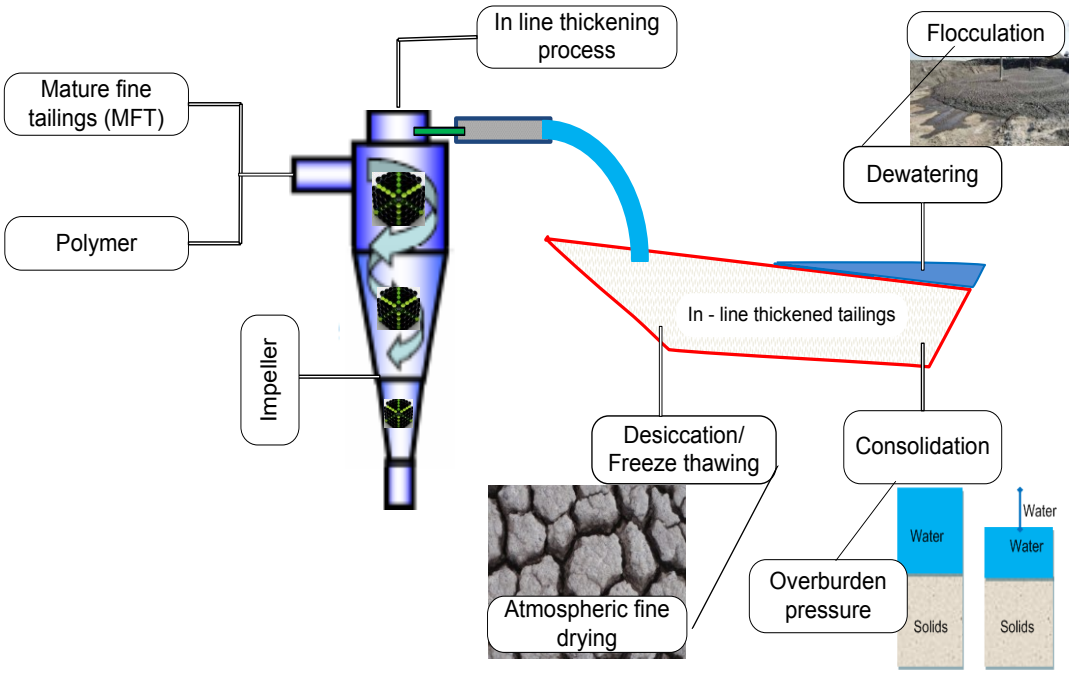

Figure 8-1: Schematic of in-line flocculation approach

The technology is not effective without the addition of chemical additive as the MFT itself does not show any dewatering potential, even after several years of deposition. Xu and Hamza (2003) reported that a high molecular weight polymer

and medium charged anions accelerated the isolation of water from fine solids, which resultantly produced paste like materials. The studies such as Ren et al. (2014); Wang et al. (2014); Farkish and Fall (2013); Mizani et al. (2013); Wells et al. (2011) and Chalaturnyk et al. (2002) were found in the literature, those discussed the solids content variations of in-line flocculated tailings in thin lift.

The dewatering along with other natural processes such as evaporation and consolidation accelerate the consolidation potential of in-line flocculation. At least four mechanisms contribute to dewatering post-deposition strength gain, i-) very short term water release – a rapid dewatering of tailings takes place due to flocs formation, ii-) dewatering due to consolidation and flocs formations in the short term (in a few weeks), iii-) strength gain by desiccation - desiccation takes place at the surface of the tailings due to evaporation (natural process), and iv-) consolidation - self weight consolidation (natural process) - self weight consolidation takes place throughout the depth of deposited tailings, when tailings are deposited in lift or a new layer of tailings is buried over another layer.

In this study, the geotechnical (undrained shear strength, void ratio, and soil water potential) properties of polymer amended tailings were examined for flocculation and natural processes such as desiccation and consolidation. MIP tests were performed to examine the microfabric of tailings.

8.2 Materials and methods

The polymer amended oil sands MFT was prepared following the guidelines as discussed in Chapter 03. The prepared tailings were transferred to three cylindrical columns of 90 cm depth and 20 cm diameter, and the tailings were deposited in a lift of 82 cm (Figure 8 - 2).

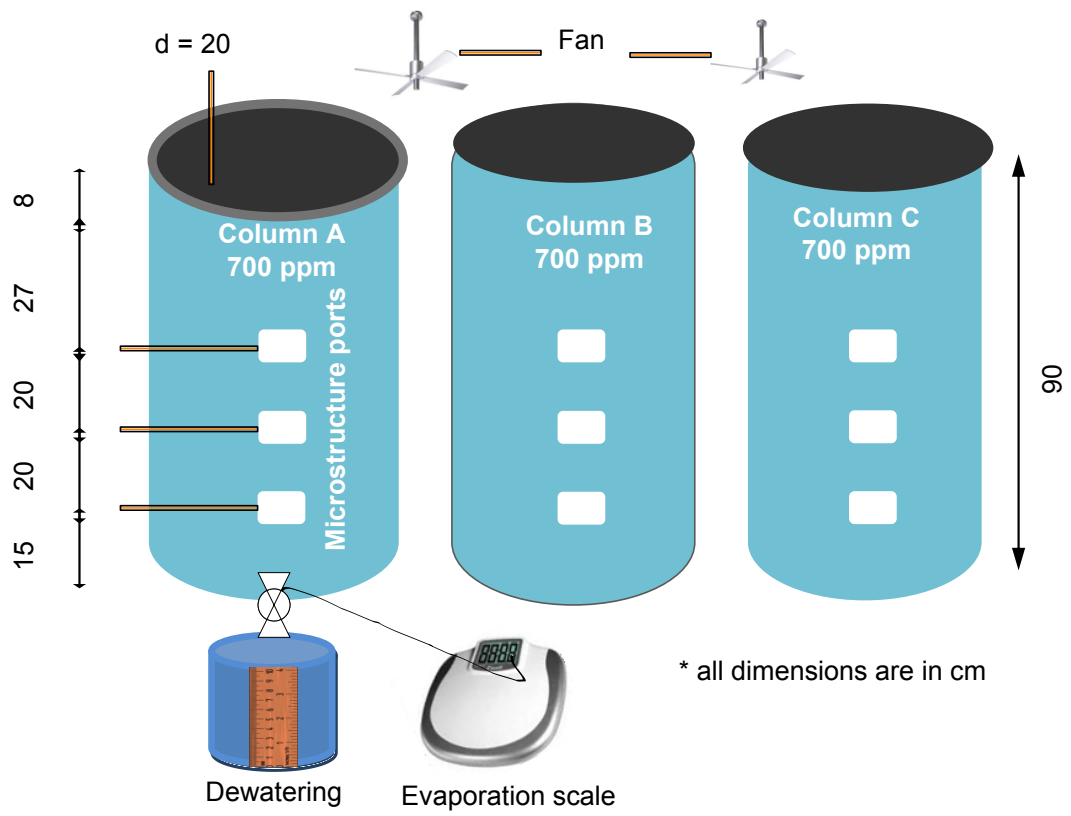

Figure 8-2: Schematic of in-line flocculated tailings.

Each column was equipped with a drainage system at the bottom to monitor successive release of water from deposited tailings. Two fans were used to control the rate of potential evaporation. The microstructure and shear strength of

polymer amended MFT was monitored at 27, 47 and 67 cm depths over time, i.e., after 09, 17 and 27 days (Figure 8 - 2).

Mercury intrusion porosimetry (MIP) tests were performed to examine the microstructure of polymer amended tailings. For these tests, the samples were collected at the depths of 27, 47 and 67 cm after 09, 17 and 27 days. A mold of 20 cm depth and 10 cm dia. was used to collect undisturbed samples from columns.

Figure 8-3: Laboratory experimental set up to examine the microstrcuture and macroscopic behaviour of polymer amended oil sands tailings in thick lift

The tailings were dug to the marked depth, and the mold was gently driven into the tailings to extract the samples. After the molds were removed from the tailings column; a sample less than 1 cm^3 was cut from the extracted specimen. In these tests, freeze dried samples were used. Vane tests were conducted to measure the undrained shear strength of tailings. The vane was gently inserted into the tailings up to depths of 27, 47 and 67 cm one by one in a single thrust (Figure 8 - 2) and rotated until the material failed in shear for the specific depth.

The variations in percent solids content, gravimetric water content and void ratio (volume change) relationships were developed over time. The dewatering (drainage) and surface flux (evaporation + decant water) of tailings were monitored to define the water release potential. For electrical conductivity, total suction and gravimetric water content, the samples were collected for each 5 cm depth of the columns after 09, 17 and 27 days. Figure 8 - 3 presents laboratory experimental set up to examine the microstrcuture and macroscopic behaviour of polymer amended oil sands tailings in thick lift

8.3 Results and discussions:

8.3.1 Volume change potential of polymer amended oil sands tailings

The tailings released significant amount of water for first week, and both dewatering and evaporation increased linearly, but after this time, the tailings showed less dewatering potential as showing in Figure 8 – 4. The tailings

attained 69% dewatering (drainage water + surface bleed water) potential in first 05 days draining off 126 mm of total 167 mm released water. The drain off potential of tailings was too low after 15 days. The tailings drained off only 0.15 mm of water after 27 days; however, the drain off potential from tailings was maximal for the first 24 hours (Figure 8 - 4).

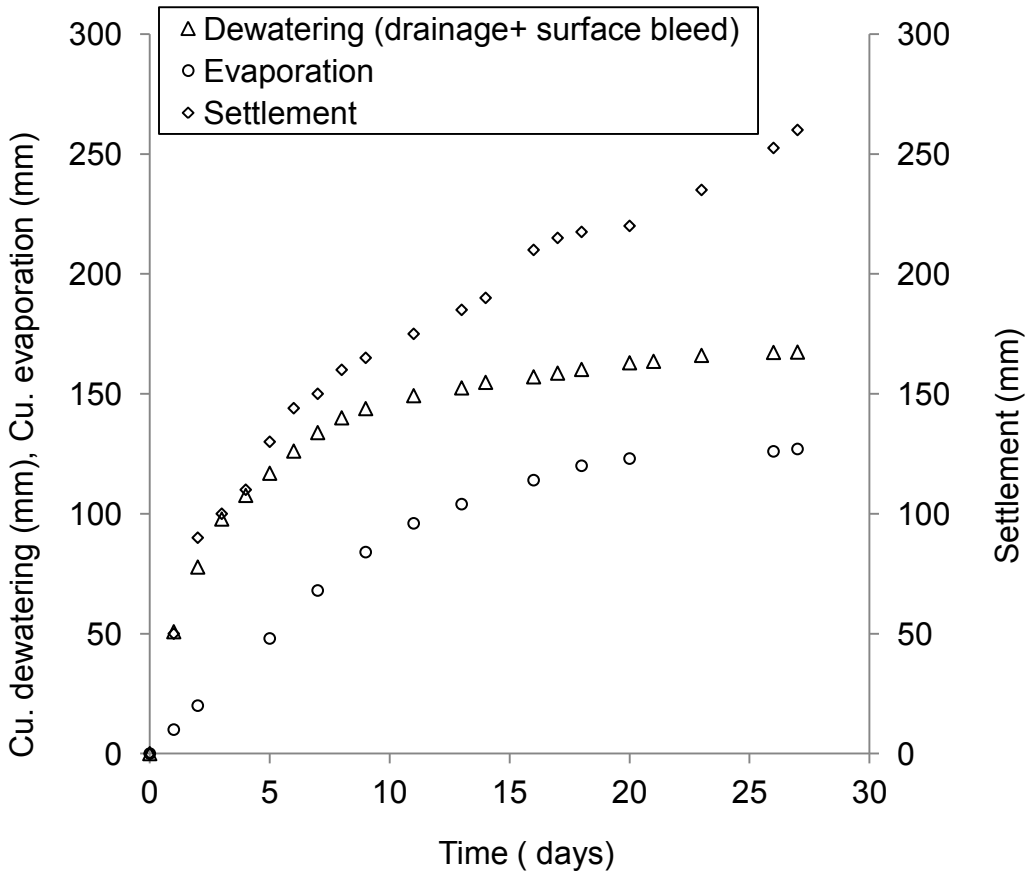

Figure 8-4: Dewatering and evaporation potential of polymer amended tailings

The tailings provided a potential evaporation (PE) of 8.50 mm / day. As a comparison to the test data as discussed in Chapter 7, the tailings showed higher

potential evaporation, and it happened due to the over release of surface water due to the fans speed.

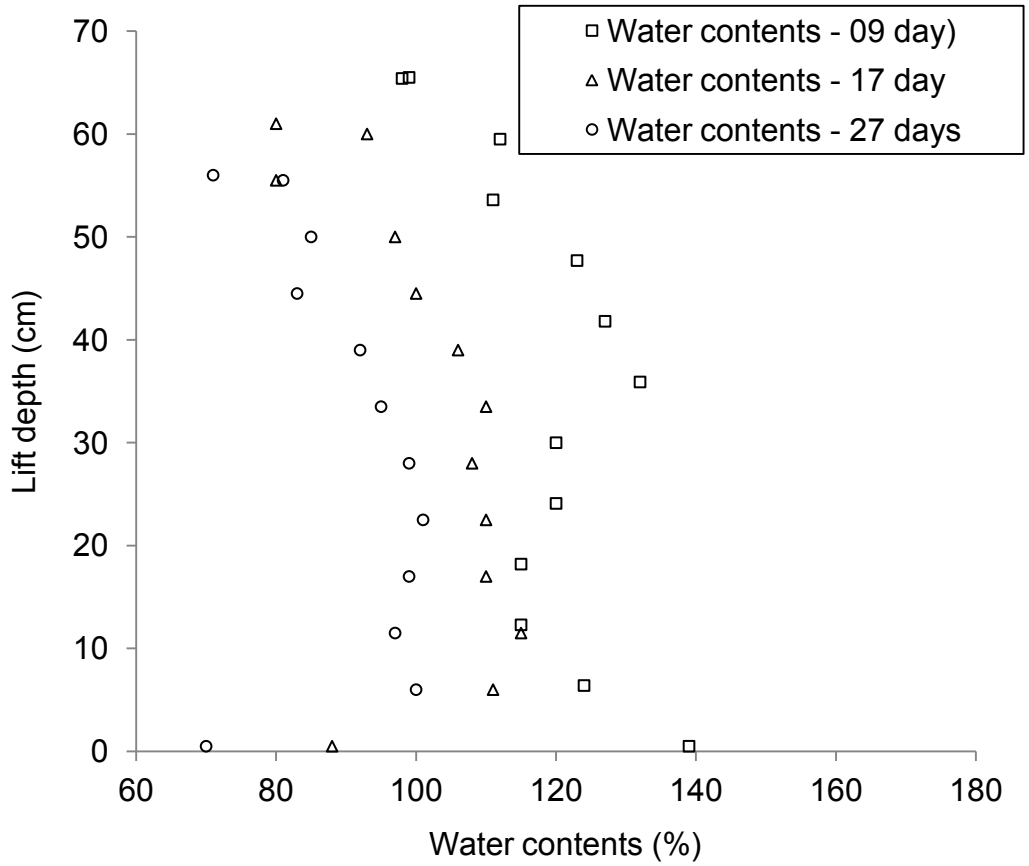

Figure 8-5: Water content variations of polymer amended tailings

The water content profiles as in Figure 8 - 5 showed that the water content of tailings varied from 139 - 98 %, 115 – 88% and 101 – 66% from top to bottom after 09, 17 and 27 days respectively. The tailings did not show uniform variations in water content along the depth of lift. The higher water content at the top lift after 09 days occurred as the tailings released water (surface bleed) to the top. Comparatively, the percent solids of tailings varied from 41 to 50; 46 to 53

and 50 to 60 along the depth after 09, 17 and 27 days respectively. The tailings generally showed lower water contents both at the top and bottom in comparison to middle depth profiles (Figure 8 – 5), and the differences was more evident after 27 days.

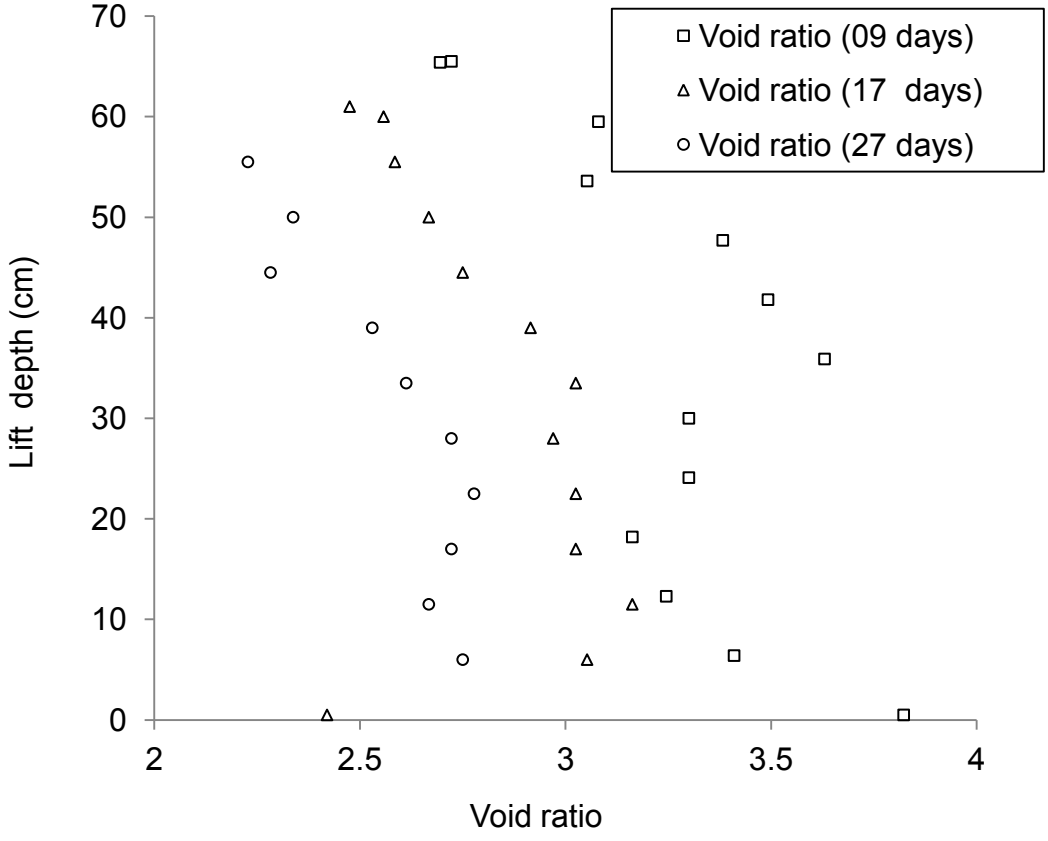

Figure 8-6: Variations in void ratio of polymer amended tailings

Comparatively, the tailings provided higher void ratio at the middle depth in comparison to top and bottom depths (Figure 8 – 6). The void ratios of tailings were calculated directly from water content assuming S=1. This assumption was

likely true in all cases except for the top of the lift, as all other void ratios were substantially higher than the shrinkage limit.

The void ratio profiles did not change significantly from 10 to 30 cm of top depth over time. At this point, the effect of desiccation and dewatering was not so influential which could alter the volume of tailings too much (Figure 8 – 6).

8.3.2 Total suction of polymer amended oil sands tailings

As in Figure 8 – 7, the tailings provided more suction at the top in comparison to the middle and bottom layers of the lift over time, and the tailings showed more suction after 09 day at 27 cm depth. The total suction varied from 20 to 232 kPa, 66 to 117 and 70 to 135 after 09, 17 and 27 days respectively after tailings deposition (Figure 8 – 7). However, the variations in total suction were not too high; however, the differences in suction were more along the depth after 09 days.

Figure 8 – 8 shows the osmotic suction profiles of polymer amended tailings over time. Like that of total suction, the osmotic suctions did not vary significantly with depth over time, but comparatively, the osmotic suction showed decreasing trend over time and differences were more along the depth after 09 day in comparison to 17 and 27 days (Figure 8 – 8).

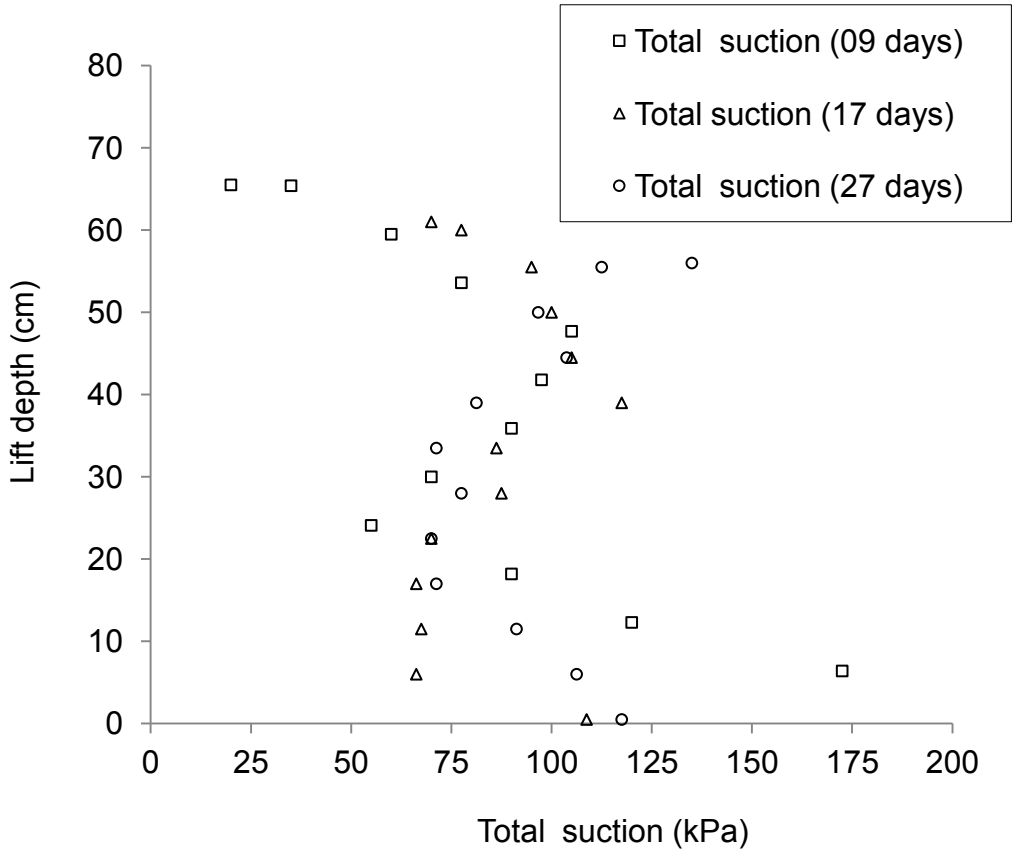

Figure 8-7; Total suction profiles of polymer amended tailings

Generally, the osmotic suction of tailings varied from 122 to 156, 56 to 77 and 26 to 52 kPa after 09, 17 and 27 days respectively (Figure 8 – 8). Fredlund and Rahardjo (1993) discussed the osmotic suction of Regina clay and the variations in the osmotic suction were minor for water contents between 23% and 32%.

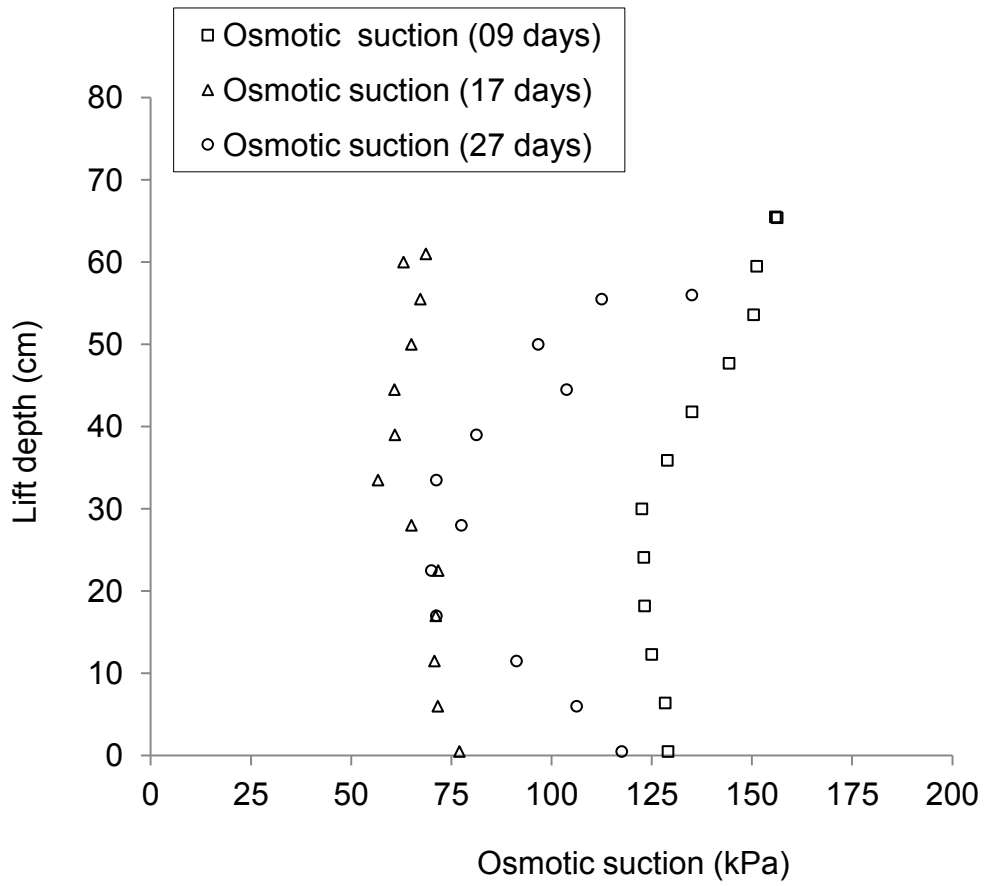

Figure 8-8: Osmotic suction profiles of polymer amended tailings

The osmotic suction decreased over time, likely due to removal of dissolved mass through drainage, and potentially some precipitation at the surface, though this was not evident in pictures.

The tailings showed minimal or zero matric suction after 09 and 17 days. However, the tailings showed some matric suction for 27 days and it varied between 19 and 109 kPa after 27 day (Figure 8 – 9). The negative value of suction as in Figure 8 – 9 was due to the fact that the accuracy of the measurements of total suction was only (+/- 100 kPa). Furthermore, the

saturation extract procedure might not yield the accurate measurement of osmotic suction. Overall, the osmotic suction dominated the total suction, though the tailings showed some matric suction over time.

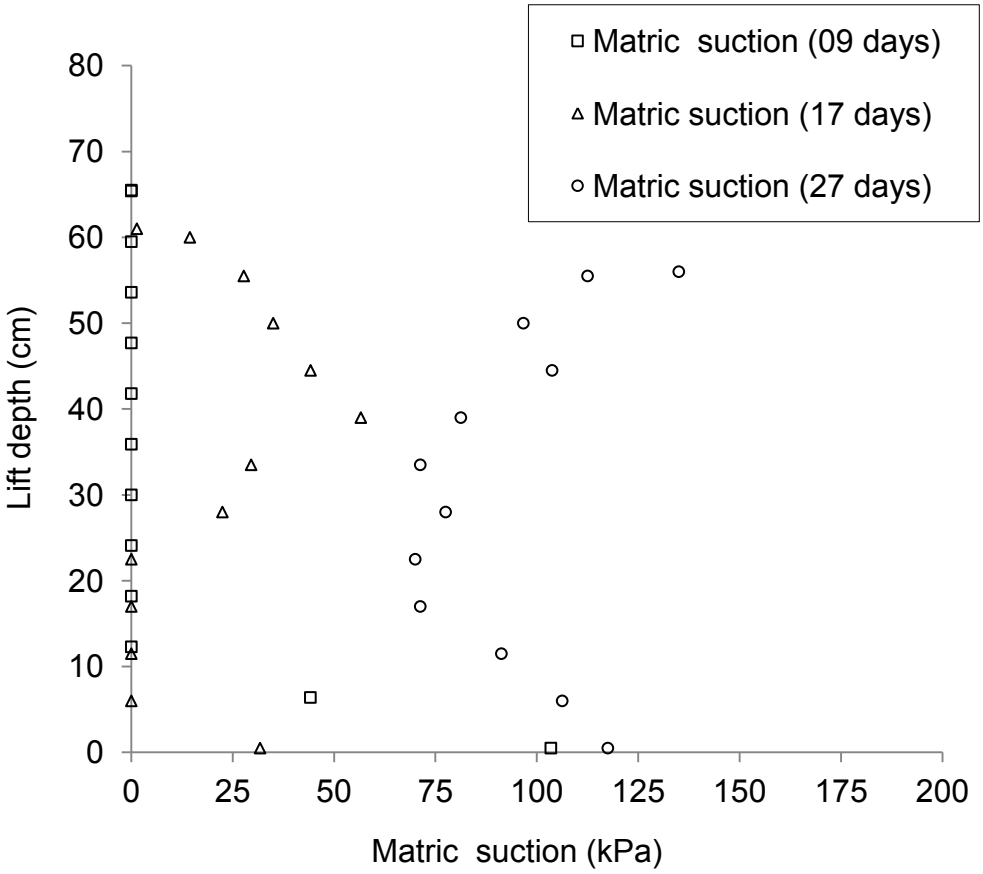

Figure 8-9: Matric suction profiles of polymer amended tailings

The tailings showed more matric suction at top and bottom layers after 27 days, which was due to desiccation and self weight consolidation. Similar studies on oil sand tailings showed that osmotic suction contributed more than 50% component of total suction (Innocent-Bernard 2013 and Rozina et al. 2015). Due to the small

influence of desiccation in these tests, the drainage or surface bleeding of dissolved mass by consolidation controlled the suction data.

8.3.3 Undrained shear strength of polymer amended oil sands tailings

The tailings showed an increase in undrained shear strength along the depth over time, and the tailings showed quite high strength after 27 days at 67 cm depth (Figure 8 – 10).

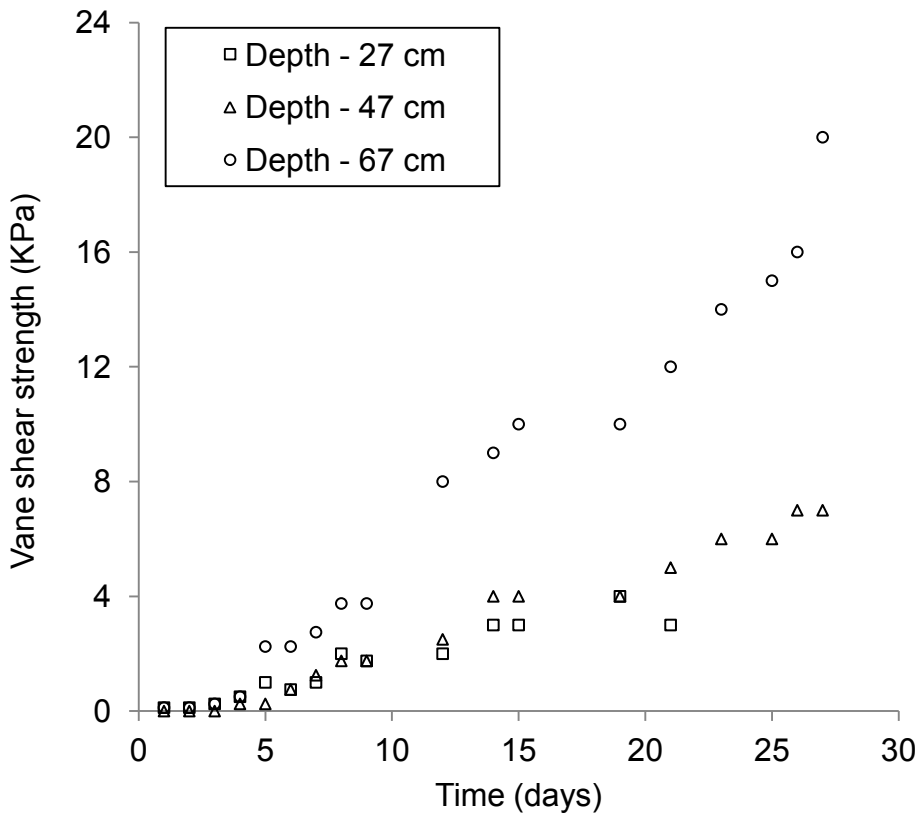

Figure 8-10: Undrained shear strength of polymer amended tailings over time

For this time, the tailings drained off sufficient quantity of total released water, which consequently increased consolidation and hence increased the strength. The tailings showed peak undrained shear strength of 20 kPa at 67 cm depth, and the strength was 7 kPa at 47 cm after 27 day. The tailings were consolidated more at the bottom due to dewatering and higher over burden pressure, which resulted in their higher strength due to lower void ratio and higher density. However, the vane was unable to provide any strength at 27 cm depth for 27 days tailings deposition due to settlement of the sample.

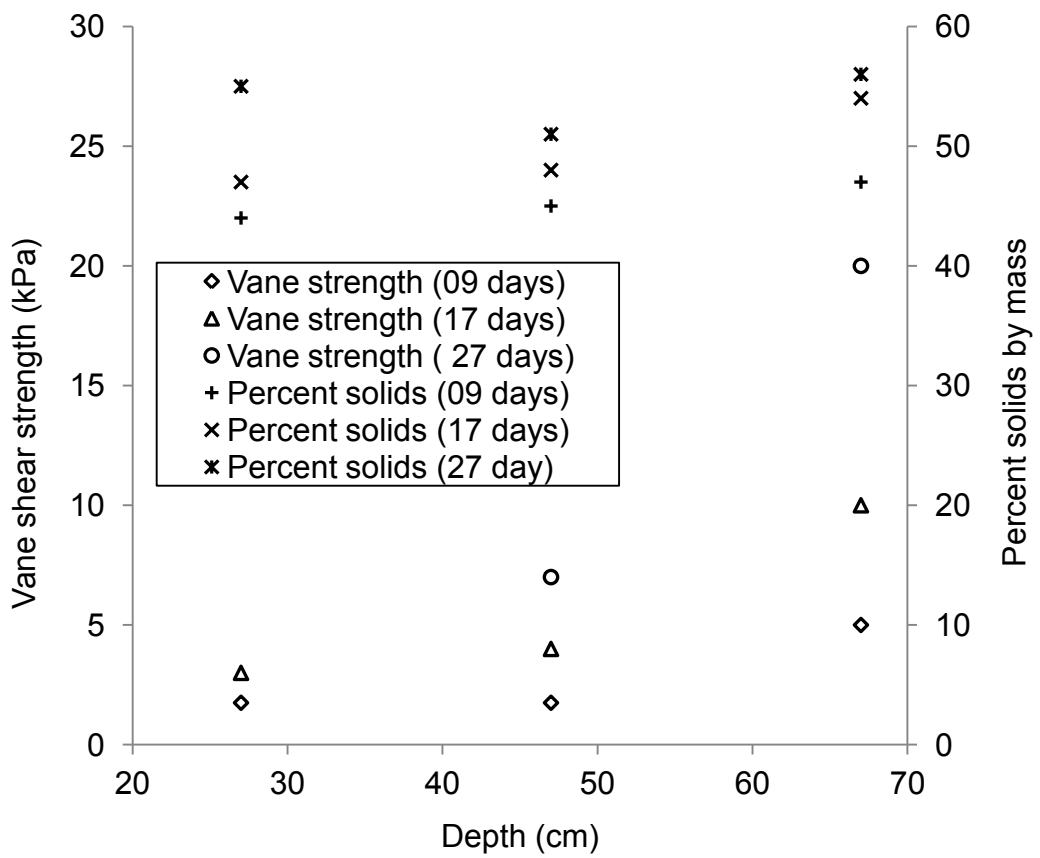

Figure 8-11: Undrained shear strength, percent solids of polymer amended tailings over time

At 27 days, the tailings showed quite high consolidation, i.e., 26 cm and the vane shear was unable to produce any strength at the top depth. At this point, the depth of tailings was not sufficient enough to determine the vane strength which might follow the criteria as set out in standard ASTM D 2573 - 08. It was discussed in the standard to insert the vane blade into the soil at least twice the length of vane blade (70 to 80 mm) to shear the materials without disturbing the adjoining soil surface; especially on the vertical edges of the vane blade. The relationship between vane strength and percent solids by mass for change in depth of the lift are highlighted in Figure 8 – 11.

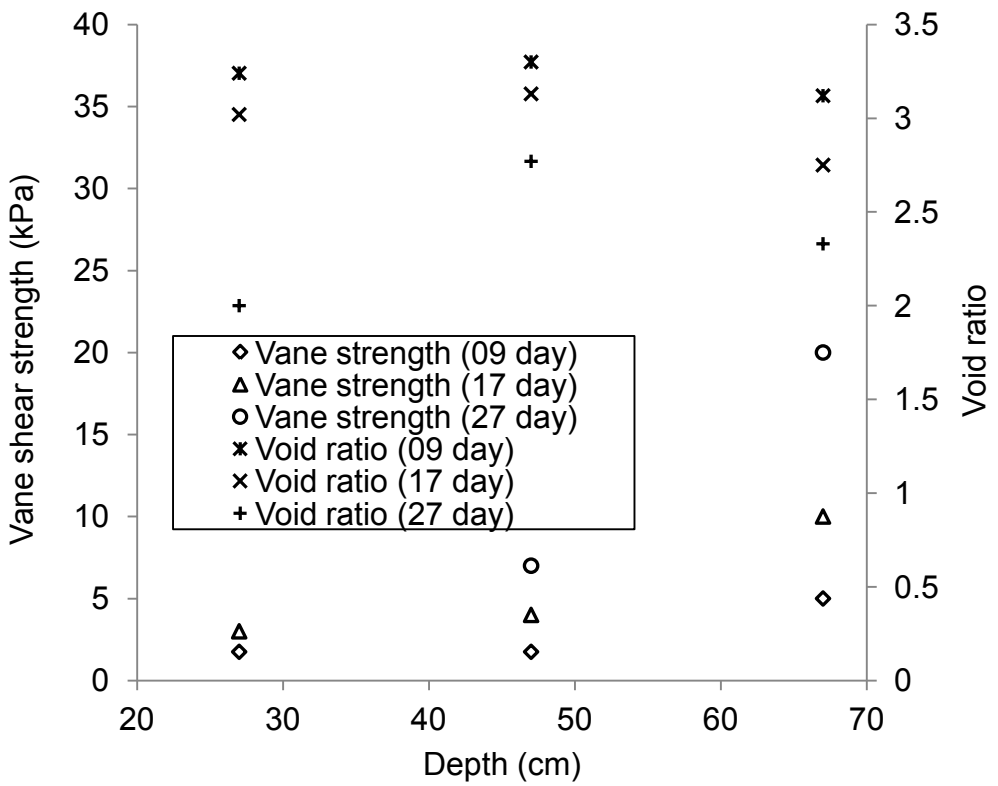

Figure 8-12: Undrained shear strength, void ratio and lift depth interactions of polymer amended tailings

The tailings showed shear strengths of 1.75, 1.75, 5 kPa at depths of 27, 47 and 67 cm corresponding to percent solids of 44, 45, and 47% respectively after 09 days. For 17 days, the tailings showed shear strength of 3, 4 and 10 kPa at depths of 27, 47 and 67 cm corresponding to solids content of 47, 48 and 54% respectively. After 27 days, the tailings showed quite high strength (20 kPa) at 67 cm depth in comparison to 47 cm depth (7 kPa), which corresponded to percent solids of 56 and 51% respectively (Figure 8 – 11).

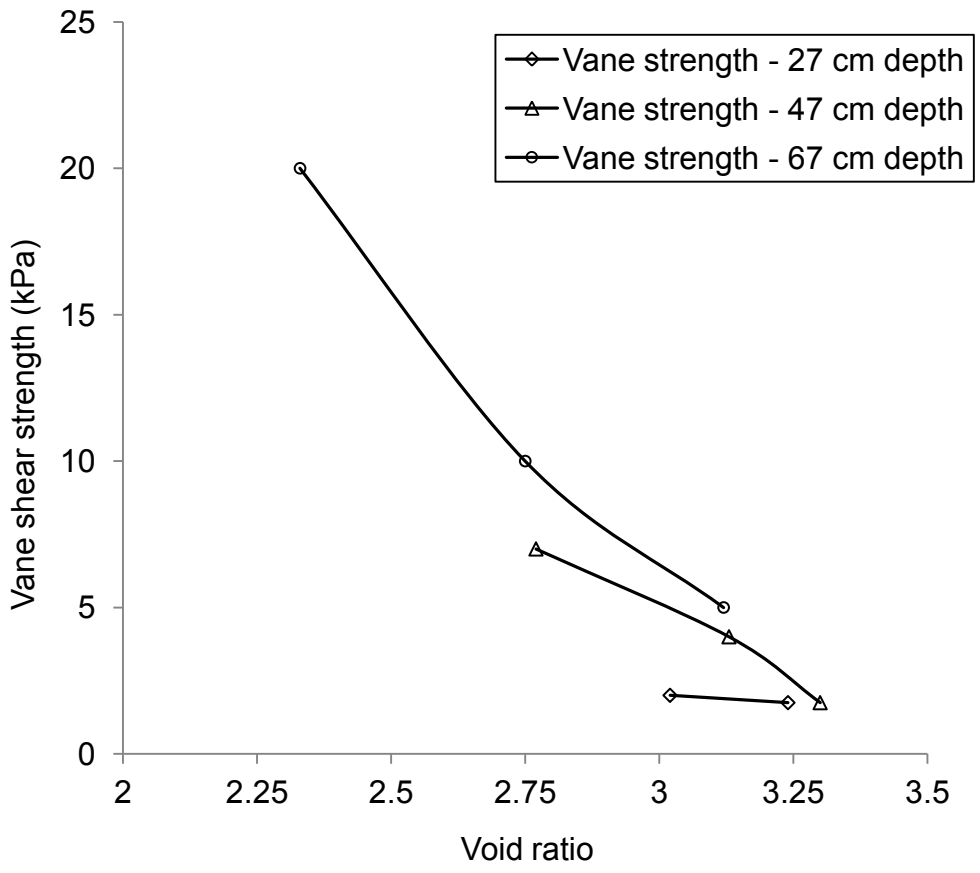

Figure 8-13: Undrained shear strength and void ratio relationships of polymer amended tailings for various depths over time

Similarly, the difference in void ratio along the depth was too high after 27 day in comparison to 09 and 17 days (Figure 8 – 12). The vane tests showed that the tailings showed some but not so significant differences in strength up to 47 cm depth, however they provided significant increase in strength at 67 cm depth over time (Figure 8 – 13) and it happened due to self weight consolidation that packed tailings more at the bottom in comparison to top and middle layers.

After 27 days, the influence of desiccation was quite notable at the top most layers and cracks development was also initiated in the tailings, which were liable to produce a major increase in strength after 27 day under the crest, but at this point, the strength could not be measured as the tailings were settled about 26 cm.

8.3.4 Mercury intrusion porosimetry test results

Figs. 8 - 14, 8 - 15 and 8 – 16 show comparison of cumulative pores size distribution (CPSD) of polymer amended fine tailings. Figure 8 – 14 showed that the tailings showed small difference in cumulative pore volume over time for 27 cm depth, however, the tailings showed quite low cumulative intrusion at this depth after 27 day..

As in Figure 8 -7, the tailings showed void ratios of 3.24, 3.02, and 2 after 09, 17 and 27 days respectively at 27 cm depth respectively, and the CPSD of tailings in Figure 8 – 14 correlated with the actual macroporosity test results. The CPSD of

tailings did not provide any major difference in pores volume for particular depth over time, however, some differences in CPSD was seen for larger pores diameter along the depth over time. The difference in CPSD was clearly observed in differential pores volume of tailings over time (Figs 8 – 17 to 8 – 19).

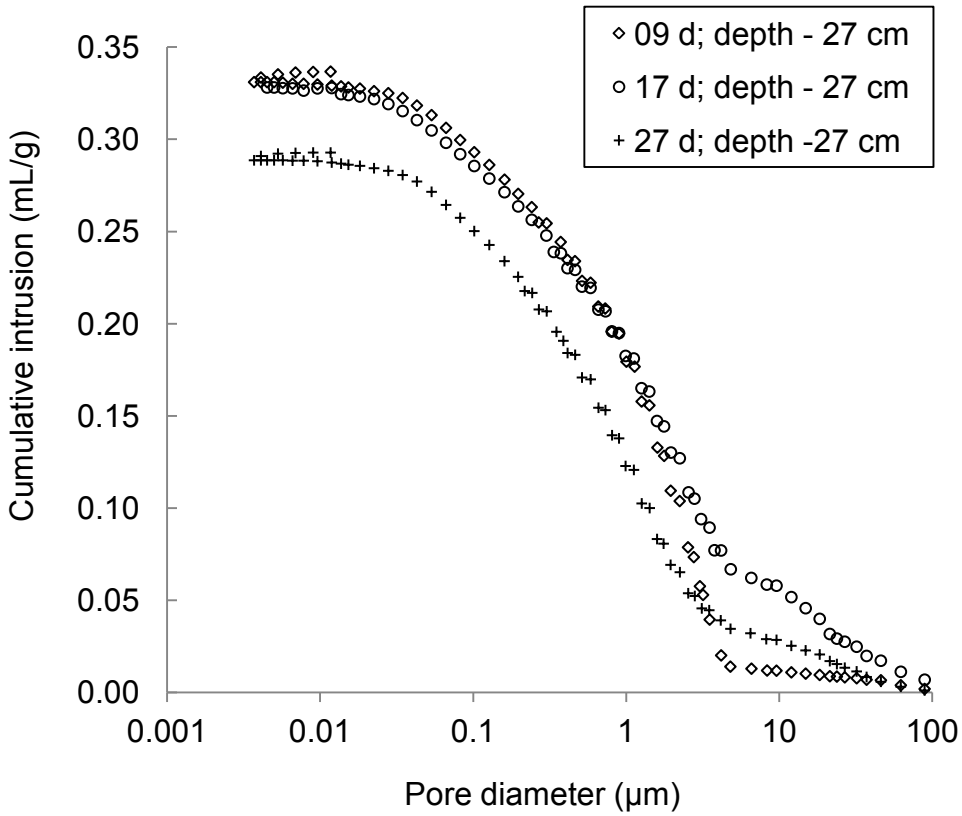

Figure 8-14: Cumulative intrusion of polymer amended tailings at 27 cm depth over time

The differential intrusion curves showed that the peak pore mode compressed and shifted towards smaller pores diameter for all depths over time. The peak pore mode of tailings lowered significantly for a particular depth over time

showing more consolidation. All the tailings provided bimodal pores size distribution along the depth over time.

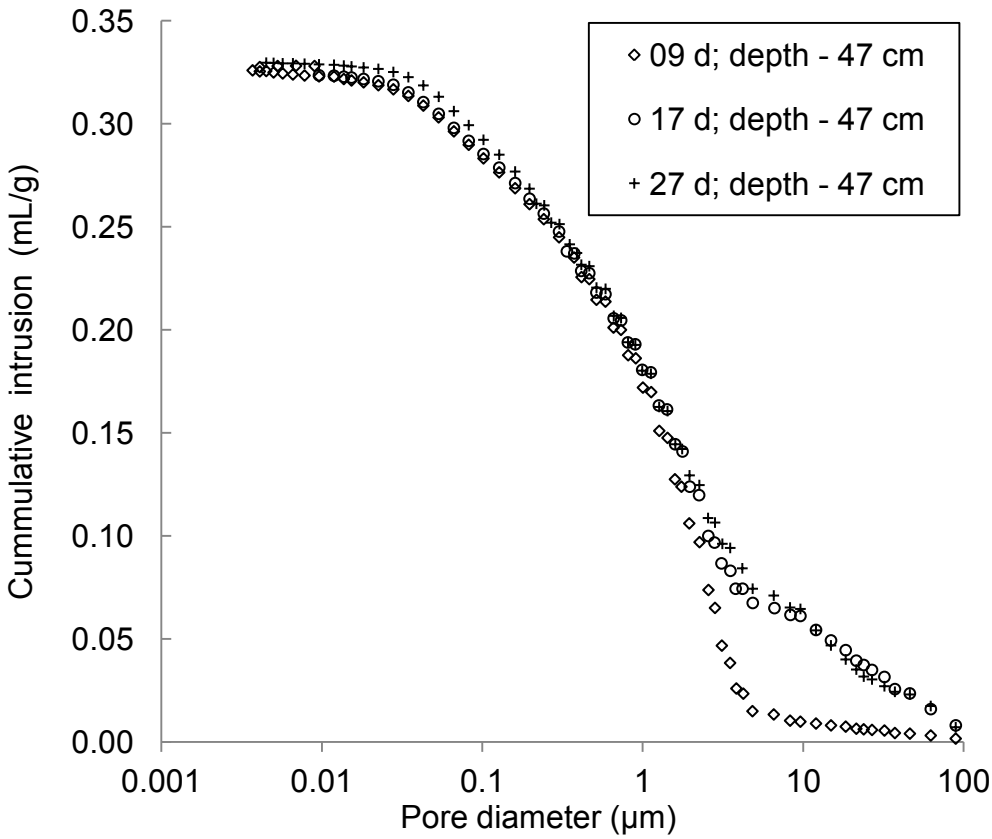

Figure 8-15: Cumulative intrusion of polymer amended tailings at 47 cm depth over time

Similarly, the log differential intrusion pore volume curves showed that the tailings shifted towards higher number of smaller pores diameter for an increase in degree of desiccation and consolidation (Figs 8 – 20 to 8 – 22), and the significant differences in PSD were noted for larger pores diameter (1 to 100 µm). The tailings fabric provided pores diameter ranging from 0.004 to 100 µm. The

bimodal PSD was mainly centered at pores diameter of 2 and 0.1 μm in all tailings. Overall, the test results showed that the pores size distribution of tailings changed along the depth over time due to change in degree of desiccation and consolidation, however, the decrease in pore volume was more near the bottom of lift due to greater influence of degree of consolidation.

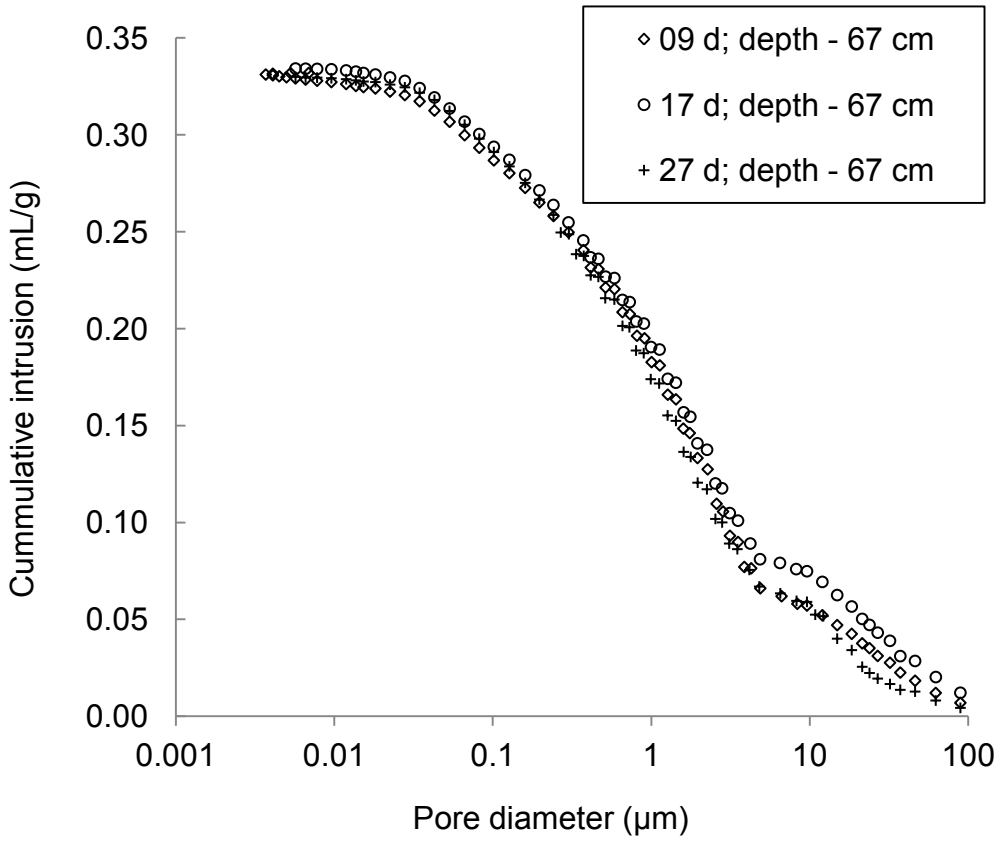

Figure 8-16: Cumulative intrusion of polymer amended tailings at 67 cm depth over time

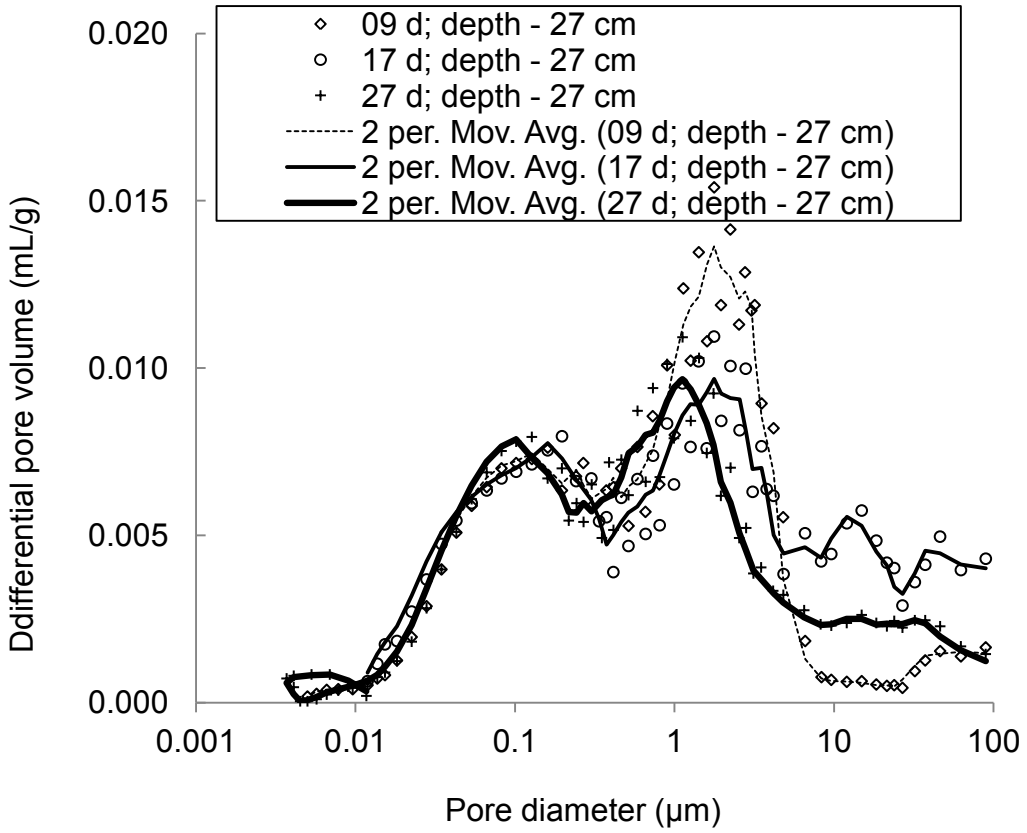

Figure 8-17: Differential pore size distribution of polymer amended tailings at 27 cm depth over time

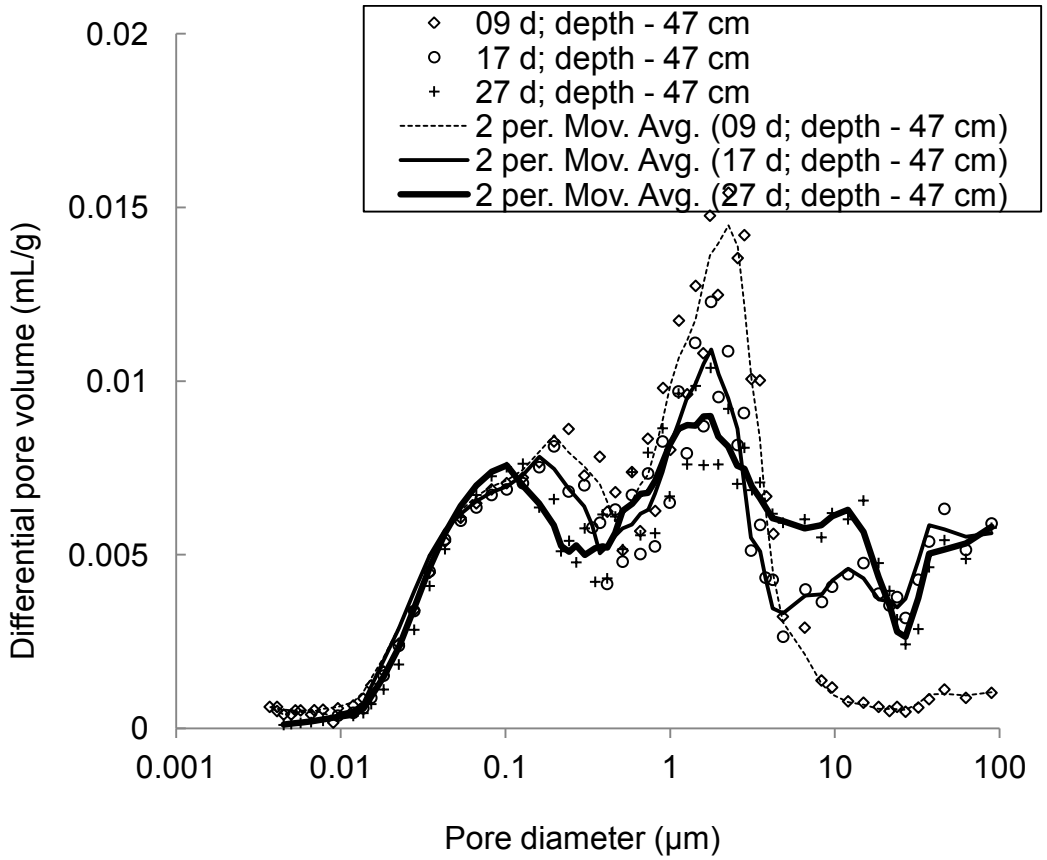

Figure 8-18: Differential pore size distribution of polymer amended tailings at 47 cm depth over time

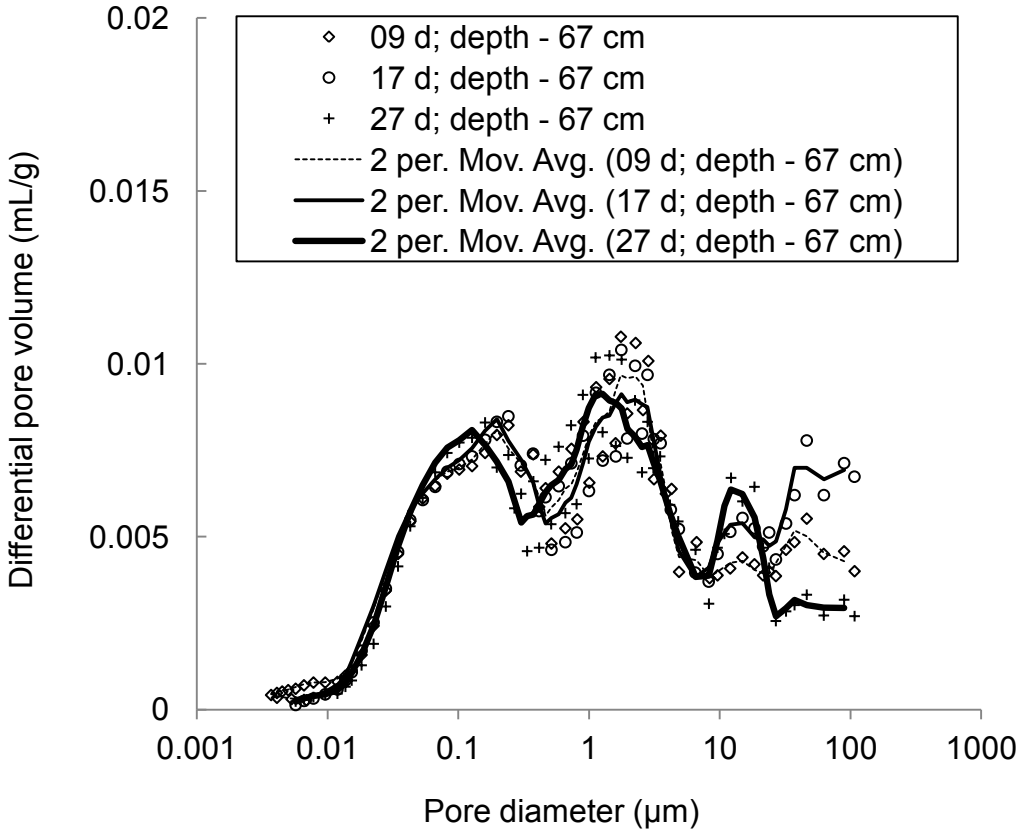

Figure 8-19: Differential pore size distribution of polymer amended tailings at 67 cm depth over time

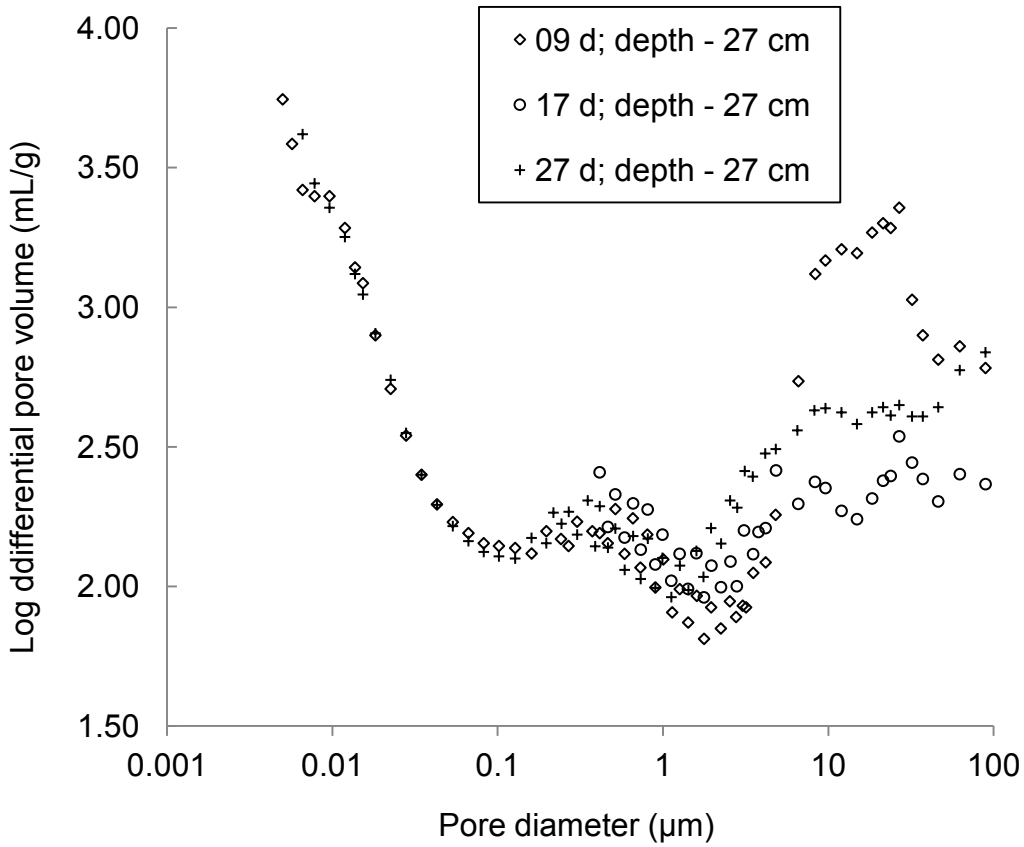

Figure 8-20: Log differential pore size distribution of polymer amended tailings at 27 cm depth over time

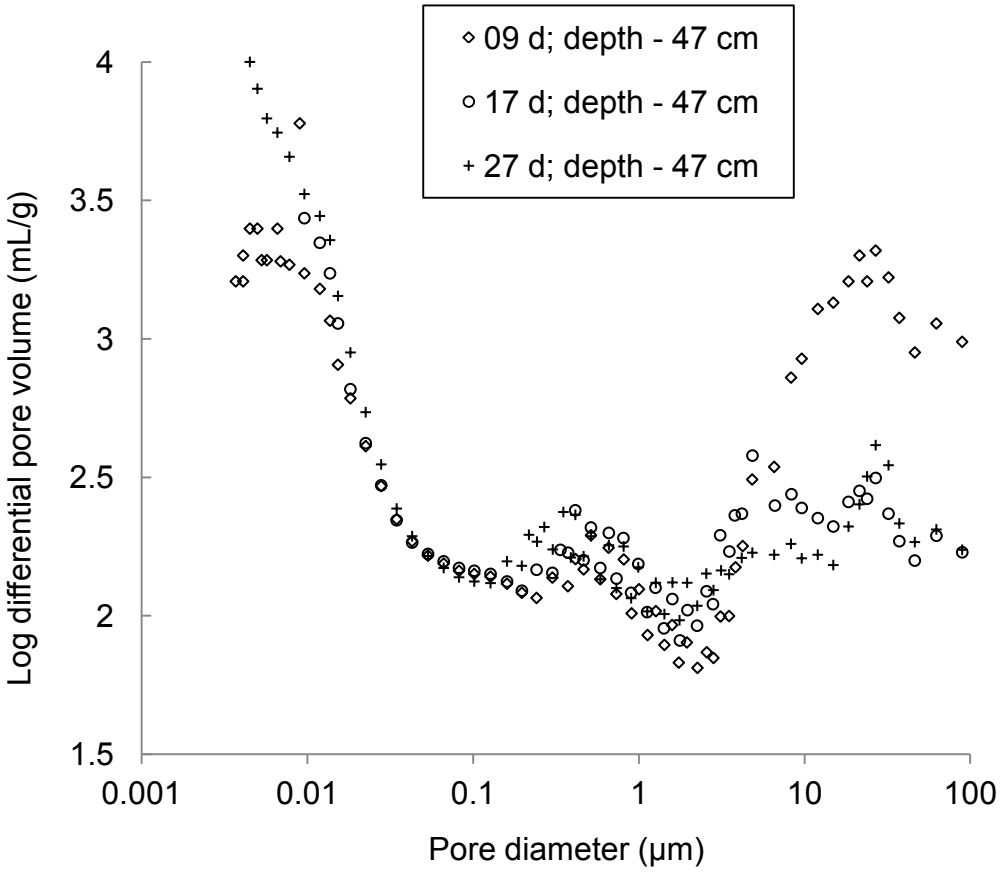

Figure 8-21: Log differential pore size distribution of polymer amended tailings at 47 cm depth over time

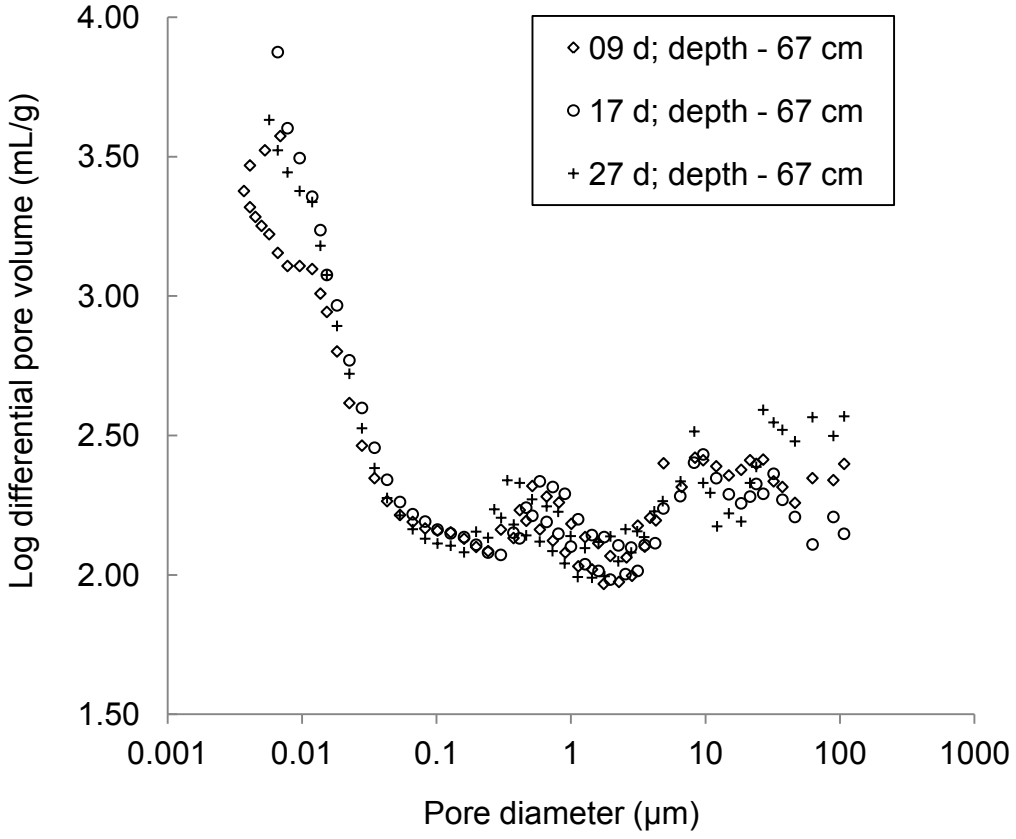

Figure 8-22: Log differential pore size distribution of polymer amended tailings at 67 cm depth over time

The test data showed that MIP technique can efficiently be used to quantify the pore size distribution of oil sands tailings like that of other materials like cement paste, soils and coal etc., as reported in the findings of Yao and Liu (2012); Monroy et al. (2010); Zhou et al. (2010); Romero and Simms (2008) and Svec and Frechet (1995).

8.4 Interaction of microstructure and macroscopic features

MIP data showed that the tailings fabric changed along the depth over time, and the peak pores mode compressed for a successive release of water or due to consolidation, despite that the stress level varied only few kPa along the depth of the lift that might not sufficient to provide major variations in PSD.

The peak of pore mode was compressed more at 67 cm depth in comparison to 27 and 47 cm depths due to self weight consolidation. Similarly, the tailings showed quite low cumulative intrusion at 27 cm depth in comparison to other depths after 27 days due to progression of desiccation. The fabric under the crest changed due to desiccation and it changed due to consolidation at bottom depth. However, the difference in fabric was not so notable at various depths for a particular time.

As a comparison to microstrcuture data, the void ratio was less at middle depth in comparison to top and bottom depths. Certainly increasing the stress level and degree of desiccation would wide up the gap in the variation of pore size distribution for various depths over time which might help largely to understand the variations in performance properties for change in tailings fabric.

8.5 Comparison of test results from different lift thicknesses

Table 8 -1 shows a comparison of macrostructure and microscopic features of polymer amended tailings deposited in two separate lifts of 30 cm and 82 cm thick. As in Table 8 – 1, the tailings of thin lift provided strength of 8 kPa after 16 days, and comparatively, the strength varied from 1.75 to 10 kPa in thick lift after 17 days; furthermore, the strength was more near the bottom in comparison to middle and top layers of thick lift. The tailings showed strength of 20 kPa after 27 days at 27 cm depth; which was comparatively quite high when compared to 16 days strength of thin lift. However, at bottom layer (67 cm depth), the tailings gave strength of 10 kPa after 17 day, which was quite comparable to thin lift strength.

Figure 8 – 23 shows a comparison of undrained shear strength for void ratio of polymer amended tailings in thin and thick lift. Both tailings did not provide any major difference in strength for larger void ratio, i.e., during earlier stage of deposition but major differences were noted for lower void ratio. For a particular void ratio, the thick lift provided more strength in comparison to thin lift, and furthermore, the tailings gave higher strength in thick lift after 16 days of deposition. At a void ratio of 2.3, the thick lift provided strength of 20 kPa as compared to 8 kPa of thin lift (Figure 8 – 23).

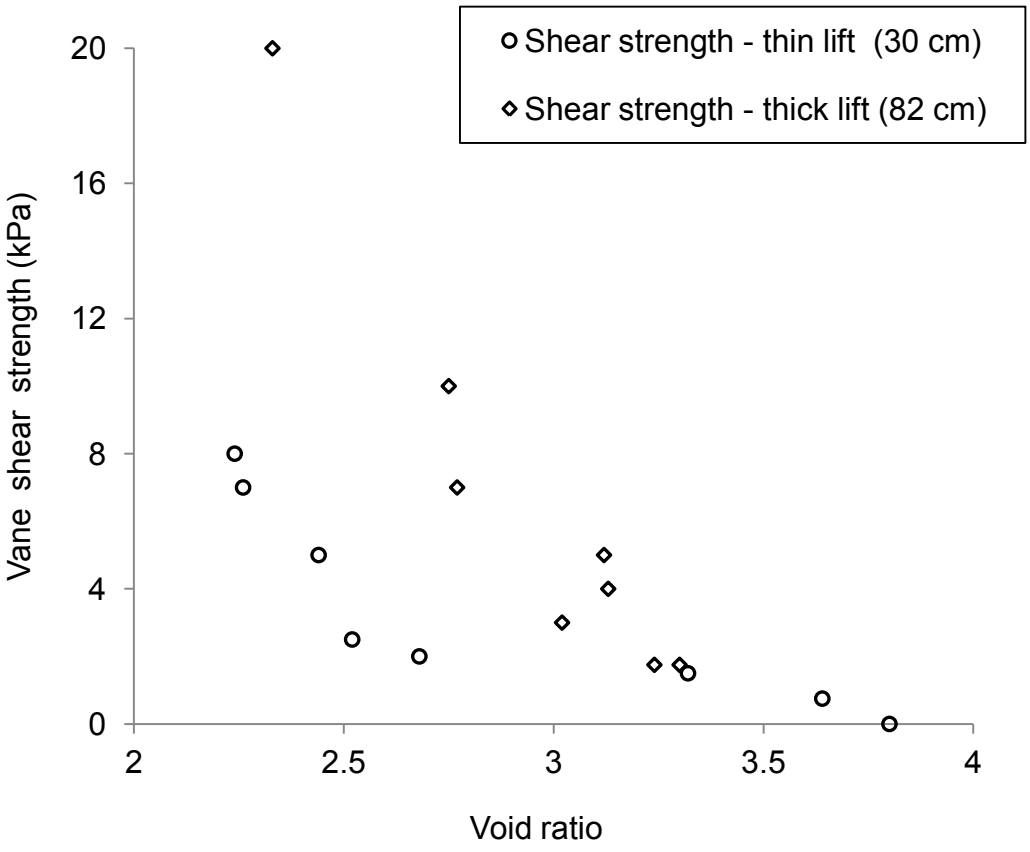

Figure 8-23: Comparison of undrained shear strength of polymer amended tailings in thin and thick lift

For thin lift, desiccation, be the major mechanism contributing to strength gain, and for thick lift, both desiccation and consolidation contributed to the strength gain of tailings. Figure 8 – 24 shows the fabric in two sets at the same void ratio for thin and thick lift. The tested sample of thin lift provided peak pore mode towards smaller pores diameter, however for thick lift, the peak pore mode was compressed and shifted towards larger pore diameter showing more flocculated fabric. This more flocculated fabric of thick lift resulted in higher strength when compared to the strength of tailings in thin lift.

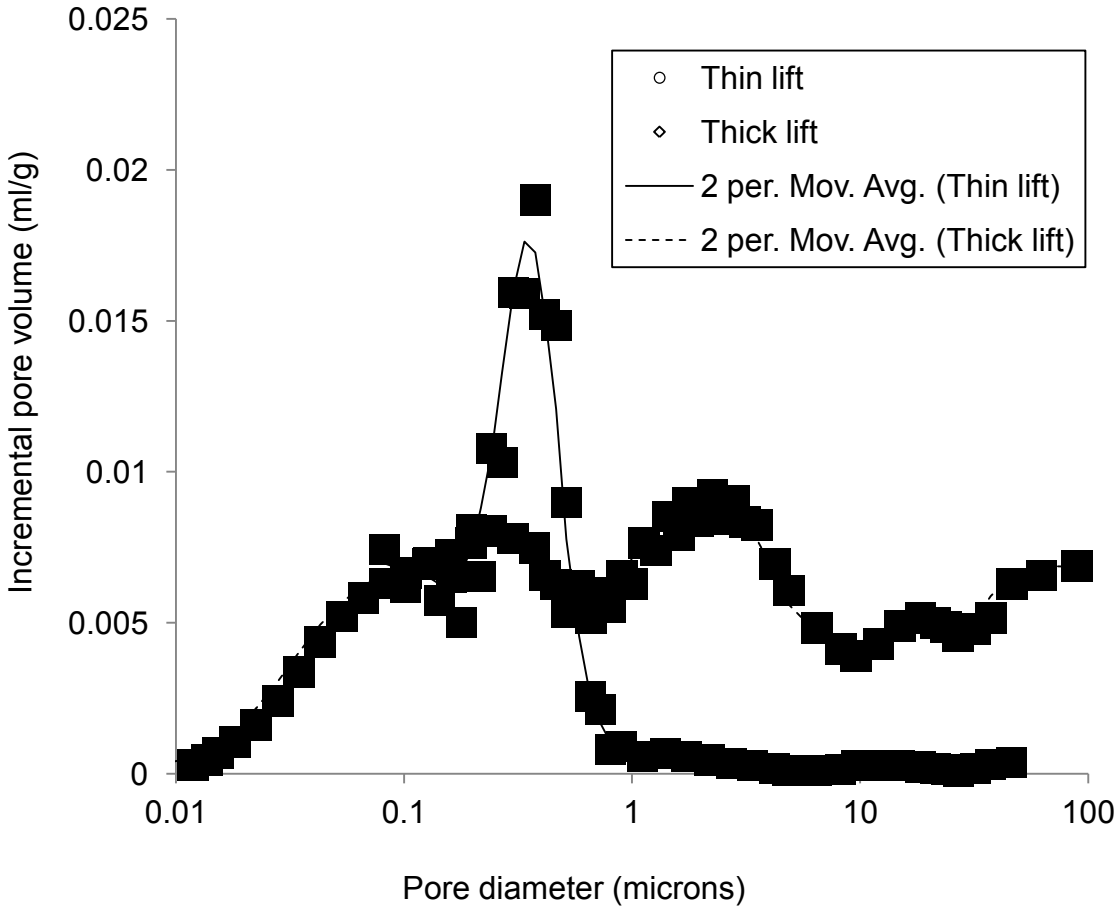

Figure 8-24: Comparison of fabric in two sets at the same void ratio for thin and thick lift

Jeeravipoolvarn (2010) reported the field observation of ILTT of Syncrude COF lagoons fine tailings and discussed that the strength of ILTT varied from 0.96 to 10 kPa in a lift of 1 m; while examined in different ponds; furthermore, the strength was more near the bottom of the ponds. The undrained shear strength of tailings varied from 1.6 kPa for a void ratio of 3.0 under the crust to 5.2 kPa for a void ratio of 2.3 near the bottom of the pond. The study also reported that the undrained shear strength of laboratory ILTT tailings varied from 0.078 to 7 kPa

corresponding to void ratio between 4.61 and 1.45, when consolidated up to a stress level of 20 kPa.

In current study, the polymer amended tailings showed vane strength of 1.75 kPa (void ratio of 3.2) under the crest and 20 kPa (void ratio of 2.33) near the bottom of thick lift. The comparison of test results showed that SNF A 3338 polymer performed very well providing higher strength when compared with Syncrude field and laboratory ILTT data for a particular void ratio.

Caldwell et al. (2014) reported the field observations of ILTT of Suncor site, and discussed that the tailings showed an increasing trend in density and strength from top to bottom of the lift. The study further added that a deposit providing 1.1 dry tonnes/m^2/yr was needed to achieve the criteria as set out in Directive 074 on economic grounds, and more ideal conditions, a deposit yield of about 2 to 3 t/m^2/yr was more desirable taken into account capital and operational costs.

At the time, the deposition of thick lifts of tailings is under consideration in oil sands industry, the integration of desiccation, consolidation along with dewatering may prove highly beneficial to achieve goals as set out in Directive 074, while tailings are deposited in thick lift. The best approach involves integrating the influence of freeze thawing with dewatering and other natural mechanisms like desiccation and consolidation considering the Northern Alberta weather conditions.

As in Table 8 – 1, major difference was noted in porosity values while comparing the actual porosity to microporosity. The variation in porosity was due to that MIP technique underestimated the PSD due to the ink bottle effect and accessible effect. Moreover, the pre-conditioning of sample also influenced the accuracy of test data as a result of volume change of tested samples.

In this study, though freeze drying method was preferred for preconditioning of tested tailings; so that to minimize the volume change, yet the samples showed major changes in volume, and it was argumented while comparing actual porosity to microporosity (void ratio) of tailings (Table 8 – 1). As the tailings at higher water content were used in this study, which were more liable to produce percent changes in volume due to their softness and wetness. Furthermore, ImageJ analysis of SEM images also showed lower microporosity that happened due to the presence of bitumen and flocs formation in polymer amended tailings.

Table 8-1: Comparison of test results of ILTT

Features		Desiccation + consolidation				Dewatering + desiccation + consolidation								
ILTT (lift)		30 cm				82 cm								
Measurements		Average				Top layer (27 cm)			Middle layer (47 cm)			Bottom layer (67 cm)		
Time (days)[3]		16				9	17	27	9	17	27	9	17	27
Polymer doses (ppm)		700	1000	1500		700								
Water contents (%)		59	60	70		115	111	80	120	109	100	111	100	88
Total suction (kPa)		880	940	780		146	88	111	80	78	70	91	102	93
Porosity	Macrostructure	0.69	0.69	0.67		0.76	0.75	0.66	0.76	0.75	0.73	0.75	0.73	0.69
	SEM	0.28	0.26	0.25		-	-	-	-	-	-	-	-	-
	MIP	0.21	0.21	0.22		0.33	0.32	0.29	0.32	0.33	0.33	0.33	0.33	0.32
Strength (kPa)[4]		8	11	4.5		1.75	3	0	1.75	4	7	5	10	20

[3] Time at which tailings were tested after their deposition in columns:
[4] The strength was measured at a depth of 15 cm from top of 30 cm thick lift

8.6 Conclusions

The addition of polymer changed the segregation nature of tailings to agglomeration which enabled tailings to release water. The post deposition dewatering, desiccation and consolidation resulted in an increase in percent solids of tailings, which consequently increased the strength of tailings. The increase in strength was more near the bottom in comparison to top layers of the lift, and comparatively, the void ratio decreased at top and bottom layers due to prevalence of desiccation and consolidation respectively with respect to middle depth.

Generally, the osmotic suction dominated the total suction in these tailings. MIP test data showed that the pores size distribution of tailings changed for all depths over time due to change in degree of desiccation and consolidation. The decrease in pore volume was more near the bottom of the lift due to more impact of self weight consolidation, and it consequently provided higher strength at the bottom layer due to lower void ratio. All tailings provided bimodal pores size distribution. Furthermore, the polymer SNF A 3338 showed better strength perspectives taken into account void ratio and percent solids when compared with Syncrude ILTT field and laboratory data sets

Chapter 9. Desiccation and subsequent consolidation of polymer amended oil sands mature fine tailings

Abstract

Polymer amended MFT deform and show subsequent change in volume because of an increase in stress level. This situation prevails in the field as one layer of tailings is buried over a desiccated layer. The aspect of this study was to study the consolidation potential of previously desiccated tailings, aided by examination of fabric using SEM and MIP. The samples were desiccated in cylindrical columns to various initial percent solids by mass and consolidated in an oedometer cell for various stress levels, and then a series of mercury intrusion porosimetry (MIP), scanning electron microscopy (SEM), total suction and electrical conductivity tests were performed. For image analysis, ImageJ software was used.

The test results showed that the hydraulic and mechanical behavior of tailings changed due to change in fabric for an increase in stress level and degree of desiccation as well. The tailings shifted towards pores of smaller diameter showing peak pore mode at smaller pore diameter for an increase in stress level. The macroscopic properties such as water potential, macroporosity and hydraulic conductivity of tailings were correlated with a change in micro fabric measurements.

9.1 Introduction and background

Various studies were reported in the literature, those employed consolidation tests to quantify the microstructure and macroscopic properties of geomaterials. Monroy et al. (2007) used mercury intrusion porosimetry and environmental scanning electron microscopy to examine the fabric of compacted London clay for various stress levels. Kierzkowksi (2007) conducted standard oedometer compression tests to investigate stress strain relationships of kaolinite clay. Cabalar (2010) performed oedometer test on coarse rotund sand – fine mixtures to study its fines content and compression behavior.

Proskin et al. (2010) examined the hydraulic conductivity, void ratio and micro fabric of mature fine tailings conducting large strain consolidation tests. Mermillod-Blondin et al. (2011) used scanning electron microscopy with automatic image analysis and energy dispersive X-ray spectrometry (EDS) to determine the mineralogical and environmental characteristics of mine tailings. Ramlochan et al. (2004) examined the microstructure and chemical features of four cemented paste backfills using SEM and energy dispersive X – ray analysis (EDX). Ouellet et al. (2008) tested cemented paste backfill performing SEM and image analysis. Nielson (2004) used x-ray CT and imaging software for microstructure evolution of five types of soils including gravel, coarse sand, medium sand, fine sand and concrete sands. However, no study has attempted to study consolidation of desiccated oil sands tailings using fabric analysis.

In this study, the hydraulic and mechanical patterns of tailings were examined for changes in pore size distribution. MIP tests and SEM tests along with imageJ analysis were performed to examine the fabric of polymer amended oil sands tailings.

9.2 Materials preparation and methods used:

The polymer amended oil sands tailings were prepared following the guidelines as discussed in Chapter 3. The prepared MFT was transferred to a cylindrical column of 30 cm depth and 30 cm diameter, and the tailings were allowed to desiccate up to certain degrees (Figure 9 – 1).

The tailings in the column were desiccated up to 58%, 71% and 80% initial solids content to examine their mechanical, hydraulic and microstructure features. For consolidation tests, the guidelines as discussed in ASTM standard ASTM D 2435/D2435M – 11 was followed. The consolidometer mold was used to extract desiccated tailings from the column. Figure 9 – 2 presents desiccated tailings in column at 80% initial solids content to examine the microstructure and macroscopic behaviour of polymer amended oil sands tailings.

The sample was left under each loading for 24 hours. Terzaghi's consolidation theory was used to estimate the hydraulic conductivity examining the coefficient of consolidation (c_v) of polymer amended oil sands tailings. The coefficient of consolidation of tailings was determined using both square root of time method

and log time method. Mercury intrusion porosimetry (MIP) and scanning electron microscopy (SEM) tests were performed for fabric analysis. ImageJ software was used to quantify the SEM micrographs.

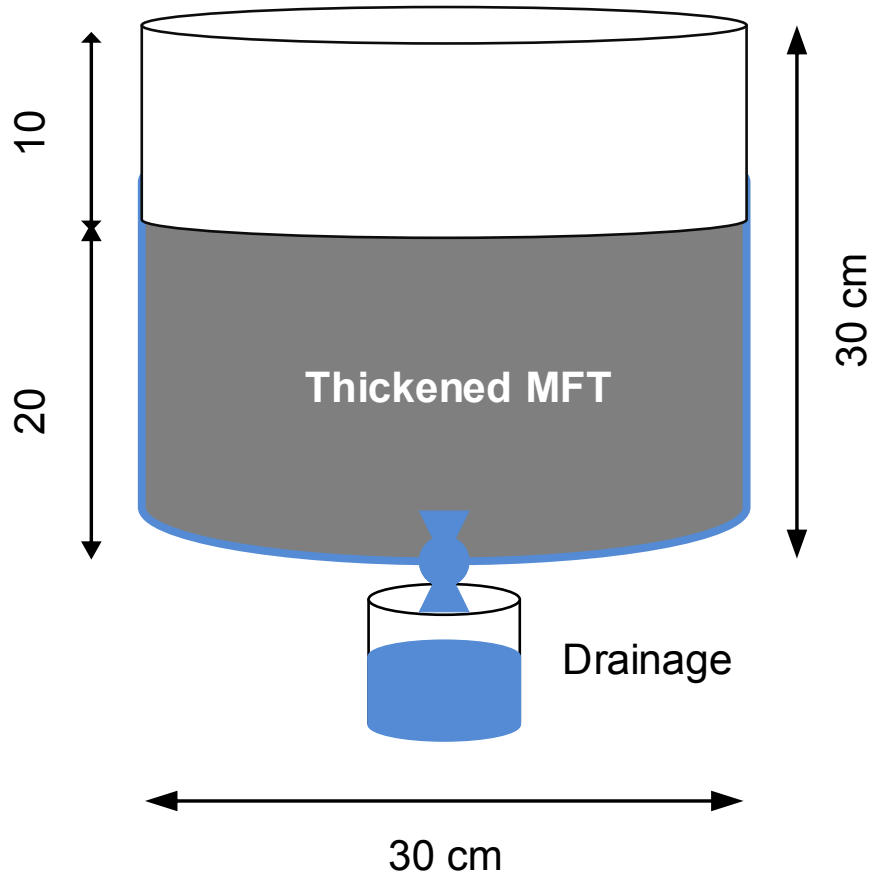

Figure 9-1: Schematic of polymer amended fine tailings for oedometer tests

The microstructure tests were conducted with unconsolidated tailings desiccated to 58, 71 and 80%, and also with initially desiccated tailings consolidated in oedometer cell up to stress levels of 20, 40 and 80 kPa. For these tests, the freeze dried samples were used. ImageJ software was used to quantify the fabric of tailings.

Figure 9-2: Desiccation of tailings in the laboratory at 80% initial solids content to examine the microstructure and macroscopic behaviour of polymer amended oil sands tailings

The total suction and electrical conductivity of tailings were examined for various degrees of desiccation and stress level, and then the osmotic suction was estimated based on electrical conductivity. For a particular sample, the total suction was recorded three times consecutively and then the average was reported in this study. In addition to this, the gravimetric water content and solids

content profiles were examined for respective stress level and degree of desiccation as well.

9.3 Results and discussions

9.3.1 Mechanical behaviour of polymer amended oil sands fine tailings

The rate of deformation of polymer amended tailings decreased with an increase in degree of desiccation and the tailings showed high volume change for 58% initial solids content as a comparison to higher initial percent solids by mass (80%). As in Figs 9 – 3 to 9 – 5, the tailings showed quite high deformation initially for initial solids content of 58 and 71% and furthermore, the rate of deformation was quite high for stress level of 2.5 kPa, after then the rate of volume change reduced considerably and the axial deformation fluctuated between 3 to 5 % of the total deformation for each stress level.

In comparison to 58 and 71% solids content, the tailings with 80% initial solids content showed less change in volume for a stress level of 2.5 kPa, after then the tailings gave almost the same change in volume varying from 3 to 5% for various stress levels.

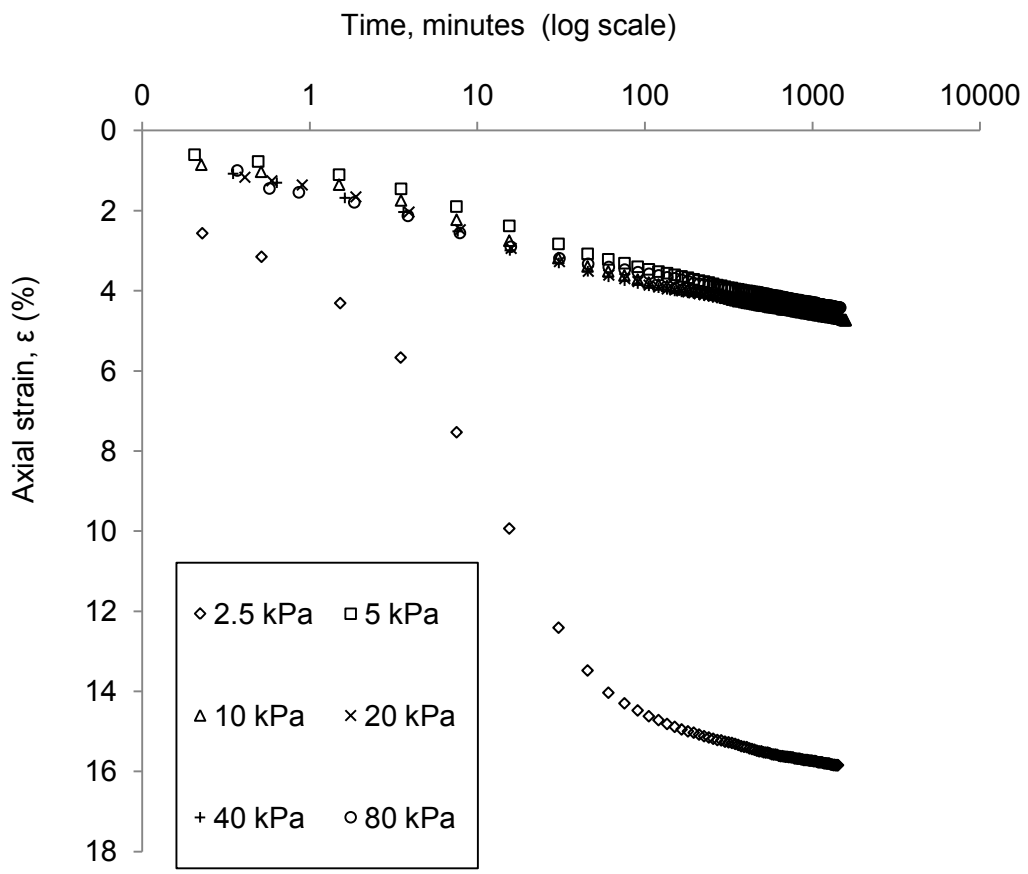

Figure 9-3: Deformation behavior of polymer amended fine tailings for initial 58 percent solids by mass

Generally, the tailings for initial solids content of 58, 71 and 80% provided axial deformation of 50%, 40% and 29% of the total mass for axial stress up to 80 kPa (Figure 9 - 6). The tailings desiccated to lower percent solids by mass provided more change in volume for an increase in stress level.

Jeeravipoolvarn (2005) discussed that the initial solids content and additive type (gypsum, phosphogypsum, lime, acid/lime, acid/flyash, alum) influenced the compressibility of the tailings, and tailings of initial higher solids content provided

less deformation in comparison to lower initial solids content, when consolidated in a consolidation cell.

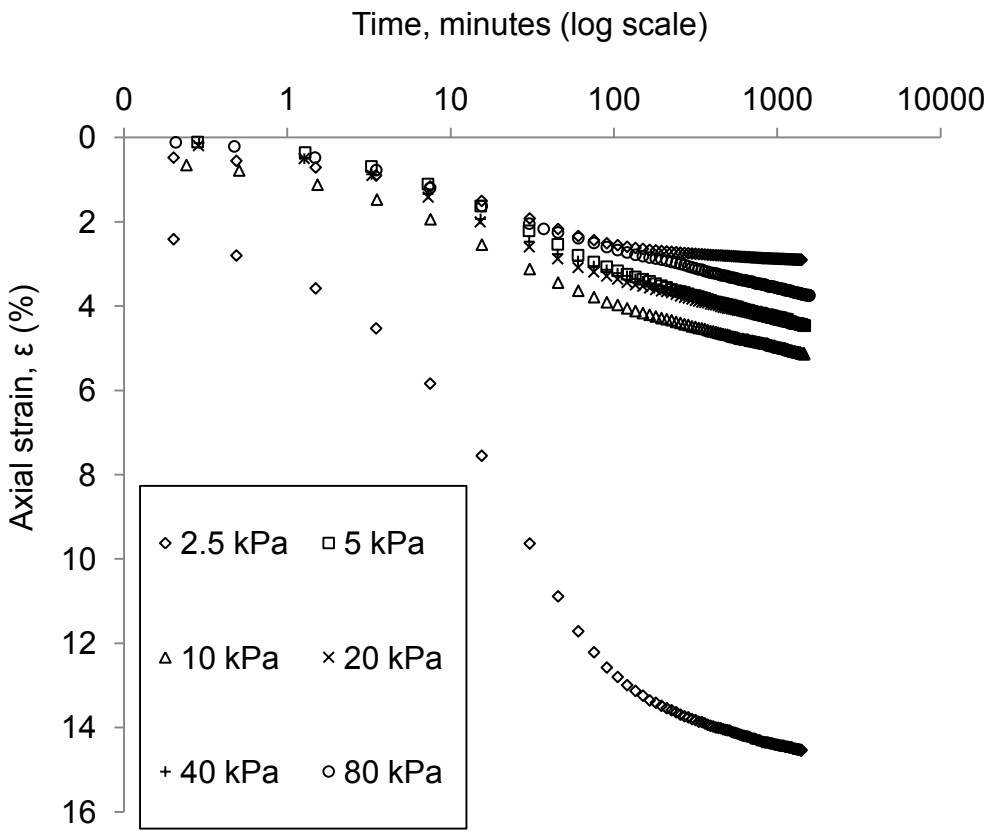

Figure 9-4: Deformation behavior of polymer amended fine tailings for initial 71 percent solids by mass

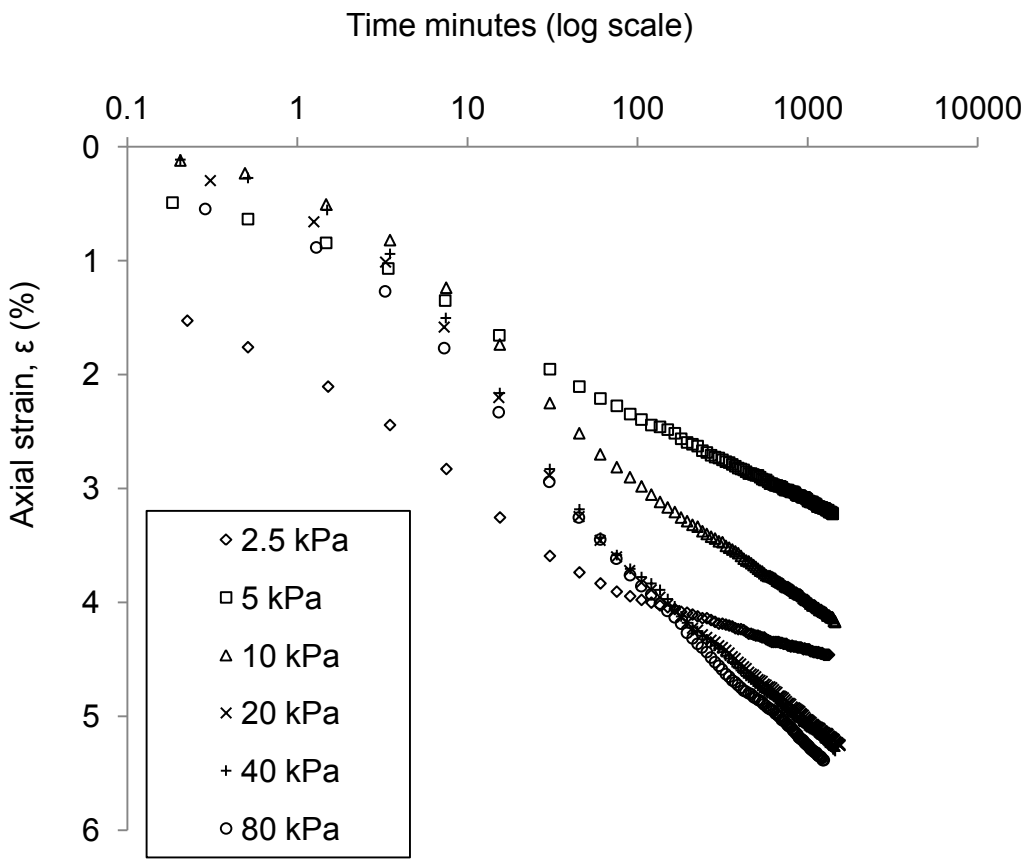

Figure 9-5: Deformation behavior of polymer amended fine tailings for initial 80 percent solids by mass

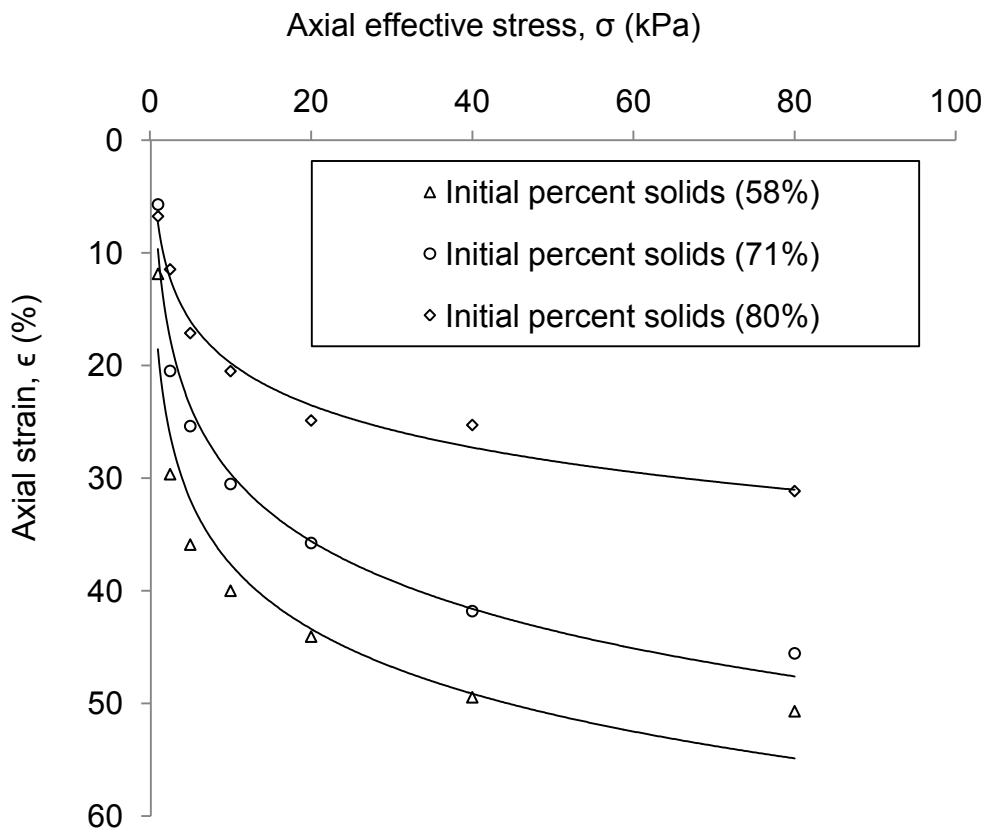

Figure 9-6: Deformation behaviour of polymer amended fine tailings for various degrees of desiccation and stress levels

9.3.2 Gravimetric water content and percent solids content of polymer amended fine tailings

As in Figure 9 - 7, the water content and percent solids profiles of tailings for lower degree of desiccation showed major changes in gravimetric water content and percent solids up to an axial effective stress of 20 kPa, after then these curves appeared overlapping to each other showing minor difference in percent solids.

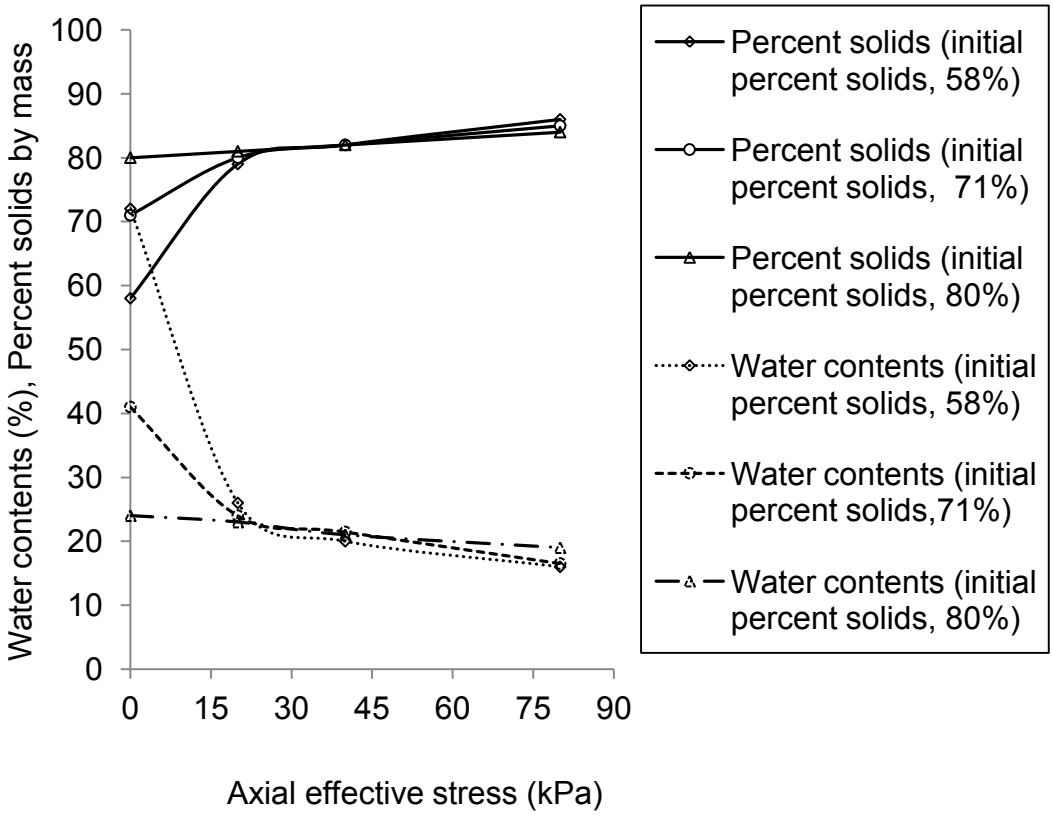

Figure 9-7: Gravimetric water content and percent solids by mass profiles of polymer amended fine tailings for various initial degrees of desiccation

The percent solids by mass of tailings for initial percent solids of 58, 71 and 80% varied from 58 - 86, 71 – 85 and 80 – 84 % respectively for 0 – 80 kPa axial stresses (Figure 9 - 7). The test results showed that the tailings desiccated to higher degree or higher percent solids by mass showed less increase in solids content with an increase in stress level. These larger changes in volume of tailings contributed to this major increase in percent solids by mass for lower degree of desiccation.

9.3.3 Hydraulic behaviour of polymer amended oil sands fine tailing

The tailings showed void ratios of 2.54, 1.64 and 1.57 for initial percent solids of 58, 71 and 80 respectively prior applying the load (Figure 9 - 8). The tailings for initial 58% solids content showed higher rate of deformation with an increase in stress level and resultantly, the rate of decrease in void ratio was more as compared to 71 and 80% initial solids content. The void ratio for 58% initial solids content decreased from 2.54 to 0.70, and it varied from 1.57 to 0.65 for 80% initial solids content. At 80 kPa stress level, the tailings showed minor difference in void ratio for various degree of desiccation but the tailings for 71% initial solids content gave slightly lower void ratio (Figure 9 - 8).

The test results showed that the deformation rate of polymer amended tailings decreased with an increase in initial percent solids. Jeeravipoolvarn (2005) discussed that the void ratio of tailings treated with additive such as gypsum and sands behaved in similar fashion to that of polymer amended tailings, when

tested for various stress levels in consolidation cell. Furthermore, the reported tailings showed lower void ratio for higher initial solids content.

Figure 9 – 9 shows total suction profiles of tailings. The tailings showed total suction of 40, 40 and 140 kPa for initial percent solids of 58, 71 and 80 respectively. There was an increase in suction with a decrease in void ratio or increase in percent solids.

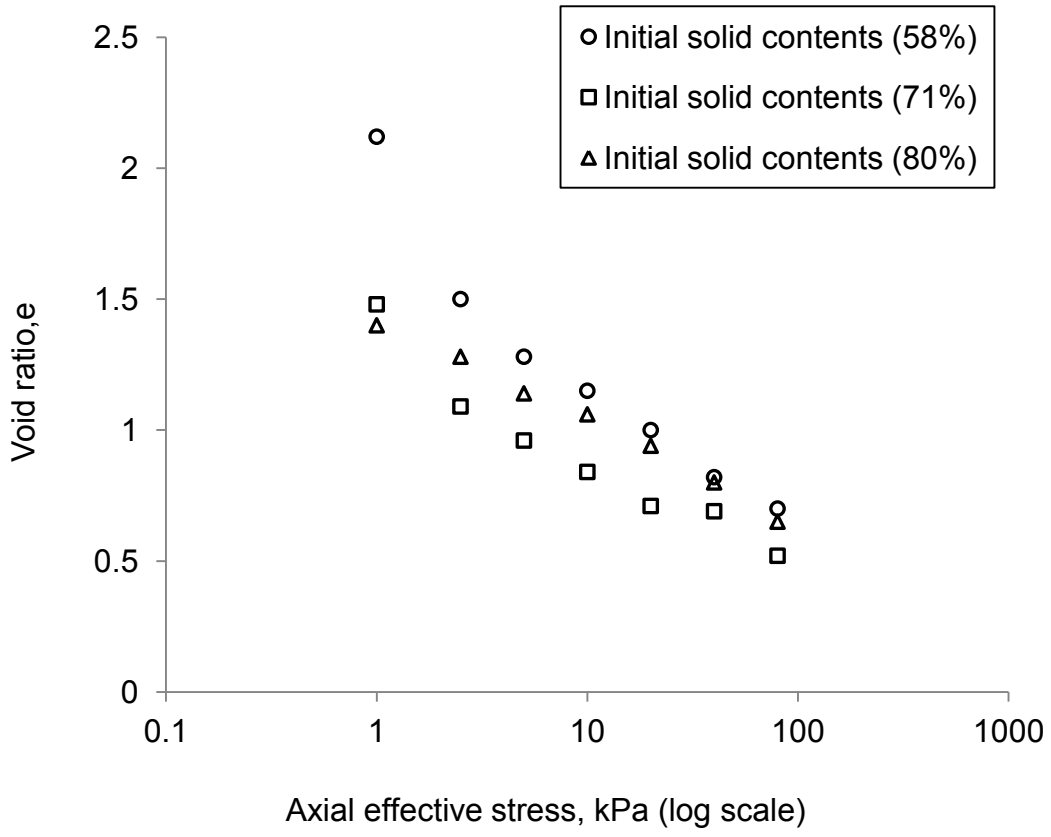

Figure 9-8: Void ratio of polymer amended oil sands tailings for various initial degrees of desiccation and consolidation

Overall, the suction varied from 40 to 490, 40 to 630 and 140 to 350 kPa for initial solids content of 58, 71 and 80 respectively with an increase in stress level up to 80 kPa. The tailings for various solids content showed significant increase in suction after 40 kPa, actually up to this point, the tailings attained significant decrease in water contents or void ratio which increased the suction values (Figure 9 – 9). Romero and Simms (2008) reported that the PSD greatly influenced the water retention curve of opalinus clay (a kaolinite – illite argillaceous rock).

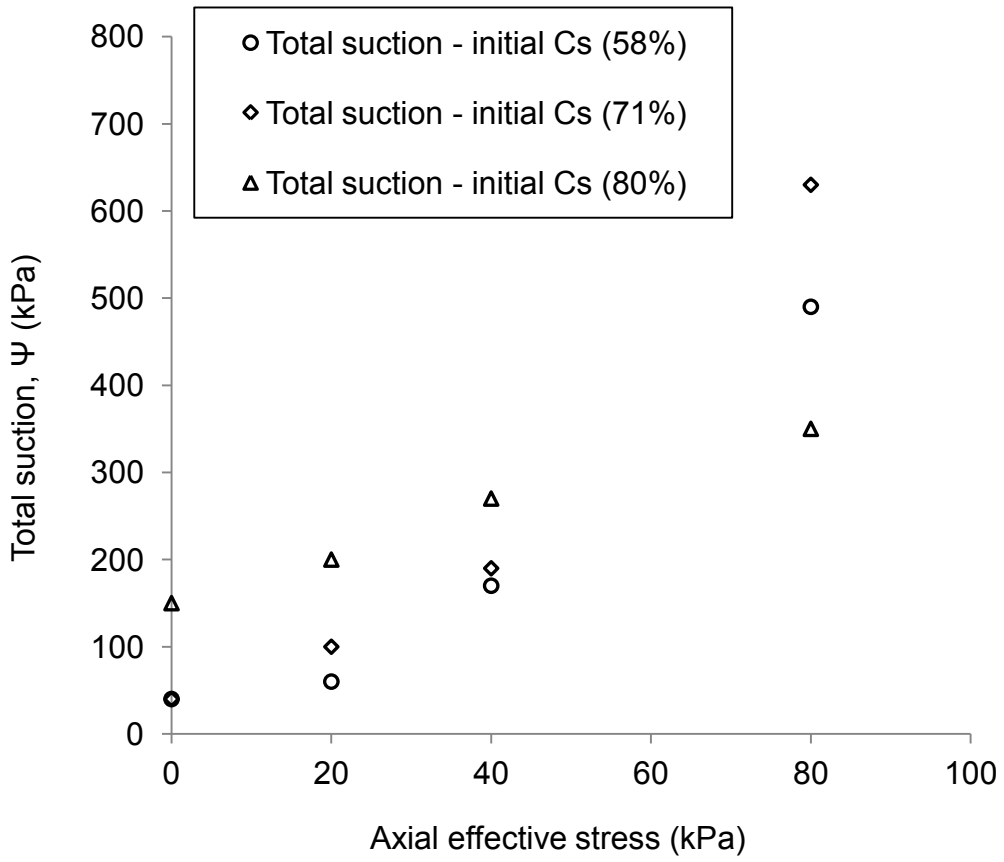

Figure 9-9: Total suction profiles of polymer amended fine tailings for various initial degrees of desiccation and consolidation

The tailings showed osmotic suction of 18, 30 and 35 kPa for various initial degree of desiccation, and no major changes were noted for change in stress level. The osmotic suction of tailings varied from 18 - 26, 20 – 30, and 35 – 60 kPa for an increase in stress up to 80 kPa (Figure 9 – 10). Fredlund and Rahardjo (1993) discussed the osmotic suction of Regina clay and the variations in the osmotic suction were minor for lower water content, i.e., from 23 to 32%.

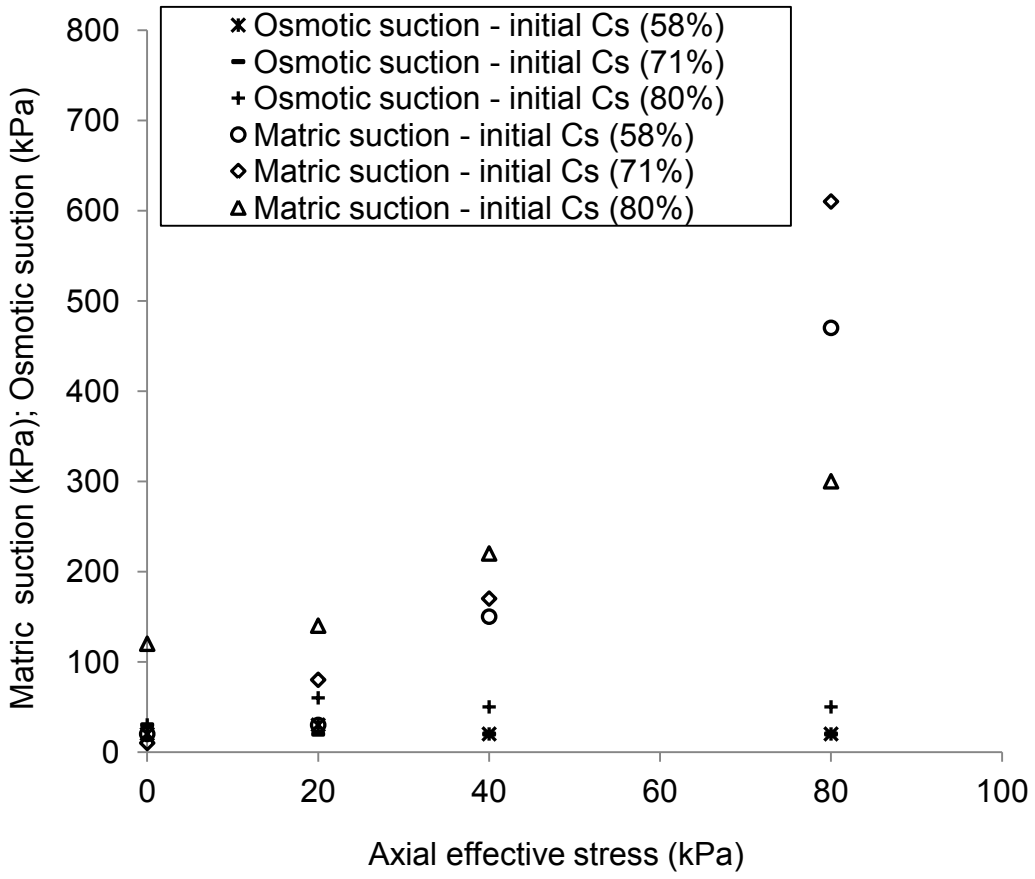

Figure 9-10: Matric suction and osmotic suction profiles of polymer amended fine tailings for various initial degrees of desiccation and consolidation

The test results showed that the osmotic suction of tailings did not vary too much for respective stress levels and/or degrees of desiccation as well. Furthermore, the osmotic suction of tailings might be biased to some extent because the saturation extract procedure was used to estimate the osmotic suction.

Now the total suction is combination of matric suction and osmotic suction. The tailings showed maximum matric suction of 464, 610 and 298 kPa at a stress level of 80 kPa for initial solids content of 58, 71 and 80% respectively (Figure 9 – 10). The matric suction of tailings varied from 22 – 464, 10 – 610, and 105 – 298 kPa for an increase in stress from 0 to 80 kPa.

It was quite uncommon as the tailings were tested under saturated condition, so the matric suction appeared larger than expected in these tailings. However, the water content of tested tailings was quite low at 40 and 80 kPa that might be enabled these tailings to provide high numbers of matric suction. The WP4 Dewpoint Potentiameter estimated the total suction equilibrating the relative humidity of the sample and the device chamber. The lower water contents (GWC - 21%) at high stress level expressed the lower relative humidity, which resulted in an increase in suction. The total suction was also biased to some extent as the WP4 Dewpoint Potentiameter simulated total suction with an accuracy of ± 0.1 MPa.

The hydraulic conductivity of tailings decreased with an increase in stress level and as expected, the tailings for initial percent solids of 58% gave higher

hydraulic conductivity values than that of 71 and 80% initial solids content initially. Proskin et al. (2010) reported similar observations when tested the oil sands tailings from Suncor lagoons. The study discussed that the tailings for lower solids content exhibited higher compressibility giving lower void ratio, and they also gave lower initial void ratio for initial higher solids content samples.

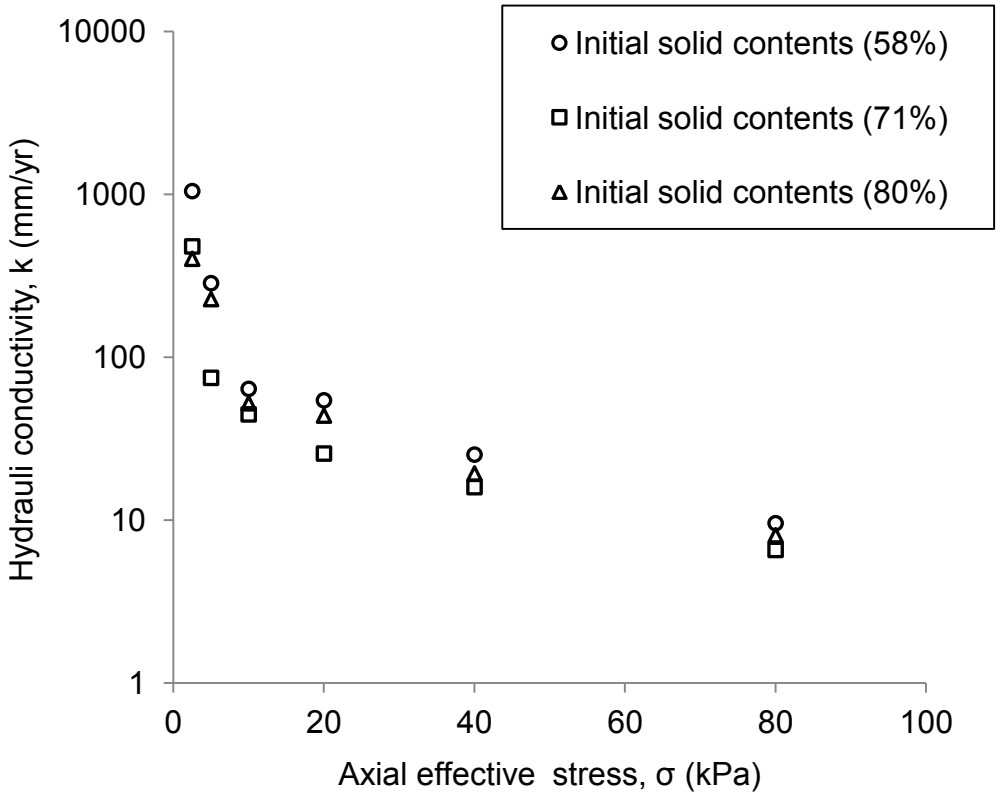

Figure 9-11: Hydraulic conductivity and axial stress relationship of polymer amended fine tailings for various initial degrees of desiccation

As in Figure (9 – 11), all tailings showed major drop in hydraulic conductivity up to an axial stress of 20 kPa, after then the curves showed less decrease in k values. As in Figure 9 – 8, the tailings of various initial solids content almost

reached to 80% volume change at a stress level of 20 kPa, so we can say that the hydraulic conductivity of tailings decreased with a decrease in void ratio.

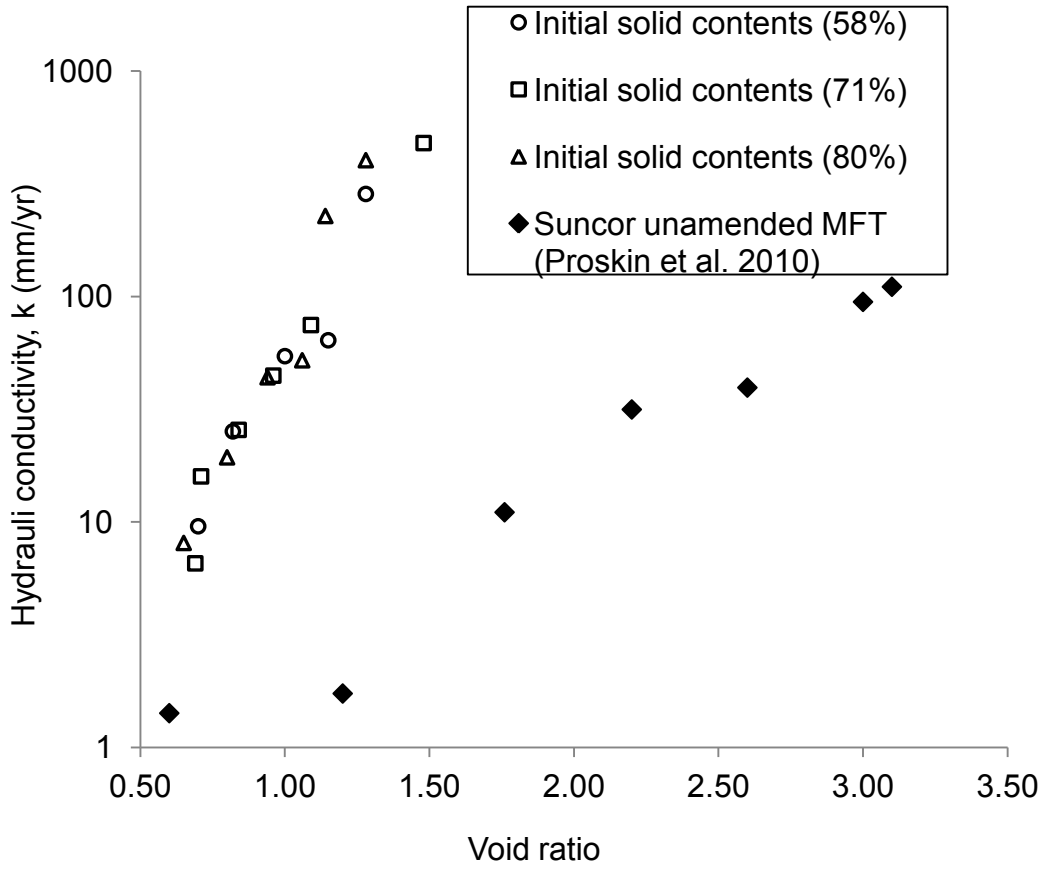

Figure 9-12: Comparative evolution of hydraulic conductivity and void ratio relationship of polymer amended fine tailings for various initial degrees of desiccation

Jeeravipoolvarn (2005) reported the hydraulic conductivity of composite tailings (CT) and discussed that the initial percent solids influenced the compressibility of oil sands tailings and the hydraulic conductivity of tailings decreased with an increase in stress level. The hydraulic conductivity of all tailings decreased with a decrease in void ratio; however, the difference in k values was not so significant

for lower void ratio. As in Figure 9 – 12, the difference in k values reduced with a decrease in void ratio for all tailings, and the data points of various tailings overlapped to each other for lower void and the difference was quite large for initial void ratio. Figure 9 – 13 present a comparison of fabric of unconsolidated and consolidated samples for various initial solids content.

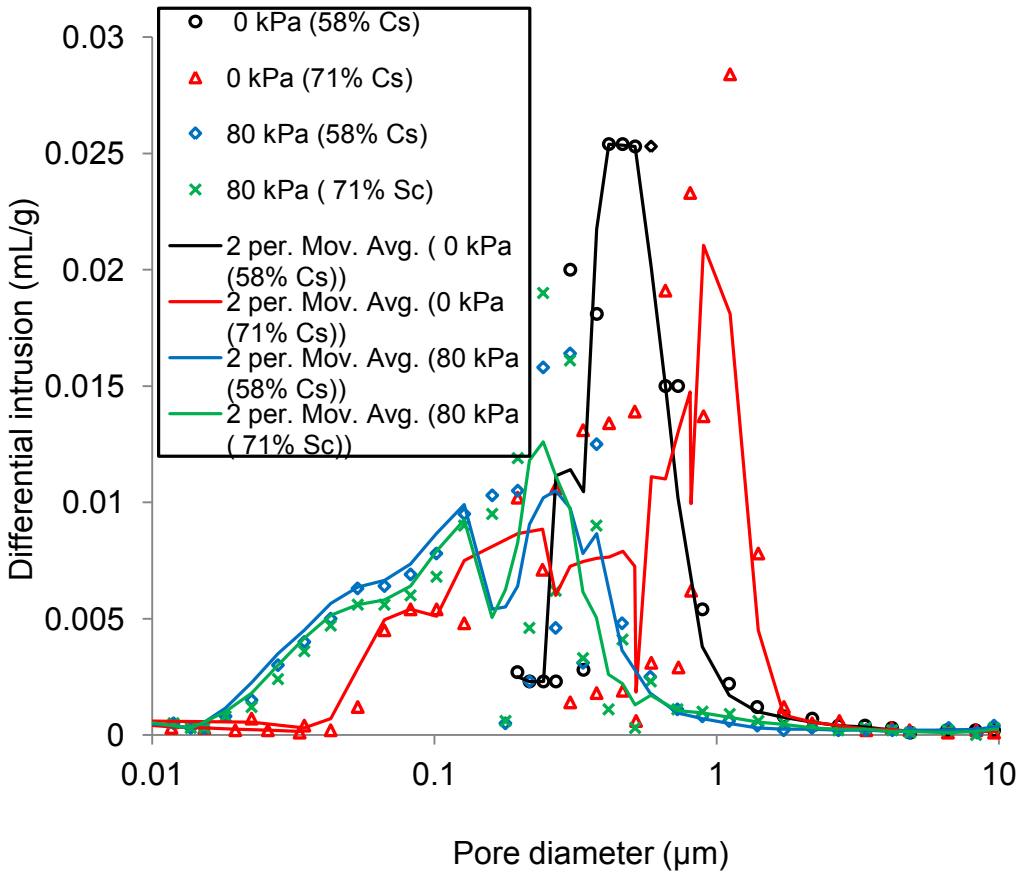

Figure 9-13: Comparison of fabric of unconsolidated and consolidated samples for various initial solids content

The test results showed that for initial solids content, the fabric behaved in different fashion showing quite significant variations in peak pore mode.

However, the peak pores mode converged at a stress level of 80 kPa proving minimal difference in PSD. This variation in fabric for initial solids content resulted in different hydraulic conductivity values initially, but for an increase in stress level, the k values attained a unique value due to similar nature of fabric.

Jeeravipoolvarn (2010) tested the hydraulic conductivity of ILTT performing large strain consolidation tests and reported that the hydraulic conductivity of tailings varied from 314 to 241 mm / yr for void ratios between 1.29 and 0.60, when the tailings of 55.4 and 55.2% initial solids content were consolidated for an axial stress up to 98 kPa.

The hydraulic conductivity of polymer amended tailings (current study) desiccated to 58% initial solids content varied from 1046 to 10 mm / year for void ratios between 1.50 and 0.70, when tested in an oedometer cell for an axial effective stress up to 80 kPa. The comparison of two tested tailings showed that the polymer amended tailings provided comparable k values to the reported test results. As an example, the polymer amended tailings gave k values in the range of 300 ~ 400 mm / annum (e = 1.29) for various initial solids, and these values were higher than that of reported study corresponding to a particular void ratio. Similarly, the polymer amended tailings showed higher hydraulic conductivity to that of acid and quick lime amended, frozen and thawed Suncor MFT for particular void ratio, as reported by Proskin et al. (2010)

Moreover, Proskin et al. (2010) reported the e – k relationship of Suncor unamended MFT (solids content – 42%) from large strain consolidation tests. A comparison of k values for unamended and polymer amended MFT is also reported in Figure 9 - 13. The hydraulic conductivity of the reported tailings varied from 1.42 to 110 mm / annum for a change in void ratio between 0.6 and 3.1, when consolidated in a consolidation cell up to stress level of 100 kPa. Comparatively, the polymer amended tailings showed quite higher hydraulic conductivity under loading conditions (Figure 9 – 12).

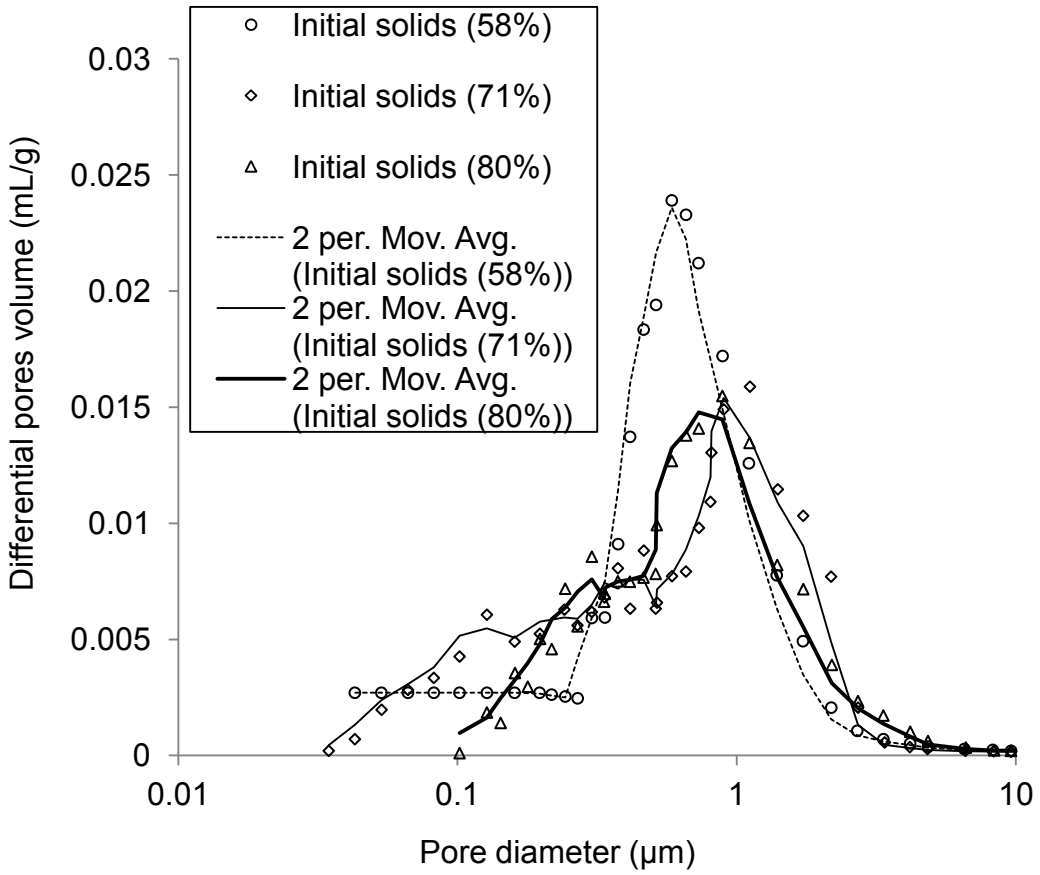

Figure 9-14: Differential pore volume distribution of polymer amended tailings desiccated to various initial solids

These test results showed that the polymer amended tailings showed major difference in k values for various initial solids content initially but with a successive increase in stress level, the difference between k values converged for all tailings and the data points protruded to each other beyond a certain level of desiccation.

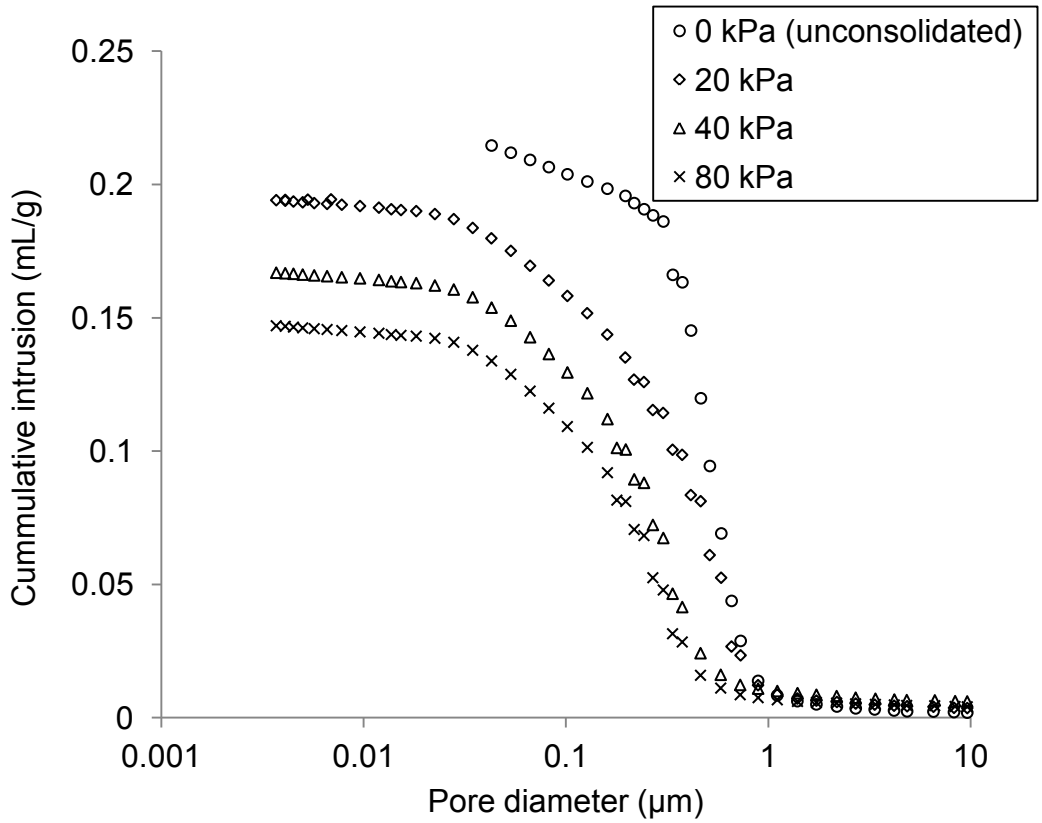

Figure 9-15: Cumulative pore volume distributions of polymer amended oil sands tailings for 58 percent solids by mass (0 kPa[5] – unconsolidated tailings)

[5] 0 kPa relates to unconsolidated tailings which were desiccated to various initial solids content in column.

9.3.4 Mercury intrusion porosimetry (MIP) test results:

Figure 9 – 14 showed that the peak of pores mode lowered for an increase in degree of desiccation, however, the diameter of peak pores mode did not differ too much for various initial solids content. Figs 9 -15 to 9 - 17 represent comparison of cumulative pores size distribution (CPSD) of polymer amended oil sands fine tailings for initial percent solids of 58, 71 and 80% at various stress levels.

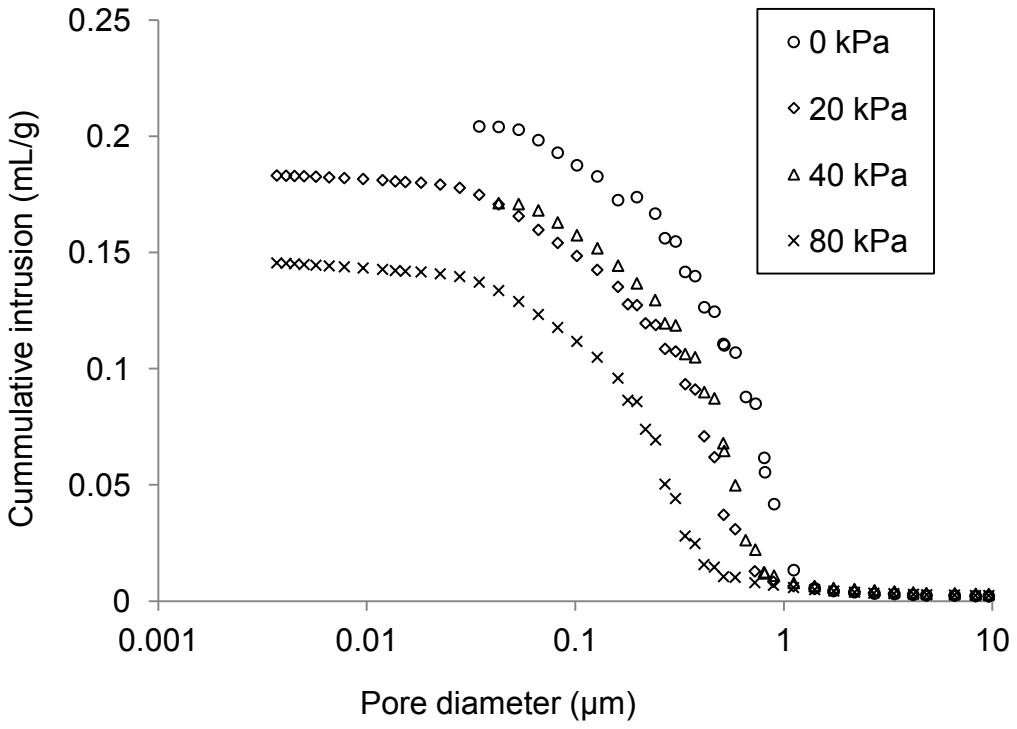

Figure 9-16: Cumulative pore volume distributions of polymer amended oil sands tailings for 71 percent solids by mass (0 kPa – unconsolidated tailings)

The unconsolidated tailings did not provide major difference in PSD for 58, 71 and 80% initial solids content, however, the cumulative pores volume of tailings decreased with an increase in initial percent solids, and it was quite natural (Figs 9 – 15, 9 – 16, 9 - 17). As in Figs 9 – 15, the cumulative intrusions of tailings for 58% initial solids content decreased with an increase in stress level, consequently showing a decrease in pores size for each incremental stress. The tailings showed almost same nature for 71 and 80% initial solids content for an increase in stress (Figs 9 -16 and 9 -17).

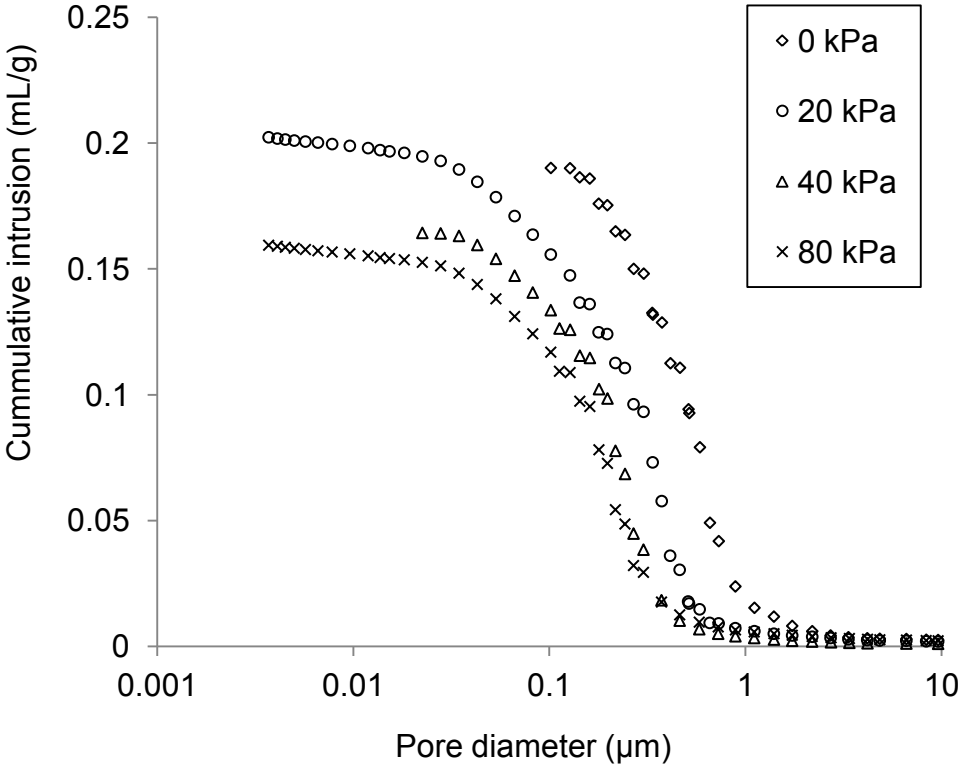

Figure 9-17: Cumulative pore volume distribution of polymer amended fine tailings for 80 percent solids by mass (0 kPa – unconsolidated tailings)

There were not too many differences in CPSD and the CPSD curves showed almost similar nature for all initial solids content with each incremental stress. Comparatively, the initial percent solids of 58% showed higher cumulative intrusions in comparison to 71 and 80% initial percent solids with each incremental stress

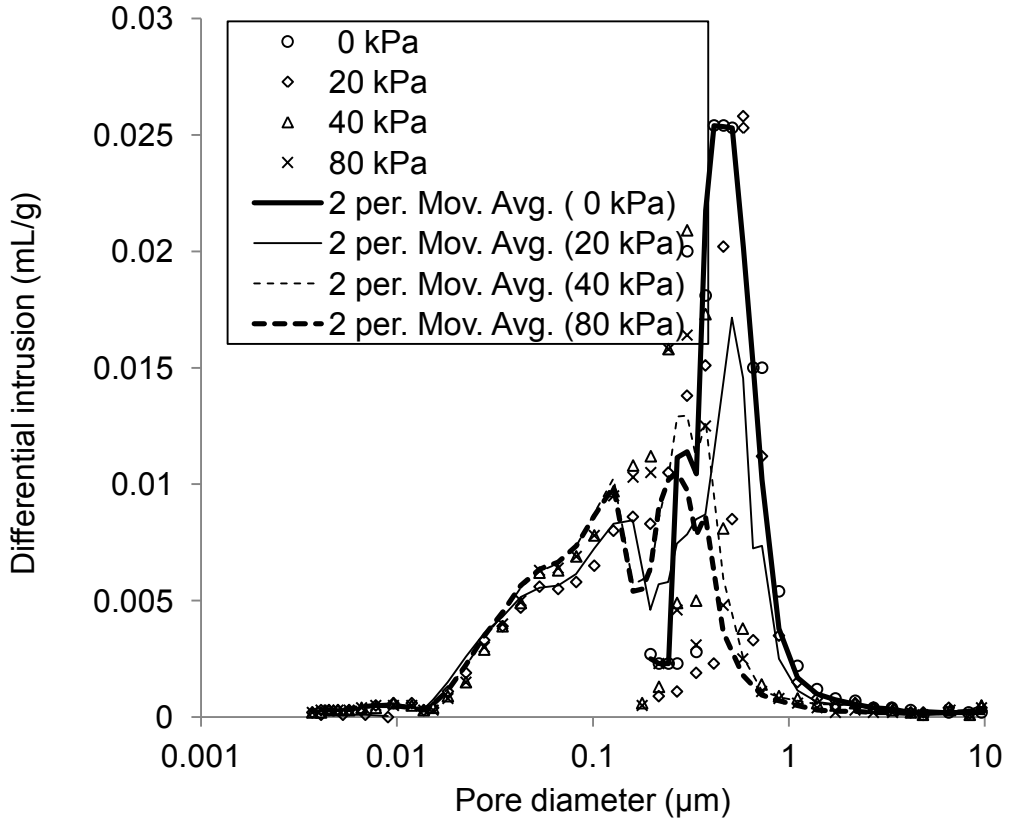

Figure 9-18: Differential pore size distributions of polymer amended fine tailings for 58 percent solids by mass (0 kPa – unconsolidated tailings)

Generally, the cumulative intrusion curves showed that the tailings were spread between 0.003 and 10 µm pores diameter, relatively giving uniform distribution

except the peak of CPSD curves lowered for each incremental stress. Furthermore, the difference in PSD of all tailings was minimal for 80% initial solids content at 40 and 80 kPa. Lee et al. (2014) examined the pore size distribution of fly ash treated gold tailings, and discussed that the cumulative pores volume of tailings varied between 0.18 and 0.14 for pores diameter ranging from 0.002 to 10 μm radii.

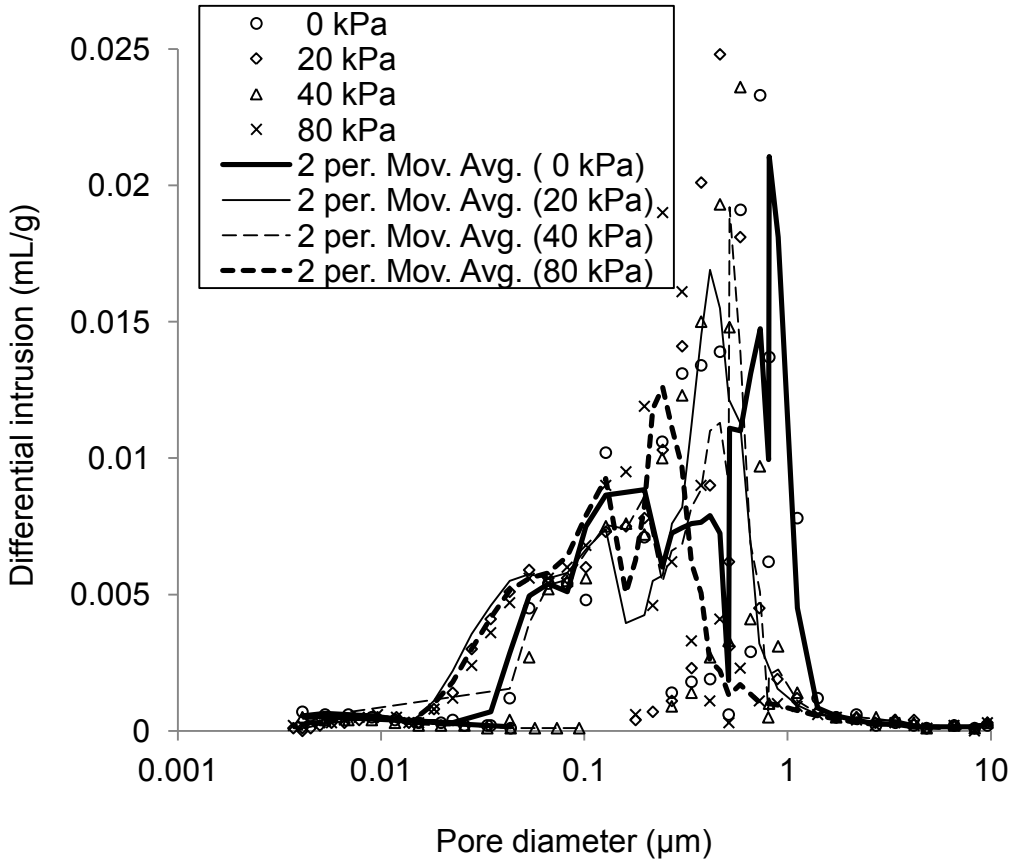

Figure 9-19: Differential pore size distributions of polymer amended fine tailings for 71 percent solids by mass (0 kPa – unconsolidated tailings)

The differential curves of tailings shifted towards smaller pores diameter with each incremental stress for various initial solids content, and the peak pore mode compressed for an increase in stress level. Furthermore, the peak pore mode also shifted towards smaller pores diameter for an increase in degree of desiccation (Figs 9 -18, 9 -19, 9 - 20).

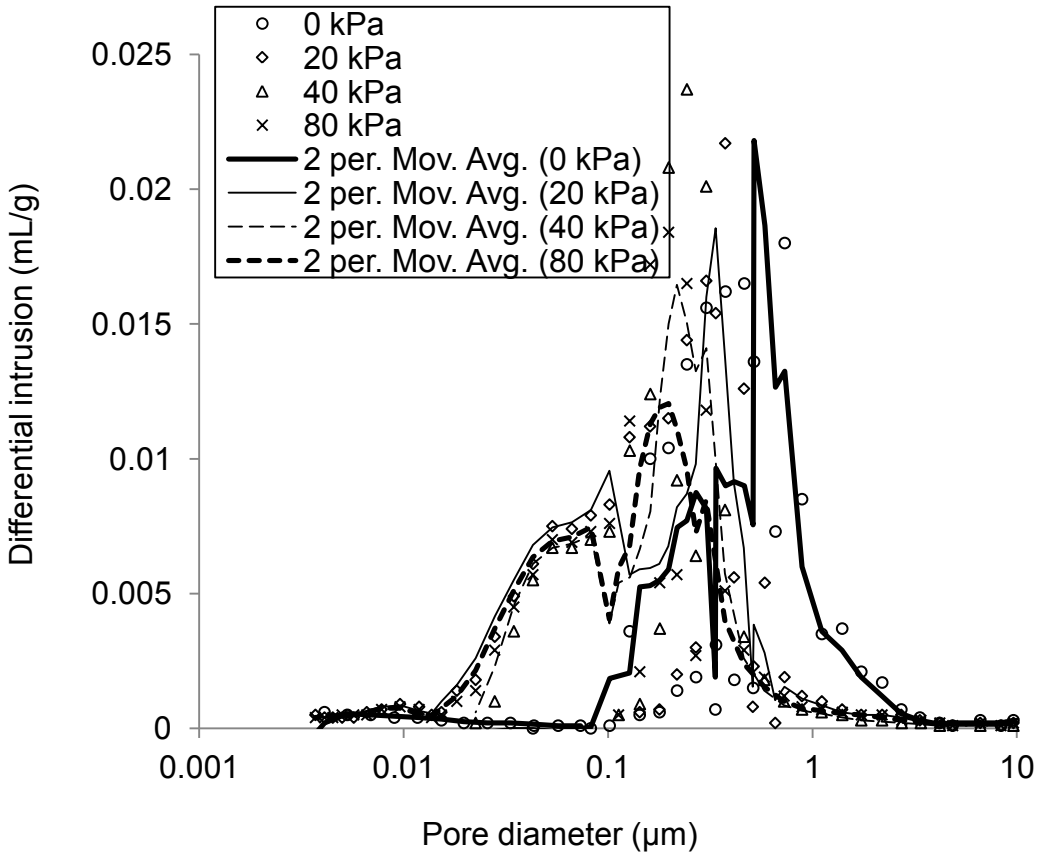

Figure 9-20: Differential pore size distributions of polymer amended fine tailings for 80 percent solids by mass (0 kPa – unconsolidated tailings)

All tailings provided bimodal pore size distribution, and the peak of pore mode reduced with each incremental stress and with increase in degree of desiccation.

However, the pores size distribution curves of polymer amended tailings provided somewhat similar trends to that of gold tailings and compacted clayey till as reported in the findings of Lee et al. (2014) and Simms and Yanful (2001).

Again, the log differential pore volume distribution of tailings showed that the tailings provided pores of smaller diameters at higher stress level, and they showed similar nature for an increase in initial degree of desiccation, and comparatively, the difference in PSD was smaller at higher stress levels as the data points overlapped to each other (Figs 9 - 21, 9 - 22, 9 - 23).

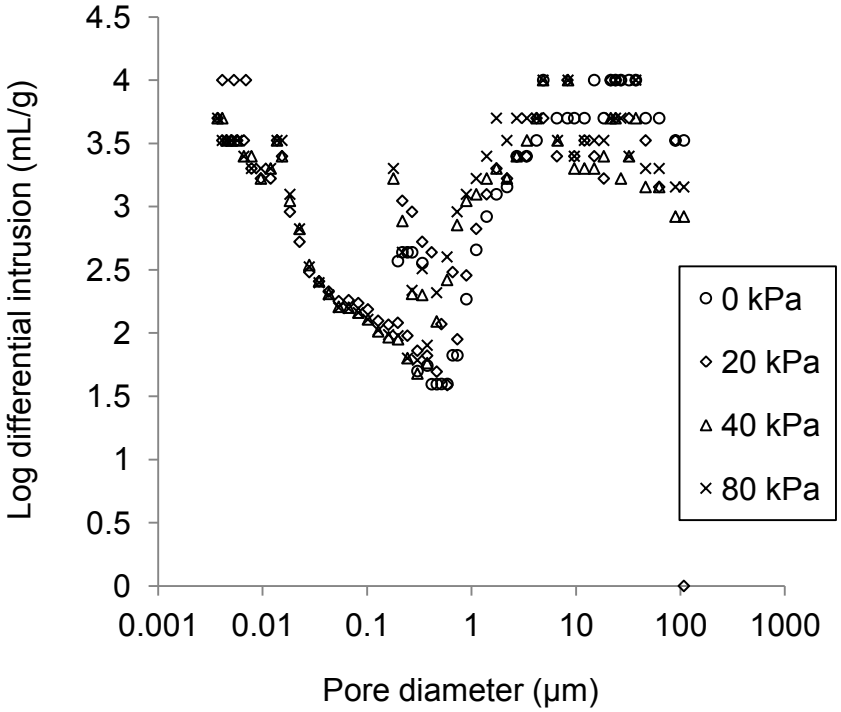

Figure 9-21: Log differential pore size distributions of polymer amended fine tailings for 58 percent solids by mass (0 kPa – unconsolidated tailings)

There were clear indications that inter – aggregate pores size centered at pore diameter of 0.5 μm. Lee et al. (2014) reported that the pore structure of gold tailings changed with the degree of desiccation. Simms and Yanful (2001) examined the pores size distribution of a clayey till during soil water characteristic curve tests and discussed that the PSD of till varied largely for various stress levels.

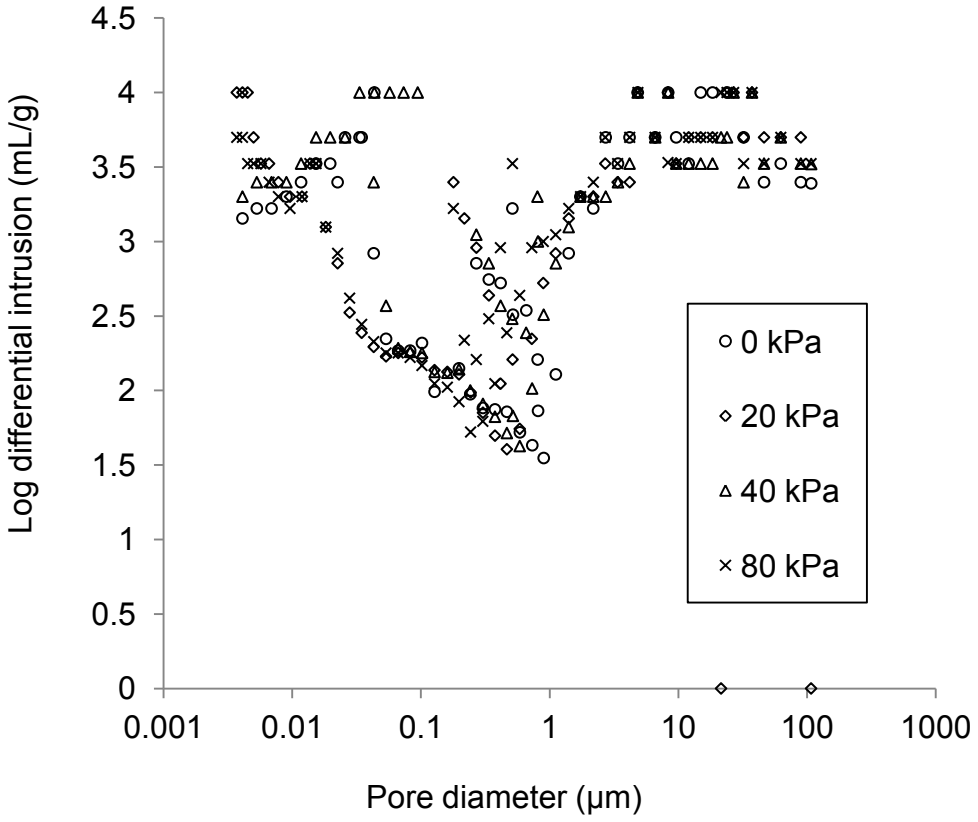

Figure 9-22: Log differential pore size distributions of polymer amended fine tailings for 71 percent solids by mass (0 kPa – unconsolidated tailings)

The test results showed that MIP technique was efficiently used to quantify the pore size distribution of flocculated tailings under loadings like that of other materials such as cement paste and clayey soils (Lee et al. 2014; Monroy et al. 2010; Zhou et al. 2010; Simms and Yanful 2004 and Abell et al. 1999).

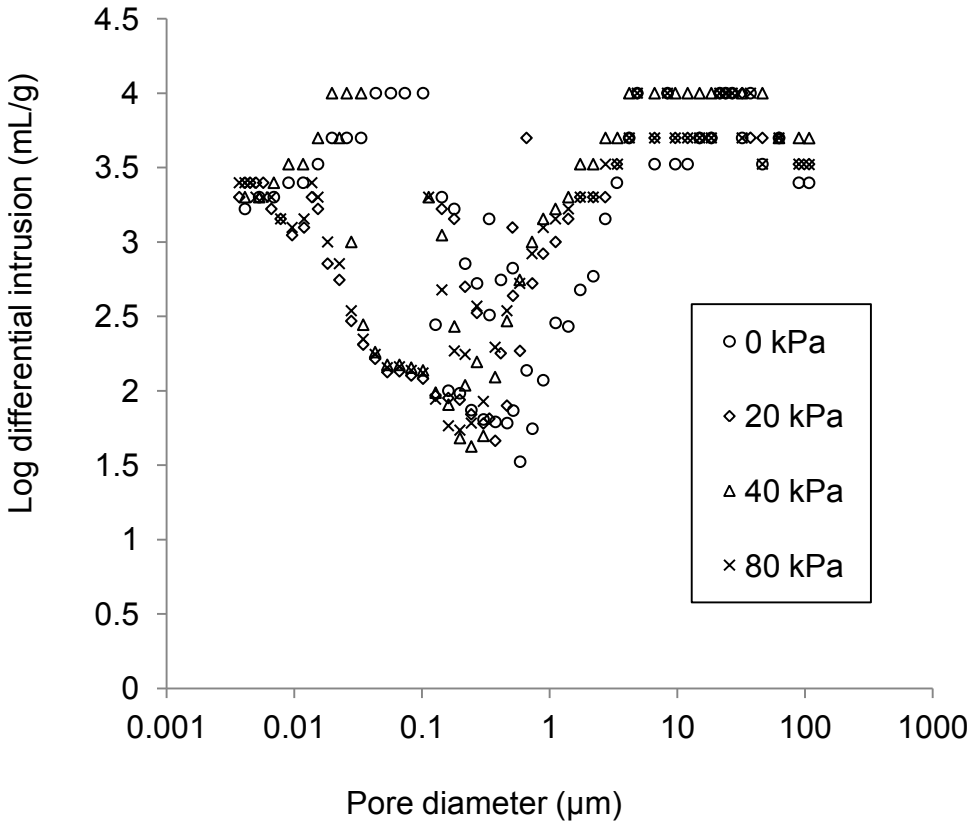

Figure 9-23: Log differential pore size distributions of polymer amended fine tailings for 80 percent solids by mass (0 kPa – unconsolidated tailings)

9.3.5 Scanning electron microscopy (SEM) test results and image analysis

Figs 9 - 24 to 9 – 26 display quantitative micro fabric measurements of SEM micrographs of polymer amended oil sands tailings.

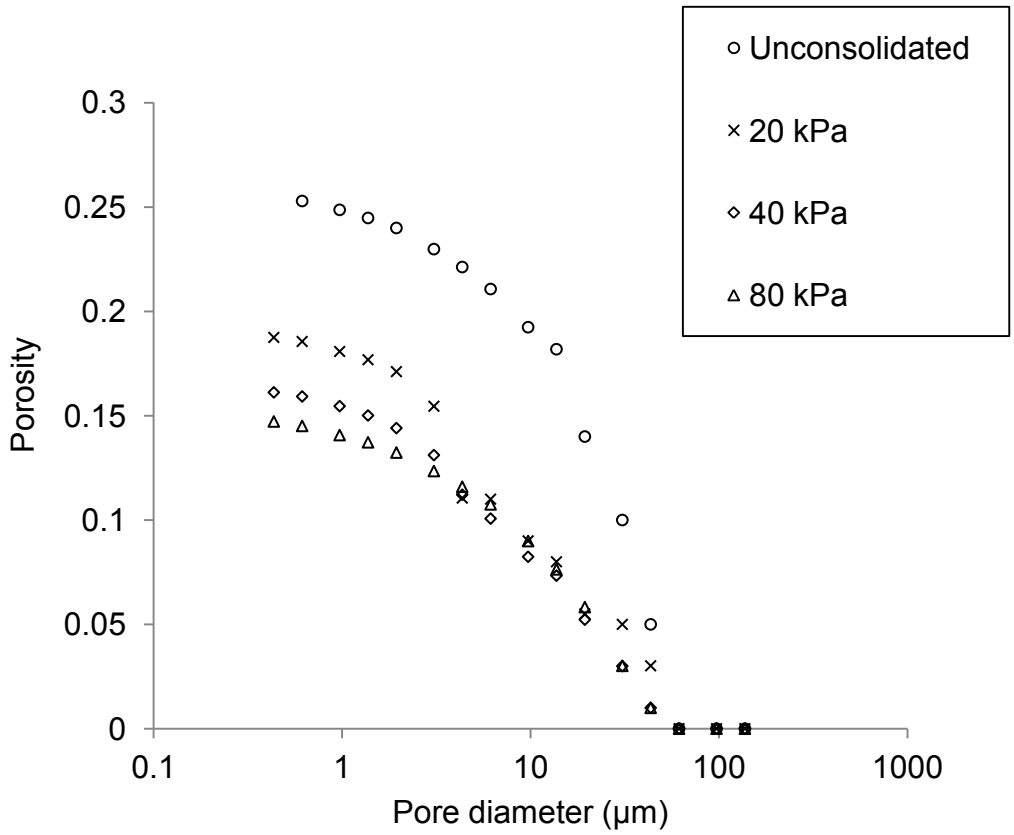

Figure 9-24: Quantitative micro fabric measurements of SEM micrographs for 58 % initial solids content

The imageJ analysis was performed with BSE images captured at a magnification of 0.5 kx, a scale of 50 μm and view field of 300 μm. SEM micrographs for image analysis are presented as appendix 4.

Furthermore, the analysis was performed at a resolution of 768 x 648 for all SEM micrographs. The specific magnification was selected to maximize the scope of the analysis, based on the particle size distribution of tailings. The resolution characterized the pixels of each image and the image processing generated and separated the individual particles based on the pixel intensity. The threshold of BSE micrographs was optimized to clearly distinguish the particles, background and adjacent grains boundaries.

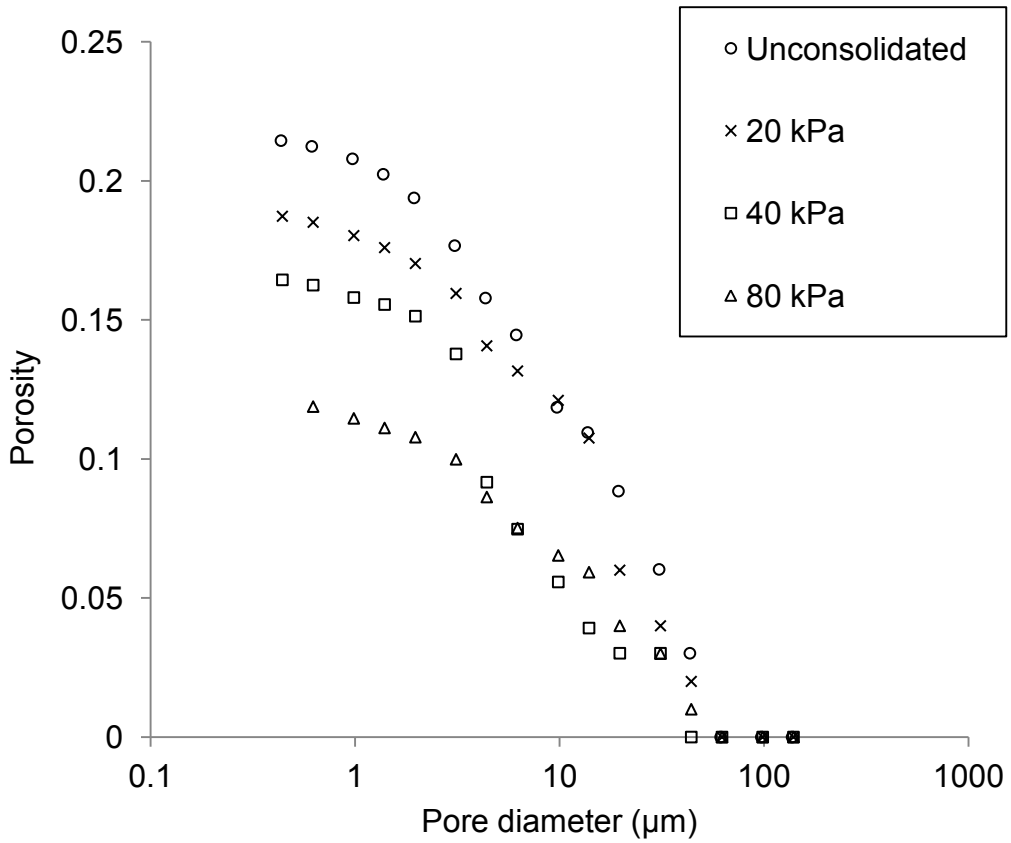

Figure 9-25: Quantitative micro fabric measurements of SEM micrographs for 71 % initial solids content

For unconsolidated oil sands fine tailings, the microporosity of tailings decreased for an increase in degree of desiccation (Figs 9 - 24 to 9 - 26). Resultantly, the unconsolidated tailings provided microporosity of 0.25, 0.22 and 0.21 for initial solids content of 58, 71 and 80 % respectively.

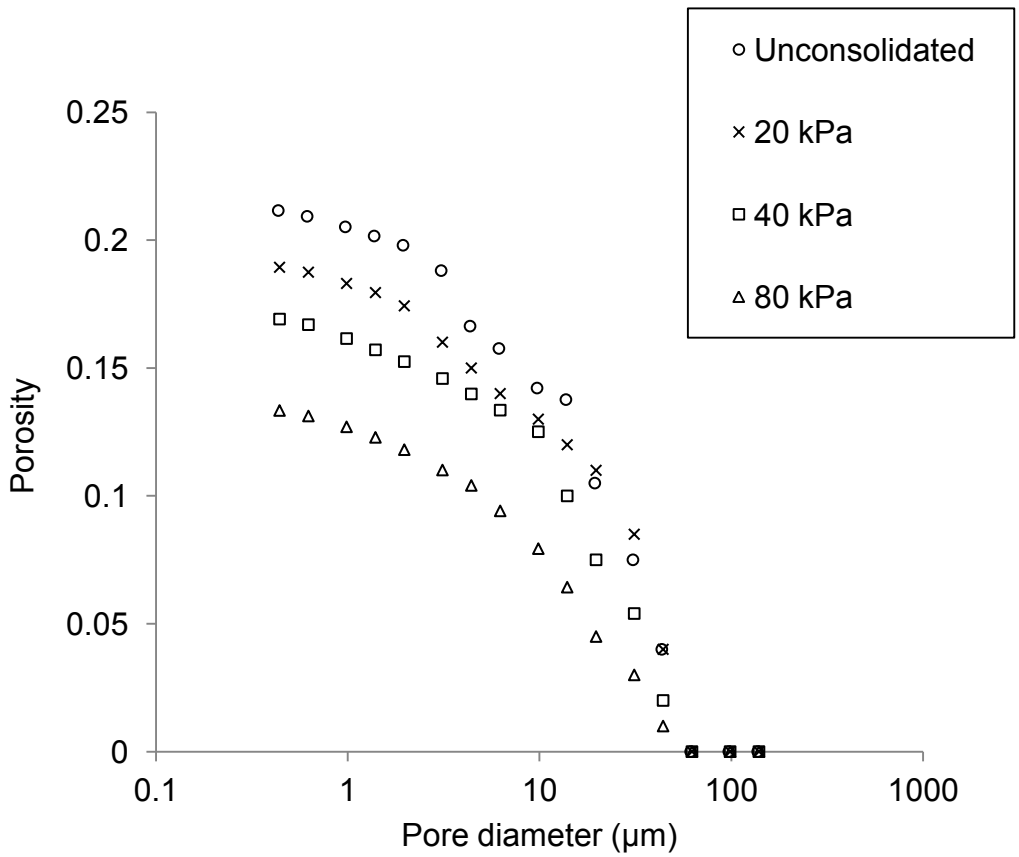

Figure 9-26: Quantitative micro fabric measurements of SEM micrographs for 80 % initial solids content

As in Figs 9 – 27 to 9 – 29, the SEM micrographs showed that the tailings fabric appeared more packed for a successive increase in initial degree of desiccation, which alternately resulted in lowering the microporosity. For visual inspection, the

images were captured at a higher magnification of 5 kx and a scale of 5 μm to clearly distinct and observe the features of the tailings fabric. Similarly, the microporosity of tailings decreased for a successive increase in stress level for a specific degree of desiccation. The increase in stress level consolidated the tailings fabric developing close interactions among the solid particles which lowered the microporosity. For 58% initial solids content, the porosity of tailings decreased from 0.25 to 0.15 for a change in stress level from 0 - 80 kPa.

The similar observations were noted for 71 and 80% initial solids content with a successive increase in stress level (Figs 9 – 25 and 9 – 26). Resultantly, each incremental stress resulted in the progressive lower of tailings fabric, which resulted in lowering their microporosity. However, the microporosity curves of tailings for various initial solids converged for an increase in stress level and the tailings did not show any difference in microporosity at a stress level of 80 kPa. According to White (1996), the smaller movement of water content and solid particles resulted in the overall deformation of oil sands tailings.

The tailings fabric showed microporosity of 0.15, 0.12 and 0.13 for 58, 71 and 80% initial solids content at a stress level of 80 kPa. All tailings behaved in similar fashion taken into account the variations in pores diameter, however, some differences were noted towards larger pores diameter for various stress levels and degree of desiccation as well. The similar findings were observed while examining SEM micrographs of tailings visually. The SEM micrographs

showed that the fabric looked more packed at higher stress level in comparison to lower stress level (Figs 9 – 27 to 9 – 29)

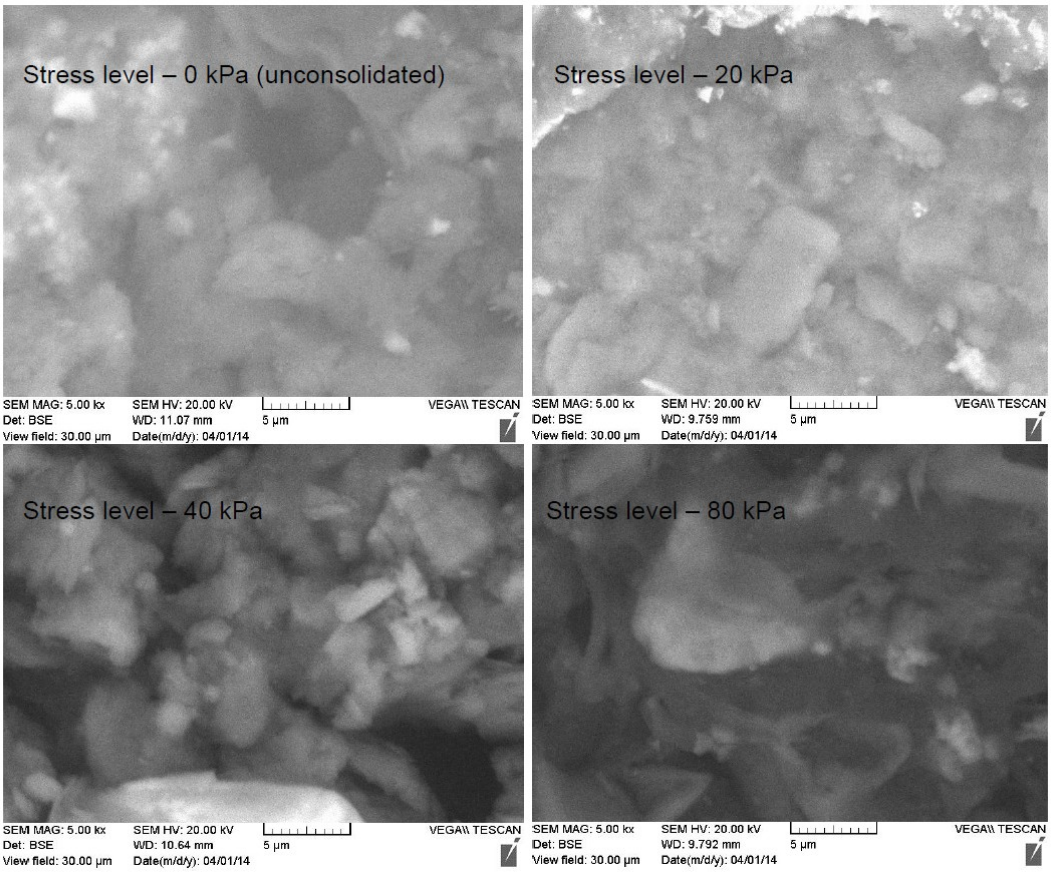

Figure 9-27: Scanning electron micrographs of polymer amended fine tailings for 58 percent initial solids content at various stress levels

The ImageJ software underestimated the gray pixel intensity to some extent due to the existence of bitumen in oil sands tailings as for grayscale images; the pixel value was a single number representing the brightness of the pixel and it appeared really difficult to adjust the threshold of SEM micrographs. Overall, gray pixel analysis test results were comparable to MIP test data, and actual

macroporosity test results to some extent. However, the larger pores diameter was dominant in gray pixel analysis as a comparison to MIP data sets. Abell et al. (1999) reported the findings of Lange et al. (1994) and discussed that the image analysis provided information about larger pores, however, the data curves of SEM looked similar to MIP, but the pores size was larger than the pore sizes simulated with MIP.

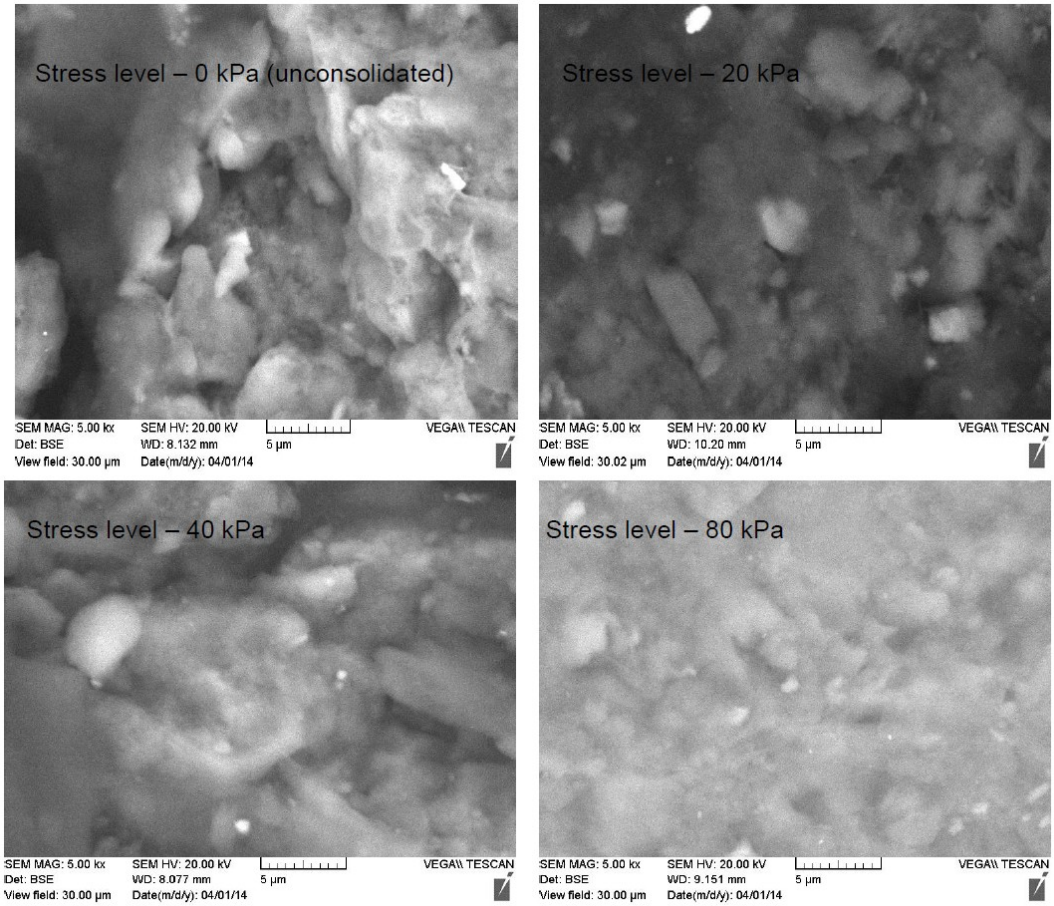

Figure 9-28: Scanning electron micrographs of polymer amended fine tailings for 71 percent initial solids content at various stress levels

ImageJ software still needs more investigation to simulate the fabric of polymer amended tailings due to presence of bitumen and flocculants even under loading conditions. The small particles of tailings appeared to blend together in SEM micrographs, and the solid and void spaces along with bitumen made it difficult to distinguish the boundaries.

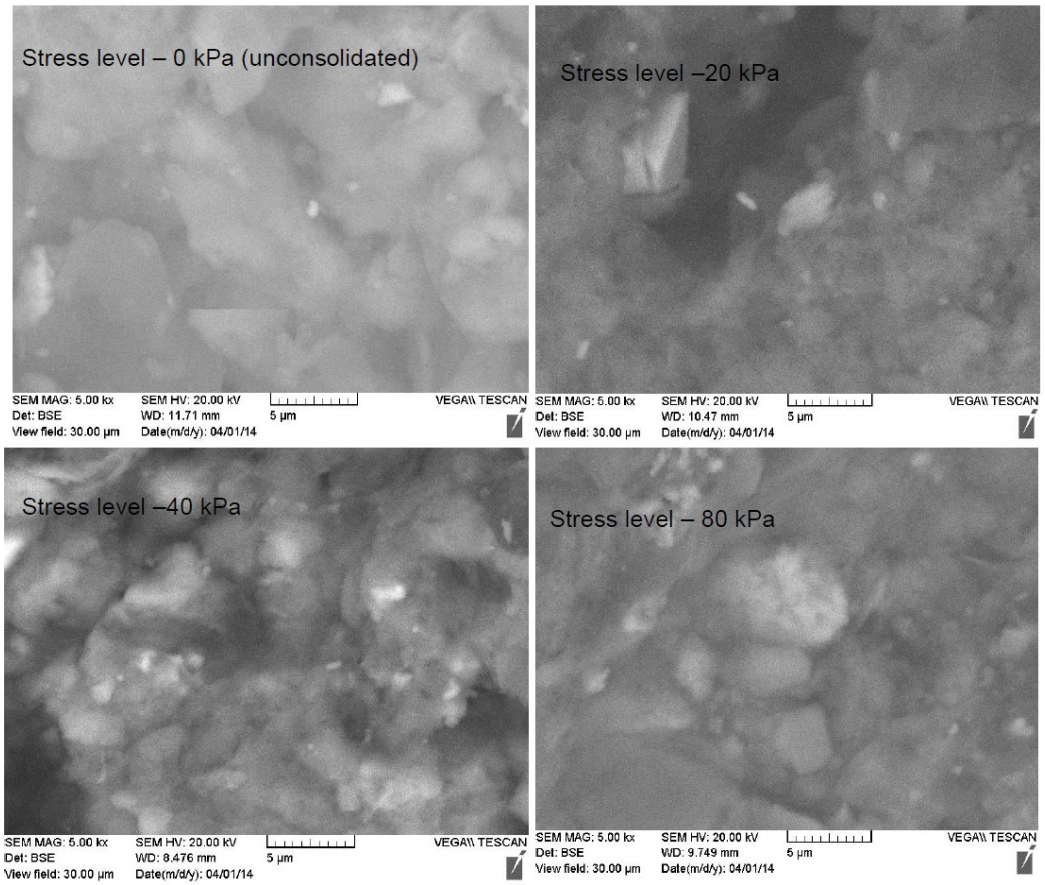

Figure 9-29: Scanning electron micrographs of polymer amended fine tailings for 80 percent initial solids content at various stress levels

9.4 Summary of oedometer tests:

Table 9 – 1 presents the summary of oedometer test data

Table 9-1: Summary of Oedometer tests data

Load inc.	σ_a(kPa)	Correc. Def, mm (ΔH)	Specimen height, mm (H)	Axial strain, ϵ_a (%)	void ratio, e	Spec. height, H_{50}.mm	Time, t_{50} (min)	T100, 100% primary cons. (min)	Coef. of consolidation, Cv (mm^2/sec), log time method	Square root of time method, t_{90}	Coef. of consolidation, square root of time method, cv (mm^2/sec.)	Coefficient of compressibility, Mv, m^2/kN
Consolidation test summary (58% initial solids content)												
Unconsolidated					2.57							
1	1	2.371	17.62	11.85	2.12							0.1261
2	2.5	5.541	14.45	27.71	1.5	16.04	9	50	0.023	5.92	0.026	0.1471
3	5	6.437	13.56	32.18	1.28	14.08	6.5	60	0.025	4.98	0.0283	0.0368
4	10	7.383	12.61	36.92	1.15	13.11	8	50	0.0176	5.5	0.0199	0.0035
5	20	8.311	11.68	41.56	1	12.19	5	32	0.0243	5.5	0.0225	0.0113

6	40	9.255	10.74	46.27	0.82	11.56	6	40	0.0173	5.0	0.0188	0.0047
7	80	10.139	9.86	50.7	0.70	10.3	4.8	40	0.0181	6.0	0.0165	0.0006
Consolidation test summary (71% initial solids content)												
Unconsolidated					1.64							
1	1	1.14	18.86	5.7	1.48							0.0625
2	2.5	4.08	15.92	20.41	1.09	17.28	18	90	0.014	7.600	0.018	0.1138
3	5	5.08	14.92	25.38	0.96	15.46	20	180	0.009	9.400	0.010	0.0257
4	10	6.1	13.9	30.51	0.84	14.45	15	108	0.011	8.010	0.011	0.0126
5	20	7.15	12.85	35.76	0.71	13.38	13	80	0.011	7.800	0.010	0.0073
6	40	8.21	11.79	39.63	0.69	12.34	10	80	0.013	6.580	0.012	0.0006
7	80	9.11	10.89	45.56	0.52	11.34	12	106	0.008	7.500	0.008	0.0026
Consolidation test summary (80% initial solids content)												
Unconsolidated					1.57							
1	1	0.5	19.50	0.975	1.4							0.0684
2	2.5	0.8922	19.10	4.61	1.28	19.43	8	30	0.038	5.78	0.040	0.0342

3	5	1.5401	18.45	7.7	1.14	18.8	10	100	0.029	6.5	0.030	0.0253
4	10	2.5159	17.48	12.58	1.06	18	12	80	0.022	7.2	0.022	0.0076
5	20	3.7119	16.28	18.56	0.94	16.96	10	85	0.024	6.5	0.024	0.0060
6	40	4.9723	15.02	24.86	0.80	15.72	12	90	0.017	7.25	0.017	0.0003
7	80	6.2311	13.76	31.15	0.65	14.42	14	200	0.012	7	0.013	0.0020

9.5 Interaction of microstructure to macroscopic features of polymer amended oil sands tailings

The void ratio of tailings decreased with an increase in initial solids content and they showed void ratio of 2.54 for 58% initial solids content which was higher in comparison to 80% initial solids content (e = 1.57). In addition to this, the void ratio of tailings decreased for each incremental stress for specific initial degree of desiccation. The pore volume of tailings decreased significantly for each incremental stress and 58% initial solids content gave quite less pore volume at 80 kPa as compared to unconsolidated tailings.

The differential and log differential pore size distribution curves showed that the tailings shifted towards pores of smaller diameters for an increase in stress level. Furthermore, the peak of pores mode compressed for each incremental stress and an increase in degree of desiccation as well. The SEM micrographs along with ImageJ analysis was supported with MIP data sets.

The tailings provided more packed structure giving pores of smaller diameters at 40 and 80 kPa, which consequently enabled tailings to give lower hydraulic conductivity. For particular initial solids content, the hydraulic and mechanical paths of tailings changed due to change in fabric for an increase in stress level. However, the hydraulic conductivity and void ratio of all tailings started converging to each other beyond a certain threshold of stress levels showing minimal gain in percent solids. The above discussion showed that the

macroscopic results were strongly correlated to changes observed in fabric measurements of the tested tailings

9.6 Conclusions

The axial deformation was high for 58% initial solids content and the percent solids varied from 58 to 86% for an increase in stress from 0 to 80 kPa, and all tailings showed minor gain in percent solids beyond a certain threshold of stress level. The tailings did not show major changes in osmotic suction for various initial degrees of desiccation, and stress levels as well. The hydraulic conductivity of tailings decreased with an increase in stress level and degree of desiccation, and it happened due to decrease in pores diameter, and ultimately, the tailings for various initial degree of desiccation attained unique hydraulic conductivity curves beyond a certain threshold of stress level. However, the polymer amended tailings provided comparable k values when tested with other test data, and k values were quite high in comparison to consolidated unamneded MFT.

MIP and SEM test results along with gray pixel analysis showed that the tailings shifted towards smaller pores diameter with an increase in degree of desiccation and an increase in stress level as well. The macroscopic results were supported by changes observed in fabric of the tested flocculated specimens. In a nutshell, the tailings of 58 % initial solids content performed in similar fashion to that of 71% and 80% solids content, so there was no efficacy to desiccate the tailings for higher initial solids content such as 71% and 80%.

Chapter 10. Comparative evaluation of microstructure of polymer amended oil sands mature fine tailings

Abstract

The main objective of this chapter is to comparatively discuss the microstrcuture data of oil sands MFT, and to highlight the sustainability of applied techniques while examining the microstructure of polymer amended MFT. Furthermore, the test data of this study was compared to some other materials test data to validate the applicability of these approaches in oil sands industry.

The data analysis showed that both MIP and SEM data was correlated with volume change for oil sands tailings. Difference in fabric data was also noted due to polymer dose. Furthermore, MIP and SEM also detected changes in fabric due to desiccation and consolidation that followed similar paths observed in other clays..

10.1 Introduction

Mercury intrusion porosimetry (MIP), scanning electron microscopy (SEM), environmental scanning electron microscopy (ESEM), micro computed tomography (μCT) and nuclear magnetic resonance (NMR) or magnetic resonance imaging (MRI) are the most commonly employed techniques to analyze the fabric of saturated and partially saturated soils.

The geometric arrangement of particles, including degree and morphology of aggregation, and pore size distribution defines soil fabric. Analysis of soil fabric has been used to explain many features of soil behaviour (Zbik et al. 2008; Simms and Yanful 2004; Simms and Yanful 2001 and Nimmo 2004). A classic example of the influence of fabric is the variation in permeability for wet of optimum in comparison to dry of optimum soils with the same porosity. The permeability of soil varies due to change in soil fabric from a relatively flocculated fabric to dispersed fabric. Similar correlations of fabric with solute convection are other clear examples of the influence of fabric (Nimmo 2004).

Nimmo (2004) stated that the size and frequency of the pores greatly influenced the hydraulic conductivity. Simms and Yanful (2002) reported that the saturated hydraulic conductivity of compacted clays showed a strong quantitative correlation with the pore-size distribution measured by MIP. Cuisiner et al. (2011) stated that the larger pore sizes influenced the hydraulic conductivity of St Quintin silt largely in addition to some other properties. Fabric analysis was used to explain differences in strength behaviour of soils and hard rock tailings with different stress histories (Dalairi et al. 2014). The above discussion showed that the properties of soils can vary as a function of fabric independent of the value of porosity.

10.2 Methods used for microstructure evaluation

In this study, quantitative and qualitative analysis of fabric of oil sands tailings was examined employing scanning electron microscopy (SEM), environmental scanning electron microscopy (ESEM) and mercury intrusion porosimetry (MIP) and were compared. Nuclear magnetic resonance was also trialed on few samples to examine the microstructure but the samples were collapsed while transferring them into the NMR tube. NMR works on the principles that it examines the microstrcuture detecting protons in samples. The addition of water further enhanced the chance of collapsing the tailings fabric at higher water content.

The studies such as Asmussen (2014); Desbois et al. (2012); Du et al. (2010); Zbik et al. (2009); Mitchell and Soga (2005); Simms and Yanful (2004, 2001) and Makula and Manuz (2000) employed SEM techniques to investigate the fabric of porous medium. Though the use of SEM is quite large in various fields relating to geomaterials but the research work is quite limited showing the use of SEM in oil sands industry. In this study, the oil sands tailings were tested for three conditions to investigate the microstrcuture.

First of all, the samples were collected from the experimental chambers to perform the image analysis on fully hydrated and original samples. A rapid freezing stage of -50 ^{o}C was applied to the samples using a low vacuum of 10^{-3} Pa.

Second, freeze-drying with sublimation was used to prepare small samples (7-8 mm^3) for SEM imaging and MIP. Mitchell and Soga (2005) preferred freeze drying method for preconditioning of samples for microstrcuture analysis. Sasanian (2011) discussed that the freeze dried samples provided better results than that of air dried samples when Nanticoke clay was tested using SEM and MIP. Third, freeze-dried samples were analyzed with and without coating the sample with gold palladium.

The aim of this exercise was to make a qualitative and quantitative comparison of polymer amended MFT micrographs. ImageJ software was used to conduct gray pixel analysis of scanning electron micrographs for quantitative measurement of tailings fabric.

10.3 Comparative evaluation of microstrcuture data

10.3.1 Mercury intrusion porosimetry (MIP) test data

10.3.1.1 Cumulative intrusions of polymer amended tailings

Figure 10 - 1 shows MIP data of oil sands tailings for various degrees of desiccation, consolidation and stress levels for a 700 ppm sample.

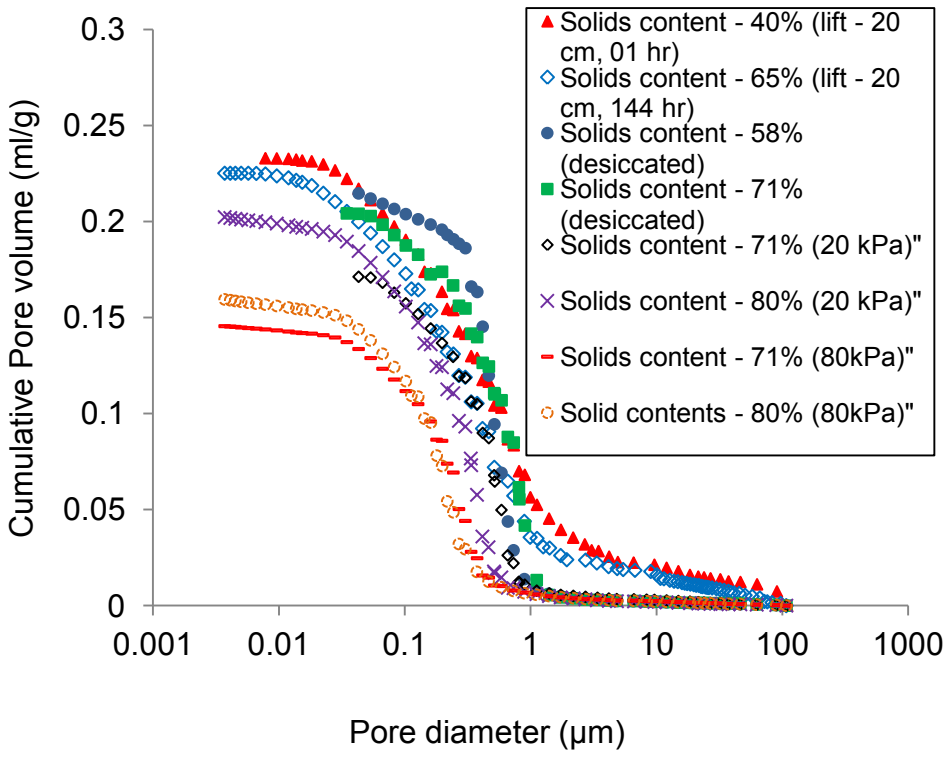

Figure 10-1: Cumulative intrusions of polymer amended tailings

In general, samples showed a decreasing proportion of frequency of larger pores with increasing desiccation and / or consolidation. Samples only undergoing self-weight consolidation showed a somewhat higher total porosity than desiccated samples with no consolidation.

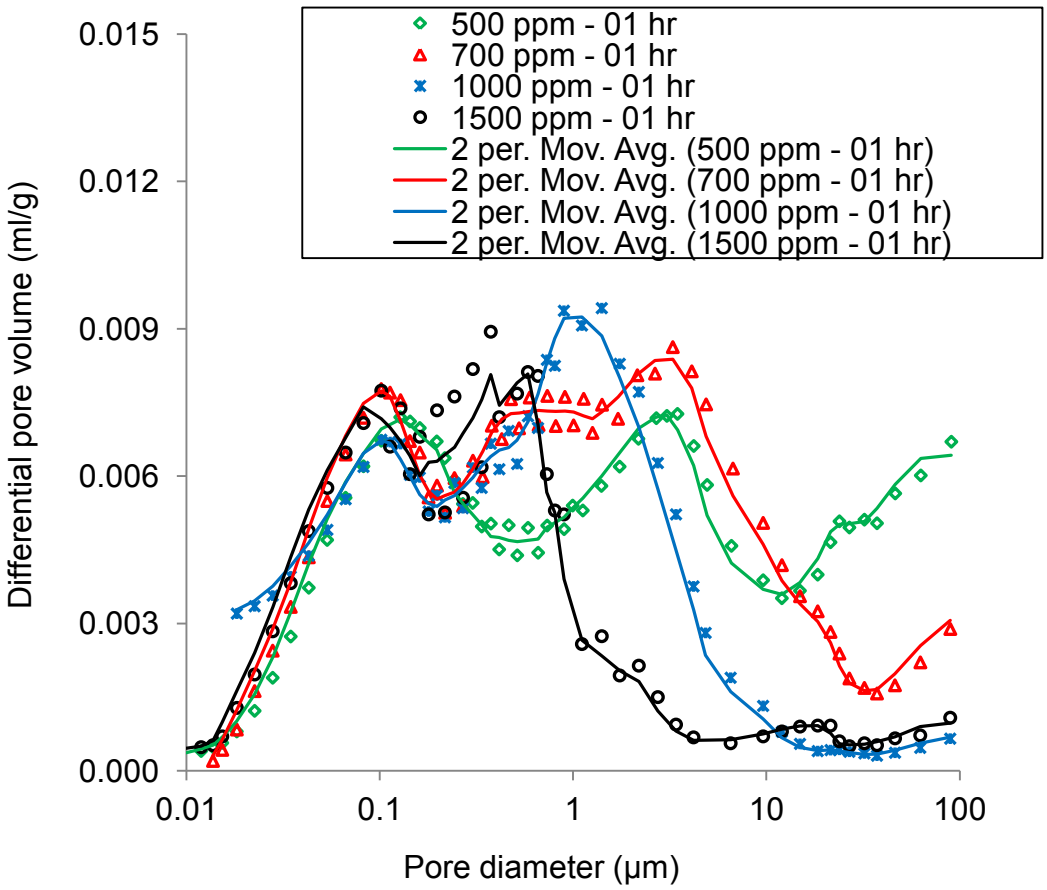

Figure 10-2: Differential pore volume distribution of polymer amended tailings for short term dewatering in thin lift (20 cm) 01 hour after polymer mixing.

10.3.1.2 Effect of difference in polymer dose

The effect of dose on the initial fabric is shown in Figure 10 - 2, which shows the different PSD for samples after 1 hour of dewatering. Both the 500 and 700 ppm samples showed a large and broad pore mode with a diameter around 3 microns. The 1000 ppm and 1500 ppm samples showed reduced peak diameters of 1 micron and 0.4 microns. The larger pores mode correlated with more regular aggregates as shown in the ESEM images in Figure 5 – 17.

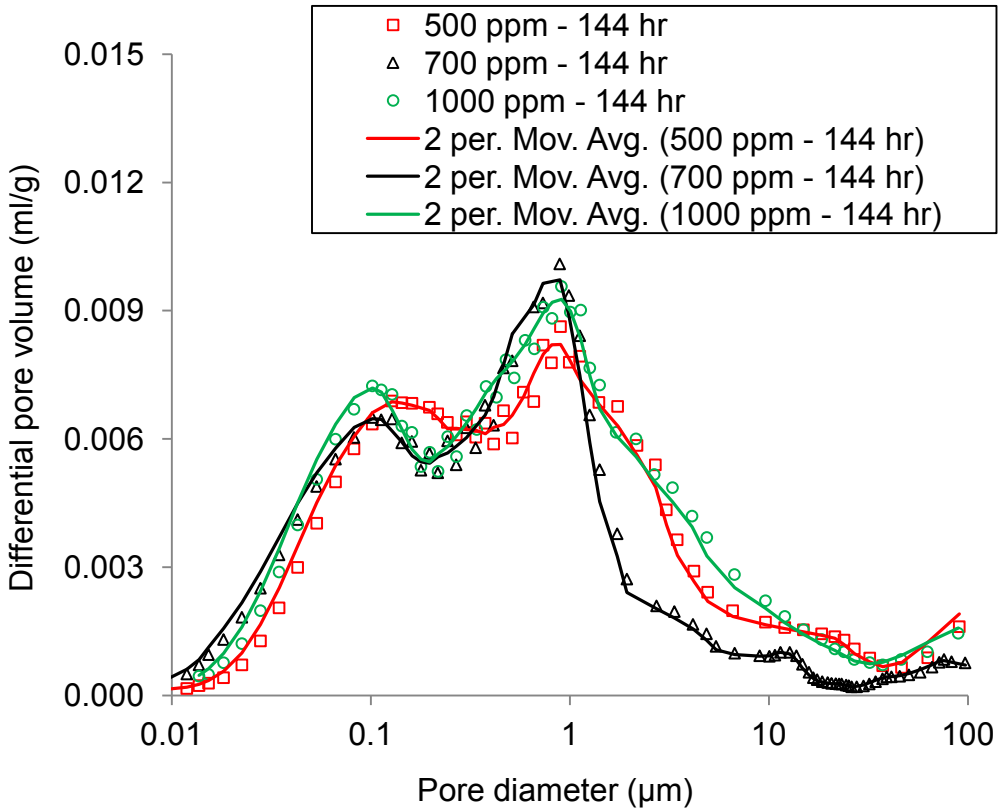

Figure 10-3: Differential pore volume distribution of amended tailings for short term dewatering in thin lift (20 cm) 144 hours after polymer mixing

10.3.1.3 Effect of consolidation

The effect of self-weight consolidation is shown in Figure 10 - 3. The change was most prominent in the 500 and 700 ppm samples, in which the large pore mode diameter was reduced to about 1 micron.

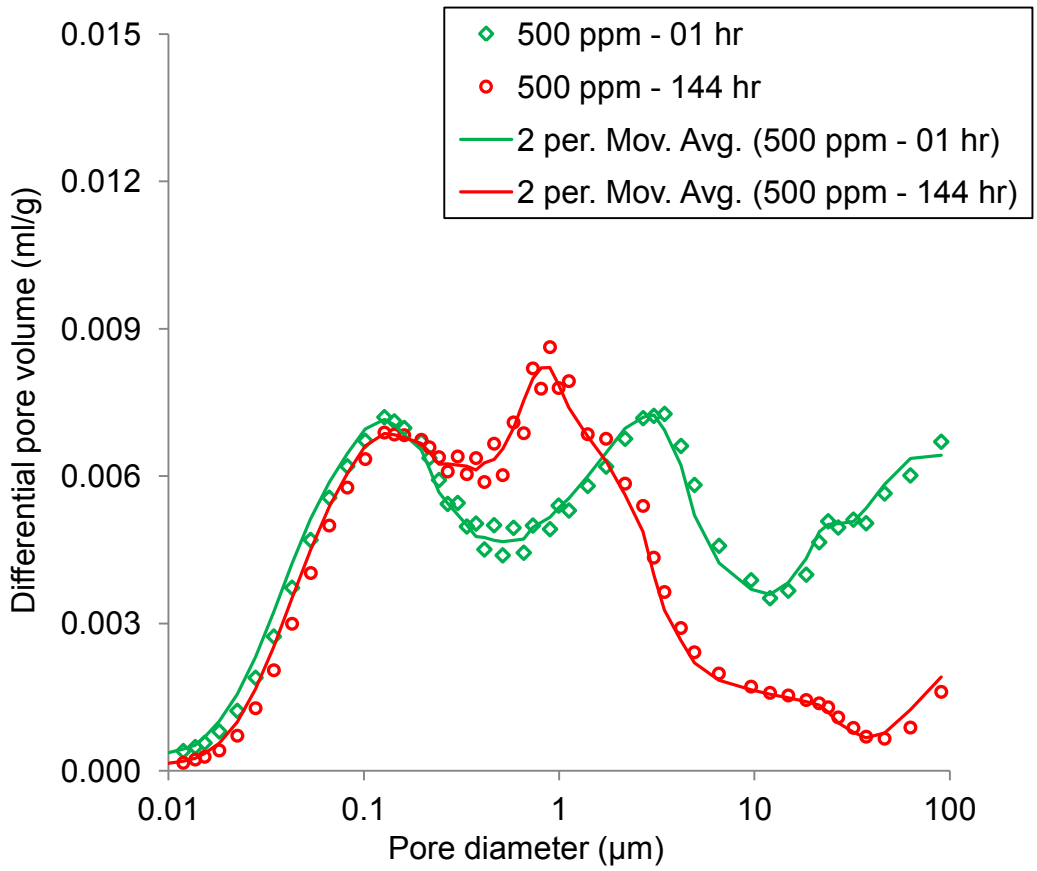

Figure 10-4: Differential pore volume distribution of polymer amended tailings for 500 ppm in thin lift (20 cm) 01 and 144 hours after polymer mixing

The PSDs converged with self-weight consolidation, though the 700 ppm sample showed a narrow pore mode, which correlated to the higher degree of consolidation of this sample observed in Chapter 6. The differences between PSDs at 1 hour and 144 hours for the 500 ppm and 1000 ppm samples are shown in Figs 10 – 4 and 10 - 5

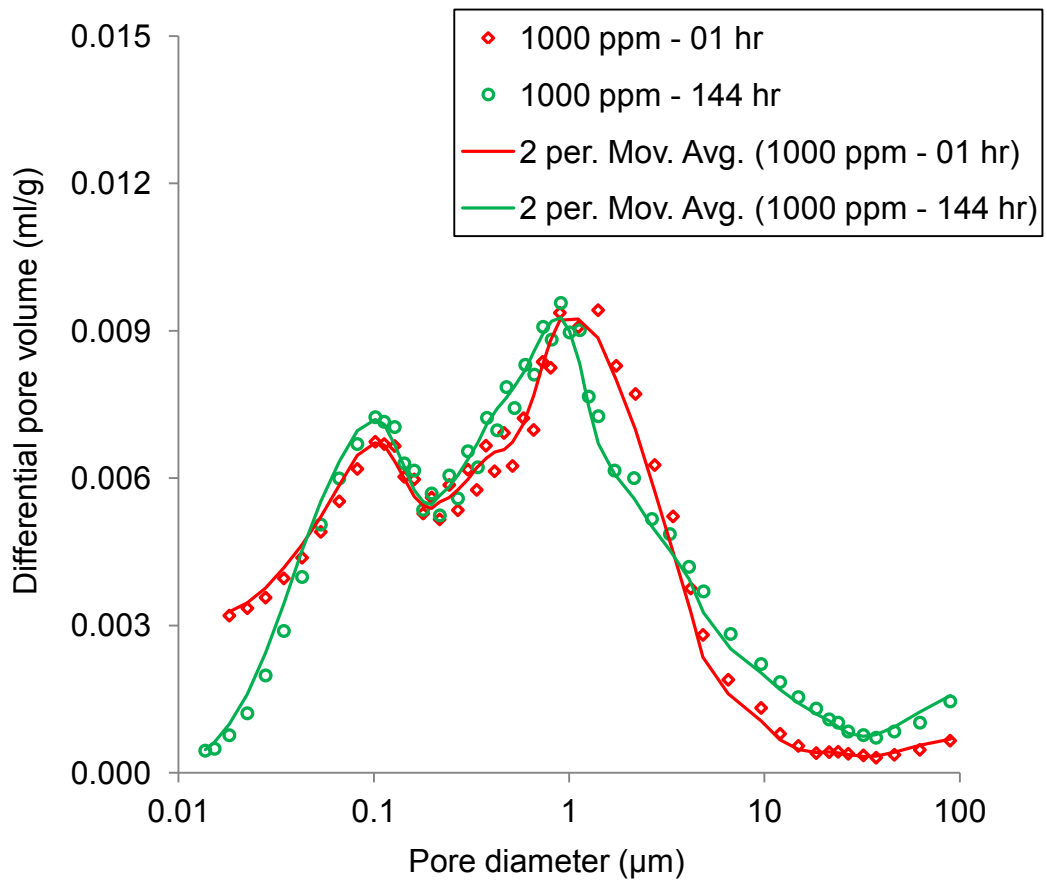

Figure 10-5: Differential pore volume distribution of polymer amended tailings for 1000 ppm in thin lift (20 cm) 01 and 144 hours after polymer mixing

The tailing deposited in lifts (Figs 10 – 3 to 10 - 5) provided larger variations in pores mode (bimodal PSD) varying between 0.01 and 100 µm, and comparatively, the desiccated and consolidated samples also shown bimodal PSD but narrow range of pores diameter varied between 0.01 and 10 µm (Figs 10 – 6 and 10 - 7).

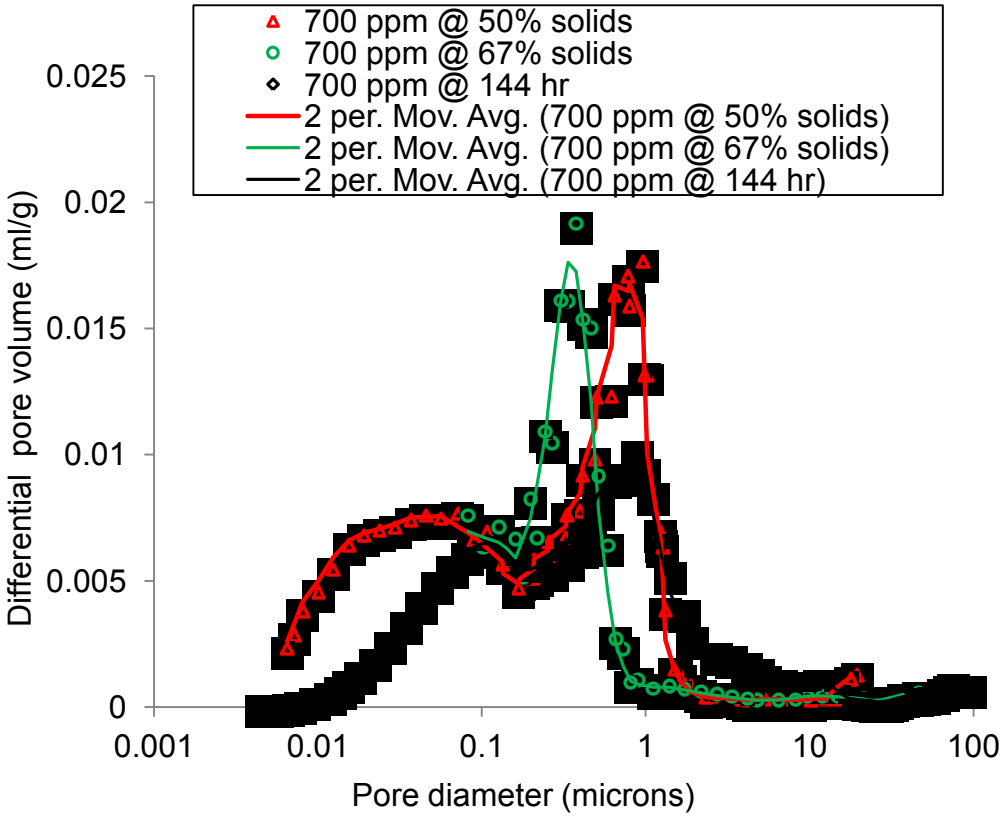

Figure 10-6: Differential pore volume distribution of polymer amended tailings for 700 ppm 144 hours after polymer mixing and different degree of desiccation

For the desiccated samples, the large pore mode increased in size, perhaps due to increase in pore accessibility due to crack development. Subsequently, the diameter of the pore mode decreased from about 0.7 to 0.3 microns (Figs 10 – 6 and 10 - 7). Similar behaviour was seen in MIP test on Halton till as shown in Figure 10 – 8. As in Figure 10 – 9, the diameter of peak pore modes decreased for desiccation and consolidation.

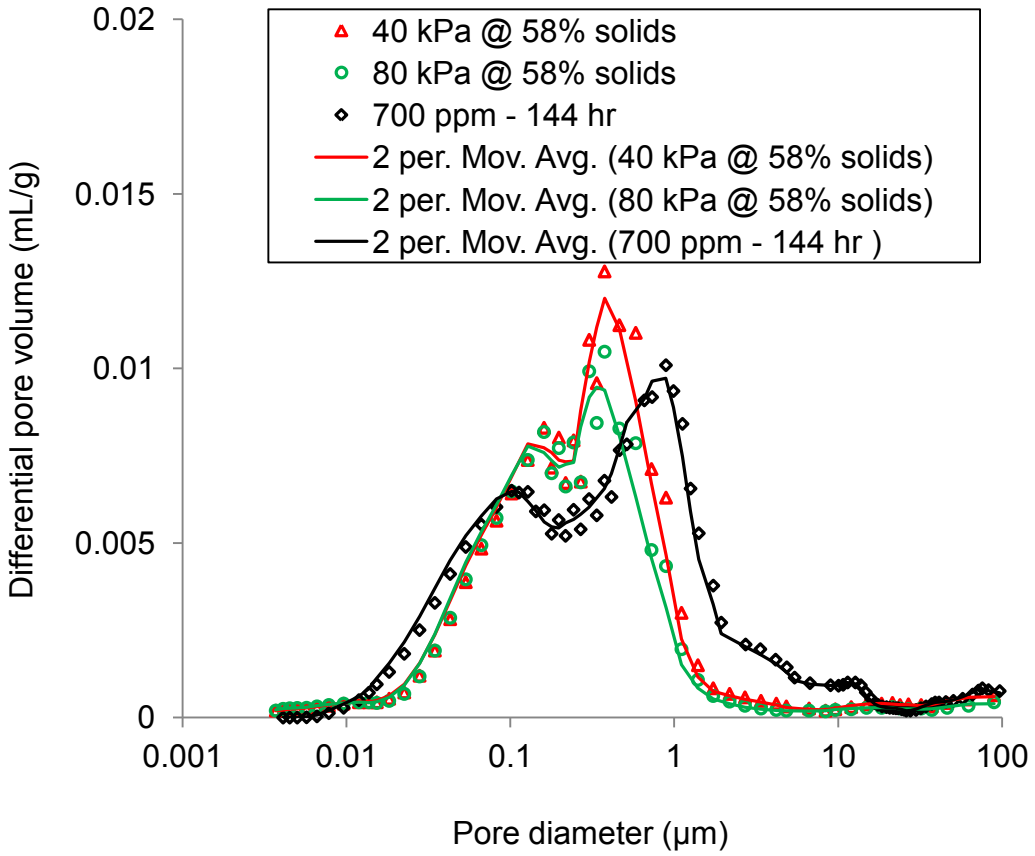

Figure 10-7: Differential pore volume distribution of polymer amended tailings for 700 ppm 144 hours after polymer mixing and for 40 and 80 kPa stress level

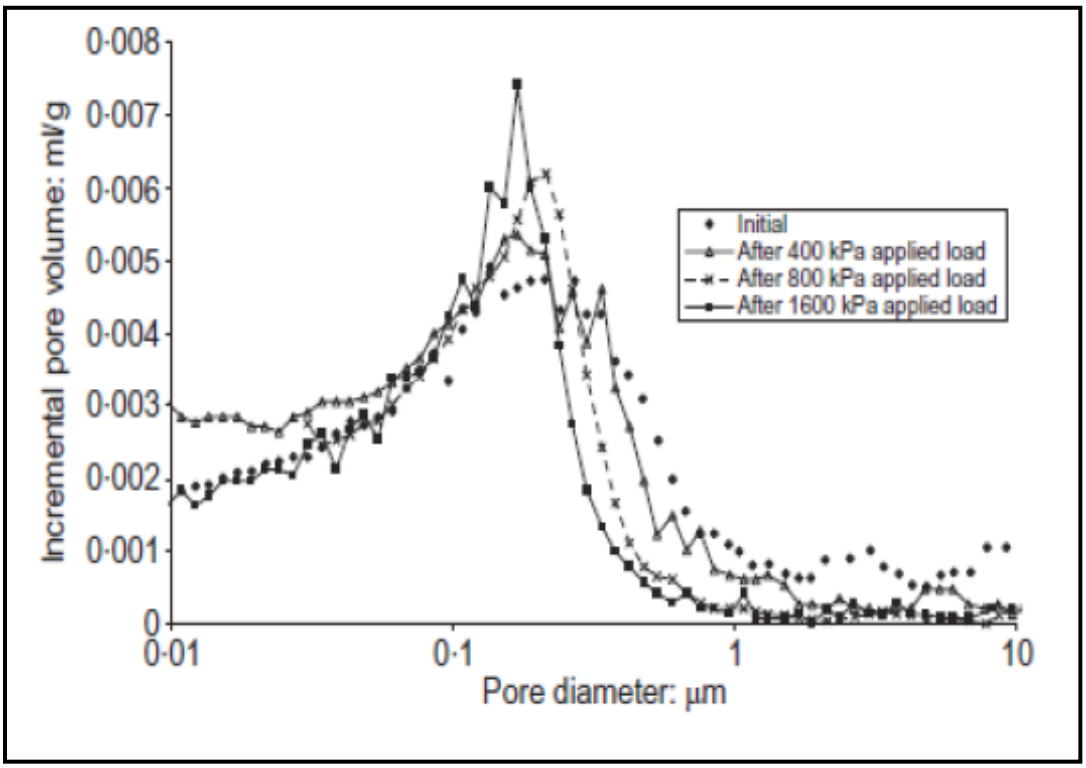

Figure 10-8: Differential pore volume distribution of Halton till (Simms and Yanful 2001)

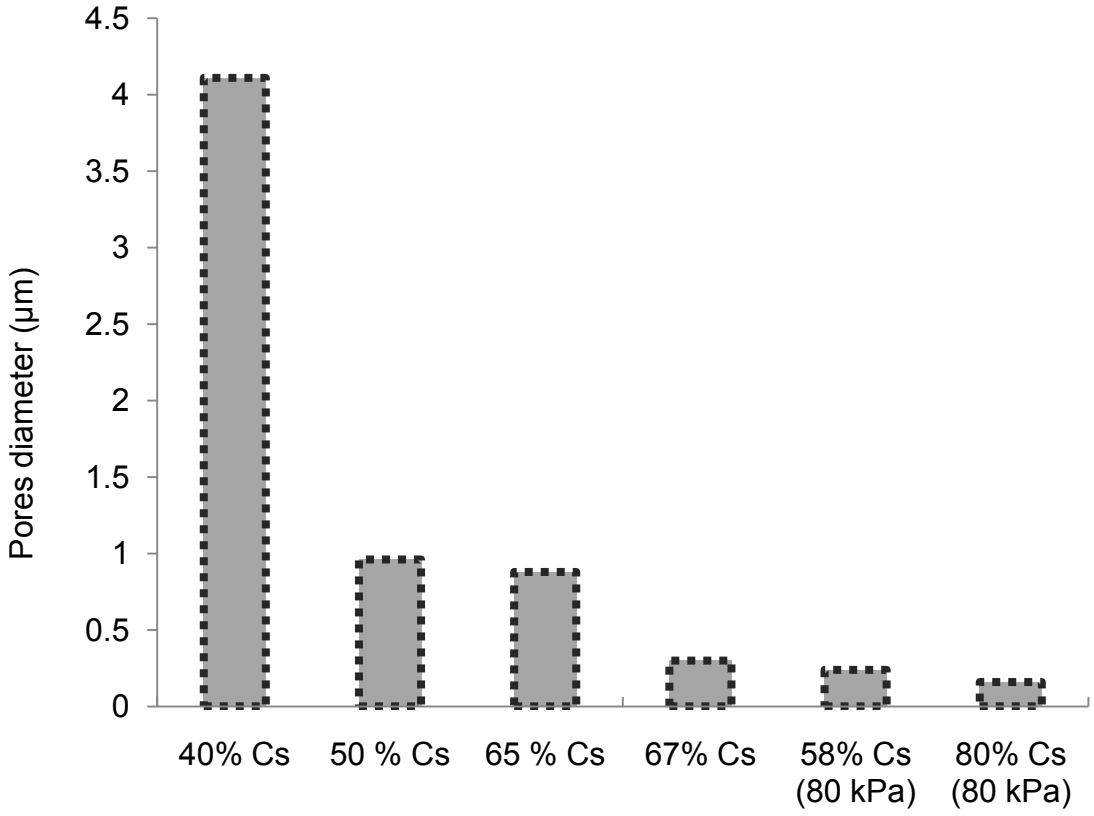

Figure 10-9: Comparison of pores mode of tailings for various conditions

10.3.2 Scanning electron microscopic (SEM) test data

10.3.2.1 Comparative evaluation of scanning electron microscopic micrographs

Figure 10 - 10 shows qualitative comparison of various scanning electron microscopic images of polymer amended oil sands tailings for various scenarios captured at a magnification of 5 kx and at a scale of 20 μm for various conditions. The comparative qualitative evaluation of micrographs showed that the specimens coated with gold palladium (Figure 10 – 10; C1) provided better quality image in comparison to uncoated (Figure 10 – 10; B1) and ESEM images (Figure 10 – 10; A1), as the fabric of tailings were more clear and distinct in freeze dried samples coated with gold palladium. Furthermore, the backscattered electron (BSE) approach provided better quality images in comparison to secondary electron approach (SE).

Figure 10 - 11 represents the scanning electron micrographs of various soils (a- FEBEX bentonite, b – 2- smectite suspension, c – 2 - kaolinite suspension. As a comparison of SEM micrographs, the SEM micrographs of tailings (Figs 10 – 10) provided comparative quality images in comparison to other materials (Figure 10 - 11), and the characterization of pore space was quite visible and distinct in SEM micrographs of oil sands tailings. The fabric of oil sands tailings (Figure 10 – 10) most commonly looked similar to FEBEX bentonite micrographs (Figure 10 – 11; a). The comparative qualitative evaluation of SEM micrographs showed

that SEM technique can effectively be used for qualitative fabric characterization of oil sands MFT.

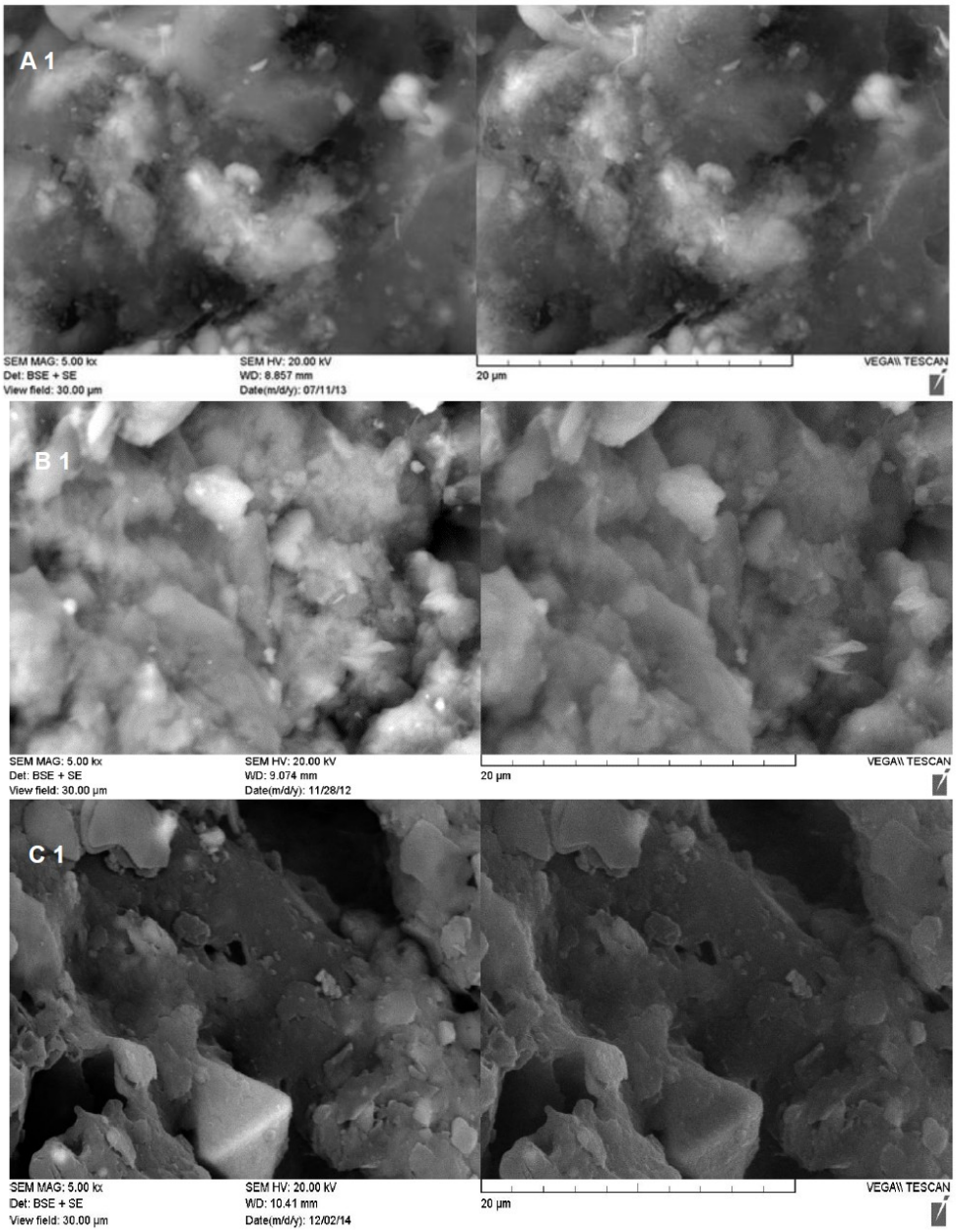

Figure 10-10: SEM micrographs of oil sands tailings (A1- ESEM image, B1 – SEM image without coating, C1 – SEM image coated with gold palladium; Left – BSE, Right – SE)

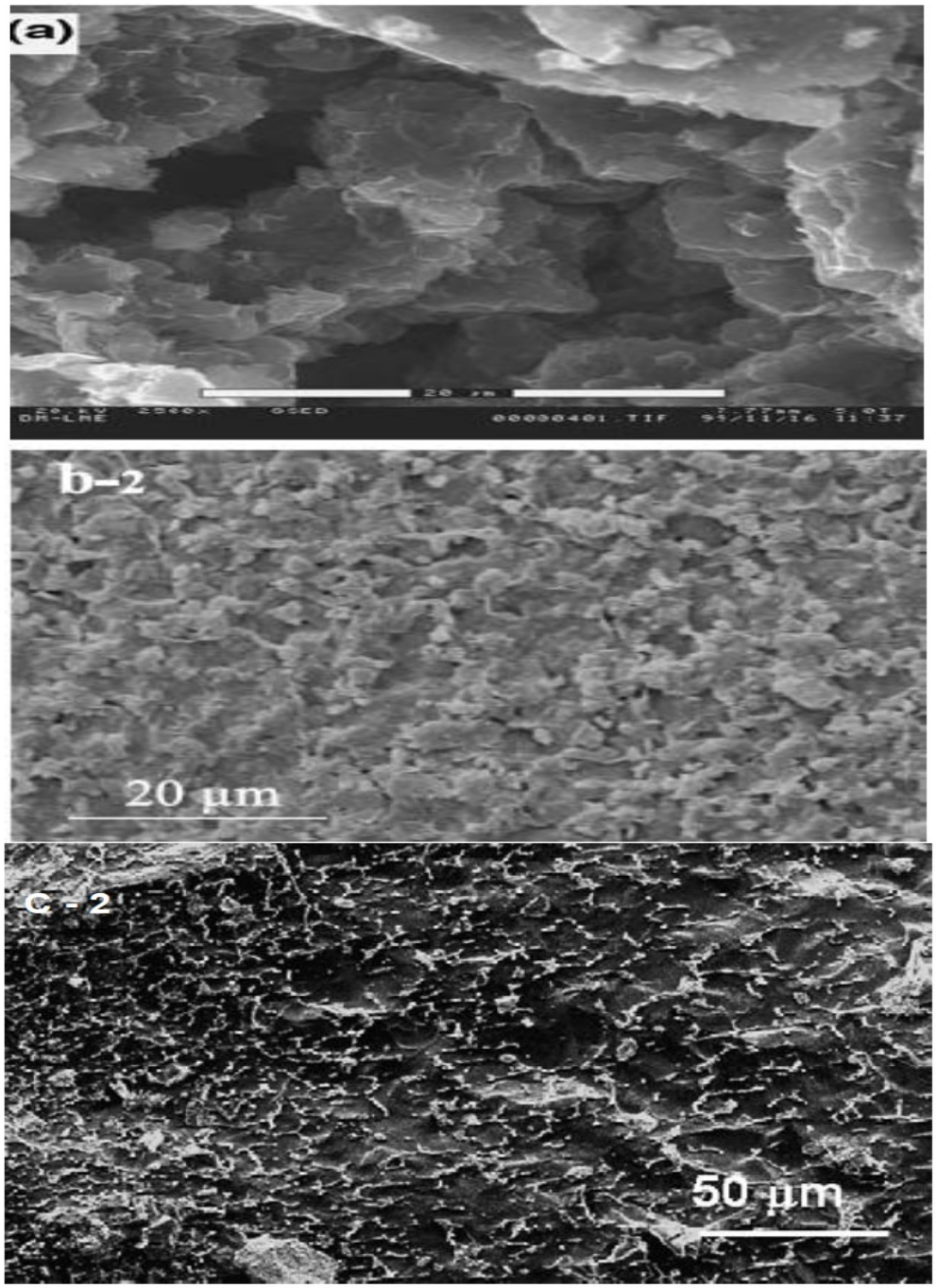

Figure 10-11: Scanning electron micrographs of various soils (a- FEBEX bentonite; ESEM (Romero and Simms 2008); b – 2- smectite suspension, SEM (Negre et al. 2004); c – 2 kaolinite suspension, SEM (Zbik et al. 2008)

Figure 10 – 12 shows backscattered ESEM micrographs for the comparative qualitative comparison of microstructure of oil sands tailings for various scenarios. All the images were captured at a magnification of 0.5 kx, with a scale of 50 μm and a view field of 300 μm. The micrographs showed that the tailings showed different structural and geometric configurations for various doses one hour after polymer mixing (Figure 10 – 12, left). The fabric of tailings appeared over flocculated for 4000 ppm. However, for 1000 ppm, the tailings provided larger regular aggregation in comparison to 500 ppm.

Similarly for a particular polymer dose, the tailings fabric changed with a successive increase in degree of desiccation or consolidation (Figure 10 – 12, right), and consequently, the successive increase in degree of desiccation resulted in more packed fabric. Furthermore, an increase in degree of desiccation resulted in a change in the cracks pattern (length and width) of tailings, and the appearance of flocs eliminated or minimized with a successive increase in degree of desiccation (Figure 10 – 12). Like that of degree of desiccation, the tailings fabric appeared different for change in depth while they were examined for various depths in a lift (Figure 10 –13). As in Figure 10 – 13 (A), the SEM micrographs showed some sort of fine cracks due to the prevalence of desiccation at the top of the lift; however, the fabric appeared more flocculated at the middle and bottom depths (Figure 10 -13 (B, C) of the lift due to higher water contents. Similarly as in Figure 10 – 14, the fabric looked different, both for unconsolidated and consolidated tailings.

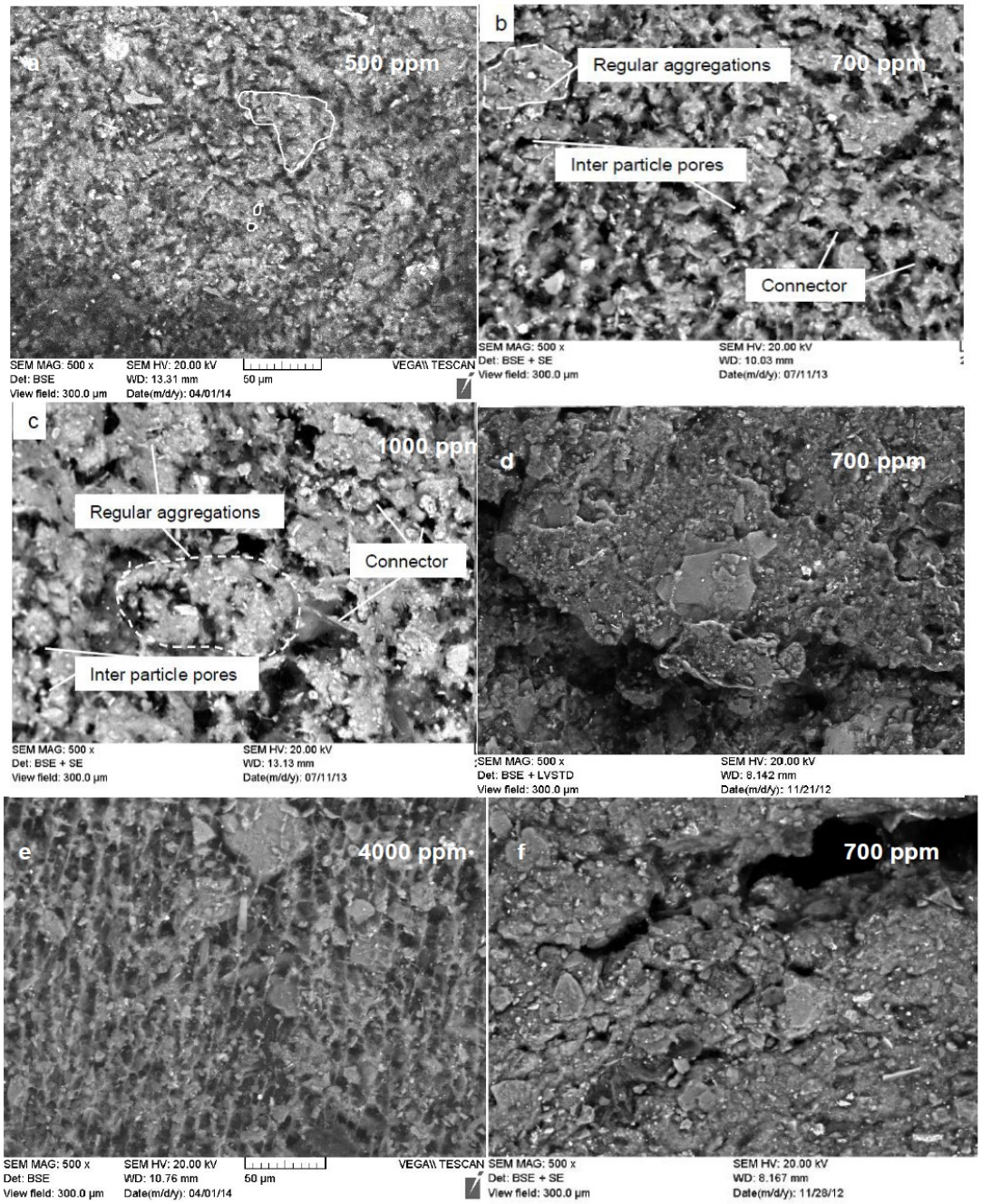

Figure 10-12: SEM micrographs of oil sands tailings (Left: a – 500 ppm (01 hr): c – 700 ppm (01 hr): e – 1000 ppm (01hr), Right: b – 700 ppm (one hour): d – 700 ppm (06 days): f – 700 ppm (17 days)

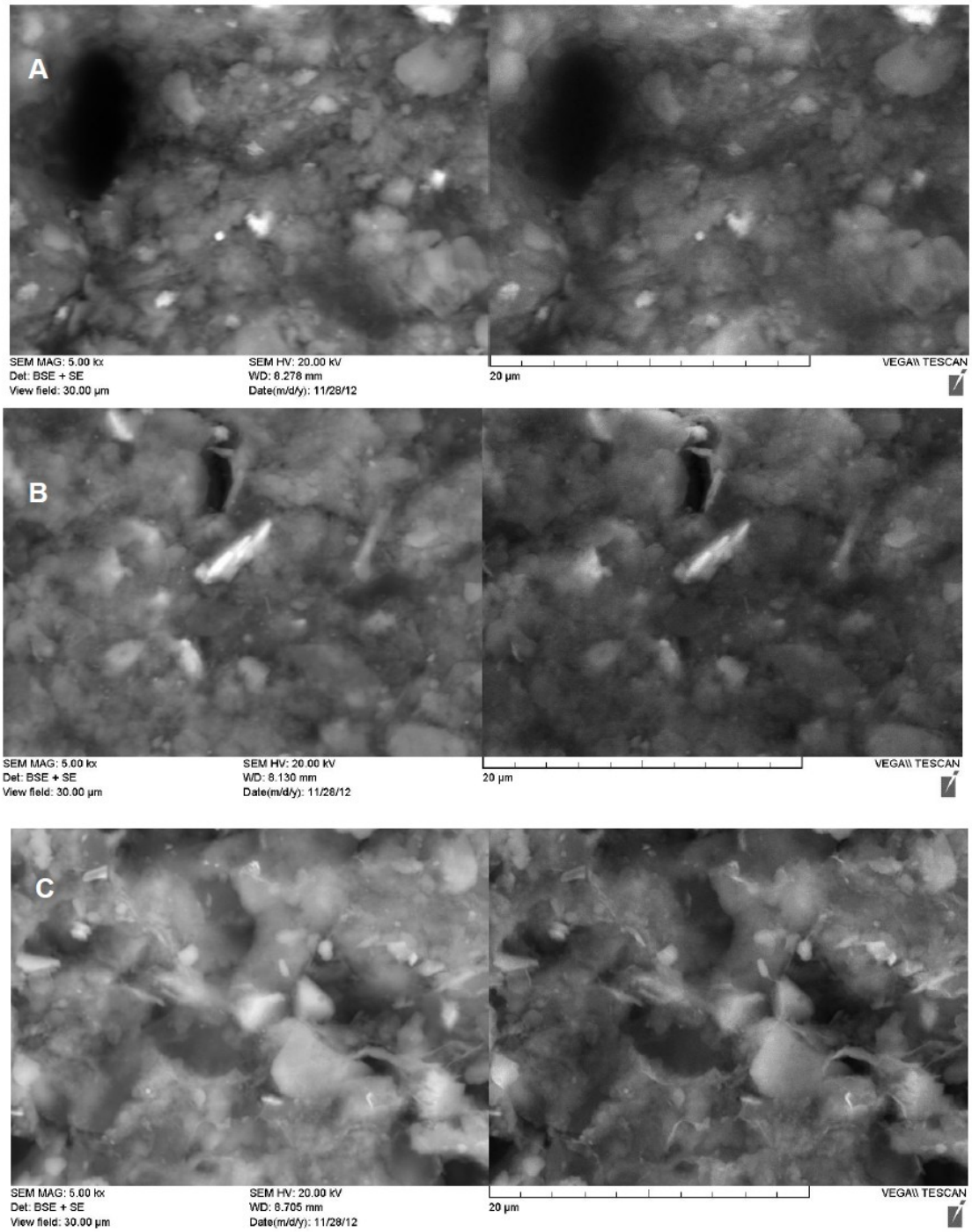

Figure 10-13: SEM micrographs of oil sands tailings for 700 ppm (A – Top depth, B – Middle depth, C – Bottom depth; Left – BSE, Right – SE

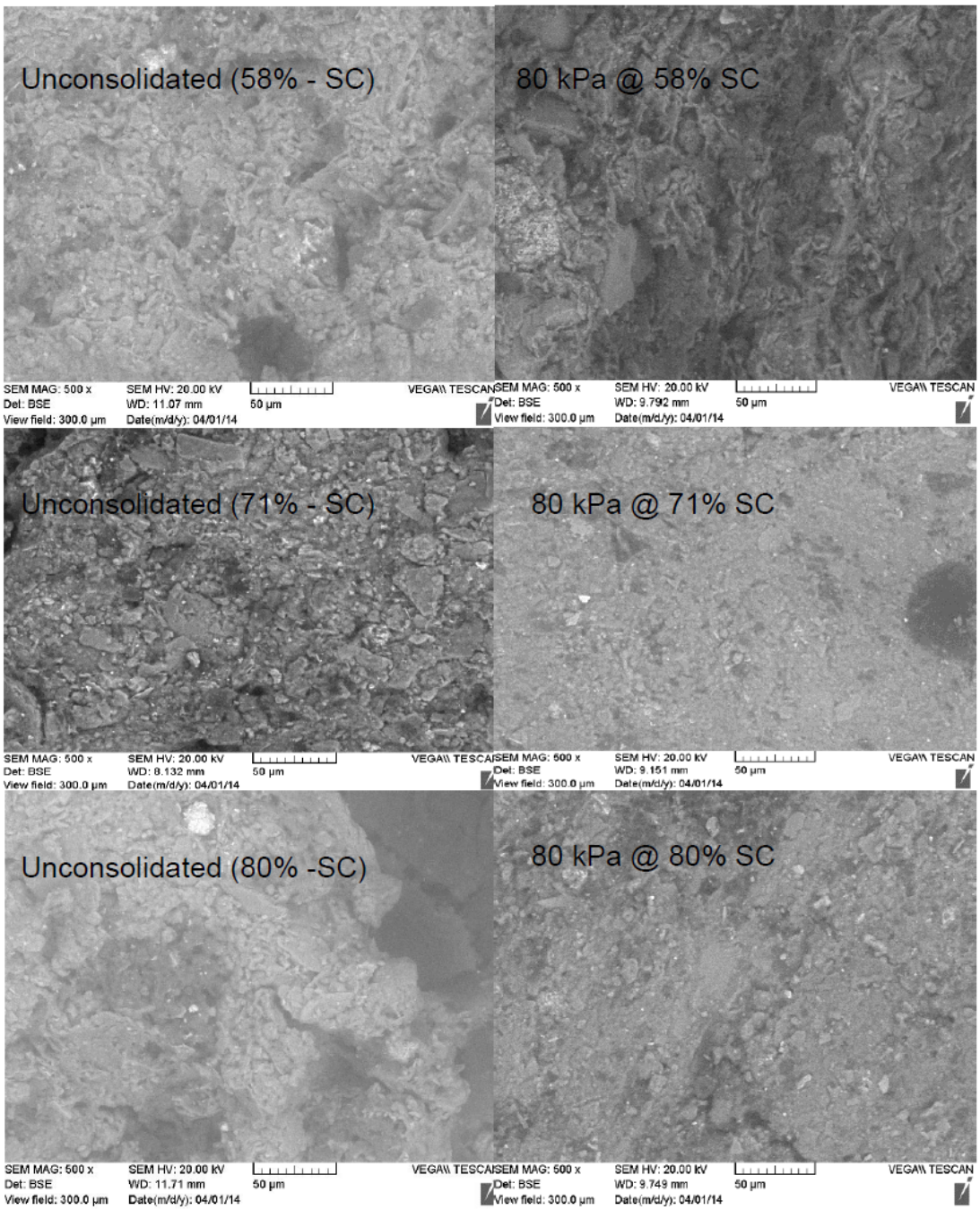

Figure 10-14: SEM micrographs of oil sands tailings for 700 ppm (Left – Unconsolidated, Right – Consolidated)

The consolidated tailings provided quite compacted fabric in comparison to unconsolidated tailings. As a comparison to MIP test data (Figure 10 – 1), the SEM micrographs for 71 and 80% solids content looked similar to each other showing minor difference in fabric. It has recently become possible using advanced image analysis software to examine aggregated porosity of SEM micrographs. Zbik et al. (2008) simulated the porosity of flocculated kaolinite sample of digitized images using STIMAN software, and the micrograph of 0.5 kx magnification was used in the analysis.

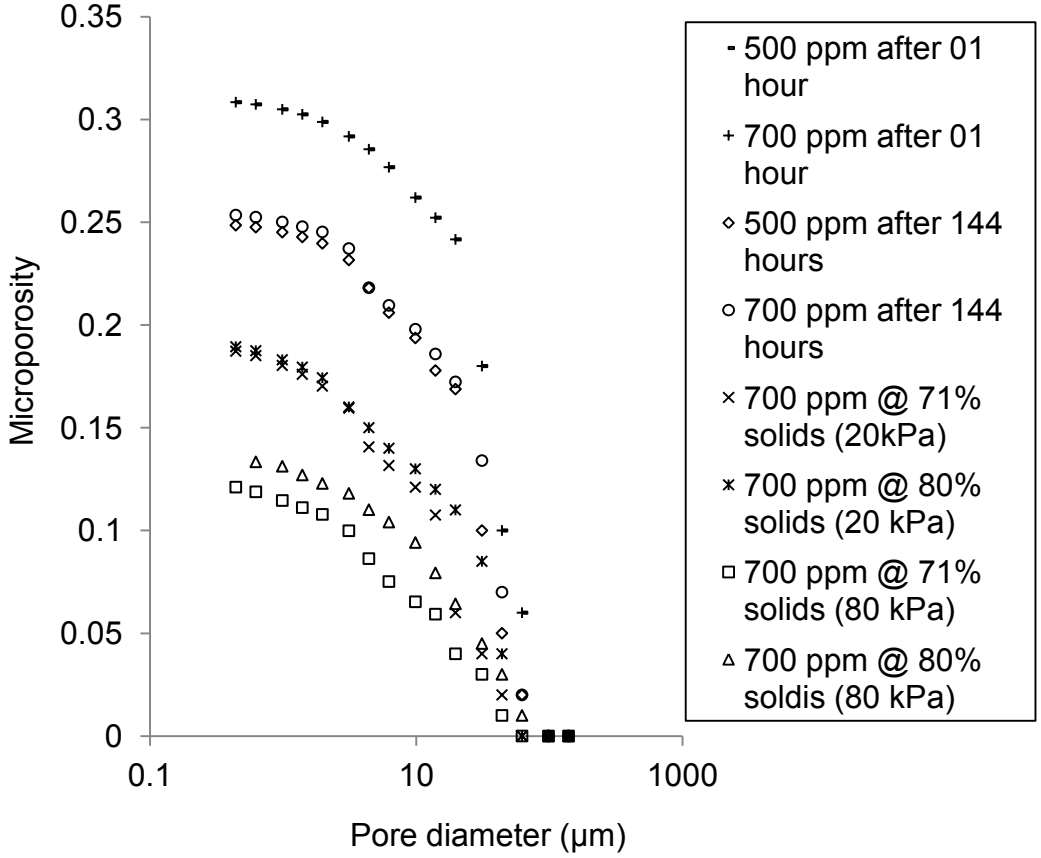

Figure 10-15: Comparative quantitative SEM micrographs data

Abell et al. (1999) examined the digital micrographs of Portland cement mortar on a Macintosh using the public domain NIH image program and disused that the mixture gave cumulative volume fraction of 0.15 and 0.13 for 0.4 and 0.6 w/c ratio. The microporosity of oil sands tailings was tested performing ImageJ analysis of SEM micrographs. Figure 10 – 15 shows the quantitative measurements of SEM micrographs.

The comparison of test results of oil sands tailings as in Figure 10 -15 showed that the microporosity of tailings decreased for desiccation and subsequent consolidation. The tailings for 700 ppm polymer dose provided microporosity of 0.31 and 0.25 respectively after 01 and 144 hours of tailings deposition. Similarly, for polymer doses of 500 and 700 ppm, the porosity did not differ too much after 01 and 144 hours. After 144 hours of tailings deposition, both 500 and 700 ppm drained off almost same quantity of water, which resulted in their comparable porosity values. The porosity of tailings reduced with an increase in stress level, and a polymer dose of 700 ppm provided high porosity values at a stress level of 20 kPa than that of 80 kPa. Similarly, the tailings did not show any difference in porosity values at 80 kPa for 71 and 80% initial solids content respectively.

The desiccation, subsequent consolidation and stress level resulted in a decrease in microporosity of tailings (Figure 10 – 15), and these results were comparable to cumulative intrusions of tailings as discussed in Figure 10 – 1 of MIP test data.

10.3.3 Comparison of MIP and SEM data

The test data presented in Figure 10 – 16 showed that a few differences were noted while comparing MIP, ESEM and SEM data sets.

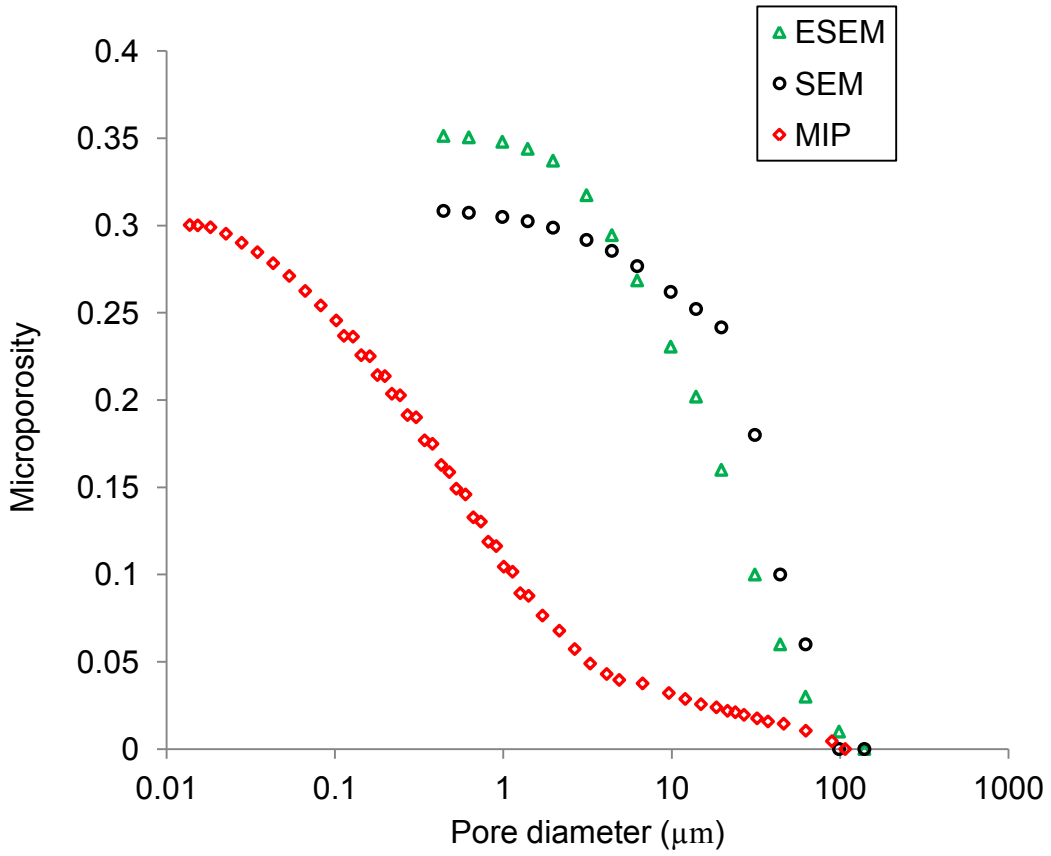

Figure 10-16: Comparison of microstructure data for 700 ppm 01 hour after polymer mixing

MIP simulated pores of smaller diameter in comparison to ESEM and SEM. Abell et al. (1999) reported the findings of Lange et al. (1994) and discussed that the shapes of the pore size distributions curves of SEM micrographs looked almost

similar to the MIP data set, but the image analysis provided pore sizes three orders of magnitude larger than MIP. However, SEM and ESEM porosity curves overlapped to each other (Figure 10 – 16). Figs 10 – 17 to 10 – 19 show comparative evaluation of both microstructure and macroscopic test data.

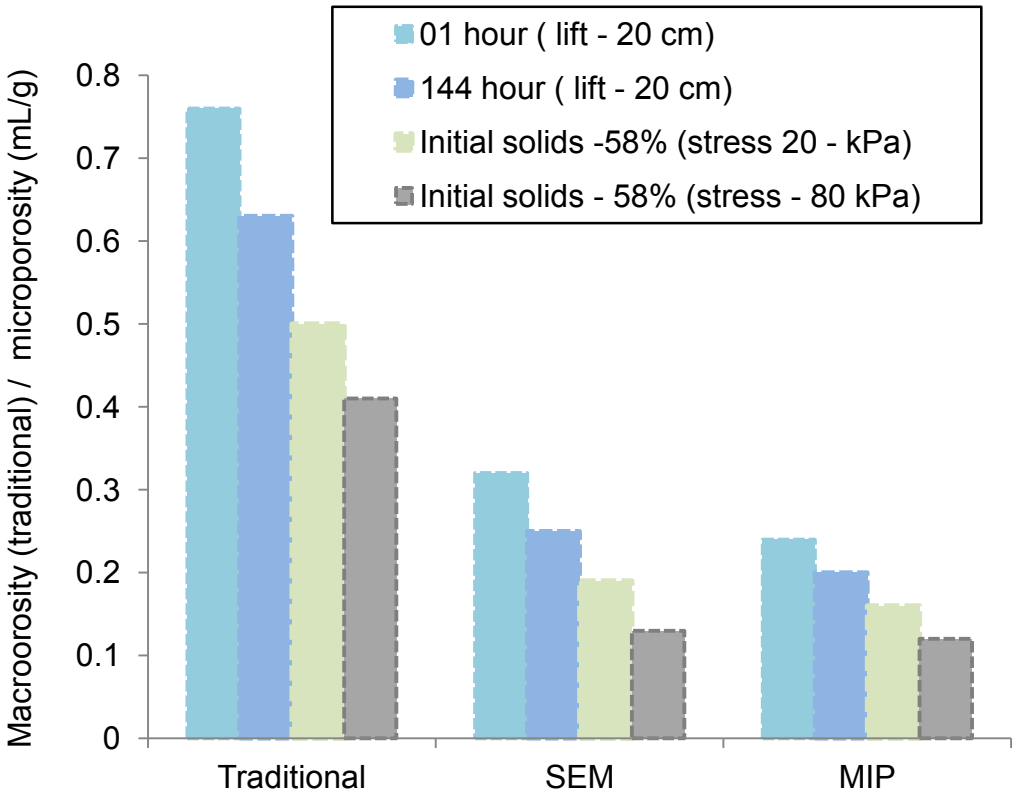

Figure 10-17: Comparison of actual porosity to SEM and MIP microporosity for specimen with 700 ppm dose

As in Figure 10 - 17, the MIP data and ImageJ analysis provided less microporosity in comparison to actual porosity of oil sands fine tailings. Similarly, as in Figure 10 – 18, various microstructure techniques such as SEM, ESEM and

MIP gave almost same microporosity 01 hour after polymer mixing, but as in Figure 10 – 19, the SEM curve fell above MIP curve showing higher microporosity, but the microporosity curves converged towards lower actual porosity, and consequently at a porosity of 0.4 (actual), both curves overlapped to each other. As the larger pores disappeared, both techniques showed good agreement in simulating the microporosity.

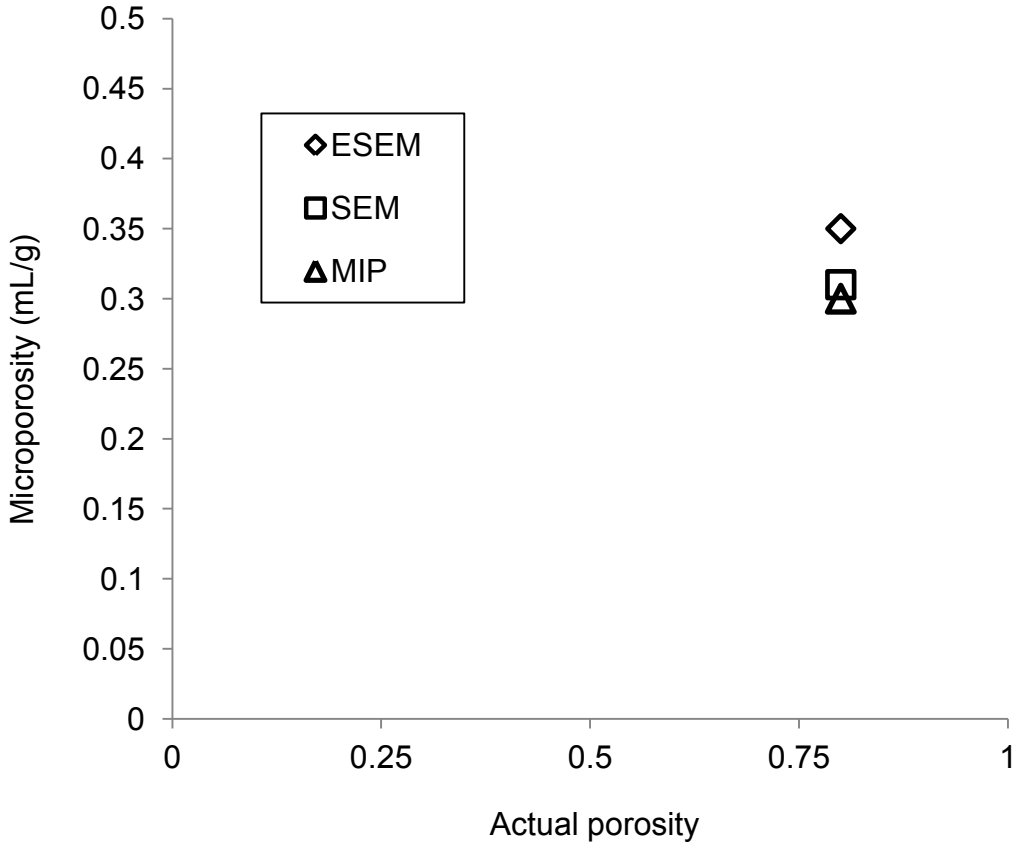

Figure 10-18: Variations in microporosity to actual porosity of tailings for 700 ppm 01 hour after polymer mixing

MIP gives a measure of pore opening rather than body sizes, and it relies on dynamic accessibility of pores to the incoming fluid. Imaging techniques are subject to some entirely different influences such as the chance and subjectivity involve in assessing pore bodies and openings.

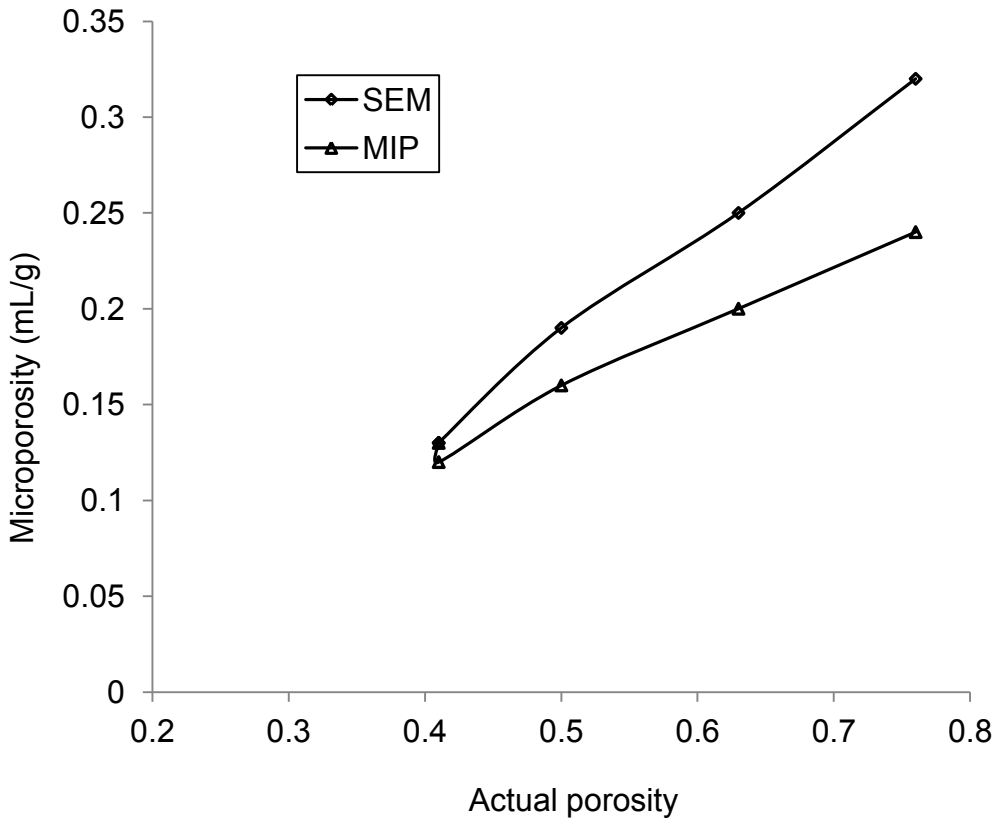

Figure 10-19: Variations in microporosity to actual porosity of tailings for 700 ppm

10.3.4 Repeatability and accuracy of microstructure test data

As in Figure 10 – 20, the imageJ analysis showed minor difference in data sets while comparing various ESEM micrographs taken at various spots of a particular

sample, and these images provided higher chances of repeatability. The data points of these tailings appeared overlapped to each other.

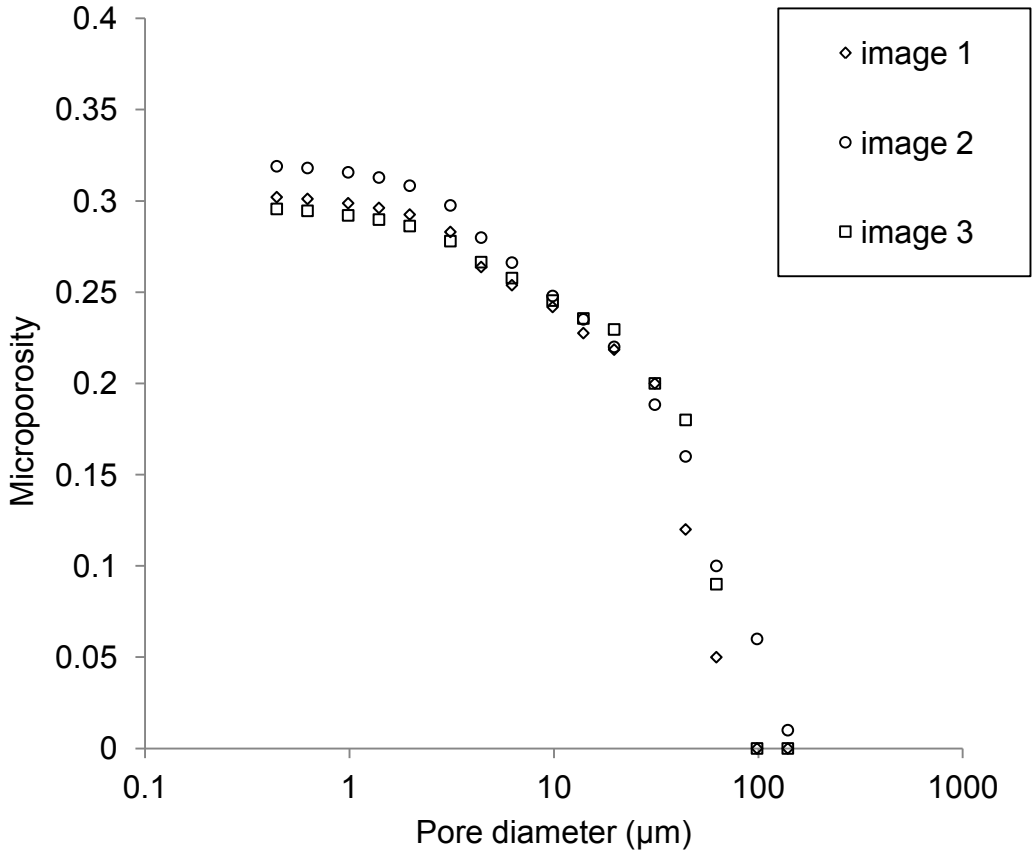

Figure 10-20: Image analysis of ESEM images captured at various locations of a particular sample

ESEM micrographs used in image analysis of Figure 10 - 20 are presented in Appendix 5. All images were captured at a magnification of 0.5 kx with a view field of 300 µm (Appendix 5).

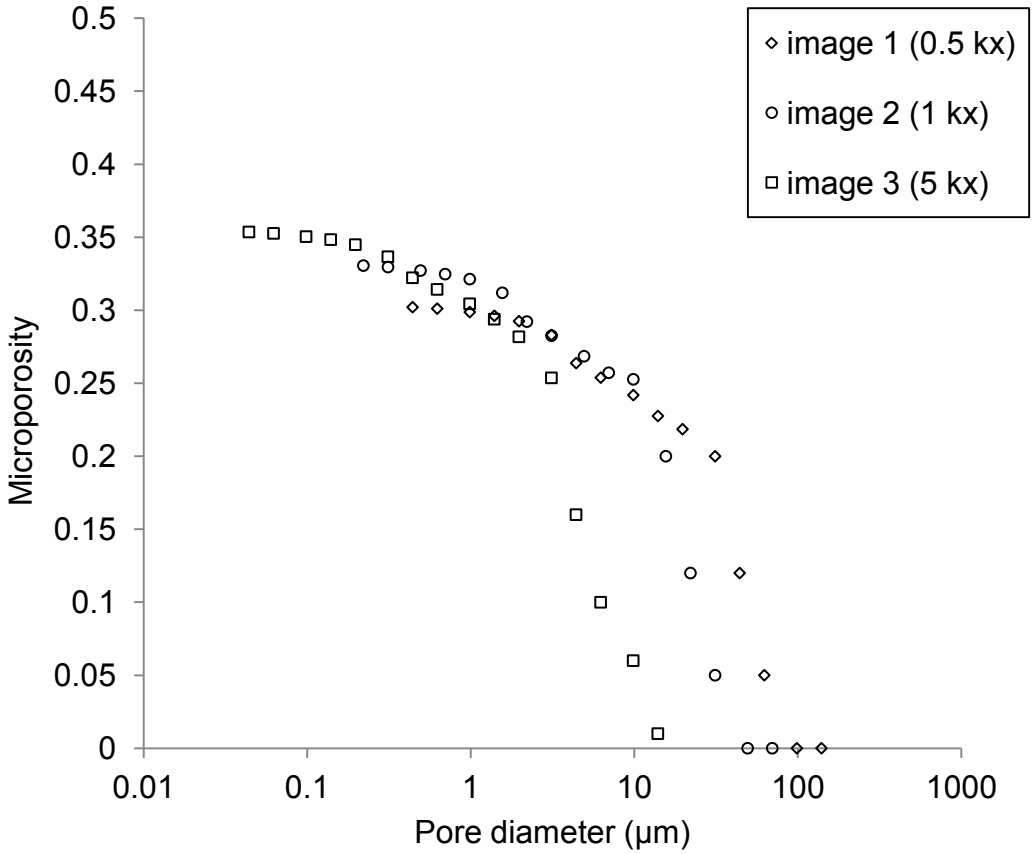

Figure 10-21: Image analysis of ESEM images of various magnifications for a particular sample of polymer amended tailings

The image analysis provided some difference towards larger diameter while analyzing a particular sample of polymer amended tailings for various magnifications as shown in Figure 10 – 21. Each image was captured at different magnification and view field as well (Appendix 6).

As in Figure 10 – 21, the frequency of smaller pores diameter increased with an increase in magnification, and the data points for all magnifications overlapped to each other showing more chances of repeatability but for larger pores diameter,

the chances of repeatability were less. The data points shifted towards smaller diameter for an increase in magnifications. ESEM micrographs for various magnifications used in image analysis of Figure 10 - 21 are presented in Appendix 6. Generally, ImageJ analysis showed larger consistency in repeatability for various images of particular sample taken at various spots than that of particular image with various magnifications.

As in Figure 10 – 20, cumulative microporosity of various images varied ± 0.05 for the pores diameter ranging from 0.4 - 5 μm giving minor or no difference in pores diameter. The data points for all images overlapped to each other for pores diameter ranging from 5 to 15 μm giving almost 100% repeatability, and for larger pores diameter (15 – 100 μm), the data points showed quite larger variations in pores diameter. Similarly as in Figure 6 – 21, the difference in pores diameter was quite larger for large pores diameter ranging from 4 to 100 μm, and data points overlapped to each other for pores diameter ranging from 0.3 to 4 μm, again showing higher probability of repeatability. Furthermore, the ImageJ software simulated the smallest pores less than 0.1 μm at higher magnification, and those were not visible at 0.5 and 1 kx magnifications.

The results showed that there was more probability of error for larger pores diameter during repetition of image analysis of a particular sample. Furthermore a variation in magnification also influenced the image analysis as the ImageJ software only simulated the smallest pores at higher magnification.

10.4 Implications of applied microstructure approaches to oil sands fine tailings

MIP and SEM appeared to be effective to measure the fabric of polymer amended oil sands MFT, but still several implications were noted while using these approaches in oil sands tailings. The oil sands MFT was consisted of 3 ~ 4 % residual bitumen and sometimes it appeared sometimes difficult to properly visualize the qualitative behaviour of scanning electron micrographs as a layer of bitumen extended over the solid particles of tailings. Similar observations were noted while examining the quantitative measurements of MFT using ImageJ software and sometimes the optimization of adjusting the threshold proved quite difficult as the tailings did not provide clear distinction between pores, bitumen and solids content. Furthermore, there was possibility to predict pores accurately while analyzing a particular image for different magnifications.

The irregular flocs formation especially at higher water content also affected the results of image analysis. It was more practical to simulate the behaviour of tailings for higher water content because the oil sand industry was more likely interested to get 5 kPa as per ERCB Directive 074 (2009) after one year of tailings deposition. ESEM provided surface images of hydrated samples generating high vacuum conditions in the chamber, so the chances of the collapse of the structure were more likely on higher side due to softness of the specimens. The collection of too wet tailings using a small mold of 1 cm^3 also disturbed the integrity of samples. Sorgi et al. (2008) stated that the sample

preparation contributed a significant part on the accuracy of SEM tested specimens. The freeze drying method preserved the microstrcuture with small changes in volume, but still the immature samples preparation influenced the integrity of initial microstructure during the dehydration process of tailings. For MIP, the ink bottle effect also affects the pore size distribution of tailing, as is well known in the literature (ASTM D4404 - 10; Zhou et al. 2010). The mercury was intruded into the dehydrated sample at high pressure, which may also disturb the physical configuration of tailings fabric

10.5 Conclusions

The comparative evaluation of MIP and SEM data showed that these techniques were able to detect changes in fabric due to differences in polymer dose, and were also able to track how the fabric of oil sands fine tailings changes under consolidation and desiccation in a similar fashion to that of other materials such as Halton till and kaolinite suspensions etc. A few differences were noted while comparing MIP and SEM data. As observed in the literature, the MIP method provided pores of smaller diameter in comparison to SEM method. The SEM micrographs coated with gold palladium provided better quality images in comparison to uncoated and naturally hydrated specimens. Repeatability of image analysis of SEM pictures was quite good in terms of total microporosity (+/- 0.05), though some variation was noted for differential porosity for the largest pores.

The differential PSD showed that the pores mode of differential curves shifted towards pores of smaller diameters for an increase in degree of desiccation and for each incremental stress level; consequently providing larger number of pores of smaller diameters. The bimodal PSD was dominant in all tailings. The tailings showed minor differences in pore size distribution beyond a certain thresholds of stress level and degree of desiccation, and the diameter of peak pore mode decreased for an increase in degree of desiccation, self weight consolidation and stress level.

Chapter 11. Summary of conclusions and recommendations

11.1 Summary of work

The scope of study was set to examine the microstructure and macroscopic behaviour of tailings for extensive range of polymer doses (500 – 4000 ppm). The SFR, LI, yield stress and microstructure of tailings were examined for this wide range of polymer doses during the very early stages of tailings deposition, i.e., 01 hour after polymer mixing. The tailings for polymer doses of 500 to 1500 ppm provided favorable results taken into account their consistency (LI), grain size distribution (SFR), slump (yield stress) and ESEM micrographs (fabric). The apparent difference in tailings fabric (size and regularity of flocs) for various doses resulted in significant variation in dewatering potential. An optimal dose for SFR and LL was 800 ppm, and the highest yield stress was at 700 ppm.

In next stage, the scope of study was limited to 500, 700, 1000 and 1500 ppm polymer doses, and the yield stress and microstrcuture of all tailings were monitored for successive release of water up to 06 days. The polymer doses of 1000 and 1500 ppm showed quite low dewatering in comparison to 500 and 700 ppm. The important observation at this point was that, though the dewatering potential of 500 and 700 ppm was quite competitive but 700 ppm provided quite high drain off potential 01 and 24 hours after tailings deposition, which consequently enabled these tailings to provide stabilized and compacted slumps, and therefore higher yield stress. The 500 and 700 ppm tailings showed smaller

and regular flocs, while the other higher doses exhibited larger flocs with irregular structure. The smaller and regular flocs may explain the improved dewatering behaviour.

In next stage, the scope of study was limited to three polymer doses: 700, 1000 and 1500 ppm. The tailings for 700 and 1000 ppm polymer doses showed the highest and almost the same strength when desiccated in columns up to 16 days in a lift of 30 cm. It was noted that cracks development was clearly seen in the fabric of all tailings at the top few cm..

Until, this point, the test results showed that 700 ppm was the best polymer dose when examined for sedimentation, self weight consolidation and desiccation; furthermore dewatering and desiccation contributed greatly to the strength of tailings. The 1500 ppm sample showed a slightly lower SL, but this did not appear to affect the consolidation and desiccation behaviour. Moreover, at high void ratio (early dewatering), 1500 ppm was somewhat stronger.

In next step, the scope of study was limited to one polymer dose, i.e., 700 ppm, and the tailings were examined in thick lift of 82 cm. During thick lift deposition, the self weight consolidation contributed largely to strength of the tailings at the middle layer and near the bottom of the lift. The influence of desiccation was quite apparent at the top of the lift as demonstrated by cracking but strengths at depth showed strong correlations with void ratio, and due to the absence of matric suction confirmed that this strength developed due to self-weight

consolidation. MIP data and ImageJ analysis of SEM images showed that the tailings shifted towards pores of smaller diameter over time for all depths, including the peak pore diameter. The consolidated samples in the thick lift retained a more flocculated structure at given water content than in the desiccated thin lift samples. This correlated with the thick lifts exhibiting a higher strength at a given void ratio than the thin lifts.

In next step of research program, the tailings were desiccated in columns to certain initial solids contents and then consolidated in an oedometer cell for various stress levels. The test results showed that the tailings hydraulic and void ratio curves converged for an increase in stress level; however, the polymer amended tailings provided comparable but high hydraulic conductivity when compared with test data from the literature of ILTT, CT and unamneded MFT as reported in a few other studies under similar loading conditions. The tailings provided major differences in microstructure for an increase in degree of desiccation and stress level as well. The test results showed that there was no efficacy to desiccate the tailings beyond a certain degree of initial solids content.

Finally, the microstructure test data of research program was comparatively evaluated, which apparently showed that the peak of the pores mode converged for release of water during short term dewatering, and the fabric of tailings was quite different for various degree of desiccation, consolidation and stress levels. However, at higher stress level, the peak pore modes for various initial solids content converged giving minimal difference in fabric, which apparently showed

that the hydraulic conductivity curves of all tailings converged to same data point beyond a certain degree of stress level. Annexures 1 to 6 present the summarized microstrcuture and macroscopic test results of the research program.

The specific conclusions of research program are as follows:

11.1.1 Conclusions:

- The addition of polymer did not largely influence the pore water chemistry of tailings, however, it lowered the metal ingredients; raised the alkalinity and the change in concentration of nutrients was minimal.
- The tailings for polymer doses of 700, 1000 and 1500 ppm provided more favorable results considering LL and SFR when compared to a range of polymer doses from 500 to 4000 ppm. SFR and LL of unamended MFT were quite low in comparison to polymer amended tailings. LL and SFR peaked at 800 ppm.
- The lower polymer doses (500 and 700 ppm) provided higher dewatering potential in comparison to higher doses. This was attributed to differences in self-weight consolidation. The polymer dose of 700 ppm showed higher dewatering than that of other doses 1 hour after polymer mixing both in 10 cm and 20 cm lifts.
- Strength, as measured by slump and vanes tests, was generally correlated with water content. However, the strength of polymer amended

tailings was substantially greater than unamended MFT at particular water content. Under drying conditions, the 1000 ppm doses gave somewhat higher strength at a given water content than that of other doses. At higher water content, higher yield stress was measured for higher polymer doses for given water content or void ratio.

- Osmotic suction was a major contributor to total suction measured in the tailings.
- Despite a clear difference in flocs formation, the tailings followed the same void ratio -hydraulic conductivity function for various polymer doses during self-weight consolidation, and the polymer amended tailings showed higher hydraulic conductivity in comparison to other materials, including unamended MFT.
- The hydraulic conductivity curves of tailings desiccated to various initial solids content and then loaded in an oedometer cell converged to each other beyond a certain threshold of stress level.
- Evaporation behaviour and associated hydro-geotechnical characteristics (SWCC, shrinkage curve) were very similar for different polymer doses (700, 100, 1500 ppm), except a slightly higher shrinkage limit for the 1500 ppm sample.
- The undrained shear strength of tailings increased with an increase in percent solids due to dewatering, desiccation and consolidation. In thick lift (~80 cm) deposition, the tailings showed higher strength at centre and near the bottom of thick lift over time. In thin lifts (~30 cm) however, the

strength of tailings enhanced largely due to prevalence of desiccation. Generally, the desiccation controlled the tailings strength in thin lift and the self weight consolidation dominated the strength at centre and near the bottom of thick lift.

- The tailings provided smooth and regular aggregation for a specified range of polymer doses (500 – 1000 ppm) during earlier stage of deposition. The fabric appeared over flocculated for too high (4000 ppm) polymer dose, however, the influence of flocs appeared to minimize or disappear with an increase in dewatering, degree of desiccation and stress level.
- MIP tests showed major differences between different polymer doses at 1 hour, furthermore 500 and 700 ppm samples showed larger peak pore diameters as compared to other doses. However, differences between doses tended to converge after self-weight consolidation and desiccation. MIP tests showed stress history effects in that desiccation and consolidation changed the shape of the PSD in different manners. The kind of changes due to desiccation and consolidation were similar to what was observed in compacted clays. PSDs of samples with different stress histories all converged to a similar PSD when the samples were consolidated to 80 kPa.
- Image analysis of SEM tests showed general agreement with MIP in terms of the trend in overall volume change. SEM, as reported in other studies

showed PSDs of higher average pore diameter, and the smaller pores were also not detected in the these studies.

- SEM with gold palladium coating provided better quality images compared to ESEM and SEM without gold coating. However, ESEM samples for high water content samples of oil sands tailings (in this study, 1 hour after dewatering) were still desirable, as very wet SEM samples might still experience volume change even under rapid freeze-drying. Image analyses on both ESEM and SEM showed slightly higher porosity for ESEM samples
- As a comparison to unamneded MFT, the polymer amended tailings showed entirely different nature providing major differences in SFR, LI, PL, LL, strength and hydraulic conductivity. These differences were clearly noted while comparing SEM micrographs and MIP test data of both unamended and polymer amended tailings.
- A few issues that might affect accuracy of microfabric measurements were identified, such as softness of tested specimens at higher water content, and the presence of bitumen.
- In practical terms, the polymer dose of 700 ppm appeared to perform well taken into account its dewatering potential, consistency, volume change, strength and fabric. In addition to this, there was no efficacy to desiccate the tailings beyond a certain degree of initial solids content.

11.2 Recommendations:

- The best aspect of this study involved investigating the interaction between micro and macro scale features of polymer amended oil sands tailings integrating various mechanisms of practical interest like drain off potential, desiccation, self weight consolidation and burial effects. However the laboratory results need to be confirmed with field measurements of microstructure. These measurements might also help to understand field scale effects on dewatering performance. The data in thick lift and thin lift simulations should be modeled using large strain consolidation software. Such an exercise might verify consolidation characteristics to be used to evaluate possible field scenarios.
- The fabric data set could be analyzed and used to improve a pore-network model such as constructed in Simms and Yanful (2005). This might lead to improve constitutive relationships integrating consolidation and desiccation, which in turn would help optimizing field deposition scenarios.
- Further work should also investigate how fabric changes in tailings over wetting and drying cycles to simulate behaviour of tailings for changing field conditions.
- Similarly, fabric investigation may be useful to characterize thixotropic behaviour of polymer amended tailings.
- For microstructure analysis, freeze drying method was preferred for preconditioning of samples and a sample of 8 ~ 10 mm^3 size was used based on the arguments of few previously conducted studies with some

other materials. The research findings suggest using the sample as thin as possible to reduce the probability of change in volume during freeze drying of specimen.

- ImageJ software still needs more investigations and modifications to simulate the gray value (black and white shades) of polymer amended oil sands fine tailings as the presence of bitumen and flocs formation may mislead to gray values

11.3 Recommendations for industry

- The influence of polymer dose occurred to be mostly in the self-weight consolidation behaviour. After self-weight consolidation, the influence of different polymer doses on subsequent desiccation and then further consolidation was not significant. Therefore, optimizing polymer dose for self-weight consolidation behaviour would be sufficient to maximize dewatering. It should be noted that the optimal point for maximum yield stress can be different from the optimal point for dewatering.
- When buried by new tailings or other surcharge, desiccated samples were initially stiffer, but then converged to the same void ratio – effective stress curve when they were consolidated. The polymer amended tailings still gave higher hydraulic conductivity at a given void ratio when compared to unamended MFT, even after desiccation and consolidation.

Annexure 1: Summary of test results - Chapter 04

Chapter 04																										
Experimental scheme		Lift	Mechanisms	Lift depth from top	Time (days)	Initial Cs (%)	Stress level (kPa)	Polymer dose	Macroscopic features															Microstrcuture		
									Liquidity index	Sand to fine ratio	Specific gravity	Water content	Percent solids	Evaporation	Dewatering	Void ratio	Suction			Hydraulic conductivity	Streng th		SEM		MI P
																	Total	Osmotic	Matric		Yield stress	Vane strength	Images	Porosity	Porosity
								ppm	-	-	-	%	%	mm	mm	-	kPa	kPa	kPa	cm/ sec	Pa	kPa	µm	%	%
Objective 1	LI and SFR	30 cm	Agglomerations and consistency					0	4.65	0.10	2.22														
								500	3.10	0.64	2.78														
								700	2.85	0.70	2.80														
								1000	2.55	1.17	2.78														
								1500	2.77	0.72	2.60														
								2000	3.23	0.72	2.52														
								3000	3.59	0.45	2.50														
								4000	3.59	0.40	2.50														

Annexure 2: Summary of test results – Chapter 05

Chapter 05																											
Experimental scheme		Lift	Mechanisms	Lift depth from top	Time (days)	Initial Cs (%)	Stress level (kPa)	Polymer dose	Macroscopic features															Microstrcuture		
									Liquidity index	Sand to fine ratio	Specific gravity	Water content	Percent solids	Evaporation	Dewatering	Void ratio	Suction			Hydraulic conductivity	Strength		Image analysis		MIP
																	Total	Osmotic	Matric		Yield stress	Vane strength	Images	Porosity	Porosity
								ppm	-	-		%	%	mm	mm	-	kPa	kPa	kPa	cm/sec	Pa	kPa	µm	%	%
Objective 2	One hour after polymer mixing	10 cm	Sedimentations + Flocculations		0.041			0				140	40	-	-	-	-	-	-	-	-	-	-	-	-
								500				129	44	0.5	2.09	3.58	280	157	122	4.32E-06	49		[6]	37	
								700				121	45	0.8	2.77	3.38	300	164	135	3.52E-06	68		[7]	35	
								1000				148	40	0.5	0.15	4.11	290	142	147	6.38E-06	33		-	43	
								1500				154	39	0.5	0.06	4.15	280	133	147	7.58E-06	30		[8]	44	
								2000				163	38	0.5	0.03	4.14	250	132	118	7.64E-06	4		-	-	
								3000				172	37	0.5	0.03	4.30	225	130	95	7.72E-06	2		-	-	
								4000				190	34	0.5	0.03	4.75	210	128	82	7.75E-06	2		[9]	51	

[6] Scattered and small aggregation
[7] Regular aggregation
[8] Irregular aggregation
[9] Over flocculated

Annexure 3: Summary of test results – Chapter 06

Chapter 06																											
Experimental scheme		Lift	Mechanisms	Lift depth from top	Time (days)	Initial Cs (%)	Stress level (kPa)	Polymer dose	Macroscopic features															Microstrcuture		
									Liquidity index	Sand to fine ratio	Specific gravity	Water content	Percent solids	Surface flux	Dewatering	Void ratio	Suction			Hydraulic conductivity	Strength		Image analysis		MIP
																	Total	Osmotic	Matric		Yield stress	Vane strength	Images	Porosity	Porosity
								ppm	-	-		%	%	mm	mm	-	kPa	kPa	kPa	cm/sec	Pa	kPa	µm	%	%
Objective 3	Short term dewatering	20 cm	Dewatering + initial short term consolidation	Average	0.041			500				143	41	4	2	3.33	280				42			33	30
					6							46	50	77	15	1.71	600			2.01E-07	185			24	58
					0.041			700				137	41	18	5	3.14	300				65			30	26
					6							59	49	81	13	1.71	650			1.37E-07	231			25	24
					0.041			1000				157	39	2	0.55	3.63	290				22			33	24
					6							88	44	58	5	2.34	420			3.52E-07	190			32	26
					0.041			1500				167	38	1	0	3.99	280				20			35	23
					6							99	42	55	4	2.95	410			7.58E-07	182			31	-

Annexure 4: Summary of test results - Chapter 07

Chapter 07																											
Experimental scheme		Lift	Mechanisms	Lift depth from top	Time (days)	Initial Cs (%)	Stress level (kPa)	Polymer dose	Macroscopic features															Microstrcuture		
									Liquidity index	Sand to fine ratio	Specific gravity	Water content	Percent solids	Evaporation	Dewatering	Void ratio	Suction			Hydraulic conductivity	Strength		Image analysis		MIP
																	Total	Osmotic	Matric		Yield stress	Vane strength	Images	Porosity	Porosity
								ppm	-	-		%	%	mm	mm	-	kPa	kPa	kPa	cm/sec	Pa	kPa	µm	%	%
Objective 4	Desiccation + consolidation	30 cm	Desiccation		1			700				107		2.5		3.64	410					0			
					5							92		30		2.68	500					1500			
					9							67		61		2.44	660					5000			
					12							62		68		2.26	710					7000			
					16							59		71		2.24	880					8000		28	21
					1			1000				129		2		3.66	350					0			
					5							86		30		2.69	600					2000			
					9							77		60		2.37	700					6000			
					12							66		67		2.21	800					9000			
					16							60		70		2.2	940					11000		26	21
					1			1500				130		2		3.82	330					0			
					5							100		25		3.09	510					600			
					9							82		52		2.91	640					3000			
					12							76		58		2.63	730					4500			
					16							70		63		2.6	780					5000		25	22

Annexure 5: Summary of test results – Chapter 08

Chapter 08																										
Experimental scheme		Lift	Mechanisms	Lift depth from top	Time (days)	Initial Cs (%)	Stress level (kPa)	Polymer dose	Macroscopic features															Microstrcuture		
									Liquidity index	Sand to fine ratio	Specific gravity	Water content	Percent solids	Cu. evaporation	Cu. dewatering	Void ratio	Suction			Hydraulic conductivity	Strength		Image analysis		MIP
																	Total	Osmotic	Matric		Yield stress	Vane strength	Images	Porosity	Porosity
								ppm	-	-		%	%	mm	mm	-	kPa	kPa	kPa	cm/sec	Pa	kPa	µm	%	%
Objective 5	Desiccation + consolidation	82 cm	Dewatering + Desiccation + self weight consolidation	Top (27 cm)	9			700				115	44	127	167	3.24	146	126	20			1750			33
					17							111	47			3.02	88	74	14			3000			32
					27							80	48			2.00	111	45	66			0			29
				Middle (47 cm)	9							120	45			3.30	80	125	0			1750			32
					17							109	48			3.13	78	68	10			4000			33
					27							100	54			2.77	70	50	20			7000			33
				Bottom (67 cm)	9							111	47			3.12	91	147	0			5000			33
					17							100	54			2.75	102	62	40			10000			33
					27							88	56			2.33	93	30	63			20000			33

Annexure 6: Summary of test results – Chapter 09

Chapter 09																											
Experimental scheme		Lift	Mechanisms	Lift depth from top	Time (days)	Initial Cs (%)	Stress level (kPa)	Polymer dose	Macroscopic features															Microstrcuture		
									Liquidity index	Sand to fine ratio	Specific gravity	Water content	Percent solids	Surface flux	Dewatering	Void ratio	Suction			Hydraulic conductivity	Strength		Image analysis		MIP
																	Total	Osmotic	Matric		Yield stress	Vane strength	Images	Porosity	Porosity
								ppm	-	-		%	%	mm	mm	-	kPa	kPa	kPa	cm/sec	Pa	kPa	µm	%	%
Objective 6	Desiccation + subsequent consolidation	30 cm	Consolidation (incremental stress)			58	0	700				72	58			2.6	40	20	20	-				25	22
							20					26	79			1	60	30	30	1.72E-07				19	20
							40					20	82			0.82	170	20	150	7.99E-08				16	17
							80					16	86			0.7	490	20	470	3.03E-08				15	14
						71	0					41	71			1.6	40	30	10	-				21	20
							20					24	80			0.71	100	20	80	8.11E-08				19	18
							40					22	82			0.69	190	20	170	5.04E-08				16	17
							80					17	85			0.52	630	20	610	2.07E-08				12	14
						80	0					24	80			1.6	150	30	120	-				21	20
							20					23	81			0.94	200	60	140	1.38E-07				19	19
							40					21	82			0.8	270	50	220	6.13E-08				17	1
							80					19	84			0.65	350	50	300	2.55E-08				13	15

Bibliography

Abedi-Koupai, J., and Mehdizadeh, H. 2007. Estimation of osmotic suction from electrical conductivity and water content measurements in unsaturated soils. *Geotechnical Testing Journal,* **31**(2)

Abell, A.B., Willis, K.L., and Lange, D.A., 1999. Mercury intrusion porosimetry and image analysis of cement based materials. *Journal of Colloid and Interface Science*, **211**(1): 39 - 44

Ahmed, S., Lovell, C.W., Diamond, S. 1974. Pore sizes and strength of compacted clay. *J Geotech Eng.,* **100**(4):407–425

Alberta Environment. 1999. Surface water quality guidelines for use in Alberta, Environment Assurance Division, November 1999.

Alberta Innovates, Energy and Environmental solutions. 2012. Oil sand tailings technology and deployment roadmap, Calgary, Alberta. Available from http://www.ai-ees.ca/

Alberta, Energy 2013. Alberta's leased oil sands area. Available from http://www.energy.alberta.ca/OilSands/pdfs/FactSheet_OilSands.pdf

AL-Zoubi, M.S. 2010. Consolidation analysis using the settlement rate-settlement (SRS) method. *Applied Clay Science*, **50**: 34 – 40

Asmussen, R.M. 2014. The Influence of microstructure on the corrosion of magnesium alloys. Ph.D. Thesis, Department of Civil and Environment Engineering, The University of Western Ontario, London, Ontario.

ASTM D2216 – 10. Standard test methods for laboratory determination of water (moisture) content of soil and rock by mass

ASTM D2435 / D2435 – 11. Standard test method for one dimensional properties of soils using incremental loading

ASTM D2573 - 08 Standard test method for field vane shear test in cohesive soil

ASTM D2974 - 07a. Standard test methods for moisture, ash and organic matter of peat and other organic soils

ASTM D422 – 63 (Reapproved 2007). Standard test method for particle size analysis of soils

ASTM D4318 – 10. Standard test methods for liquid limit, plastic limit, and plasticity index of soils

ASTM D4404 – 10. Standard test method for determination of pore volume and pore volume distribution of soil and rock by mercury intrusion porosimetry

ASTM D854 - 2000 Standard test for specific gravity of soil solids by water Pycnometer.

Bajwa, T.M. 2013. Athabasca oil sands deposit: A blessings or nuisance? http://www.mining.com/web/athabasca-oil-sands-a-blessing-or-nuisance/

Barbour, S.L. 1998. The soil-water characteristic curve: a historical perspective. *Can. J. Geotech.,* **35**(5): 873–894

Been, K., and Sills, G.C. 1981. Self weight consolidation of soft soils: an experimental and theoretical study. *Géotechnique*, **31**(4): 519-535

Beier, N., and Sego, D., 2008. The oil sands tailings research facility, Geo Interest; Geotechnical News, June 2008

Berilgen, S.A., Berilgen, M.M., and Ozaydin, I.K. 2006. Compression and permeability relationships in high water content clays. *Applied Clay Science*, **31**: 249–261

BGC Engineering Inc., 2010. Oil sands tailings technology review, oil sands research and information network, University of Alberta, School of Energy and the Environment, Edmonton, Alberta. OSRIN Report No. TR-1.

Biggs, S., Habgood, M., Graeme, J.J., and Yan, Y. 2000. Aggregate structures formed via a bridging flocculation mechanism. *Canadian Engineering Journal*, **80**(1-3): 13 – 22

Boger, D.V. 2006. Rheological concepts, In Paste and Thickened Tailings – A Guide. *Edited by Jewell R.J., and Fourier AB*., Broadway Nedlands: Australian Centre for Geomechanics.

Boger, D.V. 2013. Rheology of slurries and environmental impacts in the mining industry. *Chemical and Biomolecular Engineering*, **4**: 239 -– 257

Boratenec, D. 2003. Fundamentals of rapid dewatering of composite tailings, M.S.c. thesis, Department of Civil and Environmental Engineering, University of Alberta, Edmonton, AB.

Bothe, R., Dennis, J., Errington, J., Fahner, L., ……., and Straker, J. 2010. Shell proposed Jack Mine expansion and Pierre River Mine projects, environmental impact assessment and application review, Fort McKay Industry Relations Corporation, Alberta.

Cabalar, A. F. 2010. Applications of the oedometer, triaxial and resonant column tests to the study of micaceous sands. *Engineering Geology*, **112**: 21 – 28

Caldwell, J., Revington, A., and McPhail, G. 2014. Optimized seasonal deposition for successful management of treated mature fine tailings. In Proceedings of 17th International Seminar on Paste and Thickened Tailings, Vancouver., 8 - 12 June 2014., Joe Goodwill, InfoMine Inc: Australian Centre for Geomechanics.

Canadian Association of Petroleum Producer (CAPP), Canada's Oil and Gas Producers. Shrinking the tailings ponds: Newsletter

Carrier, W.D., III, Bromwell, L.G., and Somogyi, F. 1983. Design Capacity of Slurried Mineral Waste Ponds. *Journal of Geotechnical Engineering*, **109**(5): 699-716.

Caughill, D.L., Morgenstern, N.R., and Scott, J.D. 1993. Geotechnique of non segregating oil sand tailings. *Can. Geotech. J.,* **30**: 801- 81 1

Chalaturnyk, R.J., Scott, J.D., and Özüm B. 2002. Management of oil sands tailings. Petroleum Science and Technology, **20**: 1025-1046, DOI: 10.1081/LFT-120003695

Cuisinier, O., Auriol, J.C., Le Borgne T., and Deneele, D. 2011. Microstructure and hydraulic conductivity of a compacted lime-treated soil. *Engineering Geology*, **123:** 187 – 193.

Daliri, F., Kim, H., Simms, P., and Sivathayalan, S. 2014. Impact of desiccation on monotonic and cyclic shear strength of thickened gold tailings. *Journal of Geotechnical and Geoenvironmental Engineering,* **140**(9)

Danilatos, D.G. 1993. Introduction to the ESEM instrument. *Microscopy Research and Technology,* **25:** 354 – 371

Das, B.M. 2008. Advanced Soil Mechanics. Taylor and Francis Group, Madison Ave, New York

Delage, P. 2010. A microstructure approach to the sensitivity and compressibility of some Eastern Canada sensitive clays. *Geotechnique*, **60**(5): 353 – 368

Delage, P., Audiguier, M., Cui, Y.J., and Howatt, M.D. 1996. Microstructure of compacted silt. *Can Geotech J*., **33**:150 – 158

Delage, P., Marcial, D., Cui, Y.J. and Ruiz, X. 2006. Ageing effects in a compacted bentonite: a microstructure approach. *Geotechnique,* **56**(5): 291–304

Desbois, G., Urai, J.L., and de Bresser, J.H.P. 2012. Fluid distribution in grain boundaries of natural fine-grained rock salt deformed at low differential stress (Qom Kuh salt fountain, central Iran): implications for rheology and transport properties. *Journal of Structural Geology,* **43**: 128 – 143

Di Maio, Hueckels, T., and Loret, T. 2002. Chemo – Mechanical Coupling in Clays: From Nano – Scale to Engineering Applications. Swets & Zeitlinger B.V, Lisse, The Netherland.

Directive 074 (2009). Tailings performance criteria and requirements for oil sands mining schemes, Energy Resources Conservation Board (ERCB), Alberta

Doan, D.H., Delage, P., Nauroy, J.F., Tang, A.M, and Youssef, S. 2012. Microstructural characterization of Canadian oil. *Can. Geotech. Journal*, **49**

Du, J., Morris, G., Pushkarova, R. A., and Smart, R. St.C. 2010. Effect of surface structure of kaolinite on aggregation, settling rate, and bed density. *Langmuir,* **26**(16): 13227–13235

Dunmola, A., and Simms, P. 2010. Solute mass transport and atmospheric drying of high density gold tailings. In Proceedings of the 13th International Seminar on Paste and Thickened Tailings, Toronto, Ontario, 03 - 06 May 2010

Environmental, Defence 2008. The tar sands leaking legacy. Available from http://environmentaldefence.ca/reports/11-million-litres-day-tar-sands-leaking-legacy

Fall, M., Adrien, D., Celestin, J.C. Pokhrel, M., and Toure, M. 2009. Saturated hydraulic conductivity of cemented paste backfill. *Minerals Engineering,* **22**(15): 1307–1317

Fall, M., and Samb, S.S., 2009. Effect of high temperature on strength and microstrcuture properties of cement paste backfill. *Fire Safety Journal,* **44:** 642 – 651.

Fall, M., Celestin, J.C., and Han, F.S. 2010. Polymer modified paste fill for isolation of waste disposal sites. In Proceedings of the 13th International Seminar on Paste and Thickened Tailings, Toronto, Ontario, 03 - 06 May 2010.

Fard, M. A.H. 2011. Characterization of clay minerals in the Athabasca oil sands in water extraction and nonaqueous solvent extraction processes Ph.D. thesis. Department of Chemical and Materials Engineering, The University of Alberta, Edmonton, Alberta.

Farkish, A. and Fall, M. 2013. Rapid dewatering of oil sands mature fine tailings using super absorbent polymer (SAP). *Mineral Engineering*, **50**(51): 38 - 47

Ferreira, T., and Rasband, W. 2012. Image J/Fiji 1.46 User Guide, available from (http://imagej.nih.gov/ij/docs/guide/user-guide.pdf)

Fetter, C.W. 1994. Contaminated Hydrogeology, Wave land Press Inc., Illinois.

Fisseha, B., Bryan, R., and Simms, P. 2010. Evaporation, unsaturated flow, and salt accumulation in multilayer deposits of a paste gold tailings. *J. Geotech. Geoenviron. Eng.,* **136** (12), 1703-1712.

Fourier, A. B., and Gawu, S.K.Y., 2010. The validity of laboratory flume data for predicting beach slopes of thickened tailings deposits. In Proceedings of the 13th International Seminar on Paste and Thickened Tailings, Toronto, ON, 03 - 06 May 2010.

Fredlund, D.G. and Rahardjo, H. 1993. Soil Mechanics for Unsaturated Soil. John Wiley & Sons Inc., Hoboken. N.J.

Fredlund, D.G., and Xing, A. 1994. Equations for soil water characteristics curve. *Can. Geotech J.,* **31:** 521 - 532

Fredlund, M.D., Wilson, G.W., and Fredlund, D.G. 2002. Representation and estimation of the shrinkage curve. In Proceedings of the 3rd International Conference on Unsaturated Soils, Recife, Brazil, 10 – 13 March 2002

Fujiyasu, Y., Martin F.M., and Newson, T. 2000. Field investigation of evaporation from freshwater tailings. J. Geotech. Geoenvironment Eng., **126**: 556 - 567

Gagné, F., Douville, M., André, C., Debenest, T., Talbot, A., Sherry, J., Hewitt, L. M., Frank, R.A., McMaster, M.E., Parrott, J., and Bickerton, G. 2012. Differential changes in gene expression in rainbow trout hepatocytes exposed to extracts of oil sands process-affected water and the Athabasca River. *Comparative Biochemistry and Physiology*, **55** (2012): 551–559

Gawu, S.K.Y., and Fourie, A.B. 2004. Assessment of the modified slump test as a measure of the yield stress of high density thickened tailings. *Can. Geotech. J.,* **41**:39 – 47

Gieshe, H. 2006. Mercury intrusion porosimetry: a general practical overview, Part. Syst. Charac., 23: 1 - 11

Goodbille, F.D., and Moffett R.H. 2014. Modification of fluid fine tailing's rheological and stacking properties by in situ silica polymerisation. In Proceedings of the 17th International Seminar on Paste and Thickened Tailings, Vancouver. B.C., 8 - 12 June 2014

Government of Alberta, Canada. 2009. Environmental management of Alberta's oil sands. Available from http://environment.gov.ab.ca/info/library/8042.pdf

Griffiths, F.J., and Joshi, R.C. 1989. Change in pore size distribution due to consolidation of clays. *Geotechnique,* **39(**1): 159 -167

Guo,Y. 2012. Electrokinteic dewatering of oil sands tailings. M.E.Sc. thesis, Civil and Environmental Engineering, The University of Western Ontario, London, Ontario.

Hamza, H.A., Stanonik, H.A., and Kessica M.A. 1996. Flocculation of lime treated oil sands tailings. *Fuel,* **75**(3): 280 – 284

Heidarian, P. 2012. Effect of initial water content and stress history on water retention behaviour of mine tailings. M.A.Sc. thesis. Department of Civil and Environment Engineering, Carleton University, Ottawa, Ontario

Hein, F.J., Langenberg, C.W., Kidson, C., Berhane, H., and Berezniuk, T. 2001. A comprehensive field guide for facies characterization of the Athabasca oil sands Northern Alberta. Special Report 13, May 2001

Houlian, R.H., and Hale, C.E. 2011. Alberta mine reclamation and abandonment. In Proceedings of the Sixth International Conference on Mine Closure, Alberta, 18 – 21 September 2011

Houlian, R.H., Mian, M.H., and Lord, E.R. 2010. Oil sands tailings - technology development and regulations. In Proceedings of the 13th International Seminar on Paste and Thickened Tailings, Toronto, Ontario, 03 - 06 May 2010.

http://www.pembina.org/oil-sands/os101/alberta

Imai, G. 1979. Development of a new consolidation test procedure using seepage force. *Soils and Foundation*, **19**(3): 45-60

Innocent-Bernard, T. 2013. Evaporation, cracking and salinity in a thickened oil sands tailings. M.A.Sc. thesis, Department of Civil and Environmental Engineering, The Carleton University, Ottawa, Ontario.

James, M. 2004. Evaluating the liquefaction resistance of tailings from hard rock mining. In Proceedings of the Eleventh Tailings and Mine Waste Conference, Vail, Colorado 10-13 October 2004, pp. 89 – 101

Jeeravipoolvarn, S. 2005 Compression behaviour of thixotropic oil sands tailings. M.A.Sc. thesis, Department of Civil and Environmental Engineering, The University of Alberta, Edmonton, Alberta.

Jeeravipoolvarn, S. 2010. Geotechnical behavior of in-line thickened oil sands tailings. Ph.D. thesis. Department of Civil and Environmental Engineering, The University of Alberta, Edmonton, Alberta.

Jeeravipoolvarn, S., Scott, J.D., and Chalaturnyk, R.J. 2009. 10 m stand pipe tests on oil sands tailings: long term experimental test results and predictions. *Can. Geotech. J.*, **46:** 875–888

Kalantari, S., Ben-Awuah, E., and Askari-Nasab, H. 2013. Towards integrated oil sands mine plan and composite tailings plan. *International Journal of Mining, Reclamation and Environment*, **7**(2): 10 – 12.

Kaminsky H. A. W. 2008. Characterization of an Athabasca oil sands ore and process stream. PhD. thesis, Department of Chemical and Materials Engineering, The University of Alberta, Edmonton, Alberta

Keedwell, M.J.1984. Rheology and Soil Mechanics. Taylors & Francis Inc., New York.

Kierzkowksi, P. 2007. Oedometer creep tests of a partially saturated kaolinite clay, Experimental Unsaturated Soil Mechanics. *Springer Proceedings in Physics*, **112**: 301-307.

Kochmanova, N., and Tanaka, H. 2010. Role of microstructure in the mechanical behaviour of clay. *Geotechnical Special Publication*, **200**: 166 -171

Kodikara, J.K., Barbour, S. L., and Fredlund, D.G., 2000. Desiccation cracking of soil layers. In Proceedings of the Asian Conference in Unsaturated Soils, Balkema, Singapore, 18 -19 May 2000, pp. 693 – 698

Koumoto, T., and Houlsby, G. T. 2001. Theory and practice of the fall cone test. *Geotechnique* **51**(80): 701 - 712

Kuyucak., N., Primeau, P., Labelle, M., and Palkovits 2010. Improved dewatering characteristics of uranium tailings through controlled neutralization for paste disposal. In Proceedings of the 13th International Seminar on Paste and Thickened Tailings, Toronto, Ontario, 03 - 06 May 2010.

Lee, J. k., Shang, J.Q., and Jeong, S. 2014. Thermo-mechanical properties and microstructure of fly ash – stabilized gold tailings. *Journal of Hazardous Materials,* **276**: 323 – 331

Leong, E.C., and Rahardjo, H. 1997. Review of soil water characteristic curve equations. *Journal of Geotechnical and Geoenvironmental Engineering*, 1106 - 1117

Li, Y., Guo, J., Harbottle, D., Liu, Q., and Xu, Z. 2014. Enhancing densification by pH-switchable polymers for tailings management, In Proceedings of 17th International Seminar on Paste and Thickened Tailings, Vancouver, B.C., 8 - 12 June 2014. Joe Goodwill, InfoMine Inc., Australian Centre for Geomechanics

Mackinnon, M.D., and Boerger, H. 1986. Description of two treatment methods for detoxifying oil sands tailings pond water. *Water pollution Research Journal of Canada*, **21**: 496 - 512

Mackinnon, M.D., Matthews, W.H., and Shah, W.H., and Cuddy, R.G. 2001. Water quality issues associated with composite tailings (CT) technology for managing oil

sands tailings. *International Journal of Surface Mining, Reclamation and Environment,* **15**(4): 235 – 256

Mamer, M. 1990. Oil sands tailings technology: Understanding the impact to reclamation, Suncor Energy Inc. Canada

Manual 2003: WP4 Dewpoint Potentiameter; Decagon Devices Inc. 2365 NE Hopkins Ct. Pullman, WA 99163 - USA

Marques, M.S., Lima, H., Mandl, B., Francoeur, R., Palkovits, F., and Blois, R. 2010. Application of paste technology to mitigate the dust emissions from handling of fly and bottom ash at coal fired power plant. In Proceedings of the 13th International Seminar on Paste and Thickened Tailings, Toronto, Ontario, 03 - 06 May 2010.

Masliyah, J., Zhou, Z., Xu, Z., Czarnecki, J., and Hamza, H. 2004. Understanding water based bitumen extraction from Athabasca Oil Sands. *The Canadian Journal of Chemical Engineering,* **82** : 628 - 654

Matthews, J., Dhadli, N., House, P., and Simms, P. 2011. Field trials of thin-lift deposition of amended mature fine tailings at the Muskeg River Mine in Northern Alberta. In Proceedings of 1the 4th International Seminar on Paste and Thickened Tailings, Perth, Western Australia, 5–7 April 2011, pp. 271-280

McCarthy, D.F. 2004. Essentials of Soil Mechanics and Foundations: Basics Geotechnique. Pearson Prentice Inc., Upper Saddle River, N.J.

Meric, D. 2010. A new coupled consolidation and contaminant transport device to test a reactive core mat for remediation of contaminated, subaqueous sediments. M.Sc., thesis, Department of Civil and Environment Engineering, Northeastern University, Boston, Massachusetts.

Mermillod-Blondin, R., Benzaazoua, M., Kongolo, M., de Donato, P., Bussière, B., and Marion, P. 2011. Assessment method based on SEM-EDS and image analysis: application for fine tailings. *Journal of Minerals and Materials Characterization and Engineering*, **10** (12): 1111-1130

Mikula, R.J. 2012. Advances in oil sands tailings handling: building the base for reclamation, In Restoration and Reclamation of Boreal Ecosystems: Attaining Sustainable Development, D.H. Vitt and J.H. Bhatti, editors (Cambridge University Press, 2012).

Mikula, R.J., and Munoz, V.A. 2000. Characterization of emulsions and suspensions in the petroleum industry using Cryo-SEM and CLSM: colloids and surfaces: *Physicochemical and Engineering Aspects*, **174**: 23–36

Mitchell, J.K., and Soga, K. 2005. Fundamentals of soil behavior. John Wiley & Sons Inc., Hoboken, New Jersey

Mizani, S., and Simms, P. 2010.'Out of pipe' dewatering of thickened tailings during deposition. In Proceedings of the 13th International Seminar on Paste and Thickened Tailings, Toronto, Ontario, 03 - 06 May 2010.Broadway Nedlands: Australian Centre for Geomechanics.

Mizani, S., Solemani, S., and Simms, P. 2013. Effects of polymer dosage on dewaterability, rheology, and spread-ability of polymer amended oil sands mature fine tailings. In Proceedings of the 16th International Seminar on Paste and Thickened Tailings, Belo Horizonte., 17 - 20 June 2013., Joe Goodwill, InfoMine Inc: Australian Centre for Geomechanics.

Monroy, R., Zdravkovic, L., and Ridley A. 2007. Fabric changes in compacted London Clay due to variations in applied stress and suction, Experimental Unsaturated Experimental Mechanics. *Springer Proceedings in Physics*, **112**: 41 - 48

Monroy, R., Zdravkovic, L., and Ridley, A. 2010. Evolution of microstructure in compacted London clay during wetting and loading. *Geotechnique*, **60**(2): 105 –119

Moore, T., Zhang, C., and Pinheiro, M. 2014. Geotechnical performance of ATA – treated fluid fine tailings. In Proceedings of the 17th International Seminar on Paste and Thickened Tailings, Vancouver, B.C., 8 - 12 June 2014. Joe Goodwill, InfoMine Inc., Australian Centre for Geomechanics

Moore, T., Zhang, C., Moffett, R.H., and Odle, J. 2014. Enhanced thickened tailings performance via additional chemical treatments. In Proceedings of the 17th

International Seminar on Paste and Thickened Tailings, Vancouver, B.C., 8 - 12 June 2014., Joe Goodwill, InfoMine Inc: Australian Centre for Geomechanics.

Morgenstern, N.R., and Scott, J.D. 1995. Geotechnique of fine tailings management. In the Proceedings of the ASCE Specialty Conference on Geoenvironment, New Orleans, Louisiana, 24 - 26 February 2000, *Geotechnical Special Publication*, **46**(2): 1663- 1683.

Morris, G.E., and Żbik, M.S. 2009. Smectite suspension structural behavior. *Int. J. Miner. Process*, **93**: 20 – 25

Motta, C.S.C., Bryan, J., Komishke, B., and Kantzas, A. 2009. Study of the settling characteristics of tailings using nuclear magnetic resonance technique. *International Journal of Mining, Reclamation and Environment*, **23**(1)33–50

Munkholm, L.J., Heck, R.J., and Deen, B. 2012. Soil pore characteristics assessed from X-ray micro-CT derived images and correlations to soil friability. *Geoderma,* **181–182**: 22 – 29

Murray, E.J., and Sivakumar V. 2010. Unsaturated soils: A fundamental interpretation of soil behavior. John Wiley & Sons Inc., West Sussex

National Energy Board, Canada. 2006. Canada's oil sands opportunities and challenges to 2015: an update, an energy market assessment, June 2006.

NationMaster 2008., http://www.pembina.org/oil-sands/os101/tailings

Negre, M., Leone, P., Trichet, J., De´farge, C., Boeroa, V., and Gennari, M. 2004. Characterization of model soil colloids by cryo-scanning. *Geoderma*, **121**(1 - 2): 1 - 16

Nguyen, Q.D., and Boger, D.V. 1992. Measuring the flow properties of yield stress fluid. *In Annual Review of Fluid Mechanics*, **24**: 47-88

Nielsen, B.D. 2004. Non destructive soil testing using x-ray computed tomography. M.A.Sc. thesis, Department of Civil Engineering, Montana State University Bozeman, Montana

Nimmo, J.R. 2004. Porosity and Pore Size Distribution, in Hillel, D., ed. Encyclopedia of Soils in the Environment: London, Elsevier, v. 3, p. 295-303.

Nix, P.G., and Martin, R.W. 2006. Detoxification and reclamations of Suncor's oil sands tailing ponds. *Environmental Toxicology and Water Quality*, **7**(2): 171 - 188

Omotoso, O., and Melanson, A. 2014. Influence of clay minerals on the storage and treatment of oil sands tailings. In Proceedings of the 17th International Seminar on Paste and Thickened Tailings, Vancouver, B.C., 8 - 12 June 2014., Joe Goodwill, InfoMine Inc: Australian Centre for Geomechanics.

Onuaguluchi, O., and Eren, O. 2013. Rheology, strength and durability properties of mortars containing copper tailings as a cement replacement material. *European Journal of Environmental and Civil Engineering*, **17**(1): 19–31

Ouellet, S., Bussière B., Aubertin M., and Benzaazoua M. 2008. Characterization of cemented paste backfill pore structure using SEM and IA analysis. *Bull Eng. Geol. Environ.*, **67**: 139-152.

Owolagba, J., and Azam, S. 2013. Unsaturated soil properties of centrifuged oil sand fine tailings. In Proceedings of the 66th Canadian Geotechnical Conference on Geoscience for sustainability, Montreal, Quebec, 29 September – 03 October 2013.

Owolagba, J.O. 2013. Dewatering Behavior of Centrifuged Oil Sand Fine Tailings for Surface Deposition. M.A.Sc. thesis. Department of Environmental System Engineering, The University of Regina, Regina, Saskatchewan

Pashias, N., Boger, D.V., Summers, J., and Glenister, D.J. 1996. A fifty cent rheometer for yield stress measurement. *Journal of Rheology*, **40**: 1179 - 1189.

Peroni, N. and Tarantino, A. 2005. Measurement of osmotic suction using the squeezing technique. *Springer Proceedings in Physics*, **93**: 159-168

Pires, L.F., Borges, J. A. R., Bacchi, O.S., and Reichard, K. 2010. Twenty-five years of computed tomography in soil physics: A literature review of the Brazilian contribution. *Soil and Tillage Research*, **110**: 197-210

Price, 2008. 11 million liters a day: The tar sands leaking Legacy, Environmental Defence, 2008

Proskin, S., Sego, D., and Alostaz, M. 2010. Freeze–thaw and consolidation tests on Suncor mature fine tailings (MFT). *Cold Regions Science and Technology*, **63**: 110–120

Proskin, S., Sego, D., and Alostaz, M. 2012. Oil sands properties and freeze thaw effects. *Journal of Cold Regions Engineering*, **26**(2): 29 - 54

Ramlochan, T. Grabinsky, M.W., and Horton, R.D. 2004. Microstructure and chemical investigation of cemented paste backfills. In the Proceedings of the Eleventh Tailings and Mine Waste Conference, Vail, Colorado, 10-13 October 2004, pp. 293 – 304

Randall, E.W., Mahieu, N., and Ivanova, G.I. 1997. NMR studies of soil, soil organic matter, and nutrients: spectroscopy and imaging. *Geoderma*, **80**: 307 - 325

Ren, W., Sury, K., and Clingman, S. 2014. Enhanced thickened tailings performance via additional chemical treatments. In Proceedings of the 17th International Seminar on Paste and Thickened Tailings, Vancouver, B.C., 8 - 12 June 2014. Joe Goodwill, InfoMine Inc., Australian Centre for Geomechanics.

Riley, T.C., and Utting, L. 2014. Polymer amended modified tailings deposition – a management perspective. In Proceedings of the 17th International Seminar on Paste and Thickened Tailings, Vancouver, B.C., 8 - 12 June 2014. Joe Goodwill, InfoMine Inc: Australian Centre for Geomechanics.

Rima, U.S. 2013. Characterization and centrifuge dewatering of oil sands fine tailings. M.A.Sc thesis. The Department of Environmental Systems Engineering, University of Regina, Regina, Sakatchewan

Robinsky, E.I. 1999. Thickened tailings disposal in the mining industry. Eli. I. Robinsky Associates Limited, Toronto, Ontario

Rogers, V.V., Wickstorm, M., Liber, K., and Mackinnon, M.D. 2001. Acute and subchronic mammalian toxity of naphthenic acids from oil sands tailings. *Toxicological Sciences*, 66(27): 341 – 355

Romero E., and Simms, P. H. 2008. Microstructure investigation in unsaturated soil: A review with special attention to contribution of mercury intrusion porosimetry and environmental scanning electron microscopy. *Geotech. Geo. Engg.,* **26:** 705 – 727

Rosenqvist, I.T. 1984. The importance of pore water chemistry on mechanical and engineering properties of clayey soils*. Phil. Trans. R. Soc.,* **311** (1517): 369 - 373.

Rozina, L., Mizani, S., Malek, M., Sanchen-Sardon, M., and Simms, P. 2013. The effects of desiccation and consolidation on surface deposited thickened oil sands tailings. In Proceedings of the 14th International Seminar on Paste and Thickened Tailings, Perth, Western Australia, 5 – 7 April 2011, pp. 155 – 166

Sarsby, R.W. 2000. Environmental Geotechnique. Thomas Telford Publishing, Heron, London.

Sasanian, S. 2011. The behaviour of cement stabilized clays at high water content. Ph.D. Thesis, Department of Civil and Environment Engineering, The University of Western Ontario, London, Ontario.

Shell Canada Energy. 2012. Protocol for making flocculated mature fine tailings (MFT); Standard Operating Procedure (SOP), 17 October, 2012

Simieritsch, T., Obad j., and Dyer S. 2009. Tailing Plan Review; an assessment of oil sands company submissions for compliance with ERCB Directive 074: Tailings performance criteria and requirements for oil sands mining schemes

Simms, P.H. 2003. A fundamental study of unsaturated flow in compacted clayey soil. Ph. D. thesis, Department of Civil and Environmental Engineering, The University of Western Ontario, London, Ontario

Simms, P.H. and Yanful, E.K. 2001. Measurement and estimation of soil–pore shrinkage in a clayey till during soil-water characteristic curve tests. *Canadian Geotechnical Journal,* **38**(4): 741 - 754.

Simms, P.H. and Yanful, E.K. 2002. Predicting soil-water characteristic curves of compacted plastic soils from measured pore-size distributions. *Géotechnique,* **52(**4): 269 - 278.

Simms, P.H., and Yanful, E.K. 1999. Measurement and estimation of pore shrinkage and pore distribution in a clayey till during soil water characteristic curve tests. *Can. J. Geotech. J.*, **38:** 741 - 754

Simms, P.H., and Yanful, E.K. 2004. A discussion of the application of mercury intrusion porosimetry for the investigation of soils, including an evaluation of its use to estimate volume change in compacted clayey soils. *Géotechnique*, **54** (6): 421-426.

Simms, P.H., and Yanful, E.K. 2004. Estimation of soil water characteristics of clayey till using measured pore size distributions. *Journal of Environmental Engineering,* **130**(8): 847 - 854

Simms, P.H., and Yanful, E.K. 2005. A pore-network model for hydro-mechanical coupling in unsaturated compacted clayey soils. *Canadian Geotechnical Journal,* **42** (2): 499 - 514.

Sobkowicz, J.C. 2013. Developments in treating and dewatering oil sand tailings. In Proceedings of the 16th International Seminar on Paste and Thickened Tailings, Belo Horizonte, 17 - 20 June 2013. Joe Goodwill, InfoMine Inc: Australian Centre for Geomechanics.

Soleimani, S., Simms, P., Dunmola, A., and Freeman, G. 2014. Desiccation and consolidation in thin-lift deposition of polymer-amended mature fine tailings. . In Proceedings of the 17th International Seminar on Paste and Thickened Tailings, Vancouver, B.C., 8 - 12 June 2014. Joe Goodwill, InfoMine Inc: Australian Centre for Geomechanics

Solseng, P.B., and Wuolo, R.W., 2010. Free water from thickened tailings. In Proceedings of the 13th International Seminar on Paste and Thickened Tailings, Toronto, Ontario, 03 - 06 May 2010

Sorgi, C., DeGennaro, V. Nguyen, H.D., and Delalain P. 2008. Recent advances in ESEM analysis of partially saturated geomaterials; Unsaturated Soils, Advances in

Geo-Engineering; Proceedings of the 1st European Conference (145 – 150), E-UNSAT 2008, Durham, United Kingdom, 2 - 4 July 2008

Suncor Energy September – October. 2010. Suncor tailings ponds reclamation project; (Report 2010).

Suthkar, N.N., and Scott, J.D. 1996. Measurement of hydraulic conductivity in oil sand tailings slurries. *Canadian Geotechnical Journal*, **33**(4): 642 - 653

Svec, F., and Frechet, J. M. J. 1995. Temperature, a simple and efficient tool for the control of pore size distribution in macroporous polymers. *Macromolecules,* **28** (22): 7580-7582

Tessier, D. 1990. Behaviour and microstructure of clay minerals. *In* soil colloids and heir association in aggregate. Edited by Plenum Press, New York.

Traceable portable conductivity meter. http://www.clarksonlab.com/

Tsutsumi, A., and Tanakab, H. 2012. Combined effects of strain rate and temperature on consolidation behavior of clayey soils. *Soils and Foundations,* **52**(2): 207–215

Vanapalli, S.K., Pufahl, D.E., and Fredlund, D.G. 1999. Relationship between soil-water characteristic curves and the as-compacted water content versus soil for a clay till. In proceedings of the XI Pan-American Conference on Soil Mechanics and Foundation Engineering, Brazil, 8 – 12 August 1999, **2:** 991-998.

Wang, C., Harbottle, D., Liu, Q., and Zhenghe, X. 2014. Current state of fine mineral tailings treatment: A critical review on theory and practice. *Mineral Engineering,* **58**: 113 -131

Wang, X., Feng, X., Xu, Z., and Masliyah, J. H. 2010. Polymer aids for settling and filtration of oil sands tailings. *The Canadian Journal of Chemical Engineering*, **88:** 403- 410

Weeman, W.S. 1997. Nuclear magnetic resonance, a simple introduction to the principles and applications. *Geoderma,* **80**: 225 – 242

Wells, S., Revington, A., and Omotoso, O. 2011. Mature fine tailings drying – a technology update. In Proceedings of the 14th International Seminar on Paste and Thickened Tailings, Perth, Western Australia, 5 – 7 April 2011, pp. 155 - 166

White, T.L. 1996. Cryogenic application of clay and silt microstructure: implications for geotechnical properties. Ph.D. thesis, Department of Earth Science, Carleton University, Ottawa, Ontario

Wickland, B.E. 2006. Volume change and permeability of mixtures of waste rock and fine tailings. Ph.D. thesis, Department of Mining Engineering, The University of British Columbia, Vancouver, British Columbia.

Wilson, G.W., Fredlund, D.G., and Barbour, S. L. 1997. The effect of soil suction on evaporative fluxes from soil surfaces. *Can. Geotech. J.,* **34**: 145 – 155.

Xu, Y., and Dabros T. 2011. Alternatives to tailings ponds for oil sands tailings disposal. Natural Resources Canada

Xu, Y., and Hamza, H. (2003) Thickening and disposal of oil sand tailings. *Mining Engineering***, 55**(11): 19 – 25

Yao, Y., and Liu, D. 2012. Comparison of low-field NMR and mercury intrusion porosimetry in characterizing pore size distributions of coals. *Fuel,* **95:** 152 – 158

Yilmaz, E., Belem, T., Bussière, B., and Benzaazoua, M. 2011. Relationships between micro structural properties and compressive strength of consolidated and unconsolidated cemented paste backfills. *Cement and Concrete Composites,* **33**: 702 – 715

Zbik M.S., Du J., Pushkarova R.A., and Rogers St. C. 2009. Observation of gaseous films at solid–liquid interfaces: Removal by ultrasonic action. *Journal of Colloid and Interface Science,* **336**: 616–623

Zbik, M.S., Smart R.C., and Morris G.C., 2008. Kaolinite flocculation structure. *Journal of Colloid and Interface Science*, **328**: 73–80

Zhang, Qi. 2013. Microstructure and deterioration mechanisms of Portland cement paste at elevated temperature. Master of Engg. Thesis, The Tongi University, China.

Zhou, A., and Sheng, D. 2009. Yield stress, volume change and shear strength behavior of unsaturated soils: Validation of the SFG model. *Can. Geotech. J.,* ***46:*** *1034 – 1045*

Zhou, J., Ye, G., and van Breugal, K. 2010. Characterization of pore structure in cement-based materials using pressurization–depressurization cycling mercury intrusion porosimetry (PDC-MIP). *Cement and Concrete Research,* ***40****: 1120–1128*

Zhu, Q. 2013. Understanding the role of caustic addition in oil sands processing. M.A.Sc. thesis, Department of Chemical and Materials Engineering, The University of Alberta, Edmonton, Alberta.

Appendices

Appendix 1: SEM micrographs of tailings used in image analysis for short term dewatering

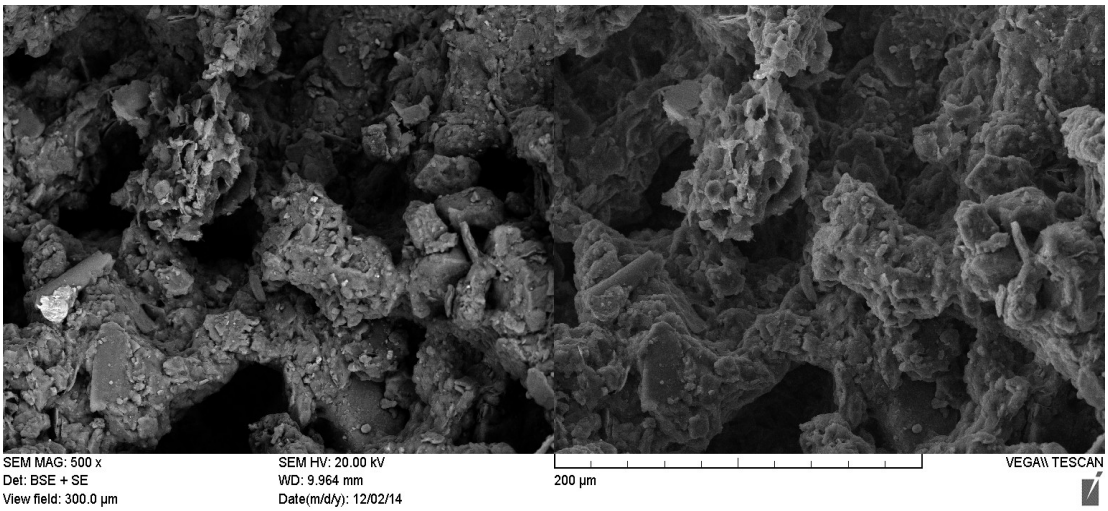

SEM micrographs of tailings for 500 ppm one hour after polymer mixing

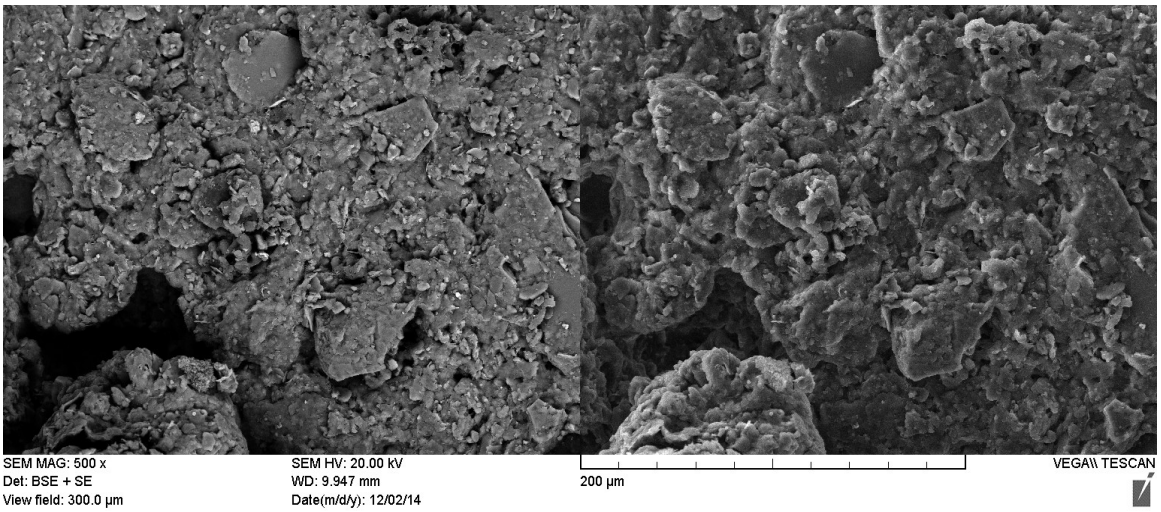

SEM micrographs of tailings for 500 ppm 144 hours after polymer mixing

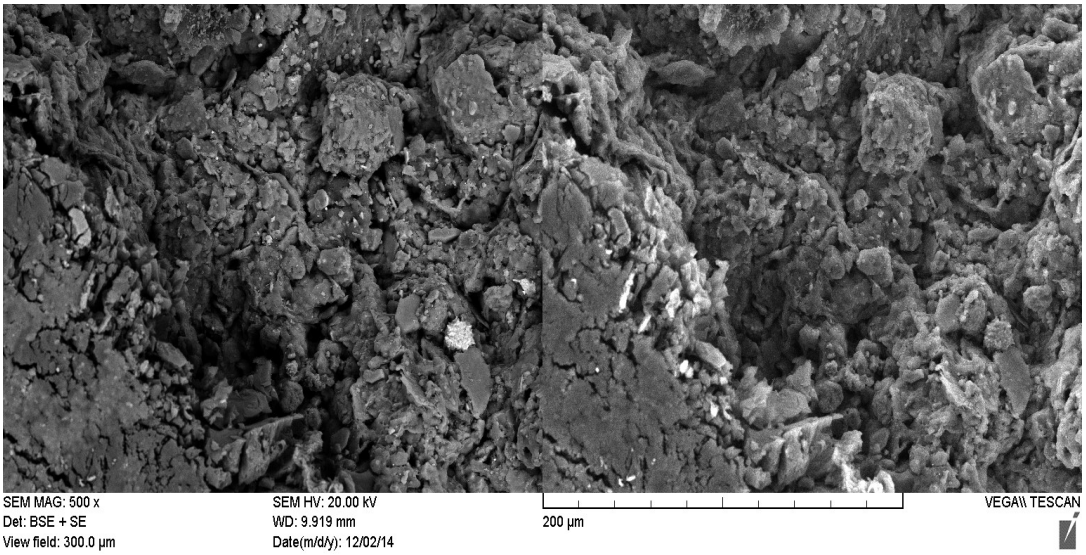

SEM micrographs of tailings for 700 ppm one hour after polymer mixing

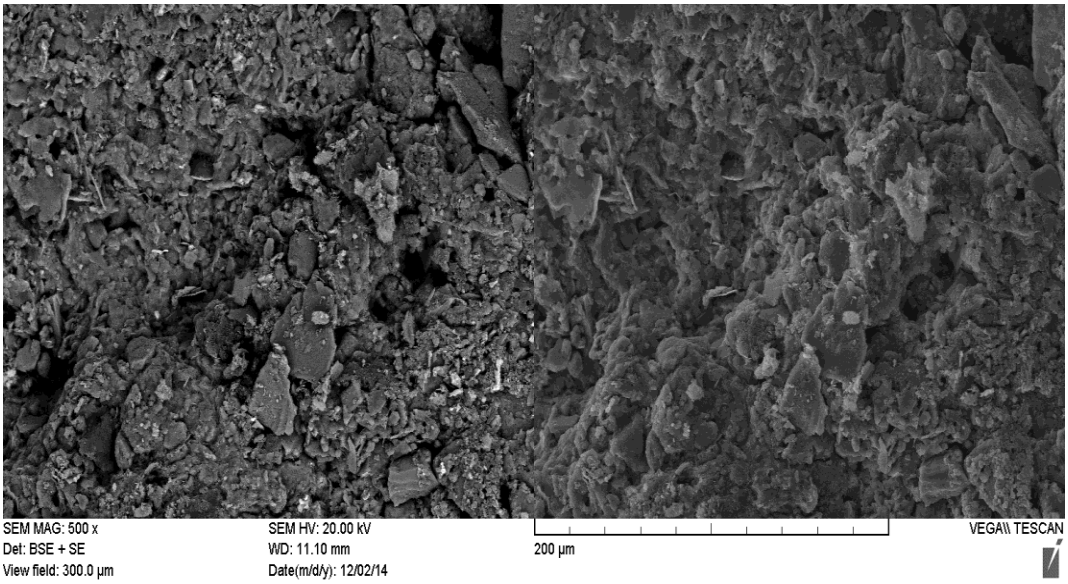

SEM micrographs of tailings for 700 ppm 144 hours after polymer mixing

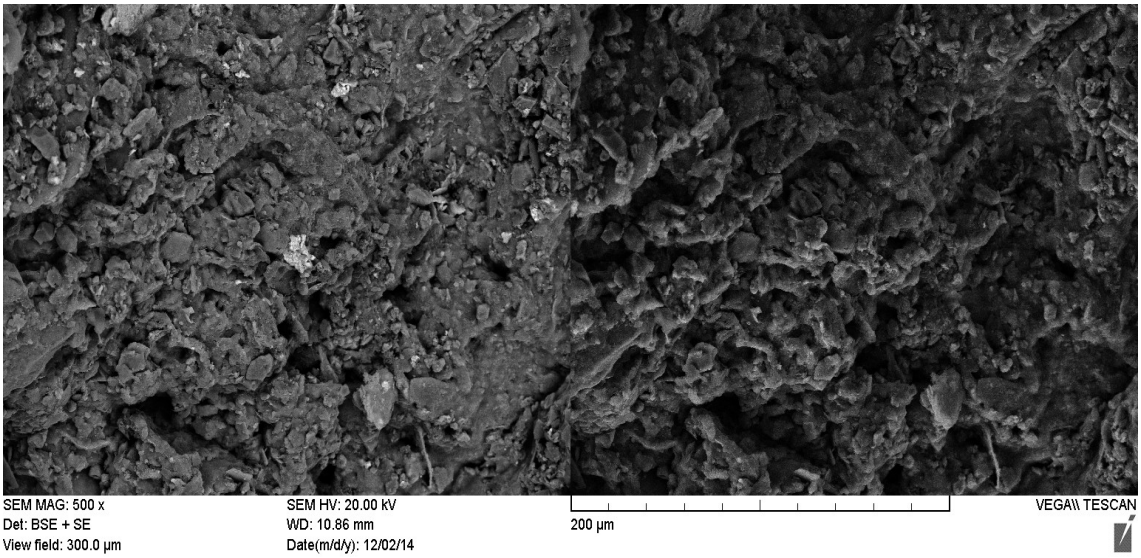

SEM micrographs of tailings for 1000 ppm one hour after polymer mixing

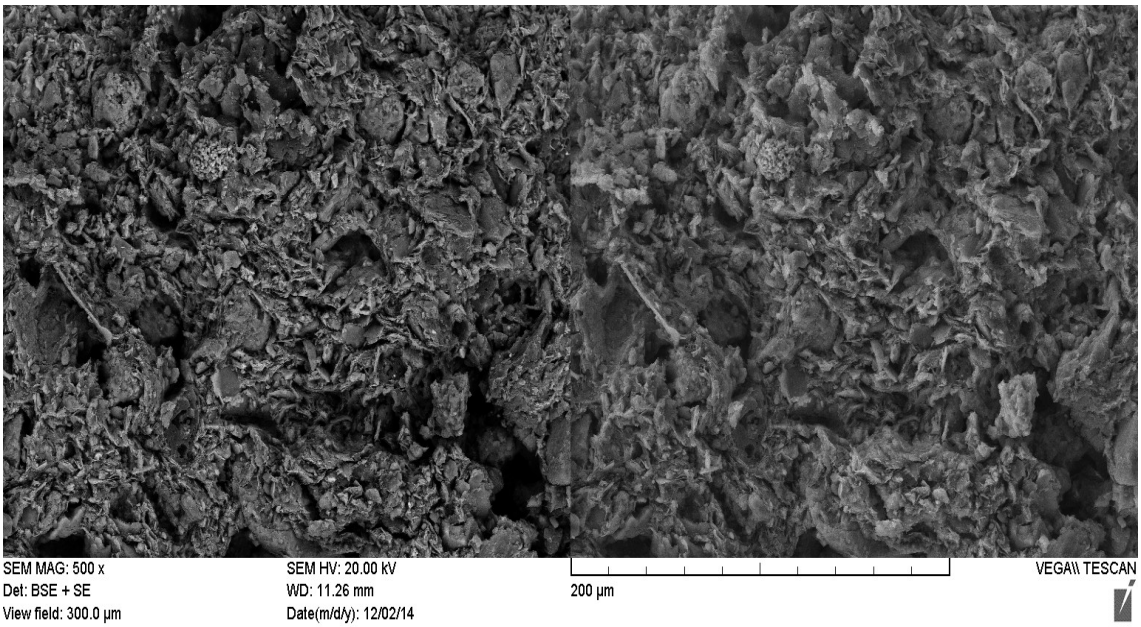

SEM micrographs of tailings for 1000 ppm 144 hours after polymer mixing

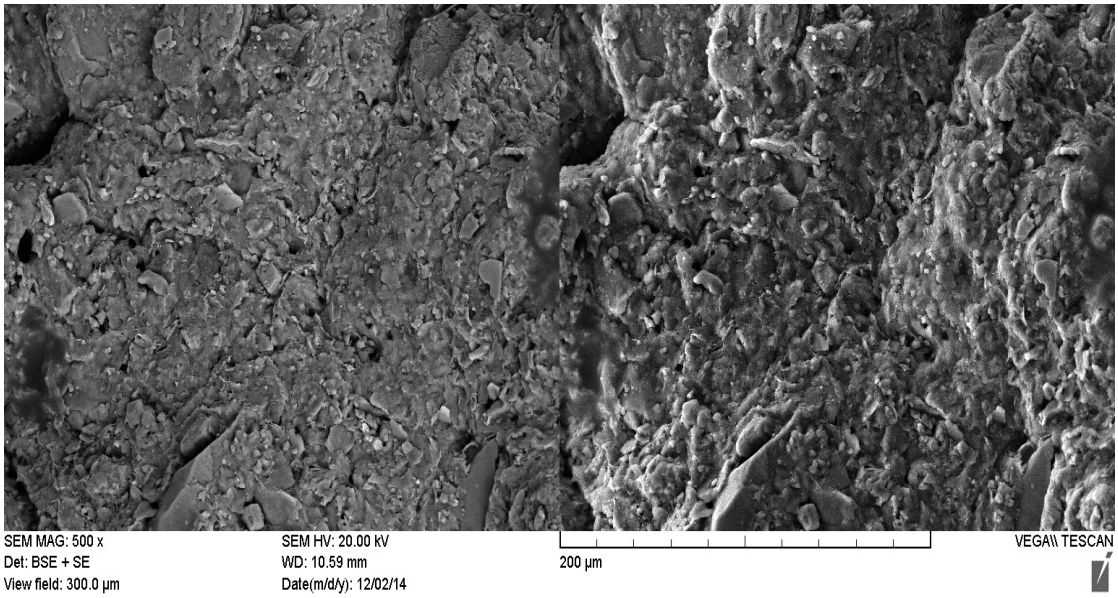

SEM micrographs of tailings for 1500 ppm one hour after polymer mixing

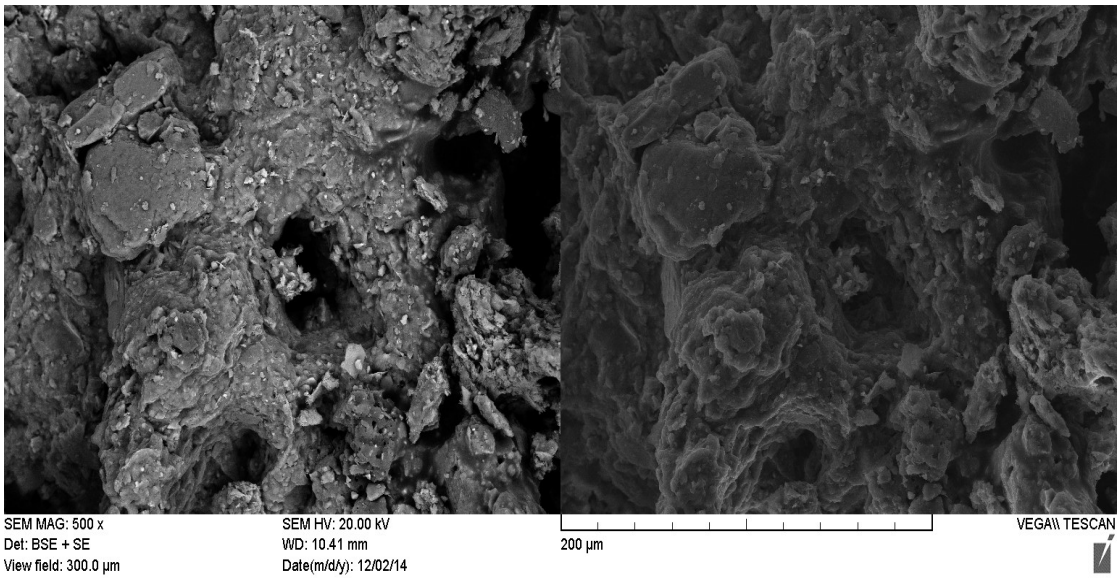

SEM micrographs of tailings for 1500 ppm 144 hours after polymer mixing

Appendix 2: ESEM micrographs of desiccated tailings from depth profiles used in image analysis

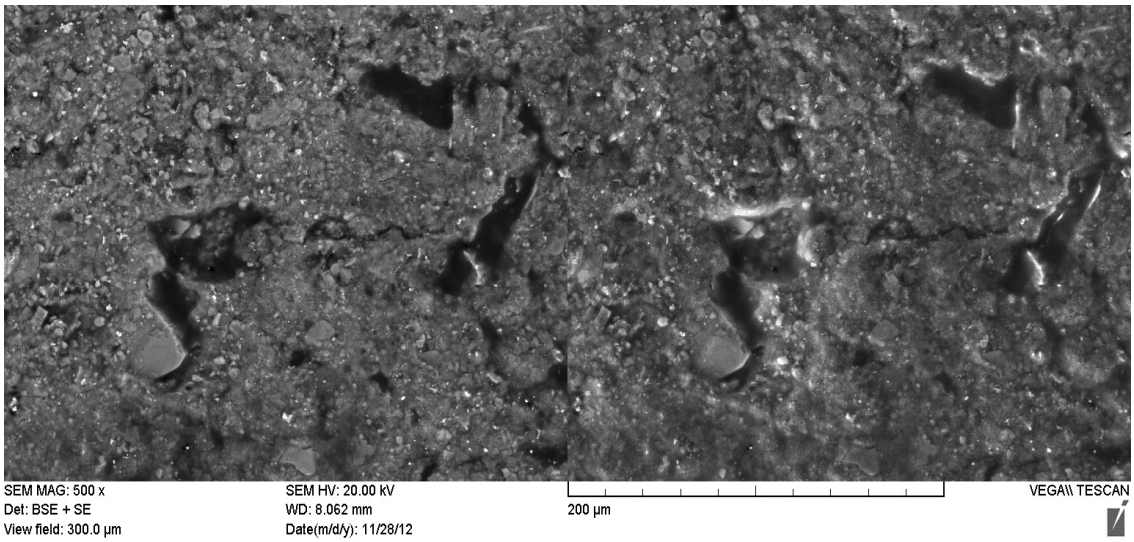

ESEM micrographs of polymer amended tailings for 700 ppm from top depth

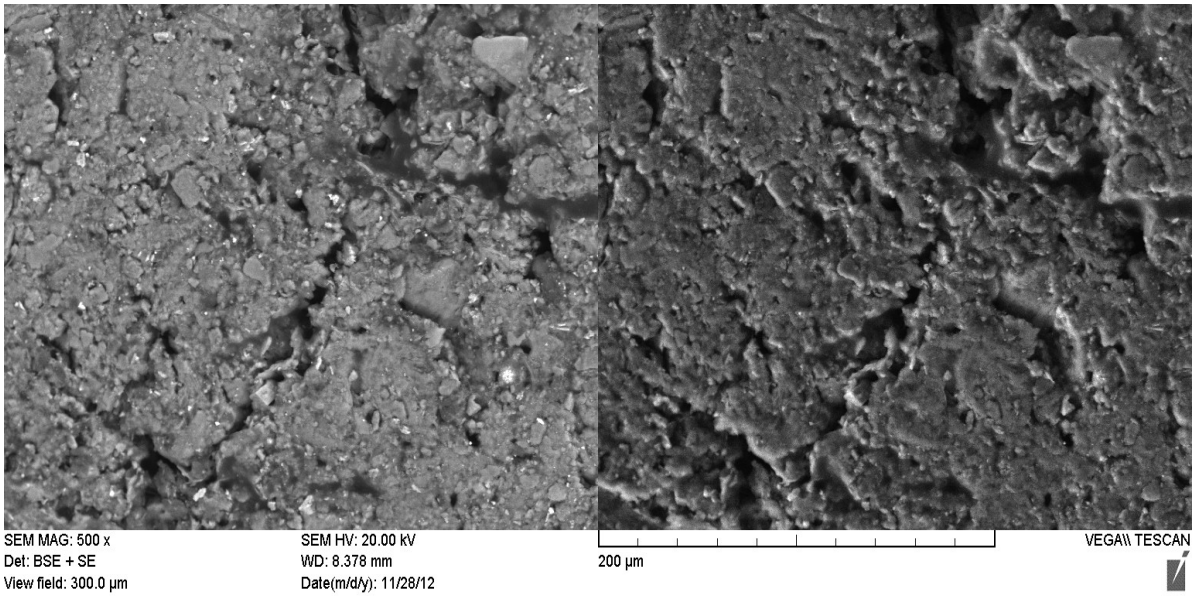

ESEM micrographs of polymer amended tailings for 1000 ppm from top depth

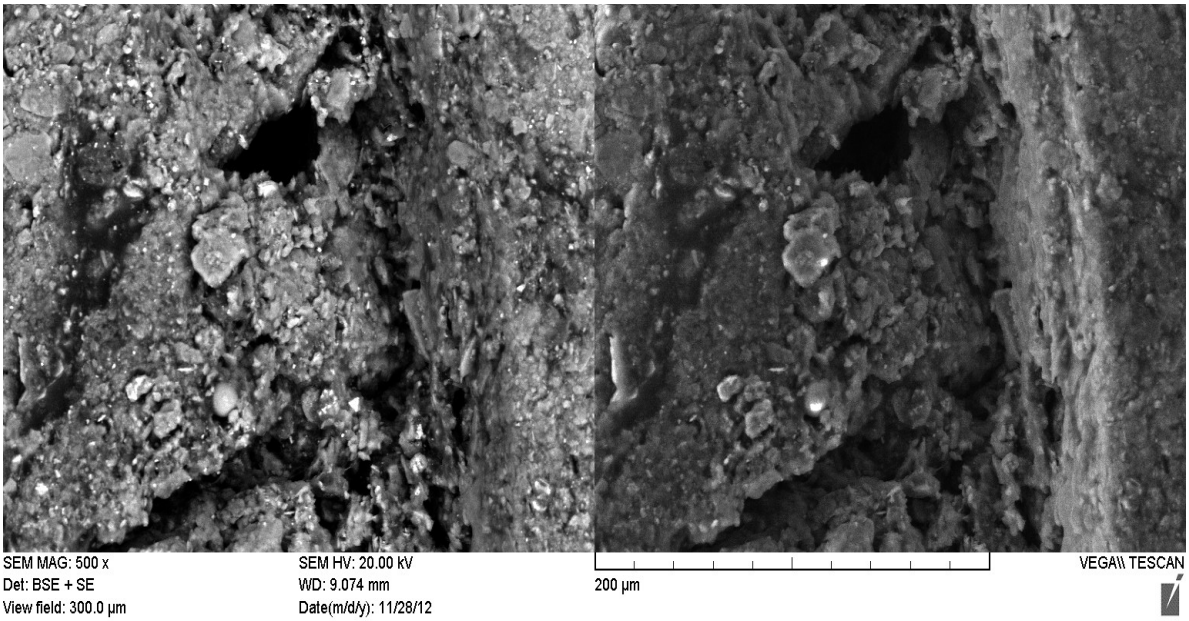

ESEM micrographs of polymer amended tailings for 1500 ppm from top depth

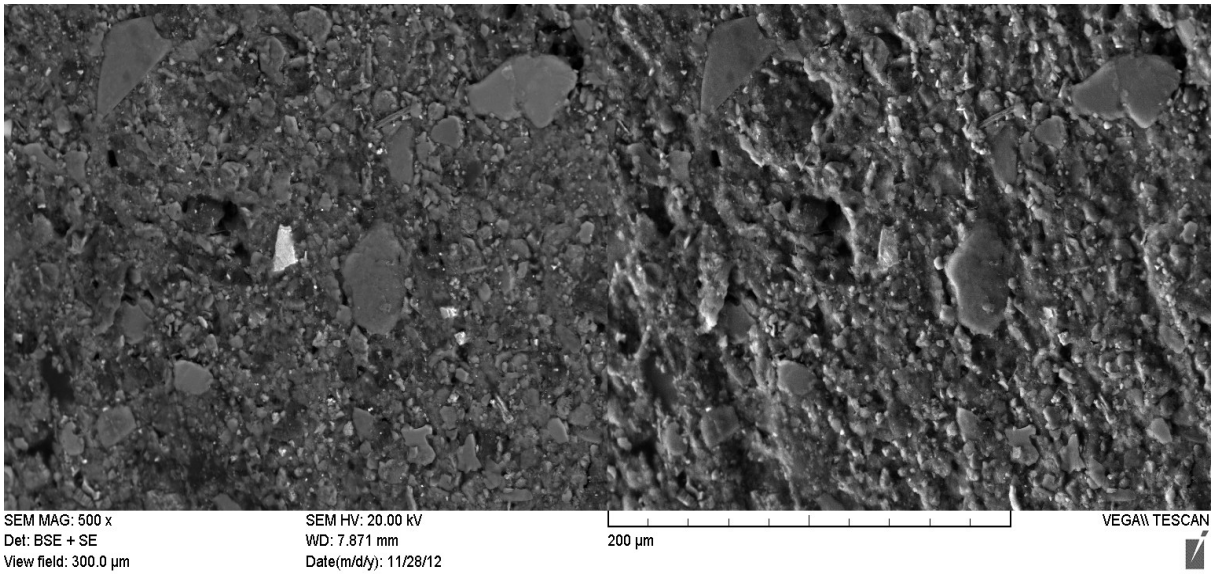

ESEM micrographs of polymer amended tailings for 700 ppm from middle depth

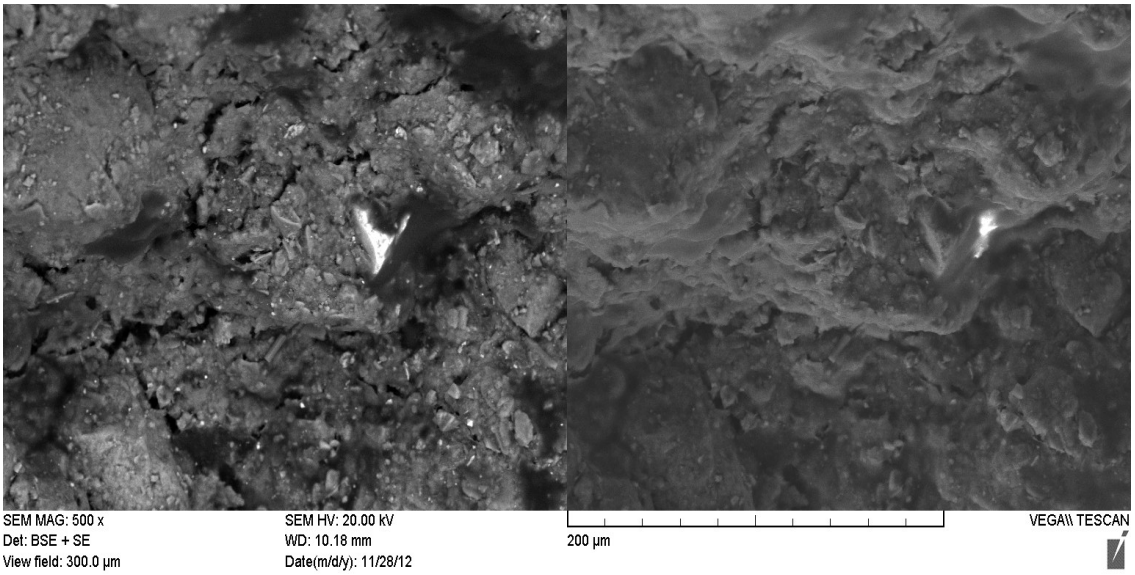

ESEM micrographs of polymer amended tailings for 1000 ppm from middle depth

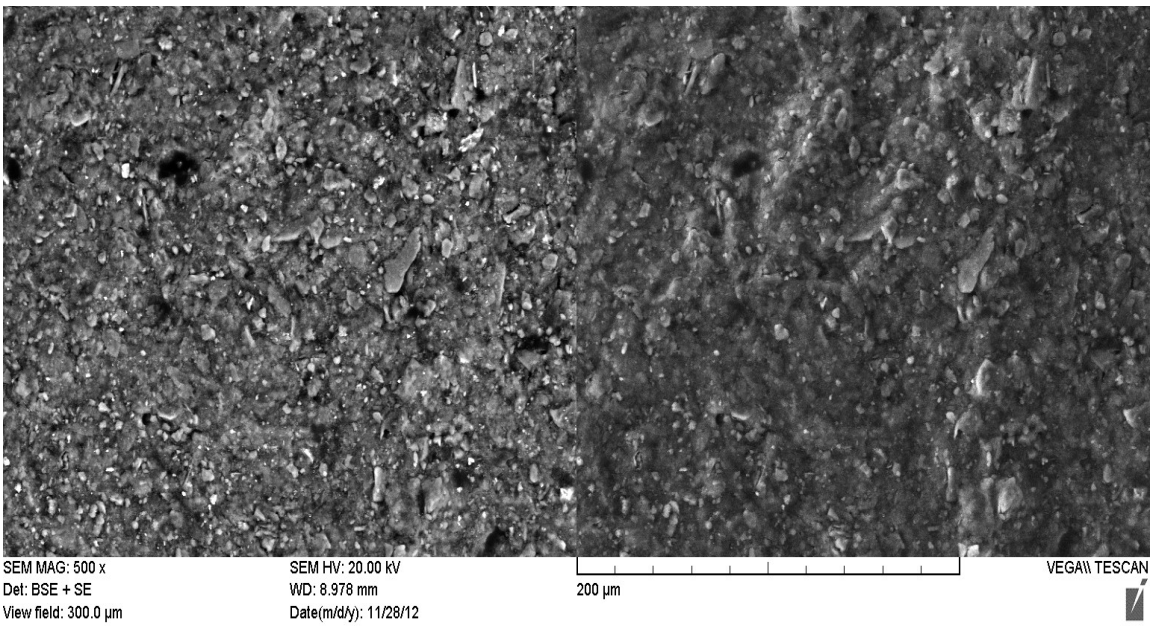

ESEM micrographs of polymer amended tailings for 1500 ppm from middle depth

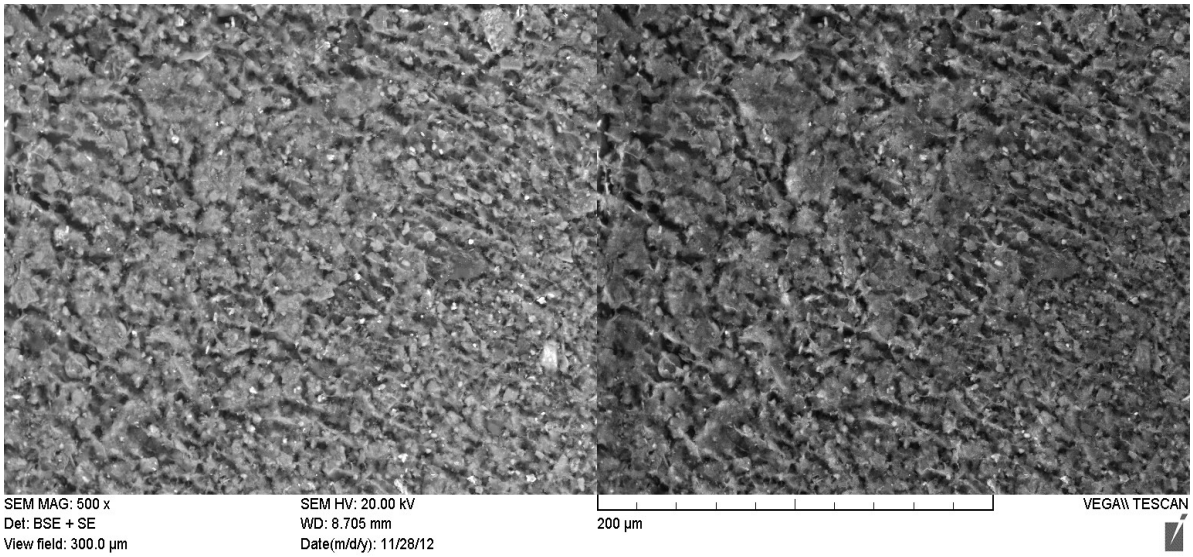

ESEM micrographs of polymer amended tailings for 700 ppm from bottom depth

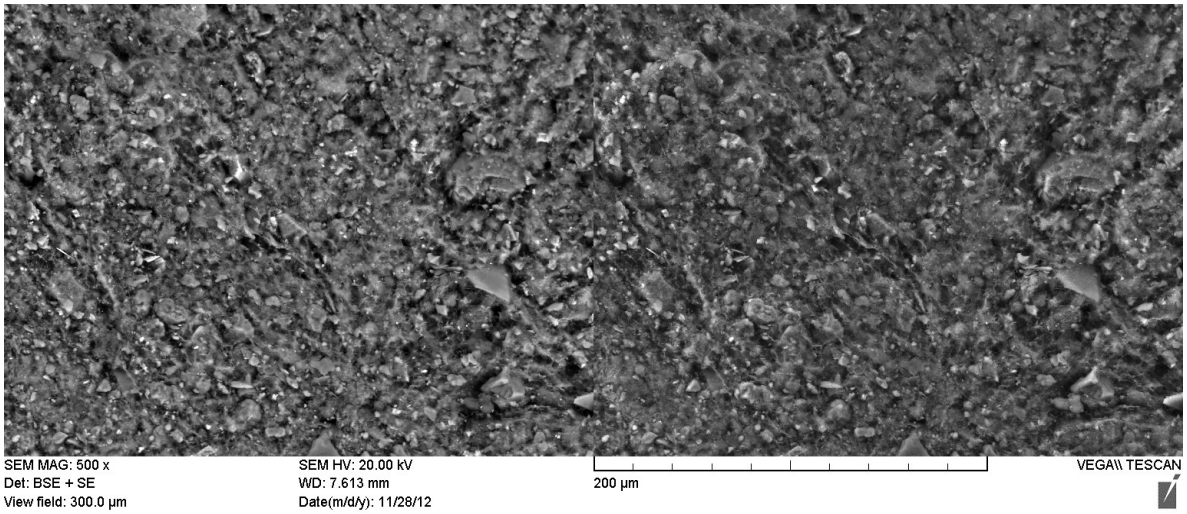

ESEM micrographs of polymer amended tailings for 1000 ppm from bottom depth

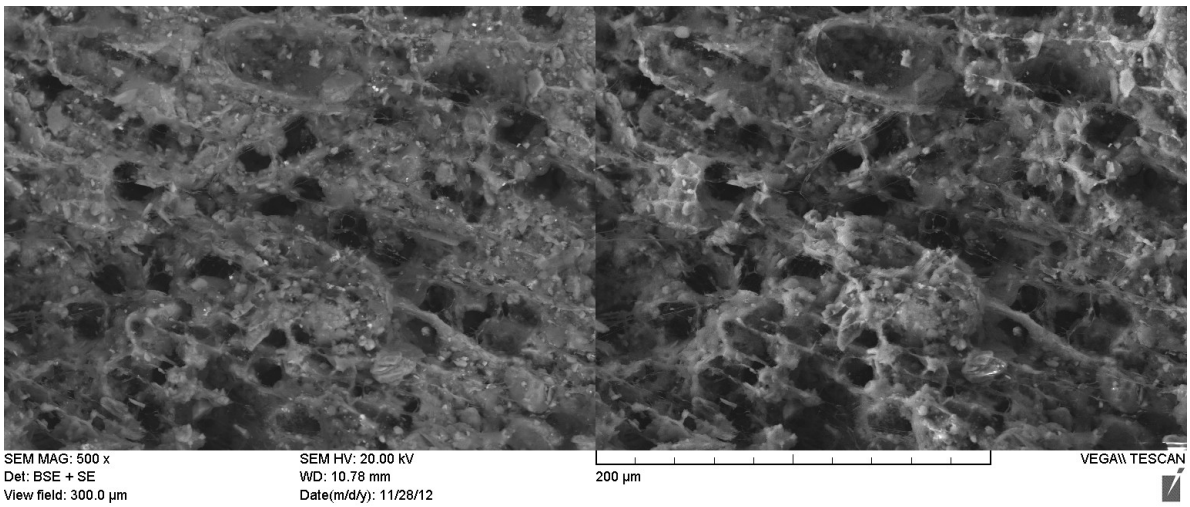

ESEM micrographs of polymer amended tailings for 1500 ppm from bottom depth

Appendix 3: ESEM micrographs of desiccated tailings used in image analysis

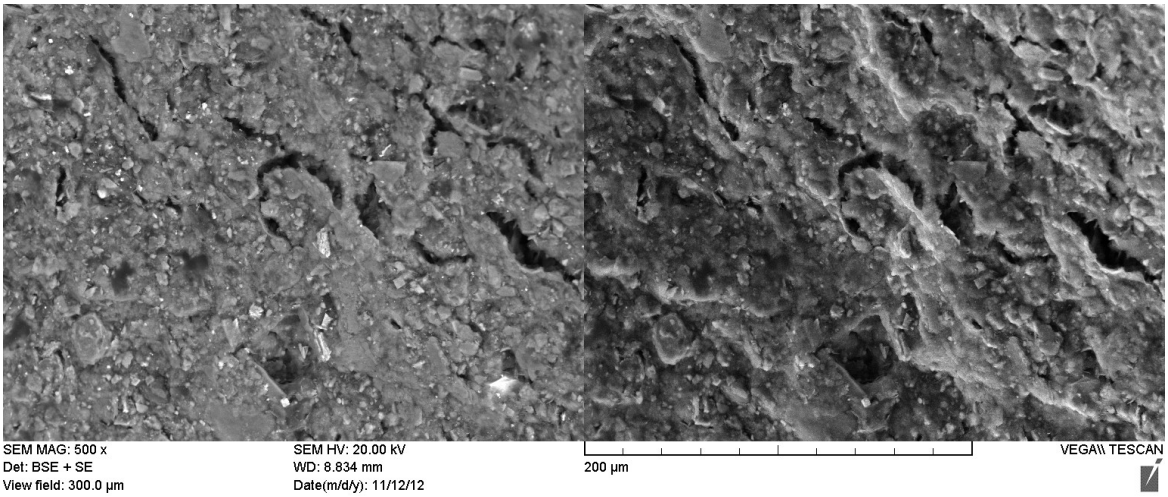

ESEM micrographs of polymer amended tailings desiccated to 103% solids content for 700 ppm

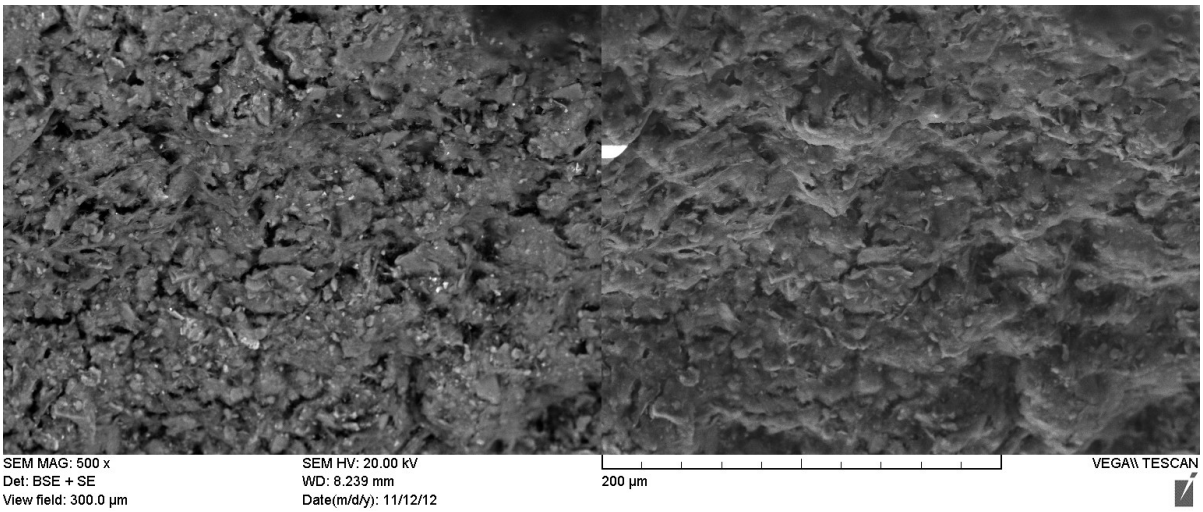

ESEM micrographs of polymer amended tailings desiccated to 103% solids content for 1000 ppm

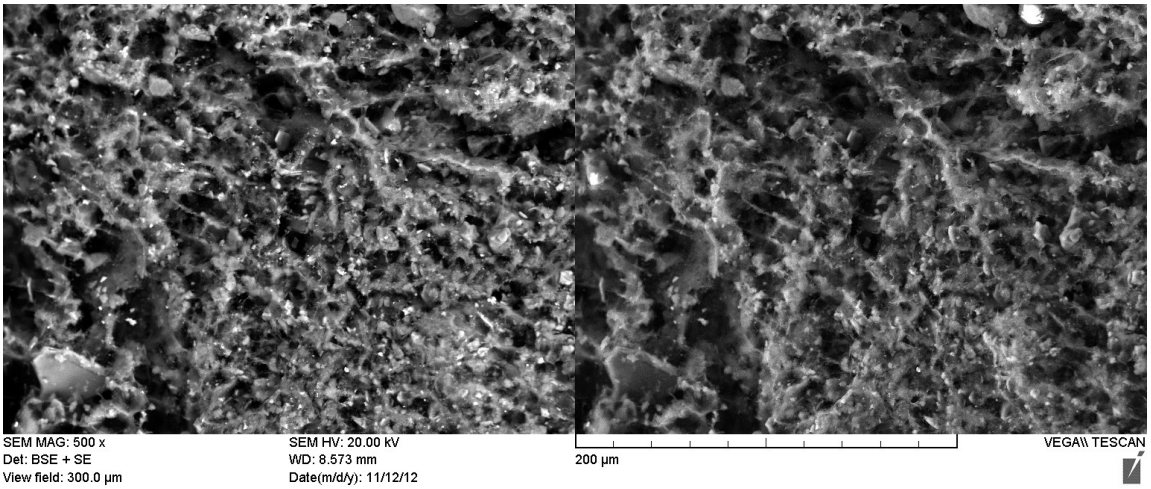

ESEM micrographs of polymer amended tailings desiccated to 103% solids content for 1500 ppm

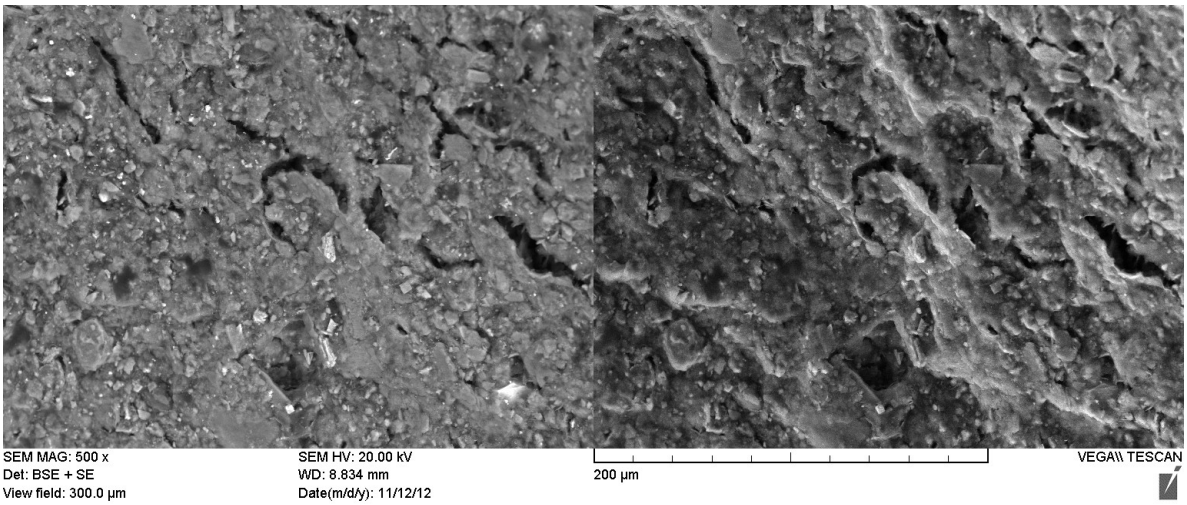

ESEM micrographs of polymer amended tailings desiccated to 50% solids content for 700 ppm

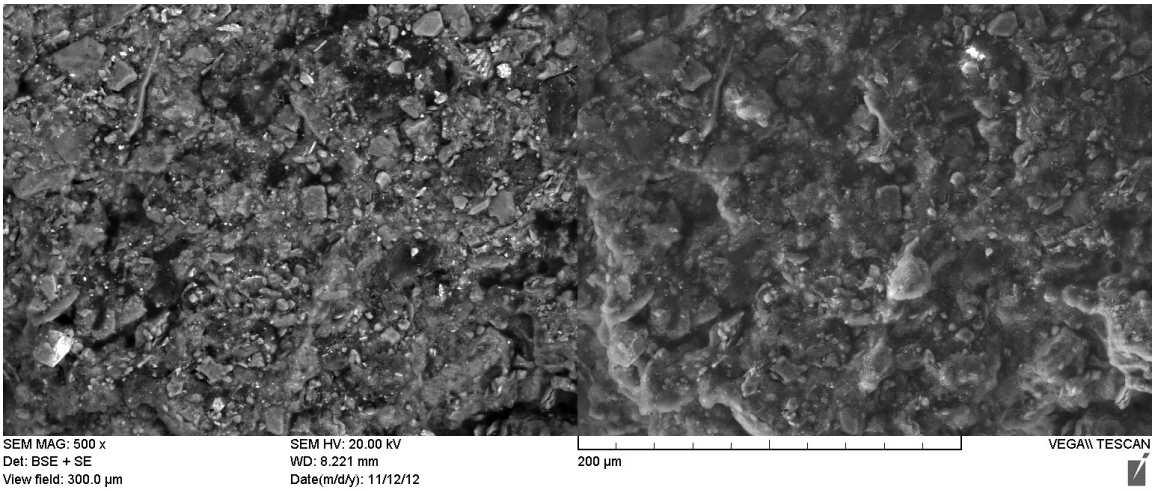

ESEM micrographs of polymer amended tailings desiccated to 50% solids content for 1000 ppm

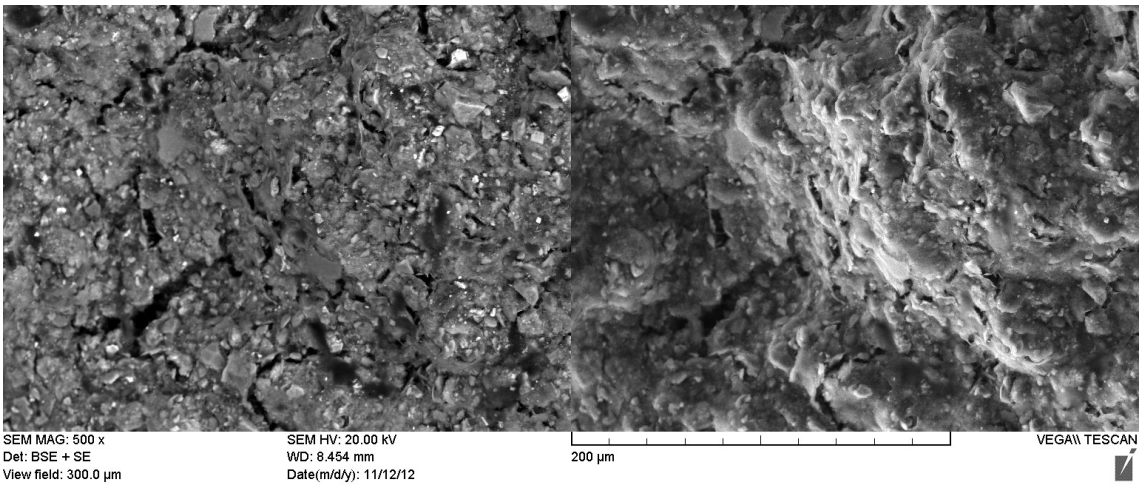

ESEM micrographs of polymer amended tailings desiccated to 50% solids content for 1500 ppm

Appendix 4: SEM micrographs of desiccated and consolidated tailings used in image analysis

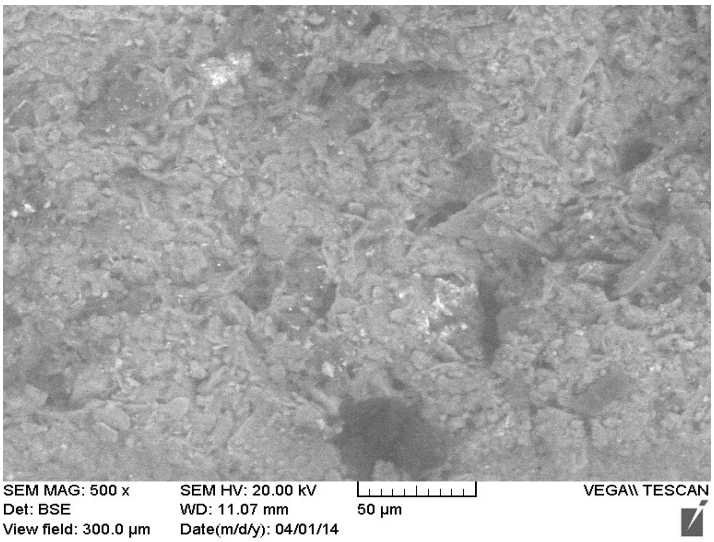

SEM micrographs of unconsolidated tailings for 58% initial solids content

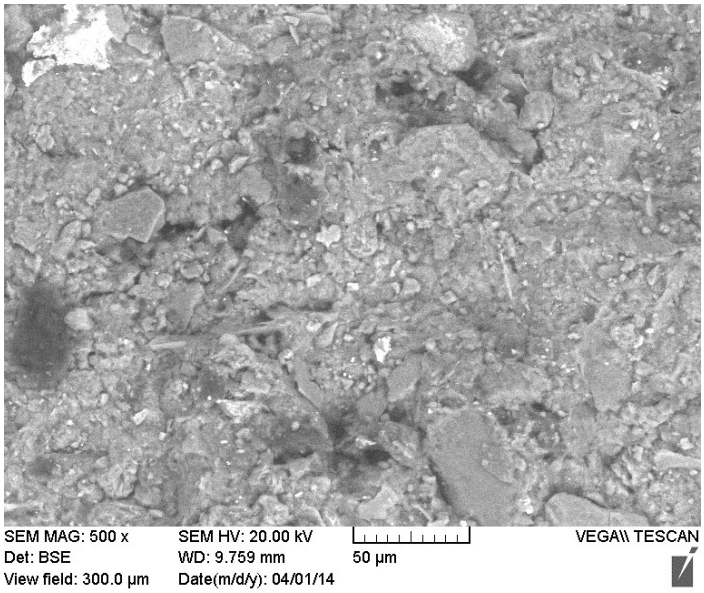

SEM micrographs of tailings at 20 kPa for 58% initial solids content

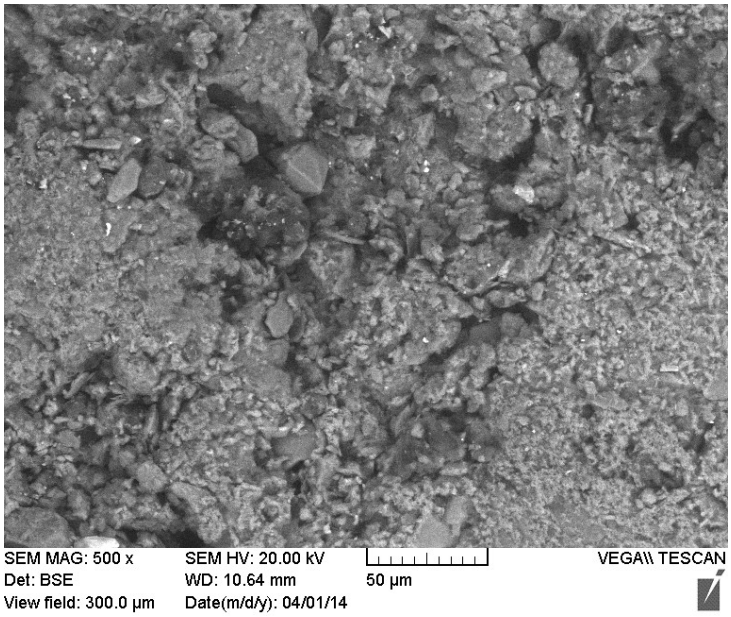

SEM micrographs of tailings at 40 kPa for 58% initial solids content

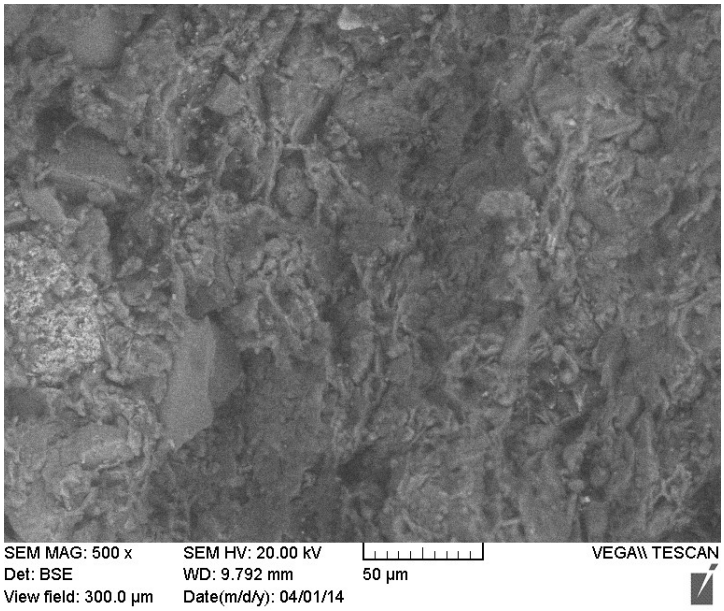

SEM micrographs of tailings at 80 kPa for 58% initial solids content

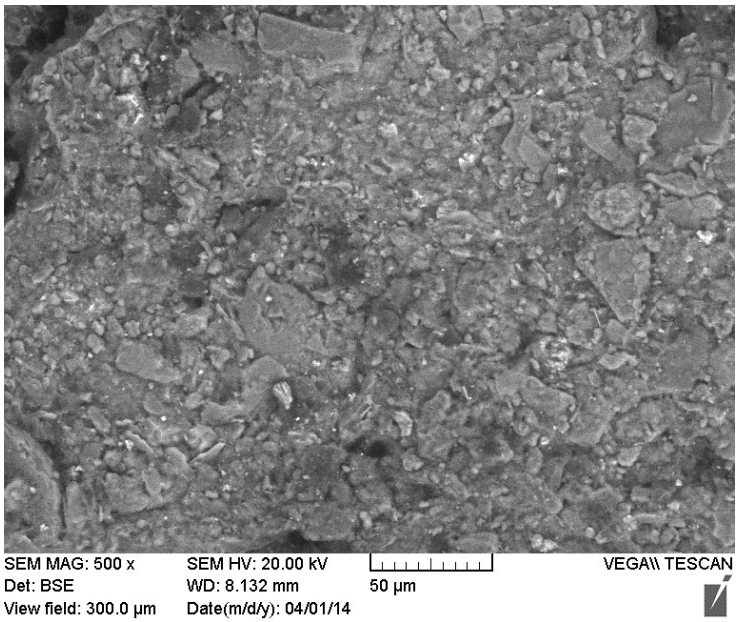

SEM micrographs of unconsolidated tailings for 71% initial solids content

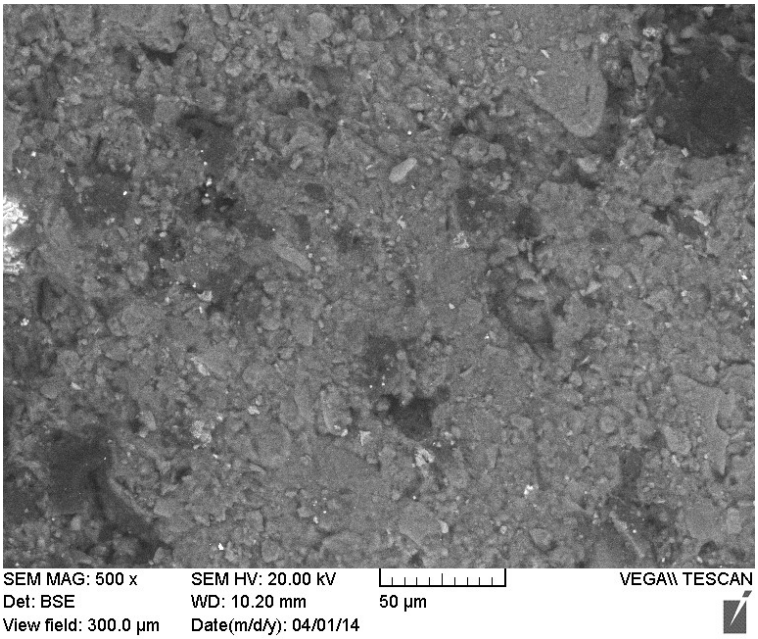

SEM micrographs of tailings at 20 kPa for 71% initial solids content

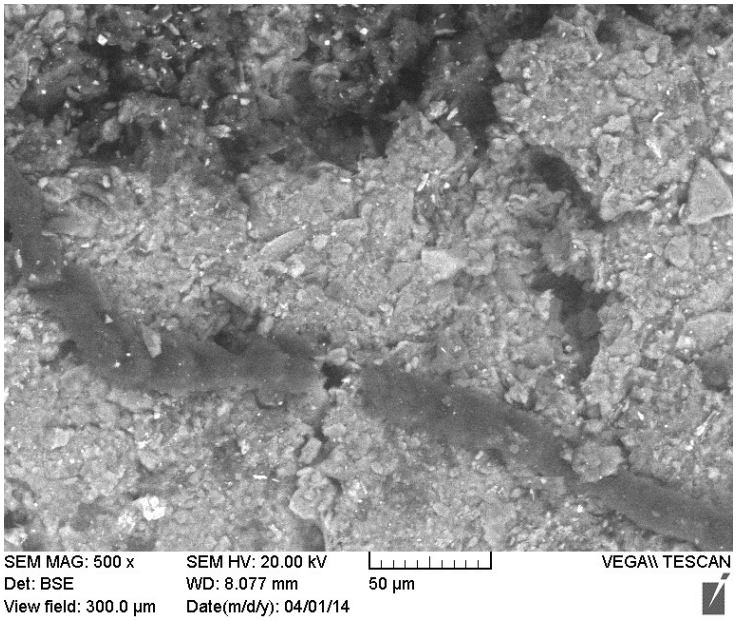

SEM micrographs of tailings at 40 kPa for 71% initial solids content

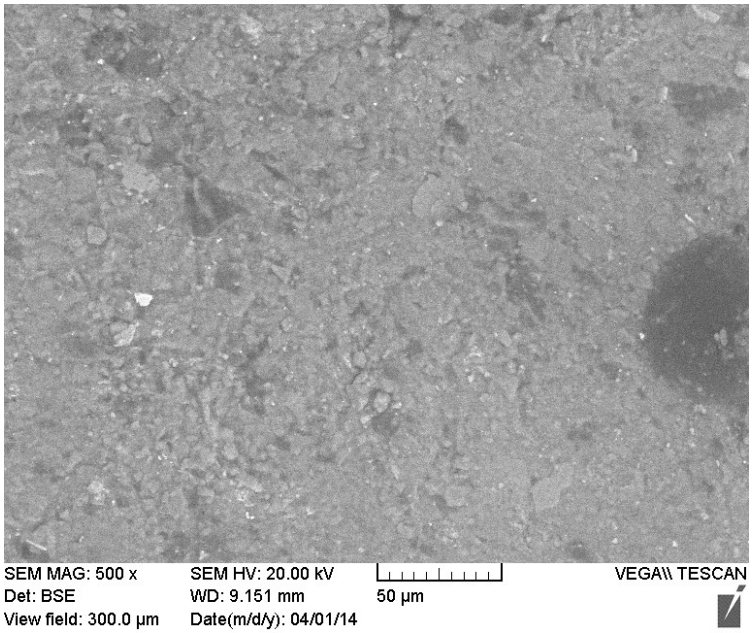

SEM micrographs of tailings at 80 kPa for 71% initial solids content

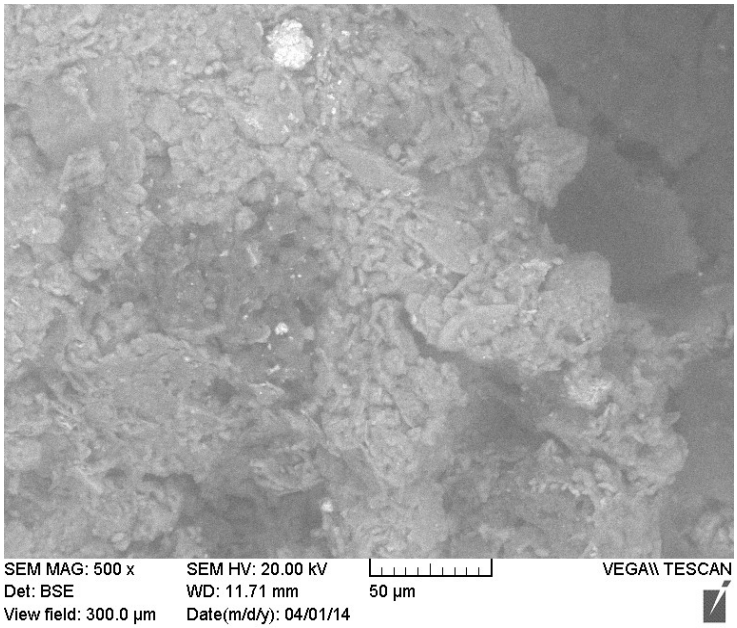

SEM micrographs of unconsolidated tailings for 80 % initial solids content

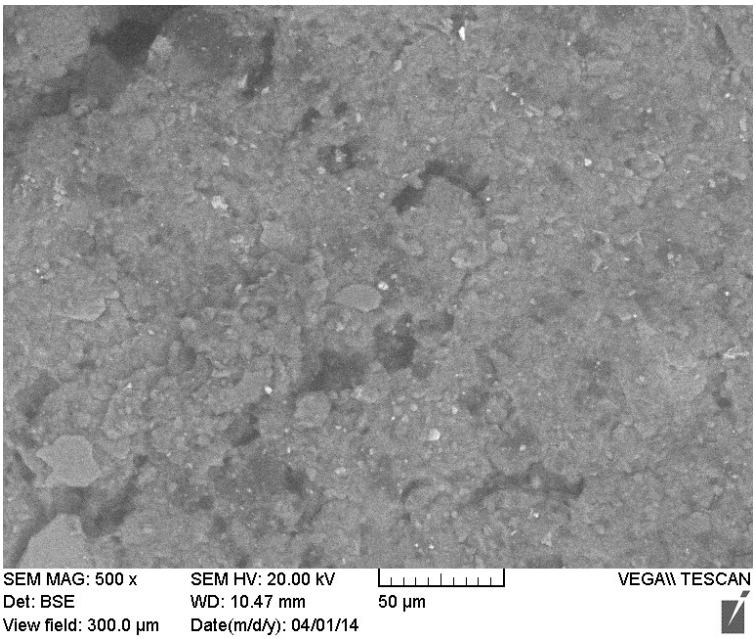

SEM micrographs of tailings at 20 kPa for 80% initial solids content

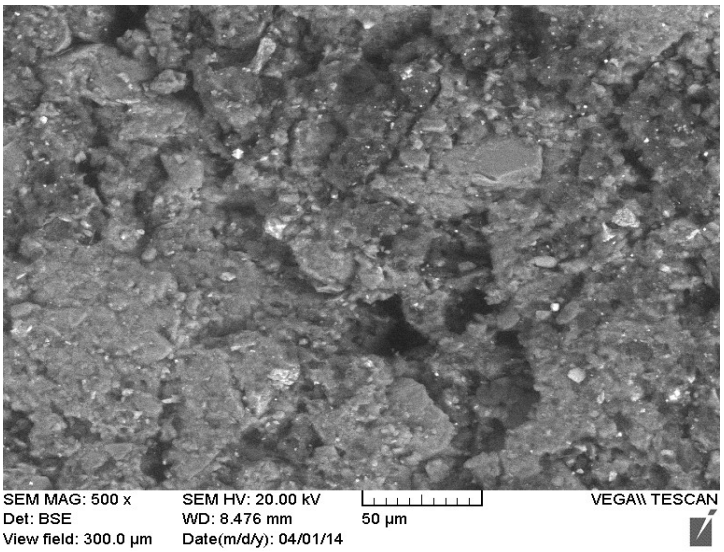

SEM micrographs of tailings at 40 kPa for 80% initial solids content

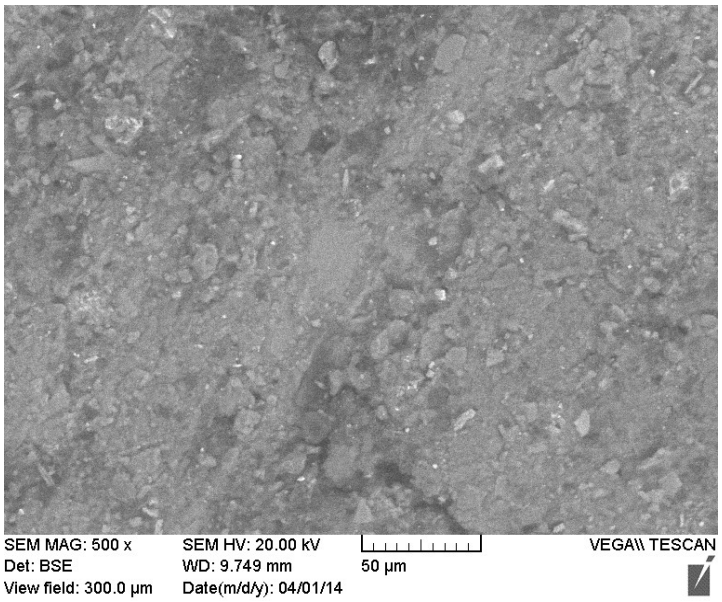

SEM micrographs of tailings at 80 kPa for 80% initial solids content

Appendix 5: ESEM micrographs of desiccated and consolidated tailings used in image analysis for repeatability

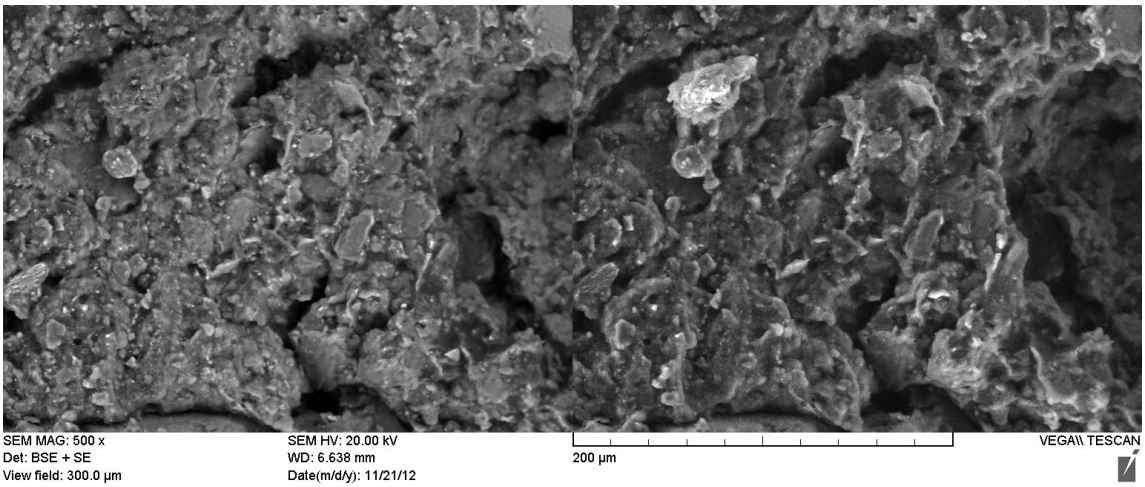

Image 1: ESEM micrographs of a desiccated and consolidated polymer amended tailings for repeatability; magnification – 0.5 kx

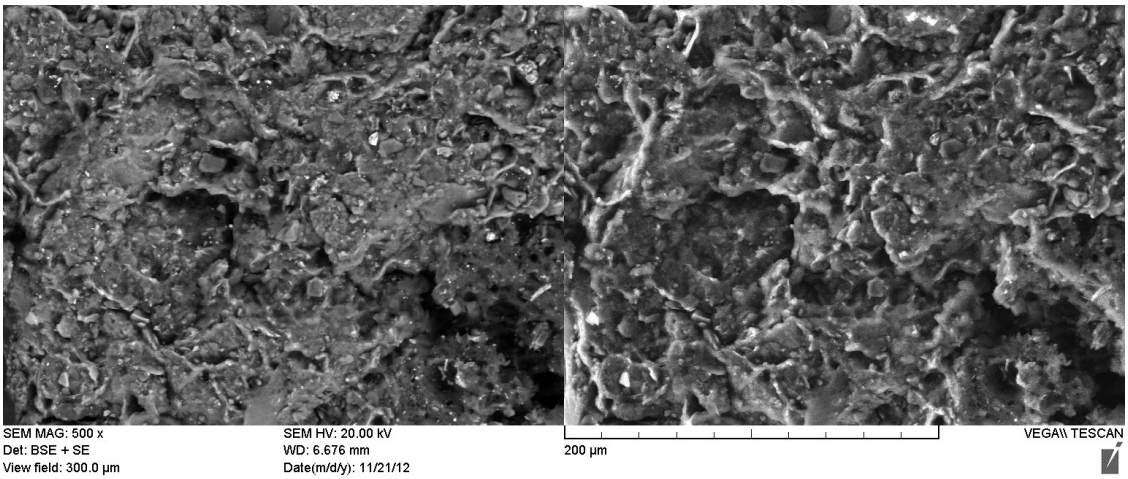

Image 2: ESEM micrographs of desiccated and consolidated polymer amended tailings for repeatability; magnification – 0.5 kx

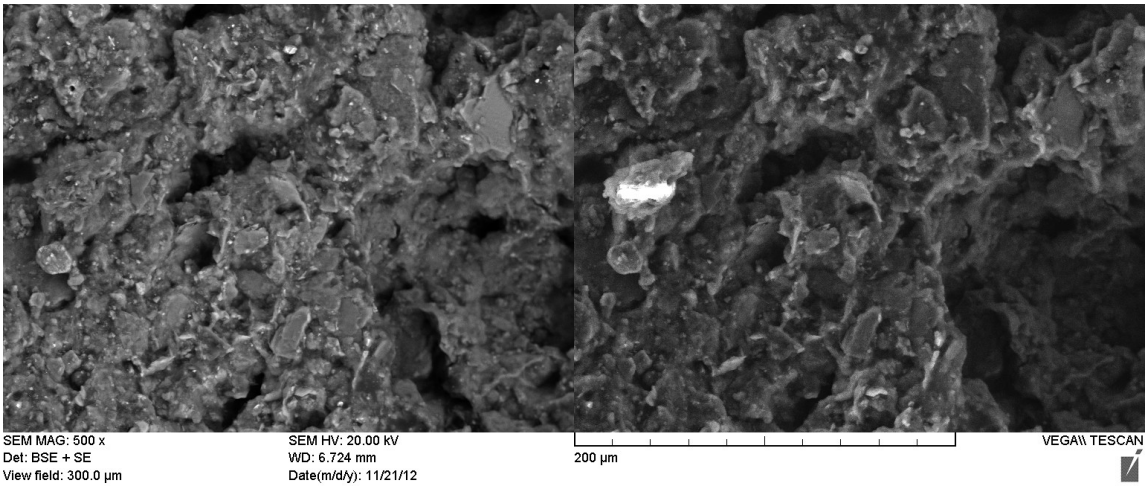

Image 3: ESEM micrographs of desiccated and consolidated polymer amended tailings for comparative evaluation for repeatability; magnification 0.5 kx

Appendix 6: ESEM micrographs of desiccated and consolidated polymer amended tailings of various magnifications for a particular sample

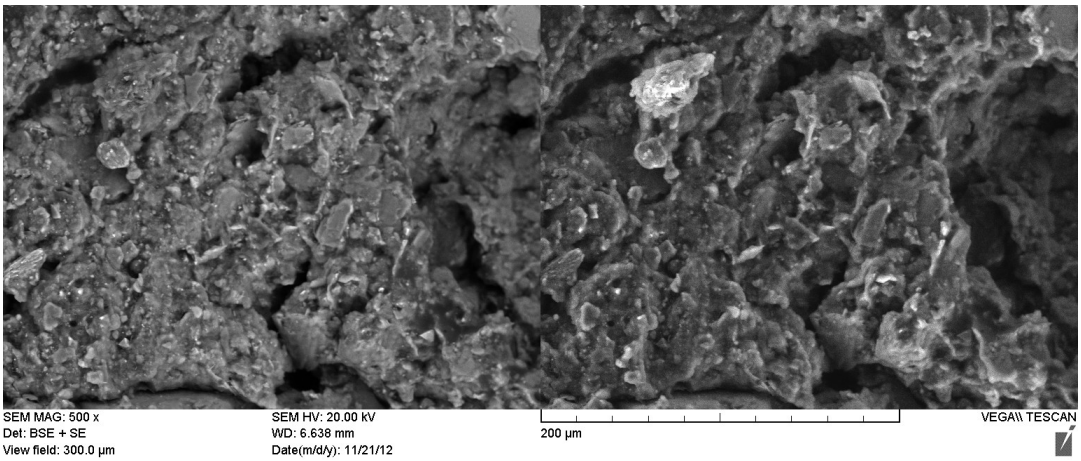

ESEM micrographs of desiccated and consolidated polymer amended tailings of various magnifications for a particular sample to check accuracy; magnification - 0.5 x

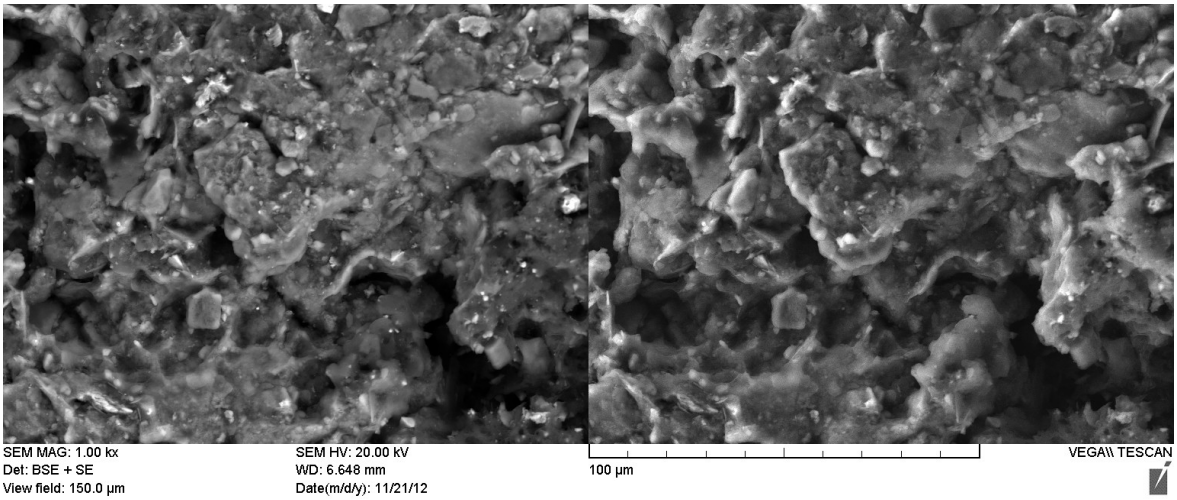

Image 2: ESEM micrographs of desiccated and consolidated polymer amended tailings for a particular sample to check accuracy; magnification – 1 kx

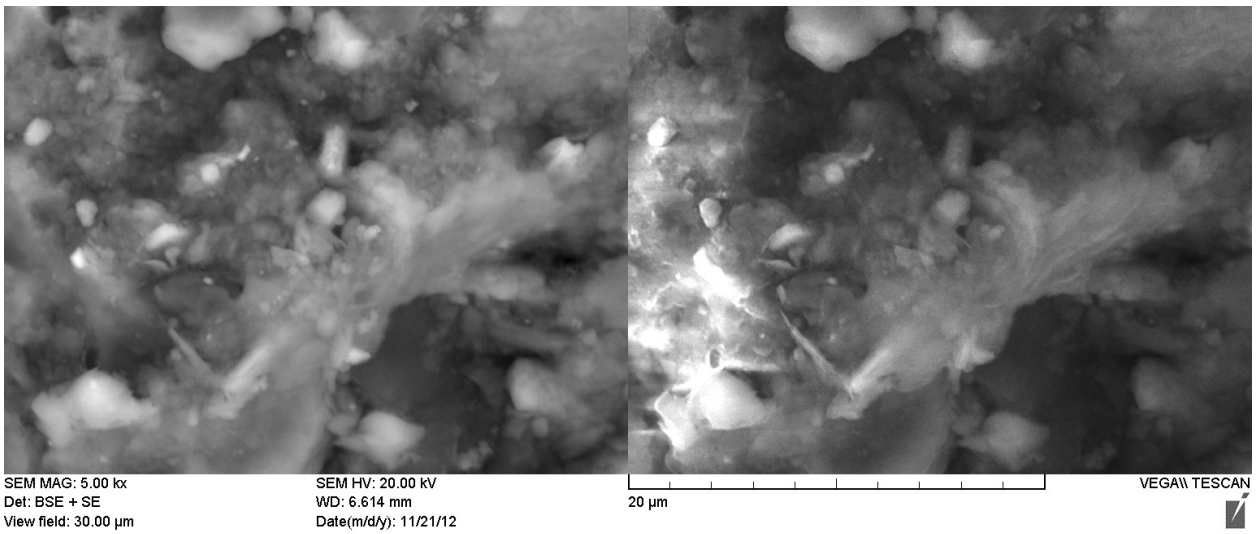

Image 3: ESEM micrographs of desiccated and consolidated polymer amended tailings for a particular sample to check accuracy; magnification – 5 kx

Appendix 7: Pictorial views of experimental set up

Laboratory experimental views to test the polymer amended oil sands tailings for desiccation

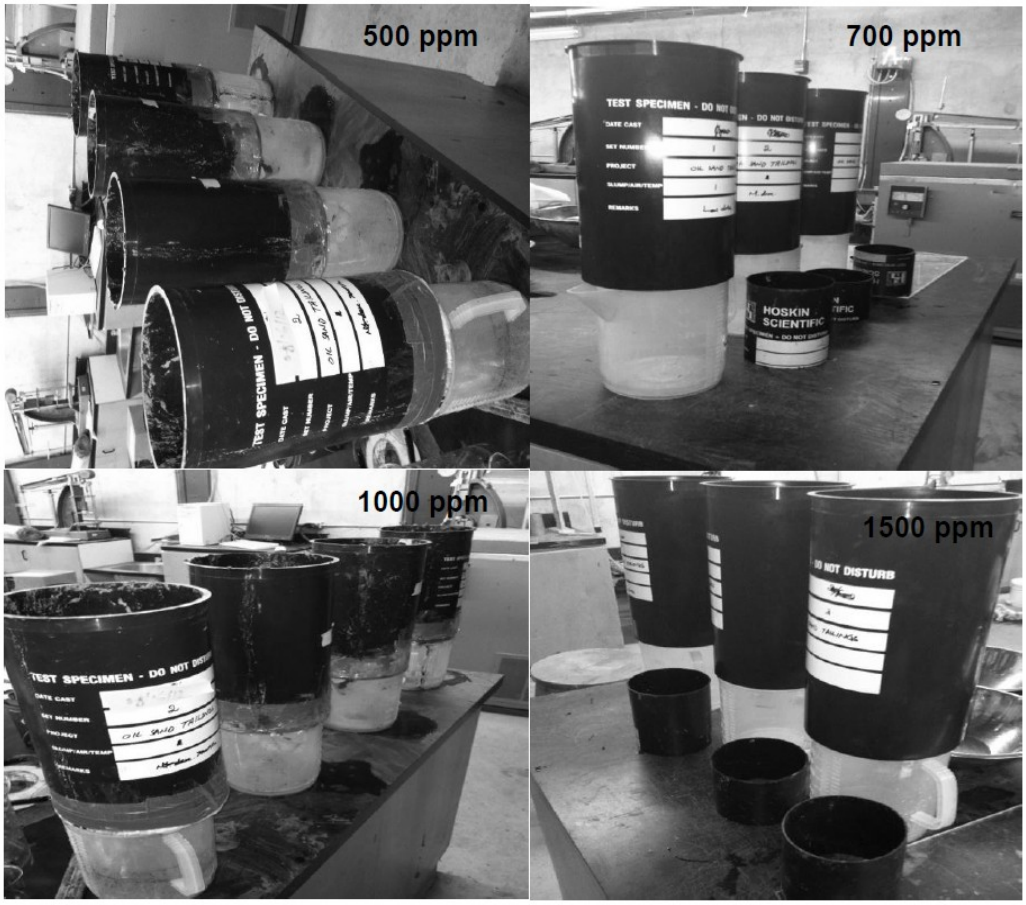

Laboratory experimental set up to examine the yield stress of polymer amended tailings for short term dewatering

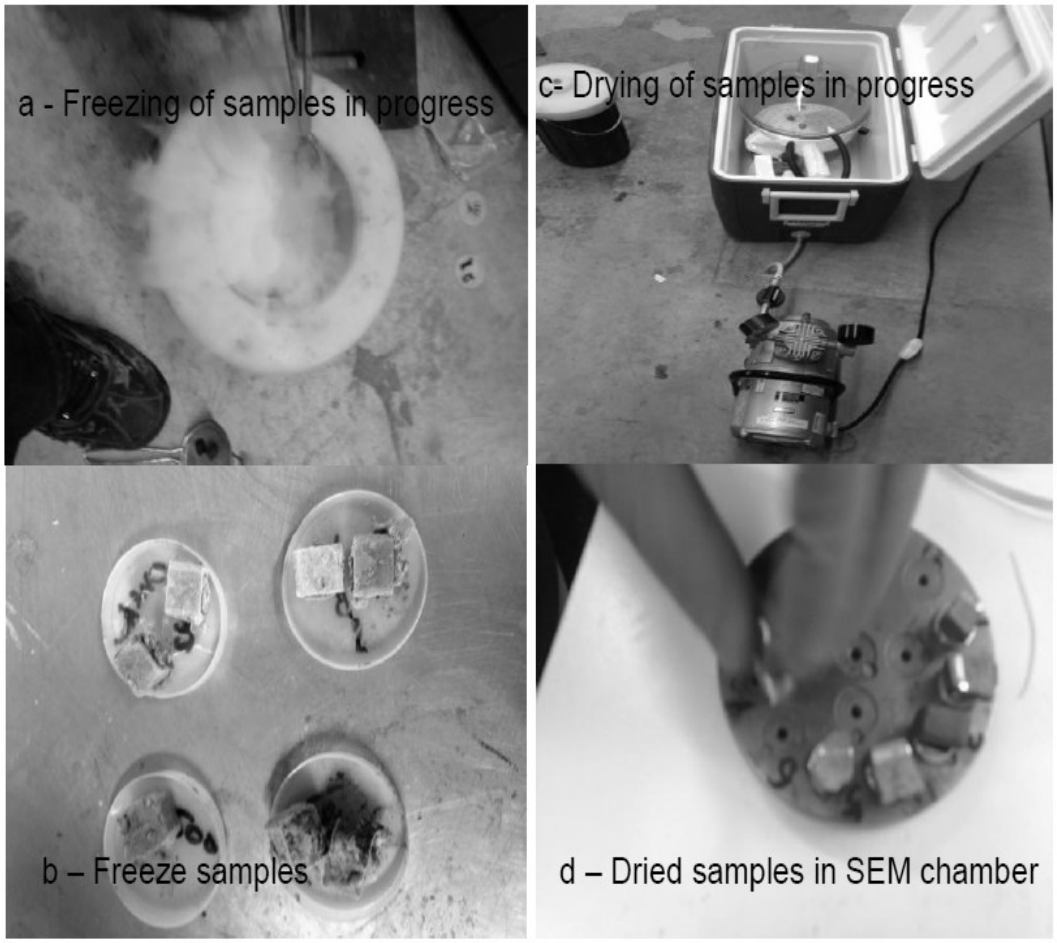

Freeze-dried samples of polymer amended oil sands mature fine tailings for SEM and MIP tests